

SEEDING ALZHEIMER'S DISEASE-ASSOCIATED TAU PATHOLOGY IN PRIMARY
NEURONS RESULTS IN EARLY AXONOPATHY AND SYNAPTIC IMPAIRMENT

By

Rebecca Lynn Mueller

A DISSERTATION

Submitted to
Michigan State University
in partial fulfillment of the requirements
for the degree of

Neuroscience – Doctor of Philosophy

2024

ABSTRACT

Alzheimer's disease (AD) is a devastating neurodegenerative disease for which there is no cure. There is a critical need for disease-modifying therapies that can help halt or even reverse the disease course. Gaining a better understanding of the mechanisms underlying the neuronal dysfunction and neurodegenerative processes observed in AD can guide the development of effective therapies. The progressive accumulation of pathological tau protein is a defining feature of AD. Tau pathology accumulates throughout the brain in a stereotypical pattern that correlates with disease severity, making it a promising target. Whether the origins of tau pathology is from cell-to-cell seeding (a prominent hypothesis in the field) or through cell autonomous routes, the subsequent functional consequences of pathogenic forms of tau require further definition. Indeed, tau is capable of seeding aggregation *in vitro* and *in vivo*, and here I leveraged this phenomenon to induce the formation of pathogenic tau in a neuron culture model of the tauopathy associated with sporadic AD. Specifically, I seeded primary neurons derived from human tau knock-in (MAPT-KI) mice with insoluble tau purified from human AD brains (AD-tau) to address critical gaps in our knowledge of the intracellular consequences of pathogenic tau. First, I performed a rigorous characterization of the model and of the seeded tau inclusions. Then, I investigated the consequences of the seeded inclusions on axon integrity and on synaptic density and function. I show that treating MAPT-KI primary neurons with AD-tau results in the progressive formation of intracellular tau pathology. I used immunological methods to show that the seeded inclusions have AD-associated modifications including phosphorylation at the PHF1, AT8, and pS422 epitopes, and conformation changes including oligomerization and exposure of an N-terminal domain (phosphatase activating domain; PAD) that is linked to axonal transport deficits. PAD activates protein phosphatase 1 (PP1), which in turn activates glycogen synthase kinase 3 β (GSK3 β).

GSK3 β phosphorylates kinesin light chains, causing these molecular motors to release their cargo. Therefore, aberrant PAD-exposure in disease may disrupt axonal transport through overactivation of this signaling pathway. I observed co-localization of active GSK3 β and cargo proteins [i.e. synaptophysin and amyloid precursor protein (APP)] with PAD-exposed tau inclusions. Furthermore, I observed PAD-exposed tau and APP colocalized in swollen processes reminiscent of axonal swellings or spheroid bodies observed in AD, which are thought to indicate an early stage of axonal degeneration. I did not observe overt axonal degeneration, or cell loss. However, the number of intact excitatory synapses was reduced in the AD-tau treated cultures. Furthermore, I used multielectrode arrays to measure the effects of the tau inclusions on neuronal function (e.g. action potential firing rate and network burst frequency). At baseline, the activity of the AD-tau treated cultures was normal. However, upon treatment with glutamate, the AD-tau treated cultures showed a significantly greater increase in network burst frequency compared to the control cultures. Furthermore, the AD-tau treated cultures showed a significantly greater decrease in network burst frequency upon treatment with an NMDA receptor (NMDAR) antagonist, suggesting that the hypersynchrony observed after glutamate addition was mediated by NMDARs. Notably, hyperexcitability, hyperactivity, and hypersynchrony are all phenotypes observed early in AD. These data demonstrate that I developed a model that recapitulates features of early neuronal dysfunction from intracellular AD-associated pathological tau. The lack of overt cell loss or axonal degeneration makes this model valuable for studying early mechanisms in AD pathogenesis, and for testing approaches to ameliorate early dysfunction and potentially prevent overt toxicity and neuronal loss in humans.

I would like to dedicate this work to my husband,
Zach,
my three-year-old son,
Owen,
and our sweet dog,
Boots.

I would also like to dedicate this work to my parents,
Jeff and Carmen, my brothers,
Eric and Matthew, my sisters,
Emily and Hayli, and my nieces and nephew,
Elliot, Natalie, Chloe and Scarlett.

ACKNOWLEDGEMENTS

I would like to thank my mentor, Nick Kanaan, for his unwavering support throughout my time in his lab. Thanks to his guidance, I am a wiser scientist, and a stronger human.

I would also like to acknowledge my committee members, Caryl Sortwell, Scott Counts, Tim Collier, and Ben Combs, for helping to steer my project into something truly exciting.

I owe a large thanks to my lab mates, past and present. I genuinely feel like they are my “found family” and it will be hard to say goodbye. I want to thank Kelly Dubois for being an amazing role model as a mother and a scientist. I appreciate the moral support from my fellow graduate students, Mohammed Alhadidy, Ahmed Atwa, and Marco Perez. I have truly enjoyed working with Matt Benskey and watching him become an independent scientist. I would like to especially thank Tessa Grabinski and Ben Combs who, along with Nick, I have known the longest. I thank Tessa for her kind, feisty, support and friendship, and Ben for his calm words of encouragement, quiet humor, and his contributions to this dissertation work.

I also thank the Translational Neuroscience department, and the Neuroscience Department. I am grateful to be able to work and learn in the midst of such intelligent and inspiring individuals.

PREFACE

At the time of writing this dissertation, major sections of Chapter 1 have already been published as a book chapter in *Tau Biology* (PMID: 32096030) and as a review in *Frontiers in Molecular Neuroscience* (PMID: 33815057). Chapters 2, 3, and 4 will be combined into a single manuscript for submission.

TABLE OF CONTENTS

LIST OF ABBREVIATIONS	ix
CHAPTER 1 Overall Introduction.....	1
INTRODUCTION.....	1
ALZHEIMER'S DISEASE.....	1
TAU BIOLOGY.....	8
NON-AD TAUOPATHIES.....	9
AXONOPATHY.....	12
SYNAPSE DYSFUNCTION AND LOSS.....	15
TAU SEEDING MODELS.....	22
DISSERTATION OBJECTIVE.....	28
REFERENCES.....	31
CHAPTER 2 Alzheimer's disease brain-derived tau seeds the formation of pathology in human tau knock-in mouse primary hippocampal neurons.....	55
ABSTRACT.....	55
INTRODUCTION.....	55
METHODS.....	59
RESULTS.....	74
DISCUSSION.....	104
REFERENCES.....	110
CHAPTER 3 Early axonopathy in MAPT-KI primary neurons seeded with human brain-derived AD-tau without overt axonal degeneration.....	120
ABSTRACT.....	120
INTRODUCTION.....	121
METHODS.....	124
RESULTS.....	133
DISCUSSION.....	148
REFERENCES.....	155
CHAPTER 4 Primary neurons seeded with human AD brain-derived tau exhibit altered NMDAR-mediated synaptic activity and loss of excitatory synapses.....	163
ABSTRACT.....	163
INTRODUCTION.....	164
METHODS.....	166
RESULTS.....	178
DISCUSSION.....	191
REFERENCES.....	198

CHAPTER 5 Overall Discussion.....	209
DISCUSSION.....	209
REFERENCES.....	222

LIST OF ABBREVIATIONS

AD	Alzheimer's disease
AD-tau	Alzheimer's brain-derived insoluble tau
aFAT	Anterograde fast axonal transport
AMPA	α -amino-3-hydroxy-5-methyl-4-isoxazolepropionic
AP5	D-2-Amino-5-phosphonopentanoic acid
APP	Amyloid precursor protein
A β	Amyloid- β
CBD	Cortical basal degeneration
CMF	Calcium and magnesium free buffer
Con	Control brain sarkosyl-insoluble proteins
CTE	Chronic traumatic encephalopathy
DIV	Day in vitro
dPBS	Dulbecco's phosphate-buffered saline
E16	Embryonic day 16
Em	Emission
Ex	Excitation
FAT	Fast axonal transport
FBS	Fetal bovine serum
FTD	Frontotemporal dementia
FTDP-17	Frontotemporal dementia with Parkinsonism linked to chromosome 1
GFAP	Glial fibrillary acidic protein
Glu	L-glutamic acid (glutamate)

GS	Goat serum
GSK3	Glycogen synthase kinase 3
His	Histidine
ICF	Immunocytofluorescence
LTD	Long term depression
LTP	Long term potentiation
MAP2	Microtubule associated protein 2
MAPT-KI	MAPT knock-in
MBO	Membrane bound organelle
MBP	Myelin basic protein
MCI	Mild cognitive impairment
MEA	Multielectrode array
MT	Microtubule
MTBR	Microtubule binding region
N	Experimental replicate
NCI	No cognitive impairment
NFDM	Non-fat dry milk
NFT	Neurofibrillary tangle
NMDAR	N-methyl-D-aspartate receptor
npGSK3	Nonphospho glycogen synthase kinase 3
NT	Neuropil thread
PAD	Phosphatase activating domain
PBS	Phosphate buffered saline

PHF	Paired helical filament
PiD	Pick's disease
PLA	Proximity ligation assay
PP1	Protein phosphatase 1
PSD95	Postsynaptic density protein 95
PSP	Progressive supranuclear palsy
PTM	Post-translational modification
RD	Repeat domain
rFAT	Retrograde fast axonal transport
SD	Standard deviation
sELISA	Sandwich enzyme-linked immunosorbent assay
SF	Straight filament
Syn	Synaptophysin
Tau-KO	Tau knockout
TBS	Tris buffered saline
TBST	TBS/0.1% TWEEN 20
TEM	Transmission electron microscopy
ThR	Thiazine Red
TNT1	Tau N Terminal 1
TOC1	Tau oligomeric complex 1
WT	Wildtype

CHAPTER 1

Overall Introduction

INTRODUCTION

Alzheimer's disease (AD) is the leading cause of dementia, affecting nearly 7 million Americans ("2024 Alzheimer's disease facts and figures," 2024). There is a critical need for disease-modifying therapies. The progressive accumulation of pathological tau protein is a defining feature of AD. Tau pathology accumulates throughout the brain in a stereotypical pattern that correlates with disease severity. Tau is capable of seeding aggregation from cell-to-cell along functionally connected networks *in vivo*, however, less is known about the specific pathological tau species that are seeded, and how the seeded tau affects neuronal health and function. I developed a relatively novel seeding model to address these gaps. I treated human tau knock-in mouse (MAPT-KI) primary hippocampal neurons with AD brain-derived tau which resulted in the formation of tau modifications (phosphorylation, conformation change and truncation) that are found in human AD, including early pretangle changes. Next, I assessed the seeded cultures for overt toxicity, axonal degeneration, and synaptic loss and dysfunction. Seeding the formation of AD-associated pathological tau in primary neurons resulted in synaptic dysfunction, mild loss of excitatory synapses, and early signs of axonopathy, without overt axon degeneration or cell death. Synapse loss is the best correlate of cognitive impairment in AD, and synaptic dysfunction occurs in early stages of AD. Identifying the mechanisms that underly synaptic toxicity could guide the development of treatments that are effective at the early disease stages of disease and could be critical for preventing or at least delaying cognitive impairment.

ALZHEIMER'S DISEASE

Alzheimer's disease (AD) is a progressive neurodegenerative disorder and the leading

cause of dementia worldwide. Age is the greatest risk factor for AD, affecting 5.0% of people age 65 to 74, 13.2% of people age 75 to 84, and 33.4% of people age 85 and older ("2024 Alzheimer's disease facts and figures," 2024). The three broad phases of AD are preclinical AD, mild cognitive impairment (MCI), and dementia due to AD. In preclinical AD, brain changes have begun despite the absence of symptoms. People with MCI experience subtle problems with memory, language, and thinking. A person is diagnosed with Dementia due to AD when the severity of memory, language, thinking and behavioral symptoms impair their ability to function in daily life. Dementia due to AD progresses from mild, to moderate, to severe. People with mild dementia due to AD are typically able to function independently in most tasks, however, they show declines in executive function. Moderate dementia due to AD is associated with worsening problems with memory and language, confusion, and decreased ability to perform activities of daily living (e.g. bathing and dressing) independently. People may have difficulty recognizing loved ones at this stage. People with severe dementia due to AD have significant impairments in verbal communication, memory and mobility and usually require constant care. Individuals with AD are at a greater risk for succumbing to blood clots, skin infections or sepsis due to impaired mobility, or aspiration pneumonia due to difficulty in swallowing.

AD is defined by the accumulation of the microtubule associated protein tau and amyloid- β ($A\beta$) into intracellular neurofibrillary tangles (NFTs) and extracellular plaques, respectively. Amyloid plaque accumulation occurs in a stereotypical pattern that is described in three stages (Braak and Braak 1991; Thal et al., 2002). $A\beta$ plaque pathology appears in the preclinical stages of AD prior to tau pathology and is initially observed exclusively in the neocortex (Phase 1). In phase 2, $A\beta$ plaque deposition progresses to allocortical regions, and appears in the entorhinal cortex and the CA1 region of the hippocampus. In phase 3, the

pathology is observed in the diencephalon, striatum, and cholinergic nuclei of the basal forebrain. The final two stages show A β pathology in the brainstem and cerebellum, respectively (Thal et al., 2002).

A β is formed by sequential cleavage of the transmembrane protein amyloid precursor protein (APP) by β -secretase followed by γ -secretase (LaFerla et al., 2007; Zhang et al., 2011). These cleavage events result in the release of a 40 or 42 amino acid A β peptide into the extracellular space. The A β 42 peptide is more prone to aggregation compared to A β 40, and is the primary fragment observed in amyloid plaques (LaFerla et al., 2007). However, several lines of evidence suggest A β oligomers are likely more toxic through mechanisms such as axonal transport disruption (Decker et al., 2010; Pigino et al., 2009; Poon et al., 2013), synaptic impairment (Li et al., 2011; Shankar et al., 2007; Wu et al., 2010), and calcium dysregulation (Alberdi et al., 2010; Arbel-Ornath et al., 2017; De Felice et al., 2007). Interestingly, evidence suggests that A β toxicity is due, at least in part, to the presence of tau. For example, A β toxicity is reduced when tau is genetically deleted from neurons in both *in vitro* and *in vivo* models (Rapoport et al., 2002; Roberson et al., 2007).

For several years, A β plaques have been the primary target of disease-modifying drug development. This is because mutations in APP or APP-processing proteins were the first identified genetic causes of AD and they cause early onset AD (LaFerla et al., 2007). Mutations in APP that cause increased β -secretase activity and/or increased aggregation of A β (e.g. Swedish and Arctic mutations, respectively) result in early onset AD. Furthermore, mutations in γ -secretase complex proteins presenilin 1 or 2 (e.g. PS1M146V) results in increased levels of A β 42, which is more prone to aggregation (LaFerla et al., 2007). Interestingly, most drugs treating A β plaques were largely unsuccessful in treating AD.

The two main classes of drugs used to treat AD are cholinesterase inhibitors and an N-methyl-D-aspartate receptor (NMDAR) antagonist. These provide modest symptom relief without changing the underlying etiology of the disease. Cholinesterase inhibitors (e.g. galantamine, rivastigmine, and donepezil) are used to treat mild to moderate AD, however, the benefits are typically modest (Marucci et al., 2021). These drugs were developed based on the loss of basal forebrain cholinergic neurons in early AD (Davies & Maloney, 1976; Hampel et al., 2018; Marucci et al., 2021; Mesulam, 2013; Sassin et al., 2000; Whitehouse et al., 1981). There is a high discontinuation rate of cholinesterase inhibitors due to side-effects (Matsunaga et al., 2018). The NMDAR antagonist, memantine, was developed to target NMDA-mediated excitotoxicity and is used to treat moderate to severe AD (Thomas & Grossberg, 2009). More recently, a class of drugs that removes A β plaques using an immunotherapeutic approach has emerged (Sevigny et al., 2016; Shi et al., 2022; van Dyck et al., 2023). Lecanemab was moderately effective at slowing cognitive and functional decline in MCI or mild AD in clinical trials (van Dyck et al., 2023), although whether this treatment improves a patient's quality of life in a significant way is currently being debated. There is clearly a critical need for disease-modifying therapies that provide significant improvements in a patient's quality of life, and ideally reverse, halt, or at least slow the progression of AD.

Researchers became keenly interested in tau when it was identified as the main component of NFTs. Indeed, NFTs are comprised of insoluble tau aggregated into straight or paired helical filaments (Brion et al., 1985; Ihara et al., 1986; Kosik et al., 1986; Nukina & Ihara, 1986). In the original AD pathological staging study, Braak and Braak tracked the distribution pattern of argyrophilic NFTs and NTs throughout the human brain using Gallyas silver stain (Braak & Braak, 1991). The staging protocol was updated using the AT8 antibody which recognizes tau that is

phosphorylated between S198 – S210 (Biernat et al., 1992; Braak et al., 2006; Braak et al., 2011; Malia et al., 2016). AT8 recognizes so-called “pretangle” tau pathology that appears before the argyrophilic NFTs. The earliest, pretangle, AT8+ tau pathology is observed in the locus coeruleus and the dorsal raphe nuclei (Braak et al., 2011; Ehrenberg et al., 2017). NFT/NT pathology is observed in the transentorhinal and entorhinal cortex (Braak stages I-II), then progresses to the hippocampus and other limbic structures (Braak stages III-IV), and finally spreads throughout much of the neocortex (Braak stages V-VI). The spatiotemporal progression and burden of tau pathology correlates with disease severity and cognitive symptoms. Braak stages I-II are associated with no cognitive impairment (NCI), also referred to as preclinical AD. Despite the absence of clinical symptoms at stages I-II, brain changes are already occurring despite the absence of symptoms. Synapse loss, neuronal loss, and neuronal hyperexcitability, for example, are some of the earliest changes in the AD brain and these events are believed to occur during NCI. The hippocampal pathology in Braak stages III-IV is associated with MCI that presents as memory impairment. By the time pathology is more widespread throughout the neocortex, Braak stages V-IV, patients have severe cognitive impairment that includes impairments in higher-order functions, aspects of judgement, and executive functions. Interestingly, the motor and sensory cortices are relatively spared until very late in AD, and this is consistent with the lack of motor symptoms AD patients.

In AD, neurons are classified based on the stage of tau pathology within the cell (Baner et al., 1989; Baner et al., 1991; Braak et al., 1994; Braak, 1993; Combs et al., 2016). Pretangle neurons contain diffuse, granular tau pathology in the soma and processes. These are believed to represent the earliest forms of pathological tau accumulation. Intermediate neurons contain a combination of granular and more compact tau inclusions within the soma with more limited

localization in processes. Mature tangle-bearing neurons contain compact classic NFTs restricted to the soma and the most proximal regions of processes. Finally, extracellular ghost tangles consist of mature NFTs that remain after the neuron is dead. Pretangle, intermediate, and mature tangle-bearing neurons are observed at all Braak stages (I-VI), though there is evidence from an analysis of human hippocampal tissue, that the proportion of pretangle neurons shows a strong negative correlation with Braak stage, and conversely, the proportion of mature tangle-bearing neurons shows a strong positive correlation with Braak stage (Combs et al., 2016).

The initial event driving monomeric tau to aggregate in disease is unclear. The current dogma is that tau monomers are modified (e.g. aberrantly phosphorylated or truncated) and this leads to formation of dimers, then oligomers, and then fibrillar tau aggregates with cross β -sheet structure. Some granular oligomers do not proceed to form filaments (termed “off-pathway” oligomers). Tau antibodies are useful for elucidating the progression of tau modifications that occur during the evolution of tau pathology in human disease. Evidence suggests that tau normally folds into a global paperclip conformation in which the N- and C-termini are in close proximity, and the C-terminus interacts with the MTBR (Jeganathan et al., 2006). Conformation changes and phosphorylation (which can induce conformation change) represent early pretangle alterations in tau that occur prior to NFT formation. The Alz50 and MC1 antibodies identified conformational changes occurring in tau at earliest stages of pathology, and immunoreactivity with each antibody is observed in pretangle neurons in postmortem AD brain. The Tau N-Terminal 1 and 2 (TNT1/2) antibodies are conformation-specific antibodies that recognize exposure of the N-terminus containing the phosphatase-activating domain (PAD; aa 2-18). The Tau Oligomeric Complex 1 (TOC1) antibody is a conformation-specific antibody raised against recombinant tau dimers and labels dimers and oligomers but not monomers or filaments (Patterson et al., 2011; Ward et al.,

2013). TNT1/2 and TOC1 immunoreactivity is observed in pretangle neurons. Pretangle neurons are also immunoreactive with phospho-specific antibodies AT8, PHF1 (phospho-S396/S404), and phospho-Ser422 (pS422). Notably, PAD-exposure is associated with phosphorylation at the AT8 epitope, and TNT1/2 immunoreactivity co-localizes with AT8, pS422, TOC1, and Alz50 in human tauopathy brain (Christensen et al., 2019; Cox et al., 2016; Kanaan et al., 2011; Tiernan et al., 2016). Immunoreactivity with Alz50, MC1, TOC1, TNT1/2, AT8, PHF1 and pS422 antibodies persists throughout tangle evolution, and is observed in the granular and compact inclusions of intermediate neurons, and in the mature tangles of NFT-bearing neurons. The TauC3 and MN423 antibodies are specific to tau truncated at D421 or E391, respectively. These antibodies recognize truncated tau monomers, however, evidence suggests that these truncation events occur after tau aggregation (Guillozet-Bongaarts et al., 2005). In human tissue, TauC3- and MN423-immunoreactive neurons were not observed in Braak stage I-II tissue, but began appearing in Braak III-IV) tissue and colocalized primarily with intermediate and mature tangle-bearing neurons, suggesting that this tau modification occurs later in the evolution of tau pathology (Combs et al., 2016; Patterson et al., 2011; Tiernan, Ginsberg, et al., 2018; Tiernan, Mufson, et al., 2018; Vana et al., 2011). The formation of β -sheet structure, identified using β -sheet dyes Thioflavin S and Thiazine Red (ThR), also occurs later in tangle evolution (Combs et al., 2016; Luna-Munoz et al., 2008; Luna-Viramontes et al., 2020; Mena et al., 1995). Accordingly, pretangle neurons do not label with ThR, instead ThR labels more compact tau inclusions (Combs et al., 2016; Patterson et al., 2011). TauC3 labelling colocalizes with pS422, and variably with ThR, suggesting that this truncation is a mid-stage event in tangle formation. MN423 labelling is more extensive than TauC3 in brain areas with severe pathology, and colocalizes extensively with ThR, suggesting that truncation at E391 occurs later (Guillozet-Bongaarts et al., 2005). In summary, these studies show

that tau undergoes a number of molecular and structural changes during the evolution of tangle pathology in human disease and that antibodies and β -sheet dyes are useful to assess these changes in tau pathology. In Braak VI entorhinal cortex, TOC1 colocalized strongly with pS422, little with MN423, and almost never with ThR (Patterson et al., 2011).

TAU BIOLOGY

Tau was discovered in 1975 as a protein that co-purified with tubulin and enhanced microtubule (MT) assembly *in vitro* (Cleveland et al., 1977a, 1977b; Weingarten et al., 1975; Witman et al., 1976). In humans, tau is expressed as six isoforms in the adult central nervous system (Wang & Mandelkow, 2016). Three of the six isoforms contain four microtubule binding repeats (4R) and alternative splicing of exon 10 results in isoforms containing three microtubule binding repeats (3R). Alternative splicing of two exons in the N-terminus results in the presence of 0N, 1N, or 2N inserts. According to this nomenclature, the six isoforms range from the shortest 0N3R isoform to the longest 2N4R isoform. The ratio of 3R to 4R isoform expression is approximately equal, though 1N isoforms are the most abundant, followed by 0N and then 2N (Wang & Mandelkow, 2016). Tau can be divided into four main domains, the N-terminus, the proline-rich domain, the microtubule binding domain, and the C-terminus. Tau is an intrinsically disordered protein, and is asymmetrically charged, with an acidic N-terminus and a positively charged MTBR and C-terminus, resulting in a low net positive charge. These properties enable tau to interact with multiple binding partners and be involved in diverse signaling roles (Brandt et al., 2020; Mueller et al., 2021; Uversky, 2015). The majority of tau is thought to be bound to MTs at any given moment, though the interaction is dynamic, allowing for tau to interact with other partners on and off MTs (~40 milliseconds residence time *in vitro*) (Janning et al., 2014; Weissmann et al., 2009). Since its initial discovery, we learned that tau interacts with a wide variety

of kinases and phosphatases to regulate axon transport, synaptic plasticity, signal transduction of insulin and neurotrophic factor pathways, and DNA and chromosomal stability (Bukar Maina et al., 2016; Combs et al., 2019; Mueller et al., 2021; Wang & Mandelkow, 2016).

Tau can undergo extensive post-translational modification (PTM). There are several phosphorylation, acetylation, methylation, ubiquitination, SUMOylation, polyamination, glycosylation, and nitration sites in tau (Alhadidy & Kanaan, 2024). PTMs have roles in regulating tau localization, degradation, and aggregation. Furthermore, PTMs can affect tau binding to MTs and MT polymerization. Some modifications associated with AD (e.g. phosphorylation at the PHF1 epitope (pS396/pS404) and PAD exposure) have roles in regulating tau function in normal conditions. Evidence suggests that phosphorylation at Ser396 is necessary for hippocampal LTD in WT mice (Regan et al., 2015). Furthermore, regulation of axonal transport through a signaling cascade initiated by PAD-exposure is thought to be a normal physiological function of tau (Mueller et al., 2021). The effects of various PTMs on tau function in physiology and in disease is an active area of investigation.

NON-AD TAUOPATHIES

There are over 20 neurodegenerative tauopathies characterized by the deposition of abnormal tau protein in the brain (Kovacs, 2018). Well known tauopathies include corticobasal degeneration (CBD), progressive supranuclear palsy (PSP), Pick's disease (PiD), chronic traumatic encephalopathy (CTE), and frontotemporal dementia with Parkinsonism linked to chromosome 17 (FTDP-17). Compared to AD, these tauopathies are relatively rare. The phenotypes of each disease are differentiated based on affected brain areas, cell types, and tau isoforms present in the tau aggregates. Most forms of tauopathies present with clinical features of frontotemporal dementia (FTD) and often have features of movement disorders (Kovacs, 2018).

Corticobasal degeneration

Cortical basal syndrome (CBS) is a progressive neurodegenerative disorder characterized by cognitive and behavioral dysfunction as well as movement disorder (Kouri et al., 2011). Classical symptoms include asymmetric rigidity and apraxia with limb dystonia and myoclonus. CBD is rare, affecting less than 1 out of 100,000 individuals per year (Constantinides et al., 2019). The average age of onset of CBD is 64 years (Constantinides et al., 2019). CBD is a primary tauopathy, and the pathological tau aggregates in CBD brains are comprised of 4R tau and are present in neurons, oligodendroglial coiled bodies and astrocytic plaques. Tau pathology is observed in the cortex, basal ganglia, diencephalon and rostral brainstem (Kovacs, 2018).

Progressive Supranuclear Palsy

Individuals with PSP exhibit FTD and progressive aphasia of speech, as well as motor symptoms, including falls, postural instability, vertical supranuclear gaze palsy, or slowing of vertical saccades. PSP affects about 6 out of 100,000 people per year (Kovacs, 2018) and the onset of PSP occurs around 66 years (Arena et al., 2015). PSP is a primary, 4R tauopathy characterized by NFTs in the subthalamic nucleus, basal ganglia, and brainstem (Kovacs, 2018). Glial tau pathology is observed as tufted astrocytes and oligodendroglial coiled bodies. PSP is characterized by atrophy affecting the basal ganglia, the frontal lobe, and the dentate nucleus of the cerebellum. A hallmark feature of PSP is the hummingbird sign visible on MRI due to atrophy of the midbrain and superior cerebral peduncle.

Pick's disease

PiD presents most often with clinical phenotypes of FTD or, rarely, with an AD-like amnesic syndrome. Reports on the average age of onset of PiD vary, with one reporting onset at 54 years (Choudhury et al., 2020). PiD is a rare, primary, 3R tauopathy characterized by

degeneration of the frontal and temporal lobes (Kovacs, 2018). Tau pathology manifests as round distinctive Pick bodies in neurons, as well as in ramified astrocytes and globular inclusions in oligodendrocytes. Pick bodies are abundant in the dentate gyrus of the hippocampus, and in cortical and subcortical regions.

Chronic traumatic encephalopathy

CTE can present initially as behavioral or mood changes, or initially as cognitive impairment (Stern et al., 2013). CTE is a mixed 3R + 4R tauopathy associated with repetitive mild head trauma (Alosco et al., 2020). Onset of CTE usually occurs 8-10 years following repetitive head trauma (Kovacs, 2015). Tau pathology in CTE is observed in neurons, oligodendroglial coiled bodies, thorny astrocytes, and granular-fuzzy astrocytes (Alosco et al., 2020; Kovacs, 2018). Tau pathology in CTE surrounds small blood vessels and distributed at the sulcal depths of the cortex. The deposition of tau pathology in CTE occurs in four stages (McKee stages I-IV), beginning as clusters of perivascular tau pathology at sulcal depths in the dorsolateral frontal cortices (McKee et al., 2023). In stage II, tau pathology is observed in frontal, temporal, and parietal cortices. In stage III, tau pathology occurs in the hippocampus, entorhinal cortex, amygdala, nucleus basalis of Meynert, substantia nigra, dorsal and median raphe, LC, and olfactory bulbs. In the final stage IV, tau pathology is observed throughout the cerebral cortex with severe pathology in the medial temporal lobe (McKee et al., 2023).

Frontotemporal dementia with Parkinsonism linked to chromosome 17

Features of FTDP-17 include cognitive impairment, behavioral and personality changes, and motor symptoms (Wszolek et al., 2006). FTDP-17 is a class of tauopathies associated with inherited mutations in the *MAPT* gene. FTDP-17 is extremely rare, however it should be considered in individuals who exhibit the onset of symptoms between 30-50 years of age and have

a family history of tauopathy (Wszolek et al, 2006). There are several tau mutations that cause FTDP-17. The P301L mutation was the first disease-causing tau mutation in FTDP-17 and subsequently is the most extensively studied. P301L-tau is a pro-aggregant form of tau and used in many animal models to study the role of tau pathology *in vitro* and *in vivo*. Using such models (as well as other mutant and modified forms of tau) the field has identified several potential mechanisms of tau-related toxicity (discussed further below).

AXONOPATHY

Axonal transport deficits and axonal degeneration in AD

Bi-directional transport of cargoes between the cell body and axon terminal is essential for maintaining neuronal function and connectivity. Anterograde axonal transport (from the soma to the terminals) is required for the delivery of synaptic proteins, organelles, ion channels, RNA, cytoskeletal proteins and more to along the axon and to the presynaptic compartment. For example, mitochondria are delivered along the axon and to the presynaptic compartment to meet local energy demands and calcium buffering needs. Retrograde axonal transport (from the axon terminals to the soma) is important for clearing damaged, misfolded, and aggregated proteins and dysfunctional mitochondria from the presynapse. Deficits in retrograde transport can lead to dysregulation of the macroautophagy pathway (a main pathway for protein degradation) which requires transport of autophagosomes to the cell body for fusion with lysosomes. Impaired clearance and degradation processes can lead to the buildup of toxic material in the cell. Axonal transport dysfunction can also impair long-distance signaling (e.g. neurotrophic signaling and stress kinase signaling). Membrane bound organelles (MBOs) and cytoskeletal components (e.g. tubulin and neurofilaments) are transported via fast axonal transport (FAT) and slow axonal transport, respectively. The anterograde-directed and retrograde-directed cargoes are driven by kinesin and

dynein motor proteins, respectively. Impaired axonal transport is thought to represent a common phenomenon underlying several neurodegenerative diseases (Combs et al., 2019; Kneynsberg et al., 2017; Kovacs, 2015). The loss of synapses early in AD is consistent with axonal transport deficits. Furthermore, brain imaging studies in AD patients show significant atrophy of axon-rich white matter structures in disease-related brain regions, and the extent to which the white matter tracts are affected is closely correlated with the degree of cognitive decline (Kneynsberg et al., 2017).

Axonal degeneration is observed in early AD and proceeds in stereotypical pattern. First, axonal enlargements known as swellings or spheroid bodies form (Raff et al., 2002; Stokin et al., 2005). Axon thinning occurs between spheroids, eventually resulting in axonal fragmentation and degradation (Kneynsberg et al., 2017; Stokin et al., 2005). During axonal degeneration, calcium-activated proteases, known as calpains, become active and facilitate breakdown of cytoskeletal components (Yin et al., 2016). The spheroid bodies contain accumulated axonal cargoes, tau, amyloid precursor protein (APP), molecular motors and cytoskeletal proteins (Stokin et al., 2005). In AD, the accumulation of cargoes in dystrophic neurites supports the role of axonal transport dysfunction in axonal degeneration (Stokin & Goldstein, 2006).

Tau regulates anterograde fast axonal transport (FAT)

Tau inclusions known as neuropil threads are present in dystrophic neurites prior to the formation of NFTs in the neuronal soma in AD (Christensen et al., 2019; Ghoshal et al., 2002; Su et al., 1997; Vana et al., 2011). Animal models of tauopathy show characteristics reminiscent of axonopathy observed in human tauopathies. Transgenic mice overexpressing 4R human tau developed accumulations of neurofilaments, mitochondria and vesicles in axonal swellings reminiscent of axonal spheroids observed in AD and other tauopathies (Christensen et al., 2019;

Mueller et al., 2021; Spittaels et al., 1999). In a separate study, mice overexpressing the six human tau isoforms (8c transgenic mice) exhibited axonal swellings and spheroids in the absence of NFTs (Duff et al., 2000). When the 8c mice were crossed with tau knockout mice to only express human tau, early axon pathology was observed, prior to the formation of pathological tau in the soma (Andorfer et al., 2003). Axonal spheroids were also present in multiple transgenic mice overexpressing mutant tau (JNPL3 mice expressing 4R/0N P301L tau and rTg4510 mice; (Lewis et al., 2000; Lin et al., 2003; Lin et al., 2005; Ludvigson et al., 2011; Mayford et al., 1996; Spires et al., 2006). Furthermore, lentiviral vector mediated delivery of WT or P301L tau into the rat hippocampus resulted in a progressive increase in swollen, fragmented, and dystrophic axons (Caillierez et al., 2013; Hebron et al., 2014). Collectively, these studies demonstrate that axonal degeneration with features reminiscent of human axonopathy is a prominent pathological feature in various animal models of tauopathy (Kneynsberg et al., 2017).

Multiple independent studies showed deficits in axonal transport due to pathological tau formation (Gotz et al., 2006; Higuchi et al., 2005; Swanson et al., 2017). Our group has elucidated a mechanism by which specific tau regulates FAT through protein phosphatase 1 (PP1)-glycogen synthase kinase-3 β (GSK3 β) signaling pathway that induces kinesin motors to release cargoes (Christensen et al., 2023; Combs et al., 2021; Combs et al., 2019; Cox et al., 2016; Kanaan et al., 2012; Kanaan et al., 2011; LaPointe et al., 2009; Morfini et al., 2002; Patterson et al., 2011; Tiernan et al., 2016). Introduction of tau monomers to the squid axoplasm did not affect anterograde or retrograde FAT (aFAT or rFAT) even at supraphysiological concentrations (Morfini et al., 2007). In contrast, recombinant wild-type tau aggregates (a mixture of oligomers and filaments) inhibited aFAT, with no effect on rFAT (LaPointe et al., 2009). Co-perfusion of the tau aggregates with PP1-specific or GSK3-specific inhibitors blocked the toxic effect on aFAT, demonstrating

activation of a PP1-GSK3 pathway as the underlying mechanism (Kanaan et al., 2011; LaPointe et al., 2009). Further studies showed that the inhibition of aFAT was dependent on an N-terminal motif (aa 2-18) termed the phosphatase-activating domain (PAD), and that PAD alone was sufficient to disrupt aFAT through the PP1-GSK3 pathway (Kanaan et al., 2011; LaPointe et al., 2009). Tau assumes a global paperclip conformation in which the N-term, MTBR, and C-term domains interact, and PAD is not exposed (Jeganathan et al., 2006). Several pathological tau species are associated with PAD-exposure. Phosphorylation at the AT8 epitope disrupts the paperclip conformation causing extension of the N-terminus and thus PAD-exposure (Christensen et al., 2023; Jeganathan et al., 2008; Kanaan et al., 2011). Furthermore, there is an FTDP-17 mutation that causes deletion of tau domains that allow flexibility for the N-term to fold onto the C-term in the paperclip formation (MTBR1 and the proline rich region) (Rovelet-Lecrux et al., 2009). As predicted, both forms of tau (AT8 and FTDP-17 mutant) disrupted aFAT as monomers in the squid, and more recently in rat primary neurons transfected with AT8 phosphomimic tau or FTDP-17 mutant tau (P301L or R5L) (Christensen et al., 2023; Combs et al., 2021; Kanaan et al., 2011). Furthermore, recombinant tau oligomers, and tau phosphorylated at Ser422 (pS422) (each associated with PAD-exposure) impaired FAT (Tiernan et al., 2016). AD-exposed tau can be identified with the conformation specific antibodies TNT1/2 (Combs et al., 2016; Kanaan et al., 2011). Axonal TNT1+ pathology is evident in subcortical white matter in early through late-stage AD, as well as in CTE, PiD, PSP and CBD (Combs et al., 2019). Together, these suggest a role for tau in axonal degeneration through PAD-exposure and the PP1-GSK3 pathway.

SYNAPSE DYSFUNCTION AND LOSS

Synaptic loss in AD

Synaptic loss is the best correlate of cognitive impairment in AD ("2024 Alzheimer's

disease facts and figures," 2024; DeKosky & Scheff, 1990; DeKosky et al., 1996; Masliah et al., 2001; Masliah et al., 1994; Scheff et al., 2007; Scheff et al., 2006; Scheff et al., 1993; Selkoe, 2002; Serrano-Pozo et al., 2011; Terry et al., 1991). Ultrastructural examination of synapses in postmortem AD tissue showed a significant reduction in synaptic numbers in frontal and temporal lobes compared to tissue from age-matched controls (DeKosky & Scheff, 1990; Scheff et al., 1993). Furthermore, decreases in synaptic number consistently correlated with cognition based on the MMSE, the Blessed test, and the dementia rating scale (DeKosky & Scheff, 1990). The regional specificity of synaptic loss appears to be consistent with the spatiotemporal pattern of tau accumulation. Illustrating this, examination of synaptic numbers in early, mid, and advanced stage AD revealed synapse loss was restricted to the hippocampus in early AD, and progressed to the neocortex in mid-advanced AD (Masliah et al., 1994). Additional studies showed synapse loss in the hippocampus in early AD first in the dentate gyrus and the CA1 region in early AD (Scheff et al., 2007; Scheff et al., 2006). A recent study used positron emission tomography was used to measure tau pathology and synaptic density in living individuals. Synaptic density correlated with tau pathology, which corroborates the early findings and provides strong evidence that tau pathology is associated with synaptic loss in AD (Wang et al., 2024).

Synaptic loss and impairment in animal models of tauopathy

Several animal models of tauopathy show synaptic dysfunction and loss. Tangle-bearing motor neurons in the spinal cord of transgenic mice overexpressing P301L tau showed a reduction in synaptic number compared to non-transgenic mouse neurons (Katsuse et al., 2006). This is consistent with studies showing that synaptophysin expression was reduced in tangle-bearing neurons in human AD tissue compared to neighboring cells devoid of NFTs (Callahan & Coleman, 1995; Callahan et al., 1999). Synapse loss and dysfunction occurred in mice overexpressing human

P301S tau at 3 months, and preceded NFT formation and neuron loss (Yoshiyama et al., 2007). In a separate study, transgenic mice overexpressing human tau harboring P301S and G2727V mutations showed signs of impaired hippocampal synaptic functioning and plasticity (Van der Jeugd et al., 2011). Overexpression of human P301L tau in layer II of the entorhinal cortex in mice (rTgTauEC) also resulted in significant reductions in pre- and postsynaptic densities in the dentate gyrus (the projection target of the EC) at 24 months (de Calignon et al., 2012). Tau_{RD} transgenic mice express the 4R repeat domain of tau with the Δ K280 mutation which has a high propensity to aggregate into tau filaments (Sydow et al., 2011). These mice showed significant reductions in synapse density at 10 months. Synapse density was rescued after turning off expression of Tau_{RD} for 4 months (corresponding with 14 months old at time of collection). Other synaptic proteins were also significantly reduced at 10 months in the Tau_{RD} including synaptophysin, drebrin, PSD95 and NMDAR1 (Sydow et al., 2011). More recently, human induced pluripotent stem cells expressing the repeat domain of tau with P301L and V337M mutations (tau-RD-LM) exhibited synaptic density reduction (Reilly et al., 2017). Furthermore, treatment of tau knockout mice with A β prevented A β -induced LTP impairment (Shipton et al., 2011). Reduction in synaptic numbers and in synaptic protein expression were observed in rTg4510 mice overexpressing P301L tau at 9-10 months (Kopeikina et al., 2013), though neuronal firing patterns are disrupted as early as 5 months (around the time of NFT formation in this model) (Menkes-Caspi et al., 2015). Furthermore, spontaneous and evoked cortical neuronal activity is reduced in rTg4510 mice at 22 months (Jackson et al., 2017). Transgenic JNPL3 mice overexpress P301L tau and show impaired LTP in hippocampal slices at 12 months (Levenga et al., 2013). Application of AD-brain derived tau oligomers to wild-type mouse hippocampal brain slices resulted in impaired LTP in the CA1 region. (Lasagna-Reeves et al., 2012). Application of recombinant human tau oligomers or AD-

tau oligomers to wild-type mouse hippocampal slices induces acute LTP impairment (Fa et al., 2016).

Long-term potentiation and hippocampal circuitry

Strengthening and weakening of synapses via long-term potentiation (LTP) and long-term depression (LTD), respectively, represents the cellular and molecular basis of learning and memory (Luscher & Malenka, 2012). N-methyl-D-aspartate receptors (NMDARs) are the primary mediators of LTP, but α -amino-3-hydroxy-5-methyl-4-isoxazolepropionic receptors (AMPA) are also involved (Luscher & Malenka, 2012). The hippocampus is the primary site of learning and memory and most of what we know about the mechanisms of LTP and LTD were discovered in the hippocampus (Bliss & Collingridge, 1993). The hippocampus is made up of the dentate gyrus, CA1, CA2, and CA3 regions. The neuronal circuitry of the hippocampus is well established. The granule cell layer of the dentate gyrus receives projections from the entorhinal cortex via the perforant pathway. Granule cells in the dentate gyrus send projections termed mossy fibers to pyramidal cells in the CA3 region. CA3 neurons send projections termed Schaffer collaterals to pyramidal cells in the CA1 region.

The role of tau in synaptic activity

There is a large body of literature supporting a role for tau in regulating synaptic function. Several independent studies show that tau is present in dendrites as well as pre and postsynaptic compartments in healthy neurons (reviewed in (Regan et al., 2017)). Indeed, 70% of post-synaptic structures in control human brains immunostained positive for tau (Tai et al., 2012). Tau mRNA is found in dendrites and dendritic spines (Malmqvist et al., 2014), suggesting that local translation may occur. Tau could also enter postsynaptic compartments via uptake from the extracellular space.

Studies consistently show that tau is involved in the regulation of LTD, while the evidence for regulating LTP is mixed. Multiple independent studies showed that tau knockout or knockdown resulted in deficits in LTD, but not LTP (Kimura et al., 2014; Regan et al., 2015; Shipton et al., 2011). In contrast, one group showed normal LTD and impaired LTP in the hippocampus of tau knockout mice (Ahmed et al., 2014). Tau interacts with the Fyn kinase and tau increases the autophosphorylation and enzymatic activity of Fyn (Lee et al., 1998; Sharma et al., 2007). Fyn phosphorylates the NMDAR subunit 2B which facilitates an interaction between the NMDAR and PSD95 and regulates LTP (Kojima et al., 1997; Nakazawa et al., 2001; Rong et al., 2001; Stein et al., 1992; Tezuka et al., 1999). Tau knockout mice showed reductions in Fyn and phosphorylated NMDAR2B in synaptosomes, suggesting a role for tau in targeting Fyn to the postsynapse (Ittner et al., 2010). This resulted in protection from pentylenetetrazole-induced seizures and excitotoxicity (Ittner et al., 2010). Notably, there is evidence for other microtubule associated proteins (MAP1A/B, MAP2) compensating for tau depletion in knockout models (Harada et al., 1994; Ma et al., 2014). Furthermore, the loss of tau-Fyn interaction in tau knockout mice was compensated for by MAP2-Fyn interactions (Liu et al., 2019). Together, these data suggest that tau has a role in LTP through interactions with Fyn, and that the lack of LTP deficits in some tau knockout animals may be due to compensatory MAP2-Fyn interactions.

A pathological role for tau in neuronal network hyperexcitability and excitotoxicity

Cortical and hippocampal hyperexcitability is a feature of early AD. In fact, neuronal hyperexcitability is observed in MCI, before the onset of dementia (Celone et al., 2006; Dickerson et al., 2005). Hyperexcitability is defined as the increased likelihood that a neuron will fire in response to a certain stimulus. Neuronal hyperexcitability was observed as a result of enhanced neuronal activity in individuals performing a memory-encoding task (Celone et al., 2006;

Dickerson et al., 2005; Hamalainen et al., 2007). Furthermore, neurons show a higher action potential firing rate frequency and lower threshold for firing in animal and cell models of tauopathy (Balez et al., 2016; Busche et al., 2008; Ghatak et al., 2019; Minkeviciene et al., 2009; Siskova et al., 2014). Interestingly, AD patients have an increased risk for epilepsy and seizures that is greater during early stages of the disease (Amatniek et al., 2006; Miranda & Brucki, 2014).

A role of tau in hyperexcitability is shown in tau knockout and overexpression models. Tau reduction ameliorates network hyperexcitability in animal models of epilepsy and AD (DeVos et al., 2013; Gheyara et al., 2014; Holth et al., 2013; Ittner et al., 2010; Pallo et al., 2016; Roberson et al., 2011; Roberson et al., 2007). Conversely, overexpression promotes network hyperexcitability in mutant tau transgenic mice. (Decker et al., 2016; Hunsberger et al., 2015; Maeda et al., 2016). Hyperexcitability can cause excitotoxicity and subsequent neurodegeneration through excess glutamate release and overactivation of NMDARs (Hardingham & Bading, 2010; Mehta et al., 2013). Indeed, overexpression of tau was shown to induce excitotoxicity in primary neurons cultures (Amadoro et al., 2006). Furthermore, treatment of neuron cultures with anti-tau antisense oligonucleotides was protective against glutamate-induced excitotoxicity (Pizzi et al., 1993).

Network hyperexcitability may involve tau-Fyn interactions. Fyn overexpression worsens hyperexcitability in hAPP mice, while knockdown reduces synaptic toxicity (Chin et al., 2005; Chin et al., 2004; Lambert et al., 1998). Recently, a study showed that phosphorylation of tau at Y18 (phosphorylation site of Fyn kinase) was necessary for NMDAR-dependent excitotoxicity (Miyamoto et al., 2017). Furthermore, there is evidence for a Fyn-independent role for tau in regulating NMDA-mediated Ca^{2+} response (Liu et al., 2020; Miyamoto et al., 2017). A role for tau in regulating excitation/inhibition (E/I) ratios may enable the protein to affect hyperexcitability

more indirectly. Along with hyperexcitability and hypersynchronization, E/I imbalance is a feature of epilepsy (Goldberg & Coulter, 2013). Interestingly, absence of tau in mouse cortical slices showed differential effects on excitatory and inhibitory neurons that ultimately reduced the E/I ratio of neural networks (Chang et al., 2021). In that study, excitatory neurons exhibited decreased action potential firing and E/I ratio without changing the excitability of the cells *per se*. In contrast, inhibitory neurons exhibited increased excitability. In this model, inhibition was promoted and hypersynchrony was suppressed (Chang et al., 2021). Together, findings from the literature suggest that there may be multiple pathways by which tau mediates excitotoxicity.

Application of oligomeric tau acutely impairs LTP

Mounting evidence suggest that soluble tau oligomers, not filaments, are the toxic species. Oligomeric tau is observed in a variety of tauopathies including AD, CBD, PSP, PiD, and CTE (Cox et al., 2016; Gerson et al., 2014; Kanaan et al., 2016; Lasagna-Reeves et al., 2012; Maeda et al., 2006; Patterson et al., 2011). In a regulatable transgenic mouse model (rTg4510), overexpression of P301L tau resulted in NFT formation, neuronal loss, and memory impairment. Remarkably, turning off tau expression rescued the memory deficits while the NFTs continued to accumulate, suggesting that the NFTs were not driving the toxicity and instead, soluble, nonfibrillar pretangle forms of tau were more likely the culprit (Santacruz et al., 2005). Aligning with this, tangle-bearing neurons in rTg4510 mice remained functionally intact as measured using two-photon Ca^{2+} imaging (Kuchibhotla et al., 2014). In a separate study, cell loss preceded tangle formation in mice overexpressing human tau (hTau mice; (Andorfer et al., 2005)). Tau oligomers were sufficient to cause synaptic and mitochondrial dysfunction in wild type mice (Lasagna-Reeves et al., 2011). Furthermore, tau oligomers impaired LTP in tau-expressing cells and in tau knockout neurons (Fa et al., 2016; Hill et al., 2019; Puzzo et al., 2020). Tau immunotherapy

rescues tauopathy-induced memory deficits in hTau and P301L mice (Castillo-Carranza, Gerson, et al., 2014; Castillo-Carranza, Sengupta, et al., 2014). Taken together, there are several lines of evidence suggesting that tau plays a role in synaptic dysfunction and this warrants further investigation.

TAU SEEDING MODELS

Tau seeding hypothesis

Pathological tau accumulates throughout the brain in a stereotypical pattern in AD and the burden of tau pathology in specific brain regions correlates with disease severity. Cell autonomous mechanisms of driving tau from a monomer to multimeric oligomers and filaments must exist, though they are not well defined currently. These triggering events could include PTMs or still undefined tau changes that lower the energy barrier for self-association. In addition, the tau seeding hypothesis provides a mechanism for how tau formed in one cell may transfer and propagate pathology to another. According to this hypothesis, pathological tau is released from a neuron and is taken up by a functionally connected neuron, where it templates the conversion of physiological monomeric tau to pathological tau in the recipient cell. Several independent studies show that tau can seed *in vitro* and *in vivo* (Boluda et al., 2015; Clavaguera et al., 2013; Gibbons et al., 2019; Guo et al., 2016; He et al., 2020; Narasimhan et al., 2017; Saito et al., 2019). Tau is released from cells in an activity-dependent manner (Pooler et al., 2013; Yamada et al., 2014). Uptake of extracellular tau aggregates can occur through heparin sulfate proteoglycans-mediated or low-density lipoprotein receptor-related protein 1-mediated endocytosis (Holmes et al., 2013; Rauch et al., 2020; Zhao et al., 2021). There is also evidence of tau transferring between neurons through tunneling nanotubes (Zhao et al., 2021). Tau uptake can occur in the somatodendritic compartment and in the axonal compartment and are transported anterogradely and retrogradely (Wu et al.,

2013).

The seeding phenomenon has proven useful in studying tau because it provides an opportunity to induce the formation of tau pathology in neuron cultures or in the brain of animal models. Seeding studies have evolved from using recombinant tau aggregates or crude tauopathy mouse brain homogenates as the seeding material to using tau purified from human AD brain (and other tauopathies). This is important because there are strain-specific differences between tau derived from various tauopathies that are recapitulated in *in vitro* and *in vivo* seeding models (Boluda et al., 2015; Clavaguera et al., 2013; Guo et al., 2016; Holmes et al., 2014; Narasimhan et al., 2017; Zareba-Paslawska et al., 2020). For example, tau derived from AD brains seeds pathological tau in neurons, while CBD-derived tau seeds aggregation in neurons and glia in wildtype mice (Narasimhan et al., 2017). Most *in vivo* seeding studies to date were performed in mice expressing mutant tau (e.g. PS19 mice) (Boluda et al., 2015; Chakrabarty et al., 2015; Guo & Lee, 2013; Holmes et al., 2014; Iba et al., 2013; Iba et al., 2015).

There are no known tau mutations that cause AD, therefore, the use of these models is not ideal for studying tauopathy associated with sporadic AD. To circumvent this drawback, some groups used transgenic hTau mice that express all six human tau isoforms (Andres-Benito et al., 2022). These mice overexpress tau and exhibit tau pathology. The 6hTau transgenic mouse model was developed to recapitulate the 3R:4R tau ratio which is approximately equal in the adult human (He et al., 2020). These mice also overexpress the six human tau isoforms by about 2-fold. To overcome the inherent drawbacks of transgenic mouse models, MAPT knock-in (MAPT-KI) mice were generated in which the entire murine *MAPT* gene was replaced with human *MAPT* using homologous recombination (Saito et al., 2019). Adult MAPT-KI mice express all six human tau isoforms at normal levels, and no mouse tau (Benskey et al., 2023; Saito et al., 2019). Tau

pathology is not observed in MAPT-KI mice out to 24 months of age (Benskey et al., 2023; Saito et al., 2019). MAPT-KI mice injected with AD-tau showed the propagation of AT8+ tau in neurites, without NFT formation or neurodegeneration (Saito et al., 2019).

Tauopathy-specific features of tau pathology are recapitulated in tau seeding models. Multiple models show that injection of pathological tau from various tauopathies recapitulate the cell-type specificity of tau pathology (Boluda et al., 2015; Clavaguera et al., 2013; Guo et al., 2016; Holmes et al., 2014; Narasimhan et al., 2017; Zareba-Paslawska et al., 2020). In a foundational study, transgenic mice overexpressing human 2N4R tau (ALZ17 line) were injected with human brain extracts from individuals who died from AD, PSP, CBD, tangle-only dementia (TD), or AGD (Clavaguera et al., 2013). The AD- and TD-injected animals showed silver-positive pathological tau inclusions reminiscent of NFTs and NTs. The tau inclusions in the AGD-tau-injected animals showed tau inclusions consistent with the small spherical or comma-shaped inclusions observed in human tissue. Oligodendrocyte tau inclusions were observed in all tauopathy-injected animals, and astrocytic tau pathology was observed in PSP (resembling tufted astrocytes), CBD (resembling astrocytic plaques), and AGD-tau-injected animals. Injection of CBD-tau, but not AD-tau, into mice overexpressing P301S tau (PS19 line) resulted in AT8+ tau inclusions in oligodendrocytes, and some astrocytes and neurons. The AT8+ tau inclusions were restricted to neurons in the AD-tau-injected mice (Boluda et al., 2015). In a separate study, WT mice were injected with sarkosyl-insoluble tau extracted from human AD, PSP, and CBD brains (Narasimhan et al., 2017). Only PSP-tau and CBD-tau seeded pathological tau in astrocytes and oligodendrocytes (Narasimhan et al., 2017). Oligodendrocytic tau pathology was also observed in mice overexpressing all six human tau isoforms (hTau line) injected with CBD-tau (Zareba-Paslawska et al., 2020). Recently, injection of mice expressing all six human tau isoforms at equal 3R/4R ratios (6hTau line) with

AD-tau, CBD-tau, PSP-tau, or PiD-tau resulted in the recapitulation of isoform-type and cell-type specificity of each tauopathy (He et al., 2020). PiD-tau seeded 3R tau pathology, while CBD-tau and PSP-tau each seeded 4R tau pathology, and AD-tau seeded mixed 3R and 4R tau pathology (He et al., 2020). Collectively, these studies highlight the importance of choosing the right animal model and seeding material to recapitulate specific diseases-associated tau species.

Characteristics of seeded inclusions

Most tau seeding studies only use the AT8 antibody to assess pathological tau. However, some have used a combination of antibodies specific to various pathological species which allows us to gain some understanding of the maturity of the tau inclusions. In one such study (Guo et al., 2016), seeded tau inclusions in WT mice injected with AD-tau were assessed with AT180 (pT231), MC1, and TG3 (conformationally altered tau pT231), which all showed increased labelling over time in the AD-tau injected animals. Some tau inclusions were AT8+/ThS+ beginning at 6 months post-injection, indicating that some of the pathological species acquired β -sheet conformation characteristic of filamentous tau (Guo et al., 2016). Notably, WT mice injected with CBD-tau or PSP-tau showed extensive ThS+ tau pathology by 3 months post-injection, while tau pathology in AD-tau mice were ThS- at that time point (Narasimhan et al., 2017).

Overt toxicity in tau seeding models

Most *in vitro* and *in vivo* tau seeding models utilizing human brain-derived tau seeds either do not assess, or lack direct evidence of overt cell loss or degeneration (Gibbons et al., 2017; Guo et al., 2016; Hayashi et al., 2021; He et al., 2020; Miao et al., 2019; Narasimhan et al., 2017; Saito et al., 2019). Mice overexpressing human 2N4R tau (ALZ17 line) injected with brain extracts from multiple human tauopathy brains exhibited extensive propagation of tau pathology in the absence of neurodegeneration out to 18 months post-injection (Clavaguera et al., 2013). Mice

overexpressing WT human 2N4R tau (Tg601) seeded with AD-brain homogenates exhibited learning and memory deficits 17 to 19 months post-injection in the absence of neurodegeneration. The impairment was correlated with increased microglia number in both hippocampi (Hayashi et al., 2021). In a separate study, injection of AD-tau into the hippocampus and overlying cortex of WT mice resulted in robust AT8+ tau pathology in anatomically connected regions, without evidence of cell loss (Guo et al., 2016). Treatment of WT mouse primary neurons with AD-tau seeded neuritic insoluble tau inclusions (Guo et al., 2016). Similarly, WT mice injected with AD-tau, PSP-tau or CBD-tau showed extensive tau pathology without neuron loss (Narasimhan et al., 2017). In a separate study, 6hTau mice injected with AD-tau, PSP-tau, CBD-tau, or PiD-tau also showed extensive tau pathology with no evidence of cell loss (He et al., 2020). Furthermore, none of the animals showed changes in LDH release, or staining of nuclei (DAPI), axons (NfL), or the somatodendritic compartment (MAP2) (He et al., 2020).

Tau seeding studies that show overt toxicity use aggressive models in which either the animal or seeding material is associated with mutant tau (Boluda et al., 2015; Congdon et al., 2016; Oakley et al., 2021). Unilateral injection of AD-brain derived tau into the hippocampus and overlying cortex of mice overexpressing P301S tau (PS19 line) induced neuronal AT8+ tau inclusions 1-month post-injection which spread to more distant sites by 6 months post-injection. This pathology was associated with a ~25% reduction in neuron number in the CA3 region of the contralateral hippocampus at 3 and 6 months post-injection (Boluda et al., 2015). In a separate study, primary neurons overexpressing 0N4R P301L tau (JNPL3 line) and treated with insoluble AD-derived tau showed significantly increased LDH levels and decreased NeuN levels, indicating overt toxicity by 7 days-post-treatment (Congdon et al., 2016). The P301S and P301L tau mutations confer an increased propensity to aggregate, and PS19 mice eventually exhibit

neurodegeneration including neuron loss and synaptic dysfunction, in the absence of seeding (Yoshiyama et al., 2007). Finally, control and P_{Sen1} L435F mutant iPSC neurons expressing TauRD-YFP were treated with brain homogenates from P301L mutant mice (rTg4510). The cells that exhibited early soma aggregate formation were associated with increased risk of subsequent cell death within 48 hours of treatment (Oakley et al., 2021).

There are infrequent reports of axonal or synaptic degeneration or dysfunction in tau seeding models. One study showed that seeding WT mice with AD-brain derived tau resulted in the reduction of PSD95 and synaptophysin without cell loss at least 4.5 months post-injection (Bassil et al., 2021). In a separate study, PS19 mouse primary neurons seeded with recombinant RD P301L tau fibrils exhibited impaired spontaneous and GABA_A antagonist-induced neuronal network activity without evidence of synapse loss (Stancu et al., 2015). Two tau seeding studies reported atrophy of functionally connected brain regions which may suggest axonal degeneration, however, there was no direct evidence. Furthermore, ALZ17 mice injected with PS19 mouse brain homogenates (containing P301S mutant tau pathology) showed no signs of axon degeneration out to 15 months post-injection (Clavaguera et al., 2009).

The studies described above primarily used insoluble tau filaments (typically sonicated prior to use) as the seeding material. There are a few examples of relatively acute toxicity following treatment with tau oligomers. WT primary cortical neurons treated with soluble AD brain-derived tau oligomers showed significant reductions in the synaptic proteins homer and bassoon 3 days post-treatment (Saroja et al., 2022). WT human iPSCs treated with recombinant soluble human 2N4R tau oligomers resulted in reduced synaptophysin and synapsin-1 immunoreactive puncta two weeks post-treatment, and this was accompanied by increased intracellular Ca²⁺ levels and decreased neurite degeneration and cell loss (Usenovic et al., 2015). In a separate study, tau

oligomers were immunoprecipitated from AD brains using the oligomer-specific T22 antibody and injected into WT mice (Lasagna-Reeves et al., 2012). Impaired object recognition was observed 3 days post-injection, but normal at 11m post-injection. Application of the tau oligomers onto WT hippocampal slices acutely inhibited LTP (Lasagna-Reeves et al., 2012). Another group showed that soluble tau oligomers from PS19 mouse brain homogenates, but not insoluble tau, induced increased LDH in 0N4R tau or P301L-overexpressing primary hippocampal neurons within 24h. Furthermore 50% neuronal loss of NeuN-positive cells and ~40% decrease in dendritic length was observed 96h after treatment with oligomers but not fibrillar tau (Jiang et al., 2019). In a separate study, authors extracted two separate populations of tau from AD brain, one enriched in high molecular weight tau oligomers (HMW) and one enriched in insoluble paired helical filaments (Mate De Gerando et al., 2023). Each population of tau seeds was injected into the hippocampus of PS19 mice, and both seeded aggregation without inducing neuron loss or changes in bassoon or PSD95 up to 3 months post-injection.

Taken together, a large body of seeding studies provide strong evidence that tau is capable of seeding pathology *in vitro* and *in vivo*, however, the effects of seeded pathological tau on neuronal integrity and function is not fully understood.

DISSERTATION OBJECTIVE

This dissertation aims to increase the knowledge of the downstream consequences of tau pathology on neuronal viability and function. I leveraged tau seeding to induce the intraneuronal formation of AD-associated pathological tau inclusions. As described above, seeding neurons with AD-derived sarkosyl-insoluble tau results in the formation of tau pathology *in vitro* and *in vivo*, however, the effects of these seeds on neuron viability and function are not well understood. To address this gap, I developed a relatively novel *in vitro* seeding model. I treated primary

hippocampal neurons derived from MAPT-KI mice with human brain-derived sarkosyl-insoluble tau (or sarkosyl-insoluble proteins from non-cognitively impaired brains (Con), or PBS as an additional control) and observed the progressive formation of intraneuronal tau inclusions. Then, I assessed the seeded cultures for signs of overt toxicity, axon degeneration, synaptic loss, or synaptic dysfunction. Gaining a better understanding of how pathological tau exerts toxic effects on cells will help develop effective therapies that treat the underlying etiology of AD.

Specific Aim 1: Identify the specific pathological tau species formed in MAPT-KI neurons seeded with AD-tau and determine if seeding results in overt toxicity.

Hypothesis: I hypothesized that treating MAPT-KI primary hippocampal neurons with human brain-derived AD-tau would seed the formation of known AD-associated pathological tau conformations (TNT1, TOC1, pS422, AT8), and that the formation of these aggregates in neurons would result in overt toxicity.

Specific Aim 1 is addressed in Chapter 2. I characterized three aspects of this seeding model: 1) the MAPT-KI cultures, 2) the AD-tau seeding material, and 3) the seeded tau inclusions. I used immunocytofluorescence (ICF) to determine what cell types are present in the MAPT-KI cultures, and biochemistry to determine the specific human tau isoforms that are were expressed *in vitro* over the time course of the seeding assay. To characterize and validate the AD-tau seeding material, I used transmission electron microscopy to identify paired helical filaments, biochemistry to identify specific tau species present in the sample, and then tested the seeding efficiency of AD-tau in RD P301S Reporter cells (HEK 293 cells expressing the fluorescently tagged-repeat domain of tau with the P301S mutation). To characterize the seeding model, I used ICF to assess the progressive formation of intracellular tau inclusions and antibodies specific to AD-associated phospho-tau (AT8, pS422, PHF1), conformationally modified tau (TNT1, TOC1), truncated tau

(TauC3, MN423), and β -sheet structure (ThR dye). To assess overt toxicity in seeded cultures, I assessed ATP levels, cell viability, cell cytotoxicity, and caspase levels in the seeded cultures. I also used ICF and biochemistry to determine cell type-specific effects of tau seeding on neuron, astrocyte, and oligodendrocyte number, and on the levels of neuron and astrocyte specific proteins.

Specific Aim 2: Determine if tau seeding in MAPT-KI cultures causes axonopathy.

Hypothesis: I hypothesized that the formation of PAD-exposed tau inclusions in seeded MAPT-KI hippocampal neurons would cause axon degeneration and deficits in action potential conduction velocity.

Specific Aim 2 is addressed in Chapter 3. I assessed calpain activity as an indirect measure of overt axon degeneration. To ascertain early signs of axon transport impairment, I used biochemistry and/or ICF to assess GSK3 β activity, and cargo protein accumulation in seeded neurons. I used ICF to assess axon degeneration. Finally, I used high density multielectrode arrays (HD-MEAs) to assess action potential conduction velocity along the axon.

Specific Aim 3: Determine if tau seeding in MAPT-KI cultures results in synaptic loss and dysfunction.

Hypothesis: I hypothesized that seeding pathological tau in MAPT-KI hippocampal neurons will result in synaptic dysfunction and overt synapse loss.

Specific Aim 3 is addressed in Chapter 4. To assess synapse loss, I used biochemistry to assess presynaptic and postsynaptic proteins in seeded culture lysates, and I used the proximity ligation assay to quantify intact excitatory synapses. To assess synaptic function, I used HD-MEAs and quantified basal and evoked action potential firing rate and network synchronicity.

REFERENCES

- 2024 Alzheimer's disease facts and figures. (2024, May). *Alzheimers Dement*, 20(5), 3708-3821. <https://doi.org/10.1002/alz.13809>
- Ahmed, T., Van der Jeugd, A., Blum, D., Galas, M. C., D'Hooge, R., Buee, L., & Balschun, D. (2014, Nov). Cognition and hippocampal synaptic plasticity in mice with a homozygous tau deletion. *Neurobiol Aging*, 35(11), 2474-2478. <https://doi.org/10.1016/j.neurobiolaging.2014.05.005>
- Alberdi, E., Sanchez-Gomez, M. V., Cavaliere, F., Perez-Samartin, A., Zugaza, J. L., Trullas, R., Domercq, M., & Matute, C. (2010, Mar). Amyloid beta oligomers induce Ca²⁺ dysregulation and neuronal death through activation of ionotropic glutamate receptors. *Cell Calcium*, 47(3), 264-272. <https://doi.org/10.1016/j.ceca.2009.12.010>
- Alhadidy, M. M., & Kanaan, N. M. (2024, Feb 28). Biochemical approaches to assess the impact of post-translational modifications on pathogenic tau conformations using recombinant protein. *Biochem Soc Trans*, 52(1), 301-318. <https://doi.org/10.1042/BST20230596>
- Alosco, M. L., Cherry, J. D., Huber, B. R., Tripodis, Y., Baucom, Z., Kowall, N. W., Saltiel, N., Goldstein, L. E., Katz, D. I., Dwyer, B., Daneshvar, D. H., Palmisano, J. N., Martin, B., Cantu, R. C., Stern, R. A., Alvarez, V. E., Mez, J., Stein, T. D., & McKee, A. C. (2020, Oct). Characterizing tau deposition in chronic traumatic encephalopathy (CTE): utility of the McKee CTE staging scheme. *Acta Neuropathol*, 140(4), 495-512. <https://doi.org/10.1007/s00401-020-02197-9>
- Amadoro, G., Ciotti, M. T., Costanzi, M., Cestari, V., Calissano, P., & Canu, N. (2006, Feb 21). NMDA receptor mediates tau-induced neurotoxicity by calpain and ERK/MAPK activation. *Proc Natl Acad Sci U S A*, 103(8), 2892-2897. <https://doi.org/10.1073/pnas.0511065103>
- Amatniek, J. C., Hauser, W. A., DelCastillo-Castaneda, C., Jacobs, D. M., Marder, K., Bell, K., Albert, M., Brandt, J., & Stern, Y. (2006, May). Incidence and predictors of seizures in patients with Alzheimer's disease. *Epilepsia*, 47(5), 867-872. <https://doi.org/10.1111/j.1528-1167.2006.00554.x>
- Andorfer, C., Acker, C. M., Kress, Y., Hof, P. R., Duff, K., & Davies, P. (2005, Jun 1). Cell-cycle reentry and cell death in transgenic mice expressing nonmutant human tau isoforms. *J Neurosci*, 25(22), 5446-5454. <https://doi.org/10.1523/JNEUROSCI.4637-04.2005>
- Andorfer, C., Kress, Y., Espinoza, M., de Silva, R., Tucker, K. L., Barde, Y. A., Duff, K., & Davies, P. (2003, Aug). Hyperphosphorylation and aggregation of tau in mice expressing normal human tau isoforms. *J Neurochem*, 86(3), 582-590. <https://doi.org/10.1046/j.1471-4159.2003.01879.x>

- Andres-Benito, P., Carmona, M., Jordan, M., Fernandez-Irigoyen, J., Santamaria, E., Del Rio, J. A., & Ferrer, I. (2022, Jan 10). Host Tau Genotype Specifically Designs and Regulates Tau Seeding and Spreading and Host Tau Transformation Following Intrahippocampal Injection of Identical Tau AD Inoculum. *Int J Mol Sci*, 23(2). <https://doi.org/10.3390/ijms23020718>
- Arbel-Ornath, M., Hudry, E., Boivin, J. R., Hashimoto, T., Takeda, S., Kuchibhotla, K. V., Hou, S., Lattarulo, C. R., Belcher, A. M., Shakerdge, N., Trujillo, P. B., Muzikansky, A., Betensky, R. A., Hyman, B. T., & Bacskai, B. J. (2017, Mar 21). Soluble oligomeric amyloid-beta induces calcium dyshomeostasis that precedes synapse loss in the living mouse brain. *Mol Neurodegener*, 12(1), 27. <https://doi.org/10.1186/s13024-017-0169-9>
- Arena, J. E., Weigand, S. D., Whitwell, J. L., Hassan, A., Eggers, S. D., Hoglinger, G. U., Litvan, I., & Josephs, K. A. (2016, Feb). Progressive supranuclear palsy: progression and survival. *J Neurol*, 263(2), 380-389. <https://doi.org/10.1007/s00415-015-7990-2>
- Balez, R., Steiner, N., Engel, M., Munoz, S. S., Lum, J. S., Wu, Y., Wang, D., Vallotton, P., Sachdev, P., O'Connor, M., Sidhu, K., Munch, G., & Ooi, L. (2016, Aug 12). Neuroprotective effects of apigenin against inflammation, neuronal excitability and apoptosis in an induced pluripotent stem cell model of Alzheimer's disease. *Sci Rep*, 6, 31450. <https://doi.org/10.1038/srep31450>
- Bancher, C., Brunner, C., Lassmann, H., Budka, H., Jellinger, K., Wiche, G., Seitelberger, F., Grundke-Iqbal, I., Iqbal, K., & Wisniewski, H. M. (1989, Jan 16). Accumulation of abnormally phosphorylated tau precedes the formation of neurofibrillary tangles in Alzheimer's disease. *Brain Res*, 477(1-2), 90-99. [https://doi.org/10.1016/0006-8993\(89\)91396-6](https://doi.org/10.1016/0006-8993(89)91396-6)
- Bancher, C., Grundke-Iqbal, I., Iqbal, K., Fried, V. A., Smith, H. T., & Wisniewski, H. M. (1991, Jan 18). Abnormal phosphorylation of tau precedes ubiquitination in neurofibrillary pathology of Alzheimer disease. *Brain Res*, 539(1), 11-18. [https://doi.org/10.1016/0006-8993\(91\)90681-k](https://doi.org/10.1016/0006-8993(91)90681-k)
- Bassil, F., Meymand, E. S., Brown, H. J., Xu, H., Cox, T. O., Pattabhiraman, S., Maghames, C. M., Wu, Q., Zhang, B., Trojanowski, J. Q., & Lee, V. M. (2021, Jan 4). alpha-Synuclein modulates tau spreading in mouse brains. *J Exp Med*, 218(1). <https://doi.org/10.1084/jem.20192193>
- Benskey, M. J., Panoushek, S., Saito, T., Saido, T. C., Grabinski, T., & Kanaan, N. M. (2023). Behavioral and neuropathological characterization over the adult lifespan of the human tau knock-in mouse. *Front Aging Neurosci*, 15, 1265151. <https://doi.org/10.3389/fnagi.2023.1265151>
- Biernat, J., Mandelkow, E., Schröter, C., Lichtenberg-Kraag, B., Steiner, B., Berling, B., Meyer, H., Mercken, M., Vandermeeren, A., & Goedert, M. (1992). The switch of tau protein to

- an Alzheimer-like state includes the phosphorylation of two serine-proline motifs upstream of the microtubule binding region. *The EMBO journal*, 11(4), 1593-1597.
- Bliss, T. V., & Collingridge, G. L. (1993, Jan 7). A synaptic model of memory: long-term potentiation in the hippocampus. *Nature*, 361(6407), 31-39. <https://doi.org/10.1038/361031a0>
- Boluda, S., Iba, M., Zhang, B., Raible, K. M., Lee, V. M., & Trojanowski, J. Q. (2015, Feb). Differential induction and spread of tau pathology in young PS19 tau transgenic mice following intracerebral injections of pathological tau from Alzheimer's disease or corticobasal degeneration brains. *Acta Neuropathol*, 129(2), 221-237. <https://doi.org/10.1007/s00401-014-1373-0>
- Braak, E., Braak, H., & Mandelkow, E. M. (1994). A sequence of cytoskeleton changes related to the formation of neurofibrillary tangles and neuropil threads. *Acta Neuropathol*, 87(6), 554-567. <https://doi.org/10.1007/BF00293315>
- Braak, H. (1993). Neuropathological staging of Alzheimer-related changes correlates with psychometrically assessed intellectual status. *Alzheimer's Disease: Advances in Clinical and Basic Research. Third International Conference on Alzheimer's Disease and Related Disorders, 1993*,
- Braak, H., Alafuzoff, I., Arzberger, T., Kretschmar, H., & Del Tredici, K. (2006). Staging of Alzheimer disease-associated neurofibrillary pathology using paraffin sections and immunocytochemistry. *Acta neuropathologica*, 112(4), 389-404.
- Braak, H., & Braak, E. (1991). Neuropathological staging of Alzheimer-related changes. *Acta Neuropathol*, 82(4), 239-259. <https://doi.org/10.1007/BF00308809>
- Braak, H., Thal, D. R., Ghebremedhin, E., & Del Tredici, K. (2011, Nov). Stages of the pathologic process in Alzheimer disease: age categories from 1 to 100 years. *J Neuropathol Exp Neurol*, 70(11), 960-969. <https://doi.org/10.1097/NEN.0b013e318232a379>
- Brandt, R., Trushina, N. I., & Bakota, L. (2020). Much More Than a Cytoskeletal Protein: Physiological and Pathological Functions of the Non-microtubule Binding Region of Tau. *Front Neurol*, 11, 590059. <https://doi.org/10.3389/fneur.2020.590059>
- Brion, J. P., van den Bosch de Aguilar, P., & Flament-Durand, J. (1985). Senile dementia of the Alzheimer type: morphological and immunocytochemical studies. In *Senile dementia of the Alzheimer type: Early diagnosis, neuropathology and animal models* (pp. 164-174). Springer.
- Bukar Maina, M., Al-Hilaly, Y. K., & Serpell, L. C. (2016, Jan 7). Nuclear Tau and Its Potential Role in Alzheimer's Disease. *Biomolecules*, 6(1), 9. <https://doi.org/10.3390/biom6010009>

- Busche, M. A., Eichhoff, G., Adelsberger, H., Abramowski, D., Wiederhold, K. H., Haass, C., Staufenbiel, M., Konnerth, A., & Garaschuk, O. (2008, Sep 19). Clusters of hyperactive neurons near amyloid plaques in a mouse model of Alzheimer's disease. *Science*, *321*(5896), 1686-1689. <https://doi.org/10.1126/science.1162844>
- Caillierez, R., Begard, S., Lecolle, K., Deramecourt, V., Zommer, N., Dujardin, S., Loyens, A., Dufour, N., Auregan, G., Winderickx, J., Hantraye, P., Deglon, N., Buee, L., & Colin, M. (2013, Jul). Lentiviral delivery of the human wild-type tau protein mediates a slow and progressive neurodegenerative tau pathology in the rat brain. *Mol Ther*, *21*(7), 1358-1368. <https://doi.org/10.1038/mt.2013.66>
- Callahan, L. M., & Coleman, P. D. (1995, May-Jun). Neurons bearing neurofibrillary tangles are responsible for selected synaptic deficits in Alzheimer's disease. *Neurobiol Aging*, *16*(3), 311-314. [https://doi.org/10.1016/0197-4580\(95\)00035-d](https://doi.org/10.1016/0197-4580(95)00035-d)
- Callahan, L. M., Vaules, W. A., & Coleman, P. D. (1999, Mar). Quantitative decrease in synaptophysin message expression and increase in cathepsin D message expression in Alzheimer disease neurons containing neurofibrillary tangles. *J Neuropathol Exp Neurol*, *58*(3), 275-287. <https://doi.org/10.1097/00005072-199903000-00007>
- Castillo-Carranza, D. L., Gerson, J. E., Sengupta, U., Guerrero-Munoz, M. J., Lasagna-Reeves, C. A., & Kaye, R. (2014). Specific targeting of tau oligomers in Htau mice prevents cognitive impairment and tau toxicity following injection with brain-derived tau oligomeric seeds. *J Alzheimers Dis*, *40 Suppl 1*, S97-S111. <https://doi.org/10.3233/JAD-132477>
- Castillo-Carranza, D. L., Sengupta, U., Guerrero-Munoz, M. J., Lasagna-Reeves, C. A., Gerson, J. E., Singh, G., Estes, D. M., Barrett, A. D., Dineley, K. T., Jackson, G. R., & Kaye, R. (2014, Mar 19). Passive immunization with Tau oligomer monoclonal antibody reverses tauopathy phenotypes without affecting hyperphosphorylated neurofibrillary tangles. *J Neurosci*, *34*(12), 4260-4272. <https://doi.org/10.1523/JNEUROSCI.3192-13.2014>
- Celone, K. A., Calhoun, V. D., Dickerson, B. C., Atri, A., Chua, E. F., Miller, S. L., DePeau, K., Rentz, D. M., Selkoe, D. J., Blacker, D., Albert, M. S., & Sperling, R. A. (2006, Oct 4). Alterations in memory networks in mild cognitive impairment and Alzheimer's disease: an independent component analysis. *J Neurosci*, *26*(40), 10222-10231. <https://doi.org/10.1523/JNEUROSCI.2250-06.2006>
- Chakrabarty, P., Hudson, V. J., III, Sacino, A. N., Brooks, M. M., D'Alton, S., Lewis, J., Golde, T. E., & Giasson, B. I. (2015, Aug). Inefficient induction and spread of seeded tau pathology in P301L mouse model of tauopathy suggests inherent physiological barriers to transmission. *Acta Neuropathol*, *130*(2), 303-305. <https://doi.org/10.1007/s00401-015-1444-x>
- Chang, C. W., Evans, M. D., Yu, X., Yu, G. Q., & Mucke, L. (2021, Oct 19). Tau reduction affects excitatory and inhibitory neurons differently, reduces excitation/inhibition ratios, and

- counteracts network hypersynchrony. *Cell Rep*, 37(3), 109855. <https://doi.org/10.1016/j.celrep.2021.109855>
- Chin, J., Palop, J. J., Puolivali, J., Massaro, C., Bien-Ly, N., Gerstein, H., Scarce-Levie, K., Masliah, E., & Mucke, L. (2005, Oct 19). Fyn kinase induces synaptic and cognitive impairments in a transgenic mouse model of Alzheimer's disease. *J Neurosci*, 25(42), 9694-9703. <https://doi.org/10.1523/JNEUROSCI.2980-05.2005>
- Chin, J., Palop, J. J., Yu, G. Q., Kojima, N., Masliah, E., & Mucke, L. (2004, May 12). Fyn kinase modulates synaptotoxicity, but not aberrant sprouting, in human amyloid precursor protein transgenic mice. *J Neurosci*, 24(19), 4692-4697. <https://doi.org/10.1523/JNEUROSCI.0277-04.2004>
- Choudhury, P., Scharf, E. L., Paolini, M. A., 2nd, Graff-Radford, J., Alden, E. C., Machulda, M. M., Jones, D. T., Fields, J. A., Murray, M. E., Graff-Radford, N. R., Constantopoulos, E., Reichard, R. R., Knopman, D. S., Duffy, J. R., Dickson, D. W., Parisi, J. E., Josephs, K. A., Petersen, R. C., & Boeve, B. F. (2020, Sep). Pick's disease: clinicopathologic characterization of 21 cases. *J Neurol*, 267(9), 2697-2704. <https://doi.org/10.1007/s00415-020-09927-9>
- Christensen, K. R., Beach, T. G., Serrano, G. E., & Kanaan, N. M. (2019, Feb 28). Pathogenic tau modifications occur in axons before the somatodendritic compartment in mossy fiber and Schaffer collateral pathways. *Acta Neuropathol Commun*, 7(1), 29. <https://doi.org/10.1186/s40478-019-0675-9>
- Christensen, K. R., Combs, B., Richards, C., Grabinski, T., Alhadidy, M. M., & Kanaan, N. M. (2023). Phosphomimetics at Ser199/Ser202/Thr205 in tau impairs axonal transport in rat hippocampal neurons. *Molecular Neurobiology*, 60(6), 3423-3438.
- Clavaguera, F., Akatsu, H., Fraser, G., Crowther, R. A., Frank, S., Hench, J., Probst, A., Winkler, D. T., Reichwald, J., Staufenbiel, M., Ghetti, B., Goedert, M., & Tolnay, M. (2013, Jun 4). Brain homogenates from human tauopathies induce tau inclusions in mouse brain. *Proc Natl Acad Sci U S A*, 110(23), 9535-9540. <https://doi.org/10.1073/pnas.1301175110>
- Clavaguera, F., Bolmont, T., Crowther, R. A., Abramowski, D., Frank, S., Probst, A., Fraser, G., Stalder, A. K., Beibel, M., & Staufenbiel, M. (2009). Transmission and spreading of tauopathy in transgenic mouse brain. *Nature cell biology*, 11(7), 909-913.
- Cleveland, D. W., Hwo, S. Y., & Kirschner, M. W. (1977a, Oct 25). Physical and chemical properties of purified tau factor and the role of tau in microtubule assembly. *J Mol Biol*, 116(2), 227-247. [https://doi.org/10.1016/0022-2836\(77\)90214-5](https://doi.org/10.1016/0022-2836(77)90214-5)
- Cleveland, D. W., Hwo, S. Y., & Kirschner, M. W. (1977b, Oct 25). Purification of tau, a microtubule-associated protein that induces assembly of microtubules from purified tubulin. *J Mol Biol*, 116(2), 207-225. [https://doi.org/10.1016/0022-2836\(77\)90213-3](https://doi.org/10.1016/0022-2836(77)90213-3)

- Combs, B., Christensen, K. R., Richards, C., Kneynsberg, A., Mueller, R. L., Morris, S. L., Morfini, G. A., Brady, S. T., & Kanaan, N. M. (2021). Frontotemporal lobar dementia mutant tau impairs axonal transport through a protein phosphatase 1 γ -dependent mechanism. *Journal of neuroscience*, *41*(45), 9431-9451.
- Combs, B., Hamel, C., & Kanaan, N. M. (2016, Oct). Pathological conformations involving the amino terminus of tau occur early in Alzheimer's disease and are differentially detected by monoclonal antibodies. *Neurobiol Dis*, *94*, 18-31. <https://doi.org/10.1016/j.nbd.2016.05.016>
- Combs, B., Mueller, R. L., Morfini, G., Brady, S. T., & Kanaan, N. M. (2019). Tau and axonal transport misregulation in tauopathies. *Tau Biology*, 81-95.
- Congdon, E. E., Lin, Y., Rajamohamedsait, H. B., Shamir, D. B., Krishnaswamy, S., Rajamohamedsait, W. J., Rasool, S., Gonzalez, V., Levenga, J., Gu, J., Hoeffler, C., & Sigurdsson, E. M. (2016, Aug 30). Affinity of Tau antibodies for solubilized pathological Tau species but not their immunogen or insoluble Tau aggregates predicts in vivo and ex vivo efficacy. *Mol Neurodegener*, *11*(1), 62. <https://doi.org/10.1186/s13024-016-0126-z>
- Constantinides, V. C., Paraskevas, G. P., Paraskevas, P. G., Stefanis, L., & Kapaki, E. (2019). Corticobasal degeneration and corticobasal syndrome: A review. *Clin Park Relat Disord*, *1*, 66-71. <https://doi.org/10.1016/j.prdoa.2019.08.005>
- Cox, K., Combs, B., Abdelmesih, B., Morfini, G., Brady, S. T., & Kanaan, N. M. (2016). Analysis of isoform-specific tau aggregates suggests a common toxic mechanism involving similar pathological conformations and axonal transport inhibition. *Neurobiology of aging*, *47*, 113-126.
- Cox, K., Combs, B., Abdelmesih, B., Morfini, G., Brady, S. T., & Kanaan, N. M. (2016, Nov). Analysis of isoform-specific tau aggregates suggests a common toxic mechanism involving similar pathological conformations and axonal transport inhibition. *Neurobiol Aging*, *47*, 113-126. <https://doi.org/10.1016/j.neurobiolaging.2016.07.015>
- Davies, P., & Maloney, A. J. (1976, Dec 25). Selective loss of central cholinergic neurons in Alzheimer's disease. *Lancet*, *2*(8000), 1403. [https://doi.org/10.1016/s0140-6736\(76\)91936-x](https://doi.org/10.1016/s0140-6736(76)91936-x)
- de Calignon, A., Polydoro, M., Suarez-Calvet, M., William, C., Adamowicz, D. H., Kopeikina, K. J., Pitstick, R., Sahara, N., Ashe, K. H., Carlson, G. A., Spires-Jones, T. L., & Hyman, B. T. (2012, Feb 23). Propagation of tau pathology in a model of early Alzheimer's disease. *Neuron*, *73*(4), 685-697. <https://doi.org/10.1016/j.neuron.2011.11.033>
- De Felice, F. G., Velasco, P. T., Lambert, M. P., Viola, K., Fernandez, S. J., Ferreira, S. T., & Klein, W. L. (2007, Apr 13). Abeta oligomers induce neuronal oxidative stress through an N-methyl-D-aspartate receptor-dependent mechanism that is blocked by the Alzheimer

- drug memantine. *J Biol Chem*, 282(15), 11590-11601.
<https://doi.org/10.1074/jbc.M607483200>
- Decker, H., Lo, K. Y., Unger, S. M., Ferreira, S. T., & Silverman, M. A. (2010, Jul 7). Amyloid-beta peptide oligomers disrupt axonal transport through an NMDA receptor-dependent mechanism that is mediated by glycogen synthase kinase 3beta in primary cultured hippocampal neurons. *J Neurosci*, 30(27), 9166-9171.
<https://doi.org/10.1523/JNEUROSCI.1074-10.2010>
- Decker, J. M., Kruger, L., Sydow, A., Dennissen, F. J., Siskova, Z., Mandelkow, E., & Mandelkow, E. M. (2016, Apr). The Tau/A152T mutation, a risk factor for frontotemporal-spectrum disorders, leads to NR2B receptor-mediated excitotoxicity. *EMBO Rep*, 17(4), 552-569. <https://doi.org/10.15252/embr.201541439>
- DeKosky, S. T., & Scheff, S. W. (1990, May). Synapse loss in frontal cortex biopsies in Alzheimer's disease: correlation with cognitive severity. *Ann Neurol*, 27(5), 457-464.
<https://doi.org/10.1002/ana.410270502>
- DeKosky, S. T., Scheff, S. W., & Styren, S. D. (1996, Dec). Structural correlates of cognition in dementia: quantification and assessment of synapse change. *Neurodegeneration*, 5(4), 417-421. <https://doi.org/10.1006/neur.1996.0056>
- DeVos, S. L., Goncharoff, D. K., Chen, G., Kebodeaux, C. S., Yamada, K., Stewart, F. R., Schuler, D. R., Maloney, S. E., Wozniak, D. F., Rigo, F., Bennett, C. F., Cirrito, J. R., Holtzman, D. M., & Miller, T. M. (2013, Jul 31). Antisense reduction of tau in adult mice protects against seizures. *J Neurosci*, 33(31), 12887-12897.
<https://doi.org/10.1523/JNEUROSCI.2107-13.2013>
- Dickerson, B. C., Salat, D. H., Greve, D. N., Chua, E. F., Rand-Giovannetti, E., Rentz, D. M., Bertram, L., Mullin, K., Tanzi, R. E., Blacker, D., Albert, M. S., & Sperling, R. A. (2005, Aug 9). Increased hippocampal activation in mild cognitive impairment compared to normal aging and AD. *Neurology*, 65(3), 404-411.
<https://doi.org/10.1212/01.wnl.0000171450.97464.49>
- Duff, K., Knight, H., Refolo, L. M., Sanders, S., Yu, X., Picciano, M., Malester, B., Hutton, M., Adamson, J., Goedert, M., Burki, K., & Davies, P. (2000, Apr). Characterization of pathology in transgenic mice over-expressing human genomic and cDNA tau transgenes. *Neurobiol Dis*, 7(2), 87-98. <https://doi.org/10.1006/nbdi.1999.0279>
- Ehrenberg, A. J., Nguy, A. K., Theofilas, P., Dunlop, S., Suemoto, C. K., Di Lorenzo Alho, A. T., Leite, R. P., Diehl Rodriguez, R., Mejia, M. B., Rub, U., Farfel, J. M., de Lucena Ferretti-Rebustini, R. E., Nascimento, C. F., Nitrini, R., Pasquallucci, C. A., Jacob-Filho, W., Miller, B., Seeley, W. W., Heinsen, H., & Grinberg, L. T. (2017, Aug). Quantifying the accretion of hyperphosphorylated tau in the locus coeruleus and dorsal raphe nucleus: the pathological building blocks of early Alzheimer's disease. *Neuropathol Appl Neurobiol*, 43(5), 393-408. <https://doi.org/10.1111/nan.12387>

- Fa, M., Puzzo, D., Piacentini, R., Staniszewski, A., Zhang, H., Baltrons, M. A., Li Puma, D. D., Chatterjee, I., Li, J., Saeed, F., Berman, H. L., Ripoli, C., Gulisano, W., Gonzalez, J., Tian, H., Costa, J. A., Lopez, P., Davidowitz, E., Yu, W. H., Haroutunian, V., Brown, L. M., Palmeri, A., Sigurdsson, E. M., Duff, K. E., Teich, A. F., Honig, L. S., Sierks, M., Moe, J. G., D'Adamio, L., Grassi, C., Kanaan, N. M., Fraser, P. E., & Arancio, O. (2016, Jan 20). Extracellular Tau Oligomers Produce An Immediate Impairment of LTP and Memory. *Sci Rep*, 6, 19393. <https://doi.org/10.1038/srep19393>
- Gerson, J. E., Sengupta, U., Lasagna-Reeves, C. A., Guerrero-Munoz, M. J., Troncoso, J., & Kaye, R. (2014, Jun 14). Characterization of tau oligomeric seeds in progressive supranuclear palsy. *Acta Neuropathol Commun*, 2, 73. <https://doi.org/10.1186/2051-5960-2-73>
- Ghatak, S., Dolatabadi, N., Trudler, D., Zhang, X., Wu, Y., Mohata, M., Ambasudhan, R., Talantova, M., & Lipton, S. A. (2019, Nov 29). Mechanisms of hyperexcitability in Alzheimer's disease hiPSC-derived neurons and cerebral organoids vs isogenic controls. *Elife*, 8. <https://doi.org/10.7554/eLife.50333>
- Gheyara, A. L., Ponnusamy, R., Djukic, B., Craft, R. J., Ho, K., Guo, W., Finucane, M. M., Sanchez, P. E., & Mucke, L. (2014, Sep). Tau reduction prevents disease in a mouse model of Dravet syndrome. *Ann Neurol*, 76(3), 443-456. <https://doi.org/10.1002/ana.24230>
- Ghoshal, N., Garcia-Sierra, F., Wu, J., Leurgans, S., Bennett, D. A., Berry, R. W., & Binder, L. I. (2002, Oct). Tau conformational changes correspond to impairments of episodic memory in mild cognitive impairment and Alzheimer's disease. *Exp Neurol*, 177(2), 475-493. <https://doi.org/10.1006/exnr.2002.8014>
- Gibbons, G. S., Banks, R. A., Kim, B., Xu, H., Changolkar, L., Leight, S. N., Riddle, D. M., Li, C., Gathagan, R. J., Brown, H. J., Zhang, B., Trojanowski, J. Q., & Lee, V. M. (2017, Nov 22). GFP-Mutant Human Tau Transgenic Mice Develop Tauopathy Following CNS Injections of Alzheimer's Brain-Derived Pathological Tau or Synthetic Mutant Human Tau Fibrils. *J Neurosci*, 37(47), 11485-11494. <https://doi.org/10.1523/JNEUROSCI.2393-17.2017>
- Gibbons, G. S., Lee, V. M., & Trojanowski, J. Q. (2019). Mechanisms of cell-to-cell transmission of pathological tau: a review. *JAMA neurology*, 76(1), 101-108.
- Goldberg, E. M., & Coulter, D. A. (2013, May). Mechanisms of epileptogenesis: a convergence on neural circuit dysfunction. *Nat Rev Neurosci*, 14(5), 337-349. <https://doi.org/10.1038/nrn3482>
- Gotz, J., Ittner, L. M., & Kins, S. (2006, Aug). Do axonal defects in tau and amyloid precursor protein transgenic animals model axonopathy in Alzheimer's disease? *J Neurochem*, 98(4), 993-1006. <https://doi.org/10.1111/j.1471-4159.2006.03955.x>

- Guillozet-Bongaarts, A. L., Garcia-Sierra, F., Reynolds, M. R., Horowitz, P. M., Fu, Y., Wang, T., Cahill, M. E., Bigio, E. H., Berry, R. W., & Binder, L. I. (2005, Jul). Tau truncation during neurofibrillary tangle evolution in Alzheimer's disease. *Neurobiol Aging*, *26*(7), 1015-1022. <https://doi.org/10.1016/j.neurobiolaging.2004.09.019>
- Guo, J. L., & Lee, V. M. (2013, Mar 18). Neurofibrillary tangle-like tau pathology induced by synthetic tau fibrils in primary neurons over-expressing mutant tau. *FEBS Lett*, *587*(6), 717-723. <https://doi.org/10.1016/j.febslet.2013.01.051>
- Guo, J. L., Narasimhan, S., Changolkar, L., He, Z., Stieber, A., Zhang, B., Gathagan, R. J., Iba, M., McBride, J. D., & Trojanowski, J. Q. (2016). Unique pathological tau conformers from Alzheimer's brains transmit tau pathology in nontransgenic mice. *Journal of Experimental Medicine*, *213*(12), 2635-2654.
- Hamalainen, A., Pihlajamaki, M., Tanila, H., Hanninen, T., Niskanen, E., Tervo, S., Karjalainen, P. A., Vanninen, R. L., & Soininen, H. (2007, Dec). Increased fMRI responses during encoding in mild cognitive impairment. *Neurobiol Aging*, *28*(12), 1889-1903. <https://doi.org/10.1016/j.neurobiolaging.2006.08.008>
- Hampel, H., Mesulam, M. M., Cuello, A. C., Farlow, M. R., Giacobini, E., Grossberg, G. T., Khachaturian, A. S., Vergallo, A., Cavedo, E., Snyder, P. J., & Khachaturian, Z. S. (2018, Jul 1). The cholinergic system in the pathophysiology and treatment of Alzheimer's disease. *Brain*, *141*(7), 1917-1933. <https://doi.org/10.1093/brain/awy132>
- Harada, A., Oguchi, K., Okabe, S., Kuno, J., Terada, S., Ohshima, T., Sato-Yoshitake, R., Takei, Y., Noda, T., & Hirokawa, N. (1994, Jun 9). Altered microtubule organization in small-calibre axons of mice lacking tau protein. *Nature*, *369*(6480), 488-491. <https://doi.org/10.1038/369488a0>
- Hardingham, G. E., & Bading, H. (2010, Oct). Synaptic versus extrasynaptic NMDA receptor signalling: implications for neurodegenerative disorders. *Nat Rev Neurosci*, *11*(10), 682-696. <https://doi.org/10.1038/nrn2911>
- Hayashi, T., Shimonaka, S., Elahi, M., Matsumoto, S. E., Ishiguro, K., Takanashi, M., Hattori, N., & Motoi, Y. (2021). Learning Deficits Accompanied by Microglial Proliferation After the Long-Term Post-Injection of Alzheimer's Disease Brain Extract in Mouse Brains. *J Alzheimers Dis*, *79*(4), 1701-1711. <https://doi.org/10.3233/JAD-201002>
- He, Z., McBride, J. D., Xu, H., Changolkar, L., Kim, S.-j., Zhang, B., Narasimhan, S., Gibbons, G. S., Guo, J. L., & Kozak, M. (2020). Transmission of tauopathy strains is independent of their isoform composition. *Nature communications*, *11*(1), 7.
- Hebron, M. L., Algarzae, N. K., Lonskaya, I., & Moussa, C. (2014, Jan). Fractalkine signaling and Tau hyper-phosphorylation are associated with autophagic alterations in lentiviral Tau and Abeta1-42 gene transfer models. *Exp Neurol*, *251*, 127-138. <https://doi.org/10.1016/j.expneurol.2013.01.009>

- Higuchi, M., Zhang, B., Forman, M. S., Yoshiyama, Y., Trojanowski, J. Q., & Lee, V. M. (2005, Oct 12). Axonal degeneration induced by targeted expression of mutant human tau in oligodendrocytes of transgenic mice that model glial tauopathies. *J Neurosci*, *25*(41), 9434-9443. <https://doi.org/10.1523/JNEUROSCI.2691-05.2005>
- Hill, E., Karikari, T. K., Moffat, K. G., Richardson, M. J. E., & Wall, M. J. (2019, Sep/Oct). Introduction of Tau Oligomers into Cortical Neurons Alters Action Potential Dynamics and Disrupts Synaptic Transmission and Plasticity. *eNeuro*, *6*(5). <https://doi.org/10.1523/ENEURO.0166-19.2019>
- Holmes, B. B., DeVos, S. L., Kfoury, N., Li, M., Jacks, R., Yanamandra, K., Ouidja, M. O., Brodsky, F. M., Marasa, J., Bagchi, D. P., Kotzbauer, P. T., Miller, T. M., Papy-Garcia, D., & Diamond, M. I. (2013, Aug 13). Heparan sulfate proteoglycans mediate internalization and propagation of specific proteopathic seeds. *Proc Natl Acad Sci U S A*, *110*(33), E3138-3147. <https://doi.org/10.1073/pnas.1301440110>
- Holmes, B. B., Furman, J. L., Mahan, T. E., Yamasaki, T. R., Mirbaha, H., Eades, W. C., Belaygorod, L., Cairns, N. J., Holtzman, D. M., & Diamond, M. I. (2014, Oct 14). Proteopathic tau seeding predicts tauopathy in vivo. *Proc Natl Acad Sci U S A*, *111*(41), E4376-4385. <https://doi.org/10.1073/pnas.1411649111>
- Holth, J. K., Bomben, V. C., Reed, J. G., Inoue, T., Younkin, L., Younkin, S. G., Pautler, R. G., Botas, J., & Noebels, J. L. (2013, Jan 23). Tau loss attenuates neuronal network hyperexcitability in mouse and Drosophila genetic models of epilepsy. *J Neurosci*, *33*(4), 1651-1659. <https://doi.org/10.1523/JNEUROSCI.3191-12.2013>
- Hunsberger, H. C., Rudy, C. C., Batten, S. R., Gerhardt, G. A., & Reed, M. N. (2015, Jan). P301L tau expression affects glutamate release and clearance in the hippocampal trisynaptic pathway. *J Neurochem*, *132*(2), 169-182. <https://doi.org/10.1111/jnc.12967>
- Iba, M., Guo, J. L., McBride, J. D., Zhang, B., Trojanowski, J. Q., & Lee, V. M. (2013, Jan 16). Synthetic tau fibrils mediate transmission of neurofibrillary tangles in a transgenic mouse model of Alzheimer's-like tauopathy. *J Neurosci*, *33*(3), 1024-1037. <https://doi.org/10.1523/JNEUROSCI.2642-12.2013>
- Iba, M., McBride, J. D., Guo, J. L., Zhang, B., Trojanowski, J. Q., & Lee, V. M.-Y. (2015). Tau pathology spread in PS19 tau transgenic mice following locus coeruleus (LC) injections of synthetic tau fibrils is determined by the LC's afferent and efferent connections. *Acta neuropathologica*, *130*, 349-362.
- Ihara, Y., Nukina, N., Miura, R., & Ogawara, M. (1986, Jun). Phosphorylated tau protein is integrated into paired helical filaments in Alzheimer's disease. *J Biochem*, *99*(6), 1807-1810. <https://doi.org/10.1093/oxfordjournals.jbchem.a135662>
- Ittner, L. M., Ke, Y. D., Delerue, F., Bi, M., Gladbach, A., van Eersel, J., Wolfing, H., Chieng, B. C., Christie, M. J., Napier, I. A., Eckert, A., Staufenbiel, M., Hardeman, E., & Gotz, J.

- (2010, Aug 6). Dendritic function of tau mediates amyloid-beta toxicity in Alzheimer's disease mouse models. *Cell*, *142*(3), 387-397. <https://doi.org/10.1016/j.cell.2010.06.036>
- Jackson, J. S., Witton, J., Johnson, J. D., Ahmed, Z., Ward, M., Randall, A. D., Hutton, M. L., Isaac, J. T., O'Neill, M. J., & Ashby, M. C. (2017, Mar 28). Altered Synapse Stability in the Early Stages of Tauopathy. *Cell Rep*, *18*(13), 3063-3068. <https://doi.org/10.1016/j.celrep.2017.03.013>
- Janning, D., Igaev, M., Sundermann, F., Bruhmann, J., Beutel, O., Heinisch, J. J., Bakota, L., Piehler, J., Junge, W., & Brandt, R. (2014, Nov 5). Single-molecule tracking of tau reveals fast kiss-and-hop interaction with microtubules in living neurons. *Mol Biol Cell*, *25*(22), 3541-3551. <https://doi.org/10.1091/mbc.E14-06-1099>
- Jeganathan, S., Hascher, A., Chinnathambi, S., Biernat, J., Mandelkow, E.-M., & Mandelkow, E. (2008). Proline-directed pseudo-phosphorylation at AT8 and PHF1 epitopes induces a compaction of the paperclip folding of Tau and generates a pathological (MC-1) conformation. *Journal of biological chemistry*, *283*(46), 32066-32076.
- Jeganathan, S., von Bergen, M., Brutlach, H., Steinhoff, H. J., & Mandelkow, E. (2006, Feb 21). Global hairpin folding of tau in solution. *Biochemistry*, *45*(7), 2283-2293. <https://doi.org/10.1021/bi0521543>
- Jiang, L., Ash, P. E. A., Maziuk, B. F., Ballance, H. I., Boudeau, S., Abdullatif, A. A., Orlando, M., Petrucelli, L., Ikezu, T., & Wolozin, B. (2019, Feb). TIA1 regulates the generation and response to toxic tau oligomers. *Acta Neuropathol*, *137*(2), 259-277. <https://doi.org/10.1007/s00401-018-1937-5>
- Kanaan, N. M., Cox, K., Alvarez, V. E., Stein, T. D., Poncil, S., & McKee, A. C. (2016). Characterization of early pathological tau conformations and phosphorylation in chronic traumatic encephalopathy. *Journal of Neuropathology & Experimental Neurology*, *75*(1), 19-34.
- Kanaan, N. M., Morfini, G., Pigino, G., LaPointe, N. E., Andreadis, A., Song, Y., Leitman, E., Binder, L. I., & Brady, S. T. (2012). Phosphorylation in the amino terminus of tau prevents inhibition of anterograde axonal transport. *Neurobiology of aging*, *33*(4), 826. e815-826. e830.
- Kanaan, N. M., Morfini, G. A., LaPointe, N. E., Pigino, G. F., Patterson, K. R., Song, Y., Andreadis, A., Fu, Y., Brady, S. T., & Binder, L. I. (2011). Pathogenic forms of tau inhibit kinesin-dependent axonal transport through a mechanism involving activation of axonal phosphotransferases. *Journal of neuroscience*, *31*(27), 9858-9868.
- Kanaan, N. M., Morfini, G. A., LaPointe, N. E., Pigino, G. F., Patterson, K. R., Song, Y., Andreadis, A., Fu, Y., Brady, S. T., & Binder, L. I. (2011, Jul 6). Pathogenic forms of tau inhibit kinesin-dependent axonal transport through a mechanism involving activation of

- axonal phosphotransferases. *J Neurosci*, 31(27), 9858-9868. <https://doi.org/10.1523/JNEUROSCI.0560-11.2011>
- Katsuse, O., Lin, W. L., Lewis, J., Hutton, M. L., & Dickson, D. W. (2006, Dec 1). Neurofibrillary tangle-related synaptic alterations of spinal motor neurons of P301L tau transgenic mice. *Neurosci Lett*, 409(2), 95-99. <https://doi.org/10.1016/j.neulet.2006.09.021>
- Kimura, T., Whitcomb, D. J., Jo, J., Regan, P., Piers, T., Heo, S., Brown, C., Hashikawa, T., Murayama, M., Seok, H., Sotiropoulos, I., Kim, E., Collingridge, G. L., Takashima, A., & Cho, K. (2014, Jan 5). Microtubule-associated protein tau is essential for long-term depression in the hippocampus. *Philos Trans R Soc Lond B Biol Sci*, 369(1633), 20130144. <https://doi.org/10.1098/rstb.2013.0144>
- Kneysberg, A., Combs, B., Christensen, K., Morfini, G., & Kanaan, N. M. (2017). Axonal Degeneration in Tauopathies: Disease Relevance and Underlying Mechanisms. *Front Neurosci*, 11, 572. <https://doi.org/10.3389/fnins.2017.00572>
- Kojima, N., Wang, J., Mansuy, I. M., Grant, S. G., Mayford, M., & Kandel, E. R. (1997, Apr 29). Rescuing impairment of long-term potentiation in t-deficient mice by introducing Fyn transgene. *Proc Natl Acad Sci U S A*, 94(9), 4761-4765. <https://doi.org/10.1073/pnas.94.9.4761>
- Kopeikina, K. J., Polydoro, M., Tai, H. C., Yaeger, E., Carlson, G. A., Pitstick, R., Hyman, B. T., & Spires-Jones, T. L. (2013, Apr 15). Synaptic alterations in the rTg4510 mouse model of tauopathy. *J Comp Neurol*, 521(6), 1334-1353. <https://doi.org/10.1002/cne.23234>
- Kosik, K. S., Joachim, C. L., & Selkoe, D. J. (1986, Jun). Microtubule-associated protein tau (tau) is a major antigenic component of paired helical filaments in Alzheimer disease. *Proc Natl Acad Sci U S A*, 83(11), 4044-4048. <https://doi.org/10.1073/pnas.83.11.4044>
- Kouri, N., Whitwell, J. L., Josephs, K. A., Rademakers, R., & Dickson, D. W. (2011, May). Corticobasal degeneration: a pathologically distinct 4R tauopathy. *Nat Rev Neurol*, 7(5), 263-272. <https://doi.org/10.1038/nrneurol.2011.43>
- Kovacs, G. G. (2015, Feb). Invited review: Neuropathology of tauopathies: principles and practice. *Neuropathol Appl Neurobiol*, 41(1), 3-23. <https://doi.org/10.1111/nan.12208>
- Kovacs, G. G. (2018). Tauopathies. *Handbook of Clinical Neurology*, 145, 355-368. <https://doi.org/https://doi.org/10.1016/B978-0-12-802395-2.00025-0>
- Kuchibhotla, K. V., Wegmann, S., Kopeikina, K. J., Hawkes, J., Rudinskiy, N., Andermann, M. L., Spires-Jones, T. L., Bacskai, B. J., & Hyman, B. T. (2014, Jan 7). Neurofibrillary tangle-bearing neurons are functionally integrated in cortical circuits in vivo. *Proc Natl Acad Sci U S A*, 111(1), 510-514. <https://doi.org/10.1073/pnas.1318807111>
- LaFerla, F. M., Green, K. N., & Oddo, S. (2007, Jul). Intracellular amyloid-beta in Alzheimer's disease. *Nat Rev Neurosci*, 8(7), 499-509. <https://doi.org/10.1038/nrn2168>

- Lambert, M. P., Barlow, A. K., Chromy, B. A., Edwards, C., Freed, R., Liosatos, M., Morgan, T. E., Rozovsky, I., Trommer, B., Viola, K. L., Wals, P., Zhang, C., Finch, C. E., Krafft, G. A., & Klein, W. L. (1998, May 26). Diffusible, nonfibrillar ligands derived from Abeta1-42 are potent central nervous system neurotoxins. *Proc Natl Acad Sci U S A*, *95*(11), 6448-6453. <https://doi.org/10.1073/pnas.95.11.6448>
- LaPointe, N. E., Morfini, G., Pigino, G., Gaisina, I. N., Kozikowski, A. P., Binder, L. I., & Brady, S. T. (2009). The amino terminus of tau inhibits kinesin-dependent axonal transport: implications for filament toxicity. *Journal of neuroscience research*, *87*(2), 440-451.
- Lasagna-Reeves, C. A., Castillo-Carranza, D. L., Sengupta, U., Clos, A. L., Jackson, G. R., & Kaye, R. (2011, Jun 6). Tau oligomers impair memory and induce synaptic and mitochondrial dysfunction in wild-type mice. *Mol Neurodegener*, *6*, 39. <https://doi.org/10.1186/1750-1326-6-39>
- Lasagna-Reeves, C. A., Castillo-Carranza, D. L., Sengupta, U., Guerrero-Munoz, M. J., Kiritoshi, T., Neugebauer, V., Jackson, G. R., & Kaye, R. (2012). Alzheimer brain-derived tau oligomers propagate pathology from endogenous tau. *Sci Rep*, *2*, 700. <https://doi.org/10.1038/srep00700>
- Lee, G., Newman, S. T., Gard, D. L., Band, H., & Panchamoorthy, G. (1998, Nov). Tau interacts with src-family non-receptor tyrosine kinases. *J Cell Sci*, *111* (Pt 21), 3167-3177. <https://doi.org/10.1242/jcs.111.21.3167>
- Levenga, J., Krishnamurthy, P., Rajamohamedsait, H., Wong, H., Franke, T. F., Cain, P., Sigurdsson, E. M., & Hoeffler, C. A. (2013, Jul 11). Tau pathology induces loss of GABAergic interneurons leading to altered synaptic plasticity and behavioral impairments. *Acta Neuropathol Commun*, *1*, 34. <https://doi.org/10.1186/2051-5960-1-34>
- Lewis, J., McGowan, E., Rockwood, J., Melrose, H., Nacharaju, P., Van Slegtenhorst, M., Gwinn-Hardy, K., Paul Murphy, M., Baker, M., Yu, X., Duff, K., Hardy, J., Corral, A., Lin, W. L., Yen, S. H., Dickson, D. W., Davies, P., & Hutton, M. (2000, Aug). Neurofibrillary tangles, amyotrophy and progressive motor disturbance in mice expressing mutant (P301L) tau protein. *Nat Genet*, *25*(4), 402-405. <https://doi.org/10.1038/78078>
- Li, S., Jin, M., Koeglsperger, T., Shepardson, N. E., Shankar, G. M., & Selkoe, D. J. (2011, May 4). Soluble Abeta oligomers inhibit long-term potentiation through a mechanism involving excessive activation of extrasynaptic NR2B-containing NMDA receptors. *J Neurosci*, *31*(18), 6627-6638. <https://doi.org/10.1523/JNEUROSCI.0203-11.2011>
- Lin, W. L., Lewis, J., Yen, S. H., Hutton, M., & Dickson, D. W. (2003, Nov). Ultrastructural neuronal pathology in transgenic mice expressing mutant (P301L) human tau. *J Neurocytol*, *32*(9), 1091-1105. <https://doi.org/10.1023/B:NEUR.0000021904.61387.95>

- Lin, W. L., Zehr, C., Lewis, J., Hutton, M., Yen, S. H., & Dickson, D. W. (2005, Dec). Progressive white matter pathology in the spinal cord of transgenic mice expressing mutant (P301L) human tau. *J Neurocytol*, 34(6), 397-410. <https://doi.org/10.1007/s11068-006-8726-0>
- Liu, G., Fiock, K. L., Levites, Y., Golde, T. E., Hefti, M. M., & Lee, G. (2020, Jul 14). Fyn depletion ameliorates tau(P301L)-induced neuropathology. *Acta Neuropathol Commun*, 8(1), 108. <https://doi.org/10.1186/s40478-020-00979-6>
- Liu, G., Thangavel, R., Rysted, J., Kim, Y., Francis, M. B., Adams, E., Lin, Z., Taugher, R. J., Wemmie, J. A., Usachev, Y. M., & Lee, G. (2019, Nov). Loss of tau and Fyn reduces compensatory effects of MAP2 for tau and reveals a Fyn-independent effect of tau on calcium. *J Neurosci Res*, 97(11), 1393-1413. <https://doi.org/10.1002/jnr.24517>
- Ludvigson, A. E., Luebke, J. I., Lewis, J., & Peters, A. (2011, Mar). Structural abnormalities in the cortex of the rTg4510 mouse model of tauopathy: a light and electron microscopy study. *Brain Struct Funct*, 216(1), 31-42. <https://doi.org/10.1007/s00429-010-0295-4>
- Luna-Munoz, J., Peralta-Ramirez, J., Chavez-Macias, L., Harrington, C. R., Wischik, C. M., & Mena, R. (2008, Nov). Thiazin red as a neuropathological tool for the rapid diagnosis of Alzheimer's disease in tissue imprints. *Acta Neuropathol*, 116(5), 507-515. <https://doi.org/10.1007/s00401-008-0431-x>
- Luna-Viramontes, N. I., Campa-Cordoba, B. B., Ontiveros-Torres, M. A., Harrington, C. R., Villanueva-Fierro, I., Guadarrama-Ortiz, P., Garces-Ramirez, L., de la Cruz, F., Hernandez-Alejandro, M., Martinez-Robles, S., Gonzalez-Ballesteros, E., Pacheco-Herrero, M., & Luna-Munoz, J. (2020). PHF-Core Tau as the Potential Initiating Event for Tau Pathology in Alzheimer's Disease. *Front Cell Neurosci*, 14, 247. <https://doi.org/10.3389/fncel.2020.00247>
- Luscher, C., & Malenka, R. C. (2012, Jun 1). NMDA receptor-dependent long-term potentiation and long-term depression (LTP/LTD). *Cold Spring Harb Perspect Biol*, 4(6). <https://doi.org/10.1101/cshperspect.a005710>
- Ma, Q. L., Zuo, X., Yang, F., Ubeda, O. J., Gant, D. J., Alaverdyan, M., Kiose, N. C., Nazari, S., Chen, P. P., Nothias, F., Chan, P., Teng, E., Frautschy, S. A., & Cole, G. M. (2014, May 21). Loss of MAP function leads to hippocampal synapse loss and deficits in the Morris Water Maze with aging. *J Neurosci*, 34(21), 7124-7136. <https://doi.org/10.1523/JNEUROSCI.3439-13.2014>
- Maeda, S., Djukic, B., Taneja, P., Yu, G. Q., Lo, I., Davis, A., Craft, R., Guo, W., Wang, X., Kim, D., Ponnusamy, R., Gill, T. M., Masliah, E., & Mucke, L. (2016, Apr). Expression of A152T human tau causes age-dependent neuronal dysfunction and loss in transgenic mice. *EMBO Rep*, 17(4), 530-551. <https://doi.org/10.15252/embr.201541438>

- Maeda, S., Sahara, N., Saito, Y., Murayama, S., Ikai, A., & Takashima, A. (2006, Mar). Increased levels of granular tau oligomers: an early sign of brain aging and Alzheimer's disease. *Neurosci Res*, *54*(3), 197-201. <https://doi.org/10.1016/j.neures.2005.11.009>
- Malia, T. J., Teplyakov, A., Ernst, R., Wu, S. J., Lacy, E. R., Liu, X., Vandermeeren, M., Mercken, M., Luo, J., & Sweet, R. W. (2016). Epitope mapping and structural basis for the recognition of phosphorylated tau by the anti-tau antibody AT8. *Proteins: Structure, Function, and Bioinformatics*, *84*(4), 427-434.
- Malmqvist, T., Anthony, K., & Gallo, J. M. (2014, Oct 10). Tau mRNA is present in axonal RNA granules and is associated with elongation factor 1A. *Brain Res*, *1584*, 22-27. <https://doi.org/10.1016/j.brainres.2013.12.033>
- Marucci, G., Buccioni, M., Ben, D. D., Lambertucci, C., Volpini, R., & Amenta, F. (2021, Jun 1). Efficacy of acetylcholinesterase inhibitors in Alzheimer's disease. *Neuropharmacology*, *190*, 108352. <https://doi.org/10.1016/j.neuropharm.2020.108352>
- Masliah, E., Mallory, M., Alford, M., DeTeresa, R., Hansen, L. A., McKeel, D. W., Jr., & Morris, J. C. (2001, Jan 9). Altered expression of synaptic proteins occurs early during progression of Alzheimer's disease. *Neurology*, *56*(1), 127-129. <https://doi.org/10.1212/wnl.56.1.127>
- Masliah, E., Mallory, M., Hansen, L., DeTeresa, R., Alford, M., & Terry, R. (1994, Jun 6). Synaptic and neuritic alterations during the progression of Alzheimer's disease. *Neurosci Lett*, *174*(1), 67-72. [https://doi.org/10.1016/0304-3940\(94\)90121-x](https://doi.org/10.1016/0304-3940(94)90121-x)
- Mate De Gerando, A., Welikovitch, L. A., Khasnavis, A., Commins, C., Glynn, C., Chun, J. E., Perbet, R., & Hyman, B. T. (2023, Aug). Tau seeding and spreading in vivo is supported by both AD-derived fibrillar and oligomeric tau. *Acta Neuropathol*, *146*(2), 191-210. <https://doi.org/10.1007/s00401-023-02600-1>
- Matsunaga, S., Kishi, T., Nomura, I., Sakuma, K., Okuya, M., Ikuta, T., & Iwata, N. (2018, Oct). The efficacy and safety of memantine for the treatment of Alzheimer's disease. *Expert Opin Drug Saf*, *17*(10), 1053-1061. <https://doi.org/10.1080/14740338.2018.1524870>
- Mayford, M., Bach, M. E., Huang, Y. Y., Wang, L., Hawkins, R. D., & Kandel, E. R. (1996, Dec 6). Control of memory formation through regulated expression of a CaMKII transgene. *Science*, *274*(5293), 1678-1683. <https://doi.org/10.1126/science.274.5293.1678>
- McKee, A. C., Stein, T. D., Huber, B. R., Crary, J. F., Bieniek, K., Dickson, D., Alvarez, V. E., Cherry, J. D., Farrell, K., Butler, M., Uretsky, M., Abdolmohammadi, B., Alosco, M. L., Tripodis, Y., Mez, J., & Daneshvar, D. H. (2023, Apr). Chronic traumatic encephalopathy (CTE): criteria for neuropathological diagnosis and relationship to repetitive head
- Mehta, A., Prabhakar, M., Kumar, P., Deshmukh, R., & Sharma, P. L. (2013, Jan 5). Excitotoxicity: bridge to various triggers in neurodegenerative disorders. *Eur J Pharmacol*, *698*(1-3), 6-18. <https://doi.org/10.1016/j.ejphar.2012.10.032>

- Mena, R., Edwards, P., Perez-Olvera, O., & Wischik, C. M. (1995). Monitoring pathological assembly of tau and beta-amyloid proteins in Alzheimer's disease. *Acta Neuropathol*, *89*(1), 50-56. <https://doi.org/10.1007/BF00294259>
- Menkes-Caspi, N., Yamin, H. G., Kellner, V., Spires-Jones, T. L., Cohen, D., & Stern, E. A. (2015, Mar 4). Pathological tau disrupts ongoing network activity. *Neuron*, *85*(5), 959-966. <https://doi.org/10.1016/j.neuron.2015.01.025>
- Mesulam, M. M. (2013, Dec 15). Cholinergic circuitry of the human nucleus basalis and its fate in Alzheimer's disease. *J Comp Neurol*, *521*(18), 4124-4144. <https://doi.org/10.1002/cne.23415>
- Miao, J., Shi, R., Li, L., Chen, F., Zhou, Y., Tung, Y. C., Hu, W., Gong, C. X., Iqbal, K., & Liu, F. (2019). Pathological Tau From Alzheimer's Brain Induces Site-Specific Hyperphosphorylation and SDS- and Reducing Agent-Resistant Aggregation of Tau in vivo. *Front Aging Neurosci*, *11*, 34. <https://doi.org/10.3389/fnagi.2019.00034>
- Minkeviciene, R., Rheims, S., Dobszay, M. B., Zilberter, M., Hartikainen, J., Fulop, L., Penke, B., Zilberter, Y., Harkany, T., Pitkanen, A., & Tanila, H. (2009, Mar 18). Amyloid beta-induced neuronal hyperexcitability triggers progressive epilepsy. *J Neurosci*, *29*(11), 3453-3462. <https://doi.org/10.1523/JNEUROSCI.5215-08.2009>
- Miranda, D. D. C., & Brucki, S. M. D. (2014, Jan-Mar). Epilepsy in patients with Alzheimer's disease: A systematic review. *Dement Neuropsychol*, *8*(1), 66-71. <https://doi.org/10.1590/S1980-57642014DN81000010>
- Miyamoto, T., Stein, L., Thomas, R., Djukic, B., Taneja, P., Knox, J., Vossel, K., & Mucke, L. (2017, May 19). Phosphorylation of tau at Y18, but not tau-fyn binding, is required for tau to modulate NMDA receptor-dependent excitotoxicity in primary neuronal culture. *Mol Neurodegener*, *12*(1), 41. <https://doi.org/10.1186/s13024-017-0176-x>
- Morfini, G., Pigino, G., Mizuno, N., Kikkawa, M., & Brady, S. T. (2007, Sep). Tau binding to microtubules does not directly affect microtubule-based vesicle motility. *J Neurosci Res*, *85*(12), 2620-2630. <https://doi.org/10.1002/jnr.21154>
- Morfini, G., Szebenyi, G., Elluru, R., Ratner, N., & Brady, S. T. (2002, Feb 1). Glycogen synthase kinase 3 phosphorylates kinesin light chains and negatively regulates kinesin-based motility. *EMBO J*, *21*(3), 281-293. <https://doi.org/10.1093/emboj/21.3.281>
- Mueller, R. L., Combs, B., Alhadidy, M. M., Brady, S. T., Morfini, G. A., & Kanaan, N. M. (2021). Tau: A Signaling Hub Protein. *Front Mol Neurosci*, *14*, 647054. <https://doi.org/10.3389/fnmol.2021.647054>
- Nakazawa, T., Komai, S., Tezuka, T., Hisatsune, C., Umemori, H., Semba, K., Mishina, M., Manabe, T., & Yamamoto, T. (2001, Jan 5). Characterization of Fyn-mediated tyrosine

- phosphorylation sites on GluR epsilon 2 (NR2B) subunit of the N-methyl-D-aspartate receptor. *J Biol Chem*, 276(1), 693-699. <https://doi.org/10.1074/jbc.M008085200>
- Narasimhan, S., Guo, J. L., Changolkar, L., Stieber, A., McBride, J. D., Silva, L. V., He, Z., Zhang, B., Gathagan, R. J., & Trojanowski, J. Q. (2017). Pathological tau strains from human brains recapitulate the diversity of tauopathies in nontransgenic mouse brain. *Journal of neuroscience*, 37(47), 11406-11423.
- Nukina, N., & Ihara, Y. (1986, May). One of the antigenic determinants of paired helical filaments is related to tau protein. *J Biochem*, 99(5), 1541-1544. <https://doi.org/10.1093/oxfordjournals.jbchem.a135625>
- Oakley, D. H., Klickstein, N., Commins, C., Chung, M., Dujardin, S., Bennett, R. E., Hyman, B. T., & Frosch, M. P. (2021, May 12). Continuous Monitoring of Tau-Induced Neurotoxicity in Patient-Derived iPSC-Neurons. *J Neurosci*, 41(19), 4335-4348. <https://doi.org/10.1523/JNEUROSCI.2590-20.2021>
- Pallo, S. P., DiMaio, J., Cook, A., Nilsson, B., & Johnson, G. V. W. (2016, Mar 1). Mechanisms of tau and Aβ-induced excitotoxicity. *Brain Res*, 1634, 119-131. <https://doi.org/10.1016/j.brainres.2015.12.048>
- Patterson, K. R., Remmers, C., Fu, Y., Brooker, S., Kanaan, N. M., Vana, L., Ward, S., Reyes, J. F., Philibert, K., Glucksman, M. J., & Binder, L. I. (2011, Jul 1). Characterization of prefibrillar Tau oligomers in vitro and in Alzheimer disease. *J Biol Chem*, 286(26), 23063-23076. <https://doi.org/10.1074/jbc.M111.237974>
- Pigino, G., Morfini, G., Atagi, Y., Deshpande, A., Yu, C., Jungbauer, L., LaDu, M., Busciglio, J., & Brady, S. (2009, Apr 7). Disruption of fast axonal transport is a pathogenic mechanism for intraneuronal amyloid beta. *Proc Natl Acad Sci U S A*, 106(14), 5907-5912. <https://doi.org/10.1073/pnas.0901229106>
- Pizzi, M., Valerio, A., Ribola, M., Spano, P. F., & Memo, M. (1993, Jun). A Tau antisense oligonucleotide decreases neurone sensitivity to excitotoxic injury. *Neuroreport*, 4(6), 823-826. <https://doi.org/10.1097/00001756-199306000-00057>
- Pooler, A. M., Phillips, E. C., Lau, D. H., Noble, W., & Hanger, D. P. (2013, Apr). Physiological release of endogenous tau is stimulated by neuronal activity. *EMBO Rep*, 14(4), 389-394. <https://doi.org/10.1038/embor.2013.15>
- Pooler, A. M., Polydoro, M., Maury, E. A., Nicholls, S. B., Reddy, S. M., Wegmann, S., William, C., Saqran, L., Cagsal-Getkin, O., Pitstick, R., Beier, D. R., Carlson, G. A., Spires-Jones, T. L., & Hyman, B. T. (2015, Mar 24). Amyloid accelerates tau propagation and toxicity in a model of early Alzheimer's disease. *Acta Neuropathol Commun*, 3, 14. <https://doi.org/10.1186/s40478-015-0199-x>

- Poon, W. W., Carlos, A. J., Aguilar, B. L., Berchtold, N. C., Kawano, C. K., Zograbyan, V., Yaoprake, T., Shelanski, M., & Cotman, C. W. (2013, Jun 7). beta-Amyloid (Abeta) oligomers impair brain-derived neurotrophic factor retrograde trafficking by down-regulating ubiquitin C-terminal hydrolase, UCH-L1. *J Biol Chem*, *288*(23), 16937-16948. <https://doi.org/10.1074/jbc.M113.463711>
- Puzzo, D., Argyrousi, E. K., Staniszewski, A., Zhang, H., Calcagno, E., Zuccarello, E., Acquarone, E., Fa, M., Li Puma, D. D., Grassi, C., D'Adamio, L., Kanaan, N. M., Fraser, P. E., & Arancio, O. (2020, Sep 1). Tau is not necessary for amyloid-beta-induced synaptic and memory impairments. *J Clin Invest*, *130*(9), 4831-4844. <https://doi.org/10.1172/JCI137040>
- Raff, M. C., Whitmore, A. V., & Finn, J. T. (2002, May 3). Axonal self-destruction and neurodegeneration. *Science*, *296*(5569), 868-871. <https://doi.org/10.1126/science.1068613>
- Rapoport, M., Dawson, H. N., Binder, L. I., Vitek, M. P., & Ferreira, A. (2002, Apr 30). Tau is essential to beta -amyloid-induced neurotoxicity. *Proc Natl Acad Sci U S A*, *99*(9), 6364-6369. <https://doi.org/10.1073/pnas.092136199>
- Rauch, J. N., Luna, G., Guzman, E., Audouard, M., Challis, C., Sibih, Y. E., Leshuk, C., Hernandez, I., Wegmann, S., Hyman, B. T., Gradinaru, V., Kampmann, M., & Kosik, K. S. (2020, Apr). LRP1 is a master regulator of tau uptake and spread. *Nature*, *580*(7803), 381-385. <https://doi.org/10.1038/s41586-020-2156-5>
- Regan, P., Piers, T., Yi, J. H., Kim, D. H., Huh, S., Park, S. J., Ryu, J. H., Whitcomb, D. J., & Cho, K. (2015, Mar 25). Tau phosphorylation at serine 396 residue is required for hippocampal LTD. *J Neurosci*, *35*(12), 4804-4812. <https://doi.org/10.1523/JNEUROSCI.2842-14.2015>
- Regan, P., Whitcomb, D. J., & Cho, K. (2017, Apr). Physiological and Pathophysiological Implications of Synaptic Tau. *Neuroscientist*, *23*(2), 137-151. <https://doi.org/10.1177/1073858416633439>
- Reilly, P., Winston, C. N., Baron, K. R., Trejo, M., Rockenstein, E. M., Akers, J. C., Kfoury, N., Diamond, M., Masliah, E., Rissman, R. A., & Yuan, S. H. (2017, Oct). Novel human neuronal tau model exhibiting neurofibrillary tangles and transcellular propagation. *Neurobiol Dis*, *106*, 222-234. <https://doi.org/10.1016/j.nbd.2017.06.005>
- Roberson, E. D., Halabisky, B., Yoo, J. W., Yao, J., Chin, J., Yan, F., Wu, T., Hamto, P., Devidze, N., Yu, G. Q., Palop, J. J., Noebels, J. L., & Mucke, L. (2011, Jan 12). Amyloid-beta/Fyn-induced synaptic, network, and cognitive impairments depend on tau levels in multiple mouse models of Alzheimer's disease. *J Neurosci*, *31*(2), 700-711. <https://doi.org/10.1523/JNEUROSCI.4152-10.2011>
- Roberson, E. D., Scarce-Levie, K., Palop, J. J., Yan, F., Cheng, I. H., Wu, T., Gerstein, H., Yu, G. Q., & Mucke, L. (2007, May 4). Reducing endogenous tau ameliorates amyloid beta-induced deficits in an Alzheimer's disease mouse model. *Science*, *316*(5825), 750-754. <https://doi.org/10.1126/science.1141736>

- Rong, Y., Lu, X., Bernard, A., Khrestchatsky, M., & Baudry, M. (2001, Oct). Tyrosine phosphorylation of ionotropic glutamate receptors by Fyn or Src differentially modulates their susceptibility to calpain and enhances their binding to spectrin and PSD-95. *J Neurochem*, *79*(2), 382-390. <https://doi.org/10.1046/j.1471-4159.2001.00565.x>
- Rovelet-Lecrux, A., Lecourtois, M., Thomas-Anterion, C., Le Ber, I., Brice, A., Frebourg, T., Hannequin, D., & Campion, D. (2009, Apr). Partial deletion of the MAPT gene: a novel mechanism of FTDP-17. *Hum Mutat*, *30*(4), E591-602. <https://doi.org/10.1002/humu.20979>
- Saito, T., Mihira, N., Matsuba, Y., Sasaguri, H., Hashimoto, S., Narasimhan, S., Zhang, B., Murayama, S., Higuchi, M., Lee, V. M. Y., Trojanowski, J. Q., & Saido, T. C. (2019, Aug 23). Humanization of the entire murine Mapt gene provides a murine model of pathological human tau propagation. *J Biol Chem*, *294*(34), 12754-12765. <https://doi.org/10.1074/jbc.RA119.009487>
- Santacruz, K., Lewis, J., Spires, T., Paulson, J., Kotilinek, L., Ingelsson, M., Guimaraes, A., DeTure, M., Ramsden, M., McGowan, E., Forster, C., Yue, M., Orne, J., Janus, C., Mariash, A., Kuskowski, M., Hyman, B., Hutton, M., & Ashe, K. H. (2005, Jul 15). Tau suppression in a neurodegenerative mouse model improves memory function. *Science*, *309*(5733), 476-481. <https://doi.org/10.1126/science.1113694>
- Saroja, S. R., Sharma, A., Hof, P. R., & Pereira, A. C. (2022, Sep). Differential expression of tau species and the association with cognitive decline and synaptic loss in Alzheimer's disease. *Alzheimers Dement*, *18*(9), 1602-1615. <https://doi.org/10.1002/alz.12518>
- Sassin, I., Schultz, C., Thal, D. R., Rub, U., Arai, K., Braak, E., & Braak, H. (2000, Sep). Evolution of Alzheimer's disease-related cytoskeletal changes in the basal nucleus of Meynert. *Acta Neuropathol*, *100*(3), 259-269. <https://doi.org/10.1007/s004019900178>
- Scheff, S. W., Price, D. A., Schmitt, F. A., DeKosky, S. T., & Mufson, E. J. (2007, May 1). Synaptic alterations in CA1 in mild Alzheimer disease and mild cognitive impairment. *Neurology*, *68*(18), 1501-1508. <https://doi.org/10.1212/01.wnl.0000260698.46517.8f>
- Scheff, S. W., Price, D. A., Schmitt, F. A., & Mufson, E. J. (2006, Oct). Hippocampal synaptic loss in early Alzheimer's disease and mild cognitive impairment. *Neurobiol Aging*, *27*(10), 1372-1384. <https://doi.org/10.1016/j.neurobiolaging.2005.09.012>
- Scheff, S. W., Sparks, L., & Price, D. A. (1993, Sep). Quantitative assessment of synaptic density in the entorhinal cortex in Alzheimer's disease. *Ann Neurol*, *34*(3), 356-361. <https://doi.org/10.1002/ana.410340309>
- Selkoe, D. J. (2002, Oct 25). Alzheimer's disease is a synaptic failure. *Science*, *298*(5594), 789-791. <https://doi.org/10.1126/science.1074069>

- Serrano-Pozo, A., Frosch, M. P., Masliah, E., & Hyman, B. T. (2011, Sep). Neuropathological alterations in Alzheimer disease. *Cold Spring Harb Perspect Med*, *1*(1), a006189. <https://doi.org/10.1101/cshperspect.a006189>
- Sevigny, J., Chiao, P., Bussiere, T., Weinreb, P. H., Williams, L., Maier, M., Dunstan, R., Salloway, S., Chen, T., Ling, Y., O'Gorman, J., Qian, F., Arastu, M., Li, M., Chollate, S., Brennan, M. S., Quintero-Monzon, O., Scannevin, R. H., Arnold, H. M., Engber, T., Rhodes, K., Ferrero, J., Hang, Y., Mikulskis, A., Grimm, J., Hock, C., Nitsch, R. M., & Sandrock, A. (2016, Sep 1). The antibody aducanumab reduces Abeta plaques in Alzheimer's disease. *Nature*, *537*(7618), 50-56. <https://doi.org/10.1038/nature19323>
- Shankar, G. M., Bloodgood, B. L., Townsend, M., Walsh, D. M., Selkoe, D. J., & Sabatini, B. L. (2007, Mar 14). Natural oligomers of the Alzheimer amyloid-beta protein induce reversible synapse loss by modulating an NMDA-type glutamate receptor-dependent signaling pathway. *J Neurosci*, *27*(11), 2866-2875. <https://doi.org/10.1523/JNEUROSCI.4970-06.2007>
- Sharma, V. M., Litersky, J. M., Bhaskar, K., & Lee, G. (2007, Mar 1). Tau impacts on growth-factor-stimulated actin remodeling. *J Cell Sci*, *120*(Pt 5), 748-757. <https://doi.org/10.1242/jcs.03378>
- Shi, M., Chu, F., Zhu, F., & Zhu, J. (2022). Impact of Anti-amyloid-beta Monoclonal Antibodies on the Pathology and Clinical Profile of Alzheimer's Disease: A Focus on Aducanumab and Lecanemab. *Front Aging Neurosci*, *14*, 870517. <https://doi.org/10.3389/fnagi.2022.870517>
- Shipton, O. A., Leitz, J. R., Dworzak, J., Acton, C. E., Tunbridge, E. M., Denk, F., Dawson, H. N., Vitek, M. P., Wade-Martins, R., Paulsen, O., & Vargas-Caballero, M. (2011, Feb 2). Tau protein is required for amyloid beta-induced impairment of hippocampal long-term potentiation. *J Neurosci*, *31*(5), 1688-1692. <https://doi.org/10.1523/JNEUROSCI.2610-10.2011>
- Siskova, Z., Justus, D., Kaneko, H., Friedrichs, D., Henneberg, N., Beutel, T., Pitsch, J., Schoch, S., Becker, A., von der Kammer, H., & Remy, S. (2014, Dec 3). Dendritic structural degeneration is functionally linked to cellular hyperexcitability in a mouse model of Alzheimer's disease. *Neuron*, *84*(5), 1023-1033. <https://doi.org/10.1016/j.neuron.2014.10.024>
- Spires, T. L., Orne, J. D., SantaCruz, K., Pitstick, R., Carlson, G. A., Ashe, K. H., & Hyman, B. T. (2006, May). Region-specific dissociation of neuronal loss and neurofibrillary pathology in a mouse model of tauopathy. *Am J Pathol*, *168*(5), 1598-1607. <https://doi.org/10.2353/ajpath.2006.050840>
- Spittaels, K., Van den Haute, C., Van Dorpe, J., Bruynseels, K., Vandezande, K., Laenen, I., Geerts, H., Mercken, M., Sciot, R., Van Lommel, A., Loos, R., & Van Leuven, F. (1999, Dec). Prominent axonopathy in the brain and spinal cord of transgenic mice overexpressing

- four-repeat human tau protein. *Am J Pathol*, 155(6), 2153-2165. [https://doi.org/10.1016/S0002-9440\(10\)65533-2](https://doi.org/10.1016/S0002-9440(10)65533-2)
- Stancu, I. C., Vasconcelos, B., Ris, L., Wang, P., Villers, A., Peeraer, E., Buist, A., Terwel, D., Baatsen, P., Oyelami, T., Pierrot, N., Casteels, C., Bormans, G., Kienlen-Campard, P., Octave, J. N., Moechars, D., & Dewachter, I. (2015, Jun). Templated misfolding of Tau by prion-like seeding along neuronal connections impairs neuronal network function and associated behavioral outcomes in Tau transgenic mice. *Acta Neuropathol*, 129(6), 875-894. <https://doi.org/10.1007/s00401-015-1413-4>
- Stancu, I. C., Ris, L., Vasconcelos, B., Marinangeli, C., Goeminne, L., Laporte, V., Haylani, L. E., Couturier, J., Schakman, O., Gailly, P., Pierrot, N., Kienlen-Campard, P., Octave, J. N., & Dewachter, I. (2014, Jun). Tauopathy contributes to synaptic and cognitive deficits in a murine model for Alzheimer's disease. *FASEB J*, 28(6), 2620-2631. <https://doi.org/10.1096/fj.13-246702>
- Stein, P. L., Lee, H. M., Rich, S., & Soriano, P. (1992, Sep 4). pp59fyn mutant mice display differential signaling in thymocytes and peripheral T cells. *Cell*, 70(5), 741-750. [https://doi.org/10.1016/0092-8674\(92\)90308-y](https://doi.org/10.1016/0092-8674(92)90308-y)
- Stern, R. A., Daneshvar, D. H., Baugh, C. M., Seichepine, D. R., Montenegro, P. H., Riley, D. O., Fritts, N. G., Stamm, J. M., Robbins, C. A., McHale, L., Simkin, I., Stein, T. D., Alvarez, V. E., Goldstein, L. E., Budson, A. E., Kowall, N. W., Nowinski, C. J., Cantu, R. C., & McKee, A. C. (2013, Sep 24). Clinical presentation of chronic traumatic encephalopathy. *Neurology*, 81(13), 1122-1129. <https://doi.org/10.1212/WNL.0b013e3182a55f7f>
- Stokin, G. B., & Goldstein, L. S. (2006). Axonal transport and Alzheimer's disease. *Annu Rev Biochem*, 75, 607-627. <https://doi.org/10.1146/annurev.biochem.75.103004.142637>
- Stokin, G. B., Lillo, C., Falzone, T. L., Brusch, R. G., Rockenstein, E., Mount, S. L., Raman, R., Davies, P., Masliah, E., Williams, D. S., & Goldstein, L. S. (2005, Feb 25). Axonopathy and transport deficits early in the pathogenesis of Alzheimer's disease. *Science*, 307(5713), 1282-1288. <https://doi.org/10.1126/science.1105681>
- Su, J. H., Deng, G., & Cotman, C. W. (1997). Transneuronal degeneration in the spread of Alzheimer's disease pathology: immunohistochemical evidence for the transmission of tau hyperphosphorylation. *Neurobiol Dis*, 4(5), 365-375. <https://doi.org/10.1006/nbdi.1997.0164>
- Swanson, E., Breckenridge, L., McMahon, L., Som, S., McConnell, I., & Bloom, G. S. (2017). Extracellular Tau Oligomers Induce Invasion of Endogenous Tau into the Somatodendritic Compartment and Axonal Transport Dysfunction. *J Alzheimers Dis*, 58(3), 803-820. <https://doi.org/10.3233/JAD-170168>
- Sydow, A., Van der Jeugd, A., Zheng, F., Ahmed, T., Balschun, D., Petrova, O., Drexler, D., Zhou, L., Rune, G., Mandelkow, E., D'Hooge, R., Alzheimer, C., & Mandelkow, E. M. (2011, Feb 16). Tau-induced defects in synaptic plasticity, learning, and memory are reversible in

- transgenic mice after switching off the toxic Tau mutant. *J Neurosci*, 31(7), 2511-2525. <https://doi.org/10.1523/JNEUROSCI.5245-10.2011>
- Tai, H. C., Serrano-Pozo, A., Hashimoto, T., Frosch, M. P., Spires-Jones, T. L., & Hyman, B. T. (2012, Oct). The synaptic accumulation of hyperphosphorylated tau oligomers in Alzheimer disease is associated with dysfunction of the ubiquitin-proteasome system. *Am J Pathol*, 181(4), 1426-1435. <https://doi.org/10.1016/j.ajpath.2012.06.033>
- Terry, R. D., Masliah, E., Salmon, D. P., Butters, N., DeTeresa, R., Hill, R., Hansen, L. A., & Katzman, R. (1991, Oct). Physical basis of cognitive alterations in Alzheimer's disease: synapse loss is the major correlate of cognitive impairment. *Ann Neurol*, 30(4), 572-580. <https://doi.org/10.1002/ana.410300410>
- Tezuka, T., Umemori, H., Akiyama, T., Nakanishi, S., & Yamamoto, T. (1999, Jan 19). PSD-95 promotes Fyn-mediated tyrosine phosphorylation of the N-methyl-D-aspartate receptor subunit NR2A. *Proc Natl Acad Sci U S A*, 96(2), 435-440. <https://doi.org/10.1073/pnas.96.2.435>
- Thal, D. R., Rub, U., Orantes, M., & Braak, H. (2002, Jun 25). Phases of A beta-deposition in the human brain and its relevance for the development of AD. *Neurology*, 58(12), 1791-1800. <https://doi.org/10.1212/wnl.58.12.1791>
- Thomas, S. J., & Grossberg, G. T. (2009). Memantine: a review of studies into its safety and efficacy in treating Alzheimer's disease and other dementias. *Clin Interv Aging*, 4, 367-377. <https://doi.org/10.2147/cia.s6666>
- Tiernan, C. T., Combs, B., Cox, K., Morfini, G., Brady, S. T., Counts, S. E., & Kanaan, N. M. (2016, Sep). Pseudophosphorylation of tau at S422 enhances SDS-stable dimer formation and impairs both anterograde and retrograde fast axonal transport. *Exp Neurol*, 283(Pt A), 318-329. <https://doi.org/10.1016/j.expneurol.2016.06.030>
- Tiernan, C. T., Ginsberg, S. D., He, B., Ward, S. M., Guillozet-Bongaarts, A. L., Kanaan, N. M., Mufson, E. J., & Counts, S. E. (2018, Sep). Pretangle pathology within cholinergic nucleus basalis neurons coincides with neurotrophic and neurotransmitter receptor gene dysregulation during the progression of Alzheimer's disease. *Neurobiol Dis*, 117, 125-136. <https://doi.org/10.1016/j.nbd.2018.05.021>
- Tiernan, C. T., Mufson, E. J., Kanaan, N. M., & Counts, S. E. (2018, Mar 1). Tau Oligomer Pathology in Nucleus Basalis Neurons During the Progression of Alzheimer Disease. *J Neuropathol Exp Neurol*, 77(3), 246-259. <https://doi.org/10.1093/jnen/nlx120>
- Usenovic, M., Niroomand, S., Drolet, R. E., Yao, L., Gaspar, R. C., Hatcher, N. G., Schachter, J., Renger, J. J., & Parmentier-Batteur, S. (2015, Oct 21). Internalized Tau Oligomers Cause Neurodegeneration by Inducing Accumulation of Pathogenic Tau in Human Neurons

Derived from Induced Pluripotent Stem Cells. *J Neurosci*, 35(42), 14234-14250.
<https://doi.org/10.1523/JNEUROSCI.1523-15.2015>

- Uversky, V. N. (2015). Intrinsically disordered proteins and their (disordered) proteomes in neurodegenerative disorders. *Front Aging Neurosci*, 7, 18.
<https://doi.org/10.3389/fnagi.2015.00018>
- Van der Jeugd, A., Ahmed, T., Burnouf, S., Belarbi, K., Hamdame, M., Grosjean, M. E., Humez, S., Balschun, D., Blum, D., Buee, L., & D'Hooge, R. (2011, Mar). Hippocampal tauopathy in tau transgenic mice coincides with impaired hippocampus-dependent learning and memory, and attenuated late-phase long-term depression of synaptic transmission. *Neurobiol Learn Mem*, 95(3), 296-304. <https://doi.org/10.1016/j.nlm.2010.12.005>
- van Dyck, C. H., Swanson, C. J., Aisen, P., Bateman, R. J., Chen, C., Gee, M., Kanekiyo, M., Li, D., Reyderman, L., Cohen, S., Froelich, L., Katayama, S., Sabbagh, M., Vellas, B., Watson, D., Dhadda, S., Irizarry, M., Kramer, L. D., & Iwatsubo, T. (2023, Jan 5). Lecanemab in Early Alzheimer's Disease. *N Engl J Med*, 388(1), 9-21.
<https://doi.org/10.1056/NEJMoa2212948>
- Vana, L., Kanaan, N. M., Ugwu, I. C., Wu, J., Mufson, E. J., & Binder, L. I. (2011, Nov). Progression of tau pathology in cholinergic Basal forebrain neurons in mild cognitive impairment and Alzheimer's disease. *Am J Pathol*, 179(5), 2533-2550.
<https://doi.org/10.1016/j.ajpath.2011.07.044>
- Wang, J., Huang, Q., Chen, X., You, Z., He, K., Guo, Q., Huang, Y., Yang, Y., Lin, Z., Guo, T., Zhao, J., Guan, Y., Li, B., & Xie, F. (2024, Apr 8). Tau pathology is associated with synaptic density and longitudinal synaptic loss in Alzheimer's disease. *Mol Psychiatry*.
<https://doi.org/10.1038/s41380-024-02501-z>
- Wang, Y., & Mandelkow, E. (2016). Tau in physiology and pathology. *Nature reviews neuroscience*, 17(1), 22-35.
- Ward, S. M., Himmelstein, D. S., Lancia, J. K., Fu, Y., Patterson, K. R., & Binder, L. I. (2013). TOC1: characterization of a selective oligomeric tau antibody. *J Alzheimers Dis*, 37(3), 593-602. <https://doi.org/10.3233/JAD-131235>
- Weingarten, M. D., Lockwood, A. H., Hwo, S. Y., & Kirschner, M. W. (1975, May). A protein factor essential for microtubule assembly. *Proc Natl Acad Sci U S A*, 72(5), 1858-1862.
<https://doi.org/10.1073/pnas.72.5.1858>
- Weissmann, C., Reyher, H. J., Gauthier, A., Steinhoff, H. J., Junge, W., & Brandt, R. (2009, Nov). Microtubule binding and trapping at the tip of neurites regulate tau motion in living neurons. *Traffic*, 10(11), 1655-1668. <https://doi.org/10.1111/j.1600-0854.2009.00977.x>

- Whitehouse, P. J., Price, D. L., Clark, A. W., Coyle, J. T., & DeLong, M. R. (1981, Aug). Alzheimer disease: evidence for selective loss of cholinergic neurons in the nucleus basalis. *Ann Neurol*, *10*(2), 122-126. <https://doi.org/10.1002/ana.410100203>
- Witman, G. B., Cleveland, D. W., Weingarten, M. D., & Kirschner, M. W. (1976, Nov). Tubulin requires tau for growth onto microtubule initiating sites. *Proc Natl Acad Sci U S A*, *73*(11), 4070-4074. <https://doi.org/10.1073/pnas.73.11.4070>
- Wszolek, Z. K., Tsuboi, Y., Ghetti, B., Pickering-Brown, S., Baba, Y., & Cheshire, W. P. (2006, 2006/08/09). Frontotemporal dementia and parkinsonism linked to chromosome 17 (FTDP-17). *Orphanet Journal of Rare Diseases*, *1*(1), 30. <https://doi.org/10.1186/1750-1172-1-30>
- Wu, H. Y., Hudry, E., Hashimoto, T., Kuchibhotla, K., Rozkalne, A., Fan, Z., Spires-Jones, T., Xie, H., Arbel-Ornath, M., Grosskreutz, C. L., Bacskai, B. J., & Hyman, B. T. (2010, Feb 17). Amyloid beta induces the morphological neurodegenerative triad of spine loss, dendritic simplification, and neuritic dystrophies through calcineurin activation. *J Neurosci*, *30*(7), 2636-2649. <https://doi.org/10.1523/JNEUROSCI.4456-09.2010>
- Wu, J. W., Herman, M., Liu, L., Simoes, S., Acker, C. M., Figueroa, H., Steinberg, J. I., Margittai, M., Kaye, R., Zurzolo, C., Di Paolo, G., & Duff, K. E. (2013, Jan 18). Small misfolded Tau species are internalized via bulk endocytosis and anterogradely and retrogradely transported in neurons. *J Biol Chem*, *288*(3), 1856-1870. <https://doi.org/10.1074/jbc.M112.394528>
- Yamada, K., Holth, J. K., Liao, F., Stewart, F. R., Mahan, T. E., Jiang, H., Cirrito, J. R., Patel, T. K., Hochgrafe, K., Mandelkow, E. M., & Holtzman, D. M. (2014, Mar 10). Neuronal activity regulates extracellular tau in vivo. *J Exp Med*, *211*(3), 387-393. <https://doi.org/10.1084/jem.20131685>
- Yoshiyama, Y., Higuchi, M., Zhang, B., Huang, S. M., Iwata, N., Saido, T. C., Maeda, J., Suhara, T., Trojanowski, J. Q., & Lee, V. M. (2007, Feb 1). Synapse loss and microglial activation precede tangles in a P301S tauopathy mouse model. *Neuron*, *53*(3), 337-351. <https://doi.org/10.1016/j.neuron.2007.01.010>
- Zareba-Paslawska, J., Patra, K., Kluzer, L., Revesz, T., & Svenningsson, P. (2020). Tau Isoform-Driven CBD Pathology Transmission in Oligodendrocytes in Humanized Tau Mice. *Front Neurol*, *11*, 589471. <https://doi.org/10.3389/fneur.2020.589471>
- Zhang, Y. W., Thompson, R., Zhang, H., & Xu, H. (2011, Jan 7). APP processing in Alzheimer's disease. *Mol Brain*, *4*, 3. <https://doi.org/10.1186/1756-6606-4-3>
- Zhao, J., Wu, H., & Tang, X. Q. (2021, May). Tau internalization: A complex step in tau propagation. *Ageing Res Rev*, *67*, 101272. <https://doi.org/10.1016/j.arr.2021.101272>

CHAPTER 2

Alzheimer's disease brain-derived tau seeds the formation of pathology in human tau knock-in mouse primary hippocampal neurons

ABSTRACT

The pathological accumulation of pathological tau is a hallmark of Alzheimer's disease (AD). Tau pathology accumulates throughout the brain in a stereotypical spatiotemporal pattern that is associated with cognitive decline. The tau seeding hypothesis offers a potential mechanism by which tau spreads. Tau is capable of seeding tau *in vitro* and *in vivo*, though less is known about the specific pathological tau species that are formed, and the consequences of tau aggregation on neuron viability. I addressed this gap by developing a relatively novel seeding model in MAPT-KI mouse primary hippocampal cultures and characterizing the seeded tau inclusions with antibodies specific to several known AD-associated tau modifications. I show that treating MAPT-KI primary cultures with AD brain-derived insoluble tau results in the progressive formation of intraneuronal tau inclusions. The tau inclusions exhibited several markers of pathogenic pre-tangle forms of tau, including PAD-exposure, oligomeric species, and phosphorylation at multiple AD-associated phosphoepitopes (i.e. AT8, PHF1, and pS422). Despite the extensive formation of tau pathology, no overt cell death or decrease in culture viability was observed. This is consistent with the majority of seeding models. Thus, this may represent a modeling approach to study the consequences (i.e., axonal and synaptic dysfunction and degeneration) of early forms of tau pathology that precede overt neurodegeneration.

INTRODUCTION

The microtubule-associated protein tau is encoded by the *MAPT* gene and expressed as six isoforms in the adult central nervous system. Alternative splicing of exon 10 in the microtubule

binding domain results in isoforms containing three or four microtubule binding repeats (3R and 4R isoforms), and alternative splicing of exons 2 and 3 in the N-terminus results in 0N, 1N, or 2N isoforms (Wang & Mandelkow, 2016). The progressive accumulation of pathological tau is a hallmark of Alzheimer's disease (AD). Intracellular neurofibrillary tangles (NFT), neuropil threads (NT), and neuritic plaques in AD are comprised of tau paired helical filaments and straight filaments containing 3R and 4R isoforms (Crowther, 1991; Fitzpatrick et al., 2017). Tau pathology accumulates throughout the brain in a stereotypical pattern, described by post-mortem Braak staging (I-VI), that correlates with cognitive decline (Braak et al., 2006; Braak & Braak, 1991; Braak et al., 2011). In early (asymptomatic) AD (Braak I-II), NFTs and NTs are restricted to the transentorhinal and entorhinal cortex. Tau accumulation continues into the hippocampus and other limbic structures (Braak III-IV), and these stages correspond with mild cognitive impairment. In late-stage AD (Braak V-VI), tau pathology is observed throughout most of the neocortex, and these stages are associated with severe cognitive impairment. Tau pathology can propagate between cells through a mechanism known as tau seeding. The tau seeding hypothesis posits that pathological tau released from a neuron is taken up by a functionally connected neuron where it acts as a template to convert normal monomeric tau into pathological tau (Gibbons et al., 2019).

Pioneering work by the Diamond and Lee groups (among others) showed that tau is capable of seeding aggregation *in vitro* and *in vivo*, respectively (Clavaguera et al., 2009; Frost et al., 2009; Guo & Lee, 2011; Guo et al., 2016; Iba et al., 2015). Wild-type and hTau mouse (overexpressing human tau isoforms) primary neurons treated with human AD brain-derived pathological tau (AD-tau) show the recruitment of endogenous tau into pathological tau (Guo et al., 2016; He et al., 2020). Injection of AD-tau into the hippocampus and overlying cortex of wild-type and hTau mice show the propagation of tau pathology along functionally connected regions ("2024 Alzheimer's

disease facts and figures," 2024; Guo et al., 2016; He et al., 2020; Narasimhan et al., 2017; Narasimhan & Lee, 2017). While several groups found evidence of tau seeding, less is known about the specific pathological species that are formed in seeded neurons, and the effect of pathological tau species on neuron viability.

Most tau seeding studies (*in vitro* and *in vivo*) only used the AT8 phospho-tau antibody to show that pathological tau was seeded. The AT8 phospho-tau antibody labels tau that is phosphorylated between S198 – S210 (Biernat et al., 1992; Goedert et al., 1995; Malia et al., 2016) and is used in the Braak staging of human tissue as it labels early pre-tangle and tangle pathologies well (Braak et al., 2006; Braak et al., 2011). AT8 is used extensively throughout the seeding literature and this form of tau is linked to pathogenic tau mechanisms (Christensen et al., 2023; Kanaan et al., 2011). There are several known AD-associated tau modifications in addition to AT8 that are identifiable with modification-specific antibodies. Furthermore, several of these specific tau modifications are linked with functional deficits. For example, aberrant exposure of the phosphatase activating domain (PAD) at the far N-terminal impairs axon transport in the squid axoplasm and in murine primary neurons (Christensen et al., 2023; Combs et al., 2021; Combs et al., 2019; Cox et al., 2016; Kanaan et al., 2012; Kanaan et al., 2011; LaPointe et al., 2009; Tiernan et al., 2016). Tau N-Terminal 1 (TNT1) is a conformation-specific antibody that binds to PAD-exposed tau (Combs et al., 2016; Kanaan et al., 2011). Tau Oligomeric Complex 1 (TOC1) is a conformation-specific antibody specific to tau oligomers that was raised against tau dimers and recognizes oligomeric tau (Patterson et al., 2011; Ward et al., 2013). Another antibody for phospho-tau that is used frequently in the AD field is PHF1, which labels phosphorylated S396/S404 tau proteins (Greenberg et al., 1992; Otvos Jr et al., 1994). A third phospho-specific tau antibody is pS422, and immunoreactivity with this antibody occurs in human tissue from AD

and other tauopathies (Guillozet-Bongaarts et al., 2006; Kimura et al., 1996; Tiernan et al., 2016; Vana et al., 2011). Importantly, AT8, pS422, and TOC1 are well-characterized markers of pre-tangle neurons (i.e. one of the earliest phases of pathological tau deposition in humans), and each antibody co-localizes with TNT1 (Christensen et al., 2019; Cox et al., 2016; Guillozet-Bongaarts et al., 2006; Kanaan et al., 2016; Kanaan et al., 2011; Tiernan et al., 2016). Furthermore, each of these modifications (except PHF1) was linked to axon transport dysfunction through PAD-exposure (Christensen et al., 2023; Combs et al., 2021; Combs et al., 2019; Cox et al., 2016; Kanaan et al., 2012; Kanaan et al., 2011; LaPointe et al., 2009; Morfini et al., 2009; Tiernan et al., 2016).

Some modifications occur later in the evolution of tangle formation. Truncation of tau at D421 and E391 are intermediate and late-stage events in tangle formation, respectively (Guillozet-Bongaarts et al., 2005). The TauC3 antibody recognizes truncated tau at D421 by caspase 3 and the MN423 antibody is specific to tau truncated at E391 (Gamblin et al., 2003; Guillozet-Bongaarts et al., 2005; Harrington et al., 1991; Novak et al., 1989). TauC3 and MN423 immunoreactivity is observed in human AD tissue (Guillozet-Bongaarts et al., 2005; Patterson et al., 2011; Tiernan, Ginsberg, et al., 2018; Tiernan, Mufson, et al., 2018; Vana et al., 2011). As opposed to tau monomers or amorphous oligomers or aggregates, tau filaments which ultimately comprise neurofibrillary tangles have cross β -sheet structure, and these can be identified using the β -sheet dyes such as thiazine red (ThR) (Combs et al., 2016; Luna-Munoz et al., 2008; Luna-Viramontes et al., 2020).

Here, I developed a tau seeding model in human tau knock-in mouse (MAPT-KI) primary hippocampal cell cultures. The entire mouse *MAPT* gene was replaced with human *MAPT* in these mice (Saito et al., 2019). Unlike hTau mice which overexpress human tau, MAPT-KI mice express

tau at normal levels. Adult MAPT-KI mice express all six human tau isoforms (Benskey et al., 2023; Saito et al., 2019). I treated MAPT-KI primary hippocampal cultures with AD-tau and show the progressive formation of intraneuronal tau inclusions associated with the early phases of tau pathology evolution in human disease. I identified the robust formation of PAD-exposed tau inclusions, thereby linking tau seeding with a tau conformation shown to impair axon and synaptic function (Mueller et al., 2021). Tau seeding does not result in cell death or overt toxicity. This model may provide a useful tool for identifying the effects of early pathological tau species on neurons that precede overt cell death (i.e. axon and synaptic dysfunction).

METHODS

Animals

Breeding pairs of human MAPT knock-in (MAPT-KI; (Saito et al., 2019)) mice were obtained from Dr. Karen Duff at Columbia University with permission from the Saito group at the Riken Center for Brain Science. These mice were used to generate an in-house colony. In these mice, murine *MAPT* was replaced with human MAPT (Saito et al., 2019) and adult MAPT-KI mice express all six human tau isoforms (Benskey et al., 2023; Saito et al., 2019). Tau knockout mice (Tau-KO; B6.129X1-Mapttm1Hnd/J; Jackson Labs, 007251) were bred in-house and used for control experiments. All mice were housed in 12h light/dark conditions with food and water provided *ad libitum*. Embryonic day 16 (E16) or E18 MAPT-KI or Tau-KO mice were used for primary neuron experiments, respectively. Timed-pregnant MAPT-KI or Tau-KO females were used to obtain fetal tissue; E0 refers to the day the vaginal plug was found. On the day of primary neuron harvest, pregnant females were euthanized by sodium pentobarbital overdose (at least 100 mg/kg) administered via intraperitoneal injection. All studies were conducted in compliance with

federal, state, and institutional guidelines and with the approval of Michigan State University's Institutional Animal Care and Use Committee.

AD-tau purification from human frontal cortex

Sarkosyl-insoluble tau was purified from human AD brain frontal cortical tissue obtained from the University of Michigan Brain Bank according to methods adapted from Narasimhan and Lee (Narasimhan & Lee, 2017). Briefly, tissue from six individuals who had AD, Braak stage V-VI, was pooled (3.5-4.5 g total). Concurrently, the same amount of frontal cortical tissue from five or six age-matched cognitively unimpaired individuals, Braak stage I-II, was pooled and used as a control throughout experiments (Con). Tissue was homogenized using a glass Dounce homogenizer in 9 volumes of ice-cold high-salt extraction buffer (10 mM Tris, pH 7.4, 10% sucrose, 0.8 M NaCl, 1 mM EDTA, 0.1% sarkosyl) supplemented on the day of use with protease (2 µg/mL pepstatin, 2 µg/mL bestatin, 2 µg/mL leupeptin, 4 mM phenylmethylsulfonyl fluoride, 10 µg/mL aprotinin) and phosphatase inhibitors (1 mM tetra-sodium pyrophosphate decahydrate, 10 mM β-glycerophosphate, 1 mM sodium orthovanadate, 1 M sodium fluoride). The homogenate was transferred to 50 mL conical tubes and centrifuged at 10,000 x g(max) for 10 min at 4 °C in a F14-14 x 50cy fixed angle rotor (Thermo Scientific, 096-145075) and Sorvall LYNX 4000 Superspeed centrifuge (Thermo Scientific, 75006581). The supernatant was filtered through a KimWipe into a 50 mL conical tube. The pellet was homogenized and centrifuged as above. The 2nd supernatant was filtered as above. This process was repeated one more time. The three supernatants were pooled into a glass beaker, the concentration of sarkosyl was increased to 1%, and the mixture was stirred with a stir bar on a stir plate for 1.5 h at room temperature. The suspension was transferred to 36 mL ultracentrifuge tubes (Beckman Coulter 355618) and centrifuged at 300,000 x g(max) at 4 °C for 60 min in a T-865 fixed angle rotor (Thermo Scientific,

51411) and Sorvall WX+ Ultra centrifuge (Thermo Fisher, 75000100). The resulting pellet was washed with 1X Dulbecco's Phosphate Buffered Saline (dPBS; Gibco, 14200-075), broken up with a pipet tip, transferred to a new 36 mL tube which was then filled with dPBS, and centrifuged at 250,000 x g(max) at 4 °C for 30 min in a T-865 8 x 36ml rotor and Sorvall WX+ Ultra centrifuge. The resulting pellet was broken up in dPBS (100 µl/g of original tissue, i.e., 450 µl dPBS for 4.5 g) and transferred to a 1.5 mL tube, then incubated on a shaker at room temperature overnight. The next day the pellet was homogenized by passing the suspension through a 21G needle, followed by a 27G needle, and sonicated (20 x 1 sec pulses at power level 1.5; Misonix, XL-2000). The homogenate was transferred to a thickwall 0.5 mL tube (Thermo Scientific, 45235) and centrifuged at 100,000 x g(max) at 4 °C for 30 min in a S120-AT3 14 x 0.5 ml rotor (Thermo Scientific, 45584) and Sorvall MTX Micro-Ultra centrifuge (Thermo Scientific, 46960). The resulting pellet was resuspended in 150 µl – 200 µl dPBS, sonicated (60 x 1 sec pulses at power level 1.5), transferred to a thickwall 0.2 mL tube (Thermo Scientific, 45233) and centrifuged at 10,000 x g(max) for 30 min at 4 °C in a S100-AT3 fixed angle rotor (Thermo Scientific, 45585) and Sorvall MTX Micro-Ultra centrifuge. The resulting supernatant containing the sarkosyl-insoluble tau (or Con proteins) was sonicated (60 x 1 sec pulses at power level 1.5), then aliquoted and stored at -80 °C until use.

Western blotting for seeding material quality control

Total protein concentrations of Con and AD-tau samples were quantified using the Bio-Rad protein assay (Bio-Rad, 5000006) as directed. Samples were diluted to 2 µg in TBS, then heated with Laemmli sample buffer (final 1X composition: 20 mM Tris, pH 6.8, 2% SDS, 6% glycerol, 1% β-mercaptoethanol, 0.002% Bromophenol Blue) at 95 °C for 5 min. Samples were loaded onto an 18-well 10% Criterion TGX Precast Midi Protein Gel (Bio-Rad 5671034) alongside 5 µl of a human tau ladder containing all six isoforms (25 ng of each isoform; rPeptide, T-1007-2) and 2 µl

All Blue Precision Plus Protein Standards (Bio-Rad, 161-0373), then run at 250V for 32 min. Proteins were transferred onto nitrocellulose membranes (Pall Life Sciences, Port Washington, NY, #66593) using a Bio-Rad transfer unit at 400 mA for 50 min. Membranes were blocked with 2% Non-Fat Dry Milk (NFD) for 1 h. Then, membranes were incubated with primary antibodies overnight at 4 °C. One membrane was incubated with 4R tau antibody (1:2000; rabbit polyclonal; CosmoBio, TIP-4RT-P01) and 3R tau antibody (1:1000; mouse IgG1; Millipore, 05-803). A second membrane was incubated with PHF1 antibody (1:50,000; mouse IgG1; Kanaan Lab; (Greenberg et al., 1992)) and R1 antibody (1:100,000; rabbit polyclonal; Kanaan Lab; (Berry et al., 2004)). Membranes were washed with TBS/0.1% Tween 20 (TBST) 3 x 5 min, then incubated with secondary antibodies (all 1:20,000) in 2% NFD for 1 h. Both membranes were incubated with IRDye 680LT goat anti-mouse IgG1 (LiCor, 926-68050) and IRDye 800CW goat anti-rabbit (LiCor, 926-32211). Membranes were washed 3 x 5 min in TBST then imaged using a Li-Cor Odyssey infrared imaging system with Li-Cor ImageStudioLite 5.2 software.

Recombinant tau proteins

Recombinant hT40 and hT39 (2N4R and 2N3R, respectively) with 6 x histidine C-terminal tags were made as previously described (Combs et al., 2017). Briefly, DNA plasmids, pT7C hT40 C-His or pT7C hT39 C-His, were transformed into T7 Express Competent *E. coli* cells (New England Biosciences, Ipswich, MA, C2566). Cells were grown in Luria broth and IPTG was used to induce expression of the plasmid DNA. Cells were pelleted, then lysed, and tau was purified through a sequence of heavy metal affinity, size exclusion, and anion exchange chromatography steps using an AKTA fast protein liquid chromatography system. First, the majority of non-target proteins were eliminated using a HiTrap TALON crude column (Cytiva, 28953767) that binds the polyhistidine tag on tau. Next, I used a HiPrep 16/60 Sephacryl S500 HR size exclusion column

(Cytiva, 28935606) to further purify tau proteins. Finally, I used a HiTrap Q HP anion exchange column (Cytiva, 17115401) to separate tau from fractions containing DnaK protein, a bacterial Hsp70 homologue that coelutes with recombinant tau from bacteria. Tau was concentrated within the range of 1.5 – 5 mg/mL and 1 mM of dithiothreitol (DTT) was added to reduce disulfide bonds. Single use aliquots were stored at -80 °C until use.

Arachidonic acid-induced tau aggregation in vitro

Recombinant hT40 and hT39 monomer and aggregate samples were made as previously described (Combs et al., 2017) for use as standard curves in sandwich enzyme-linked immunosorbent assays (sELISAs). Briefly, stocks of 250 mM DTT, 1 M NaCl, 250 mM HEPES (pH7.6) and 1 mM EDTA were diluted in filtered ultrapure water to 5 mM DTT, 100 mM NaCl, 10 mM HEPES and 0.1 mM EDTA (adding each reagent in that order). Next, tau was added to a final concentration of 4 μ M. An arachidonic acid stock was made immediately prior to use by diluting arachidonic acid (peroxide-free, Cayman Chemicals, Ann Arbor, MI 90010.1) to 2 mM in 100% ethanol (Sigma, 459836-100ML). Arachidonic acid was added to the tau reaction to a final concentration of 150 μ M. Ethanol vehicle alone was added to the monomer reactions. Reactions were rocked gently by hand to mix. Tau monomers were immediately aliquoted and frozen at -80 °C and the aggregation reactions were allowed to proceed overnight at room temperature. Aggregate reactions were aliquoted and stored at -80 °C.

Sandwich enzyme-linked immunosorbent assays (sELISAs)

High-binding capacity 96-well plates (Corning, 3590) were coated with 50 μ l/well of capture antibody (2 ng/ μ L) in borate saline buffer (100 mM boric acid, 25 mM sodium tetraborate decahydrate, 75 mM NaCl, 250 μ M thimerosal) for 1 h. The capture antibodies used were Tau5 (mouse IgM; Kanaan Lab; (Carmel et al., 1996; LoPresti et al., 1995)), TNT1 (mouse IgG1;

Kanaan Lab; (Combs et al., 2016; Kanaan et al., 2011)), or TOC1 (mouse IgM; Kanaan Lab; (Patterson et al., 2011; Ward et al., 2013)). Plates were washed 2x with 200 μ l/well of ELISA wash solution (100 mM boric acid, 25 mM sodium tetraborate decahydrate, 75 mM NaCl, 250 μ M thimerosal, 0.4% BSA and 0.1% tween-20, pH 9.0) then blocked with 200 μ l/well of 5% non-fat dry milk made in ELISA wash solution for 1 h. Plates were washed twice, then 50 μ l/well of each sample was applied to the plate for 1.5 h. For total tau quantification, standard curves using hT40 and hT39 monomers were prepared in TBS (80 nM – 0.0625 nM; 1:2 dilution). AD-tau and Con samples were diluted 1:2500 and 1:5000, and additional Con samples were prepared at 1:250 and 1:500 in TBS. For identification of pathological tau species, hT40 monomers and aggregates were serially diluted 1:4 from 80 nM to 0.001 nM (Tau5 and TNT1) or from 200 nM – 0.003 nM (TOC1). AD-tau and Con samples were diluted as above.

For cell lysate experiments, hT40 monomers and aggregates were diluted 1:4 from 85.7 nM – 0.002 nM (Tau5 and TNT1) or from 214.26 nM – 0.007 nM (TOC1). Lysates were adjusted to 20 μ g in TBS. Plates were washed 4x, then incubated with 50 μ l/well of detection antibody (R1; 1:5,000) in blocking buffer for 1.5 h. Plates were washed 4x and then incubated for 1 hr in 50 μ l/well secondary antibody Goat anti-rabbit HRP diluted 1:5,000 for AD-tau and Con experiments or 1:10,000 for cell lysate experiments in blocking buffer. Plates were washed 4x and reactivity was detected by adding 50 μ l/well of 3,3',5,5' tetramethylbenzidine substrate (Sigma, T0440). The reactions were quenched with 50 μ l/well of 3.6% H₂SO₄ and absorbance was read at 450 nm. Absorbance data (an inverse log scale measure) were converted to percent light absorbed (a linear scale conversion) using the following equation %Absorbance = (1 – 10^{-x})*100, where x is absorbance.

Tau RD P301S cell seeding assay

RD Biosensor Cells (Tau RD P301S FRET Biosensor cells; ATCC, CRL-3275) were plated in a poly-D-lysine-coated 96-well plate (Corning, 354461) at a density of 12,000 cells/well in 100 μ l/well of RD media [DMEM (Gibco, 11995-065), 10% FBS, 1% Pen/Strep (Gibco, 15140-122), 1X GlutaMAX (Gibco, 35050-061)]. The next day, cells were treated with PBS, Con or AD-tau delivered via lipofection. Each treatment (PBS, Con or AD-tau) was diluted in OptiMEM (Gibco, 31985-062). In parallel, Lipofectamine 2000 (ThermoFisher Scientific, 11668019) was diluted in OptiMEM to 28 nM AD-tau and Con matched to AD-tau for total protein amount. After 20 min, the treatment and Lipofectamine reagents were combined for an additional 20 min. Next, the Lipo/Treatment mixtures were added to the cells (20 μ l/well). After 48 hours, cells were fixed with 37 °C pre-warmed 4% paraformaldehyde in cytoskeleton buffer (10 mM MES, 138 mM KCl, 3 mM MgCl₂, and 4 mM EGTA, pH 6.1) for 20 min, then washed 3 x 5 min with TBS. DAPI (0.5 μ g/mL) was added to the first wash.

Transmission electron microscopy (TEM)

Samples were incubated on 300 mesh Formvar carbon coated copper grids (Electron Microscopy Sciences, 215-412-8400) for 1 min. Grids were washed 1x with ultrapure water, 1x with 2% uranyl acetate, and negatively stained with 2% uranyl acetate for 1 min. Grids were imaged using a JEOL JEM-1400 Plus electron microscope at 80 kV equipped with an AMT XR81 digital camera and AMT software version 602.6 (Advanced Microscopy Techniques).

Primary Neurons

Glass-bottom 18-well chamber slides (Ibidi, 81817) were coated with 0.5 mg/mL poly-D-lysine (Sigma, P7886-100MG) in borate buffer [12.5 mM sodium borate decahydrate (VWR, MK745706) and 50 mM boric acid (Sigma, B6768-1KG)] overnight at room temperature, then

washed 4x with sterile deionized water. Embryonic day 16 or 18 pups were obtained from timed pregnant MAPT-KI mice or Tau-KO mice, respectively. Primary neurons were harvested and dissociated as described previously (Mueller et al., 2023). Briefly, hippocampi were dissected and transferred to ice-cold calcium and magnesium-free buffer [CMF; 1X Dulbecco's PBS (Gibco, 14200-075), 0.1% glucose (Sigma, G7528), 2.5 µg/mL Amphotericin B (Gibco, 15290-026), and 50 µg/mL Gentamicin (Gibco, 15710-072)]. Next, the tissue was washed 4x with 5 mL of cold CMF, then incubated with warm 0.125% trypsin (Gibco, 15090-046) in CMF for 15 min at 37 °C. The cells were washed 2x with cold CMF, then digestion was halted by adding 3 mL of trypsin inactivation solution [Hank's Balanced Salt Solution (Gibco, 24020-117), 20% Newborn Calf Serum (Gibco, 16010-167) and 1X DNase I solution (10X stock: 5 mM sodium acetate (Sigma S5636), 1 µM calcium chloride (Sigma, C7902), 0.5 mg/mL DNaseI (Fisher, NC9185812)]. The cells were triturated using a 3 mL syringe with progressively smaller diameter needles: 30x with a 14G needle, 30x with a 15G needle, 20x with a 16G needle, 20x with an 18G needle, and 15x with a 21G needle. The single-cell suspension was layered on fetal bovine serum (FBS; Invitrogen, 16000044) and centrifuged at 200 x g for 5 min at 4 °C. The FBS was removed and the cells were resuspended in 1 mL of warm Neurobasal Media Plus (Gibco, A3582901) supplemented with 2% B27 Plus (Gibco, A3582801), and 1% GlutaMAX (Gibco, 35050061), with antibiotics: 2.5 µg/mL Amphotericin B and 50 µg/mL Gentamicin. Cells were plated in NBM Plus media: 25,000 cells/well in 100 µl/well for 18-well chamber slides and poly-D-lysine coated 96-well plates (Corning, 354461), or 150,000 cells/well in 500 µl/well for poly-D-lysine coated 24-well plates (Fisher, 08-774-124). Cells were maintained in a humidity-controlled incubator at 37 °C, and 5% CO₂. Fresh NBM Plus was added to cells every other day: 5 µl (18-well chamber slides and 96-well plates) or 75 µl (24-well plates) per well.

Treatment of primary hippocampal cultures

Primary hippocampal cultures were treated on DIV5 with 28 nM of AD-tau (based on the tau concentration determined by total tau sandwich ELISA), Con (matched to the total protein concentration of the AD-tau samples), or dPBS. Treatments were prepared in fresh NBM Plus media and prewarmed to 37 °C. The treatments were mixed briefly by vortex immediately before addition to cells. The treatments were added directly to the cell culture media in a spiral pattern, then the culture plate or slide was gently rocked to mix, and returned to the incubator.

MAPT-KI seeding time course assay

Primary neurons were plated in poly-d-lysine coated 96-well plates at a density of 25,000 cells/well. The cultures were treated with PBS, Con, or AD-tau on DIV5. at 9d, 17d, or 26d post-treatment (corresponding to DIV14, 22, or 31). Cells were fixed with ice-cold methanol at 20 °C to remove soluble tau. ICF was performed using TNT1 and Tuj1 antibodies as described in the ICF section below. Cells were imaged using a Lionheart FX Automated Microscope (BioTek Instruments) and analyzed by Gen5 Software. Twelve images per well were captured at 10x magnification with DAPI (ex 377/em 447), GFP (ex 469/em 525) and RFP (ex 531/em 685) filter cubes. Pixel intensity and size thresholds were applied to the GFP and RFP channels to detect Tuj1+ axonal area (GFP) and TNT1+ seeded aggregates (RFP). The number of RFP objects (tau inclusions) was normalized to axonal surface area (Tuj1).

Western blotting of primary neuron lysates

Cells were collected in cell lysis buffer (20 mM Tris, 0.5 mM DTT, 150 mM NaCl, 0.5% Triton X-100, 2 µg/mL pepstatin, 2 µg/mL bestatin, 2 µg/mL leupeptin, 4 mM phenylmethylsulfonyl fluoride, 10 µg/mL aprotinin, 1 mM tetra-sodium pyrophosphate decahydrate, 10 mM β-glycerophosphate, 1 mM sodium orthovanadate, 1 M sodium fluoride, pH7.5). Phosphatase

inhibitors were excluded from the lysis buffer for the tau isoform experiments. Lysates were sonicated and total protein was quantified using the Bio-Rad protein assay (Bio-Rad, 5000006) as directed. For the tau isoform blots, 27.5 μ L of each lysate (~18-46 μ g; collected on DIV 5, 14, 22 or 31) were combined with fresh protease inhibitors were added as above and the samples were dephosphorylated in the presence of FastAP Thermosensitive Alkaline Phosphatase (1:5; Thermo Scientific, EF0652) at 37 °C for 3 h. Then, lysates were heated with Laemmli sample buffer (final 1X composition: 20 mM Tris, pH 6.8, 2% SDS, 6% glycerol, 1% β -mercaptoethanol, 0.002% Bromophenol Blue) at 95°C for 5 min. Samples were loaded onto 12-well 10% Tris-Glycine Plus Midi Gels (Invitrogen, WXP01012BOX) alongside 1.75 μ l of All Blue Precision Plus Protein Standards and 3 μ l of human tau ladder at 250V for 40 min.

For the neuron and astrocyte protein expression blots, 15 μ g/lane of each lysate (collected 26d post-treatment; DIV31) were heated with sample buffer at 95°C for 5 min, then run on a 26-well Criterion TGX Precast 4-20% gel (Bio-Rad, 567-1095) at 250V for 32 min. Proteins were transferred onto nitrocellulose membranes (Pall Life Sciences, Port Washington, NY, #66593) using a Bio-Rad transfer unit at 400 mA for 50 min. Membranes were blocked in 2% Non-Fat Dry Milk (NFDM) for 1 hour. Then, membranes were probed with primary antibodies overnight at 4 °C. For the tau isoform blots, membranes were incubated with Tau12 antibody (1:200,000; mouse IgG1; Kanaan Lab; (Combs et al., 2016; Horowitz et al., 2006)) and Tuj1 β -III tubulin antibody (1:10,000; mouse IgG2a; (Caccamo et al., 1989)). For the neuron and astrocyte protein expression blot, the membrane was cut just above the 37 kDa marker and the top portion was incubated with Tuj1 antibody (1:10,000) and glial fibrillary acidic protein (GFAP, 1:1000; rabbit; DAKO Z0334), and the bottom portion was incubated with GAPDH antibody (1:2,000; rabbit; Cell Signaling Technology, 5174). Membranes were washed with TBS/0.1% TWEEN 20 (TBST) 3 x 5 min, then

incubated with secondary antibodies (1:20,000) in 2% NFDM for 1h. For the tau isoform blots, membranes were incubated with IRDye 680LT goat anti-mouse IgG1 (LiCor, 926-68050) and IRDye 800CW goat anti-mouse IgG2a (LiCor, 926-32351). For the neuron and astrocyte protein expression blot, the top portion of the membrane was incubated with IRDye 800CW goat anti-mouse IgG2a and IRDye 680LT goat anti-rabbit (LiCor, 926-68021) and the bottom portion of the membrane was incubated with IRDye 680LT goat anti-rabbit. Membranes were washed 3 x 5 min in TBST then imaged using a Li-Cor Odyssey infrared imaging system. Li-Cor ImageStudioLite 5.2 Software was used to quantify the signal intensity of the bands. Signal intensities for GFAP and Tuj1 bands were normalized to GAPDH.

Immunocytofluorescence (ICF)

Cells were fixed (on DIV21 unless otherwise stated) with warm 4% paraformaldehyde in cytoskeleton buffer (10 mM 2-(N-morpholino)ethanesulfonic acid, 138 mM KCl, 3 mM MgCl₂, and 4 mM EGTA, pH 6.1) for 20 min at room temperature then washed 3 x 5 min with TBS (500 mM Tris, 150 mM NaCl pH 7.4). Cells were incubated with blocking buffer (5% goat serum, 1% BSA, 0.2% Triton-X in TBS) for 1 h. Then, cells were incubated with primary antibodies in 2% goat serum-TBS (GS-TBS) overnight at 4°C. Cells were washed 3 x 5 min with TBS, then incubated with secondary antibodies (all 1:500 in 2% GS-TBS) for 1 h. Cells were washed 3 x 5 min with TBS. When DAPI was included, it was added to the first wash (1:10,000; Thermo, D1306).

The following combinations of primary and secondary antibodies were used. All secondaries were from purchased from Thermo.

1) AP14 microtubule associated protein 2 (MAP2) antibody (1:10,000; mouse IgG1; Kanaan Lab; (Binder et al., 1986; Caceres et al., 1984; Kalcheva et al., 1994; Tucker et al., 1988)) + GFAP

antibody (1:4,000) + myelin basic protein antibody (MBP; 1:2,000; chicken; Invitrogen, PA1-10008); Alexa Fluor goat anti-mouse IgG1 488 + Alexa Fluor goat anti-rabbit 568, Alexa Fluor goat anti-chicken 647.

2) TNT1 (1:20,000) + Tuj1 (1:5000); Alexa Fluor goat anti-mouse IgG1 568 + Alexa Fluor goat anti-mouse IgG2a 488.

3) TNT1 (1:20,000) + TOC1 (1:1000) + Tuj1 (1:5000); Alexa Fluor goat anti-mouse IgG1 568 + Alexa Fluor goat anti-mouse IgM 647 + Alexa Fluor goat anti-mouse IgG2a 488.

4) TNT1 (1:20,000) + CST MAP2 (1:250) + Tuj1 (1:5,000); Alexa Fluor goat anti-mouse IgG1 568 + Alexa Fluor goat anti-mouse IgG2a 488 + Alexa Fluor goat anti-rabbit 405.

5) TNT (1:40,000) + GFAP (1:4,000); Alexa Fluor goat anti-mouse IgG1 568 + Alexa Fluor goat anti-rabbit 488.

6) Thiazine Red; then TNT1 (1:40,000); Alexa Fluor goat anti-mouse IgG1 488.

7) MAP2 (1:10,000) + GFAP (1:4,000); Alexa Fluor goat anti-mouse IgG1 488 + Alexa Fluor goat anti-rabbit 568.

8) MBP (1,2000); Alexa Fluor goat anti-chicken 488.

Trypsin extraction

To remove extracellular proteins, DIV26 cells were treated with 0.06% trypsin-EDTA for 3 min at room temperature, then immediately fixed with 4% paraformaldehyde in cytoskeleton buffer and washed as above. Cells were then used in ICF studies to help determine whether the tau pathologies were intra- or extracellular.

Dual-IgG1 ICF using Fab fragments and biotinylated antibodies

Fixed cells were incubated with blocking buffer as above. Next, cells were incubated with TNT1 antibody (1:40,000) overnight at 4 °C. Cells were washed 4x 5 min with TBS then incubated with

Alexa Fluor 488 goat anti-mouse IgG (H+L) AffiniPure Fab fragments (sets 1 and 2; 1:500; Jackson ImmunoResearch, 115-547-003) or Alexa Fluor 594 goat anti-mouse IgG (H+L) AffiniPure Fab fragments (set 3; 1:500; Jackson ImmunoResearch, 115-587-003) in 2% GS-TBS for 1 h. Cells were washed 4 x 5 min with TBS then incubated with primary antibodies in 2% GS-TBS for 1 hr. One set was incubated with pS422 antibody (1:1000; rabbit; Abcam, 79415), biotinylated PHF1 antibody (1:100), and Tuj1 antibody (1:5,000). A second set was incubated with biotinylated AT8 antibody (1:100; mouse IgG1-biotin; Thermo Scientific, MN1020B) and Tuj1 antibody (1:5,000). A third set of cells was incubated with biotinylated TauC3 antibody (1:100; mouse IgG1; Kanaan Lab; (Gamblin et al., 2003)) and Tuj1.

Cells were washed 4 x 5 min with TBS then incubated with secondary antibodies in 2% GS-TBS. The first set was incubated with Alexa Fluor goat anti-rabbit 647 (1:500; Thermo Fisher, A21244), Alexa Fluor streptavidin 568 (1:1000; Thermo Fisher, S11226), and DyLight goat anti-mouse IgG2a 405 (1:500; Jackson ImmunoResearch, 115-475-206). The second set was incubated with Alexa Fluor streptavidin 568 (1:1000) and Alexa Fluor goat anti-mouse IgG2a 405 (1:500). Cells were washed 4 x 5 min with TBS. The third set was incubated with Alexa Fluor streptavidin 488 (1:1000) and DyLight goat anti-mouse IgG2a 405 (1:500).

Thiazine Red Staining

Cells were fixed in warm 4% paraformaldehyde in cytoskeleton buffer as above. Prior to ICF, cells were stained with 0.005% Thiazine Red (Sigma, S570435) in 50% EtOH/TBS for 15 min at room temperature. Cells were washed 3 x 1 min with 50% EtOH/TBS, then 3x 5 min with TBS.

Confocal imaging

Images were obtained using a Nikon A1+ laser scanning confocal microscope system equipped with solid-state lasers (405, 488, 561, and 640) and Nikon Elements AR software. All images in

an experiment were acquired at 20x, 40x or 60x magnification using identical acquisition settings (i.e. gain, offset, laser intensity, pinhole size, resolution, scan speed, and step-size for z-stacks). Maximum projections of Z-stack images were used to create figure images. Images were prepared for publication using ImageJ (version 2.14.0/1.54f), Adobe Photoshop (version 25.9.1), and Adobe Illustrator (version 28.5).

CellTiter-Glo Assay

To determine if the formation of pathological tau in the MAPT-KI neurons was toxic to the cells, I used two cell viability assays. First, cell viability was measured using a CellTiter-Glo Assay kit (Promega, G7570). This assay quantifies ATP which is proportional to the number of viable cells.

Cells were plated in a poly-D-lysine coated 96-well plate (Corning, 354461) at 25,000 cells/well in 100 μ l/well of NBM Plus. At 28d post-treatment, ATP was quantified using a CellTiter-Glo Assay kit according to the manufacturer's instructions. CellTiter-Glo reagent was added directly into the cell media at a 1:1 ratio. The reaction was mixed on a shaker at room temperature for 2 min, then developed for 10 min. Then, each reaction was transferred to a solid white well plate and luminescence was recorded using a Promega GloMax plate reader.

ApoTox-Glo Assay

Cell viability, cytotoxicity and caspase-3/7 activity were measured using an ApoTox-Glo Triplex assay kit (Promega, G6320). Two protease substrates, one cell-permeant and one cell-impermeant, are used in this assay. The cell-permeant substrate is cleaved to generate a fluorescent signal proportional to the number of living cells. The cell-impermeant substrate is cleaved by proteases that are released from cells that have lost membrane integrity, this fluorescent signal is proportional to the number of dead cells. After measuring fluorescence, cells were lysed and a luminogenic

caspase-3/7 substrate was added. Luminescence is proportional to the amount of caspase activity present.

Cells were plated in a black walled/clear bottom poly-D-lysine coated 96-well plate (ThermoFisher, 152037) at 25,000 cells/well in 100 μ l/well of NBM Plus. At 26d post-treatment, cell viability, cytotoxicity and caspase activity were measured using an ApoTox-Glo Triplex Assay kit as directed. First, 20 μ l of Viability/Cytotoxicity Reagent was added directly into the cell media and the reaction was mixed on a shaker at room temperature for 30 s, then returned to incubator for 1 h. Fluorescence was measured using a Promega GloMax plate reader with the following filter cubes: 405_{Ex}/495-505_{Em} for viability; 490_{Ex}/510-570_{Em} for cytotoxicity. Then, 100 μ l of Caspase-Glo 3/7 Reagent was added to each well and the plate was mixed for 30 s then incubated at room temperature for 30 min. Then, 180 μ l of each reaction was transferred to a solid white well plate and luminescence was recorded using a Promega GloMax plate reader.

Experimental design and statistical analyses

Each independent experimental replicate (N) represents a single primary cell culture derived from one timed pregnant MAPT-KI or TKO female. Each primary cell culture was generated by pooling the hippocampi from multiple E16 fetuses from a single timed-pregnant female. Experiments that underwent data and statistical analysis each had three treatment groups (PBS, Con, and AD-tau), and each experiment had a sample size of three or more (as indicated in the figure legends). The data were assessed for normality and equal variance assumptions using the Shapiro-Wilk test normality test and the Brown-Forsythe variance test. When both were not met, nonparametric statistical tests were used to analyze the data. Experiments that met the normality and equal variance assumptions were analyzed with a one-way analysis of variance test followed by Tukey's post hoc test when overall significance was achieved. For nonparametric analyses, the Kruskal-

Wallis test was used followed by the Dunn's post hoc test when overall significance was achieved. Significance was defined as $p \leq 0.05$. Data are shown as mean \pm standard deviation for parametric tests or as median \pm interquartile range for nonparametric tests. Analyses were performed using GraphPad Prism 10 software (version 10.2.3).

RESULTS

Primary MAPT-KI culture characterization

The MAPT-KI mice were generated by replacing the entire mouse *MAPT* gene with human *MAPT* (Saito et al., 2019, Benskey et al., 2023). Adult MAPT-KI mice express all six human tau isoforms (Figure 2.1A) (Saito et al., Benskey et al.). Only 3R tau is expressed during development in humans and mice (Takuma et al., 2003; Goedert and Jakes, 1990; Wang and Mandelkow, 2015). The relative expression levels of the six human tau isoforms in MAPT-KI primary neuron cultures was not investigated previously. Here, the expression of each tau isoform in MAPT-KI culture lysates collected on DIV5, 14, 22 and 31 was quantified. Western blots probed with the human-specific total tau antibody, Tau12, showed that the 0N3R tau isoform was the predominant isoform expressed from DIV5-31 and the only isoform detected at DIV5 (Figure 2.1). At DIV14, 22 and 31, the 0N4R, 1N3R, 1N4R, and 2N3R isoforms are detectable on western blot (Figure 2.1). The 2N4R isoform was not detectable on western blot at any of the time points analyzed.

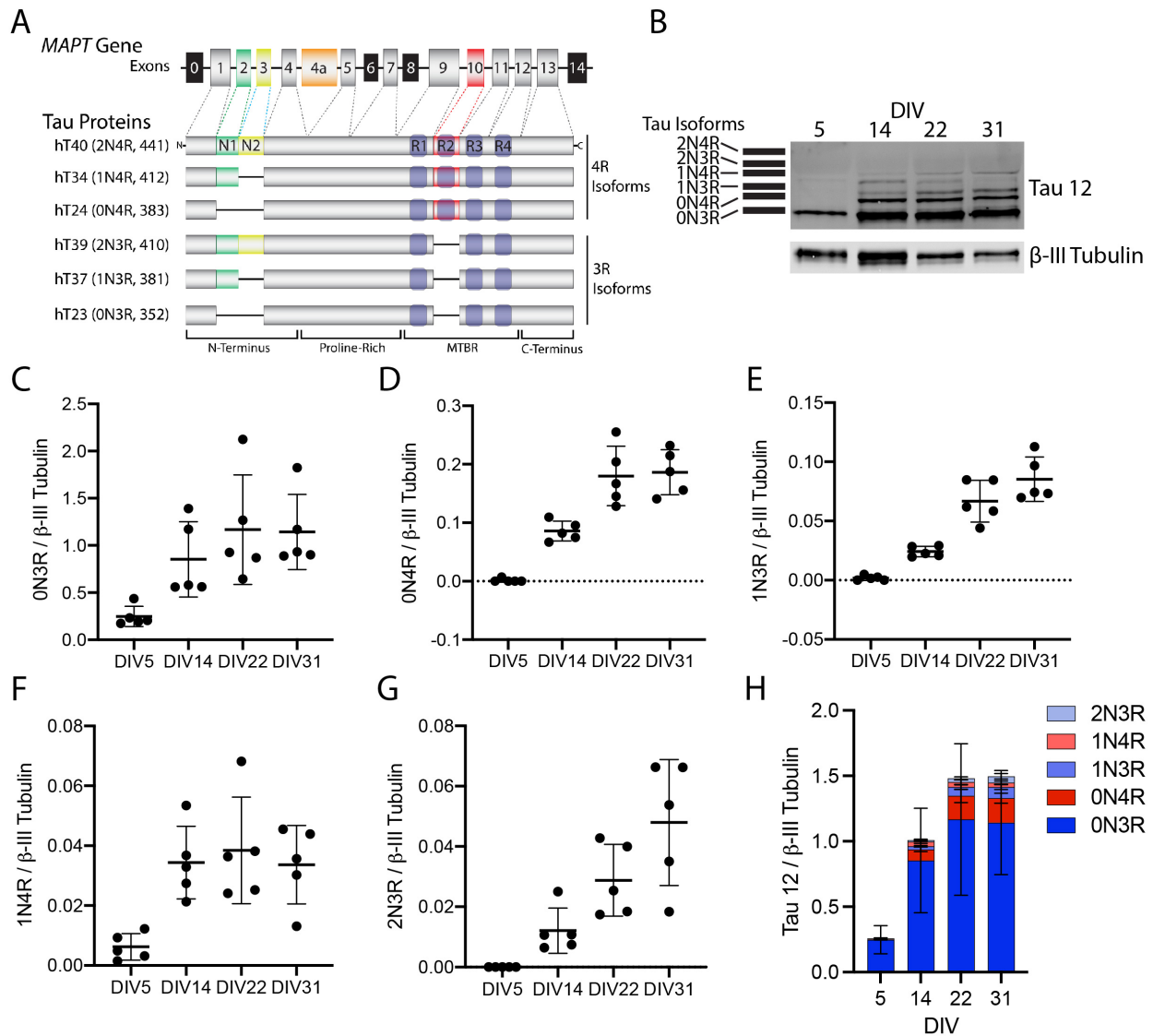


Figure 2.1. Primary hippocampal cultures from MAPT-KI mice express multiple 4R and 3R human tau isoforms. A) The six primary adult CNS human tau isoforms that are expressed in the MAPT-KI mice (murine *MAPT* was replaced with human *MAPT*). B) Representative western blot of MAPT-KI primary hippocampal neuron lysates collected on DIV5, 14, 22, and 31, probed with Tau12 (human tau) and β -III tubulin (Tuj1) antibodies. Note that each isoform, 2N4R, 2N3R, 1N4R, 1N3R, 0N4R and 0N3R positions are shown with a digital ladder. C-G) The intensity of the 2N3R (C), 1N4R (D), 1N3R (E), 0N4R (F) and 0N3R (G) isoform bands were quantified and normalized to β -III tubulin. Note that 2N4R was not detectable.

Figure 2.1 (cont'd).

H) The relative tau isoform expression levels at each time point is displayed in the same graph to demonstrate isoform expression differences. N=5; each individual replicate represents a separate primary neuron harvest from a unique timed pregnant MAPT-KI female.

Immunocytofluorescence was used to characterize the cellular composition of the MAPT-KI cultures. Mature cultures (DIV21) were fixed and immunolabelled with a neuron-specific MAP2 antibody, an astrocyte-specific GFAP antibody, and an oligodendrocyte-specific MBP antibody (Figure 2.2A). Each cell type (labeled within the same well) was manually counted using total enumeration in the images collected. The cultures were composed of ~66% neurons, ~33% astrocytes, and ~1% oligodendrocytes (Figure 2.2B). Taken together, these data show that mature MAPT-KI hippocampal cultures (DIV21 and older) express five of the six human tau isoforms, the cultures are primarily comprised of neurons and astrocytes, with a small oligodendrocyte component.

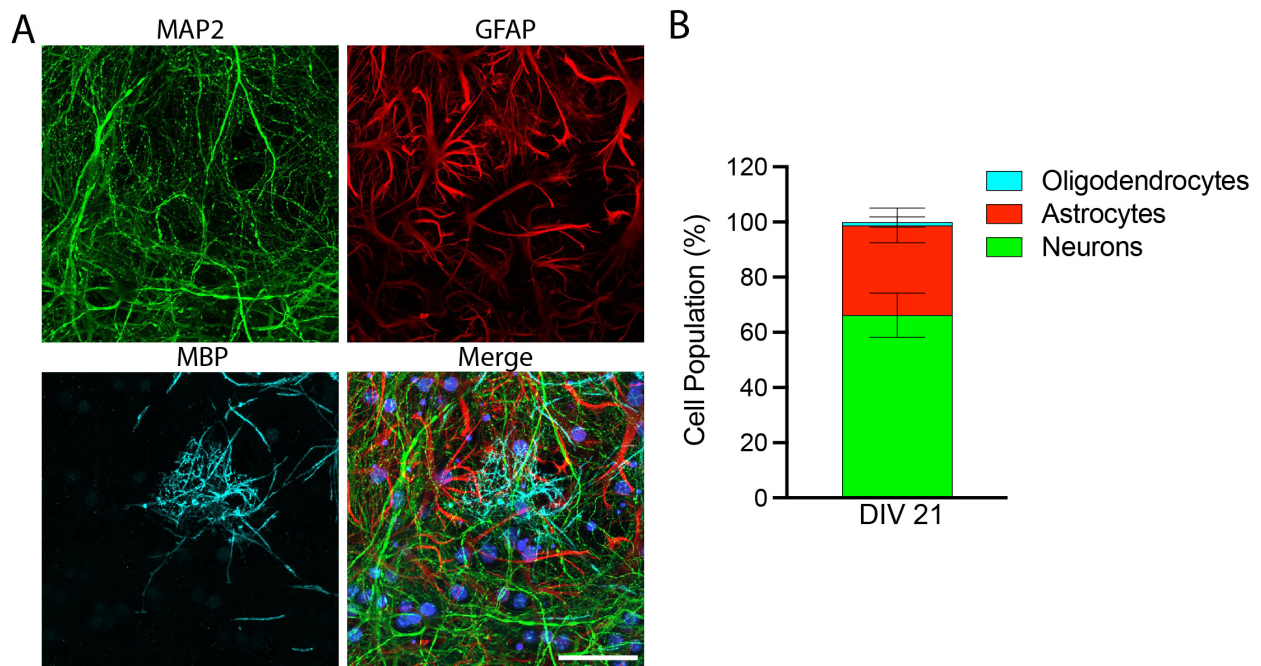


Figure 2.2. Neurons and astrocytes are the primary cellular components of mature MAPT-KI primary hippocampal cultures. A) Primary cultures were fixed on DIV21 and immunolabelled with MAP2 (neurons; green), GFAP (astrocytes; red), and MBP (oligodendrocytes; cyan) antibodies in the same well. Scale bar = 50 μ m. B) Each cell type was manually counted and divided by the total cell number (% cell population). N=3; Images are representative of findings in each experimental replicate which were derived from separate neuron harvests from a unique timed pregnant MAPT-KI females.

Seeding material contains pathological tau species

Seeding material (AD-tau) was purified from post-mortem late-stage AD (Braak stage V-VI) human forebrain tissue. The purification protocol yields a final sample that is enriched in sarkosyl-insoluble tau. To control for other sarkosyl-insoluble proteins, the same purification protocol was followed using tissue from cognitively intact age-matched individuals (Con, Braak stage I-II). The final supernatant containing AD-tau or Con proteins was in 1X dPBS (PBS), and PBS was used as an additional vehicle control in experiments. In our hands, Con and AD-tau

preparations contained 0.07 - 0.64% or 3.6 - 11.4% tau, respectively. I observed paired helical filaments in the AD-tau sample with characteristic helical morphology on TEM (Figure 2.3A). Western blots indicate that AD-tau contains PHF1+ tau species (Figure 2.3B), and both 3R and 4R isoforms were detected (Figure 2.3C). These species were not detected in the Con sample on Western blots (Figure 2.3B and C). Sandwich ELISAs confirm that that Con samples contain low tau levels, while AD-tau contains higher levels of total tau (Tau5; Figure 2.3D). I also confirmed that AD-tau contained pathogenic forms of tau, specifically, the AD-tau samples contained PAD-exposed (TNT1; Figure 2.3E) and oligomeric (TOC1; Figure 2.3F) tau species. In contrast, Con samples contained little to no detectable TNT1 and TOC1 reactivity (Figure 2.3E).

The seeding capacity of the brain-derived samples was verified using the HEK293 P301S Biosensor cells (Holmes et al., 2014). Upon seeding with AD-tau, the fluorescent protein-tagged pro-aggregant tau fragment expressed in the HEK cells was sequestered into bright puncta detectable using microscopy (Figure 2.3G). A small amount of seeding was observed in the cells treated with Con sample (Figure 2.3G), which is consistent with substantially lower levels of tau pathology in these disease stages (i.e. Braak I-II). Together, these results show that AD-tau contains known AD-associated pathological forms of tau that can seed tau pathology *in vitro*.

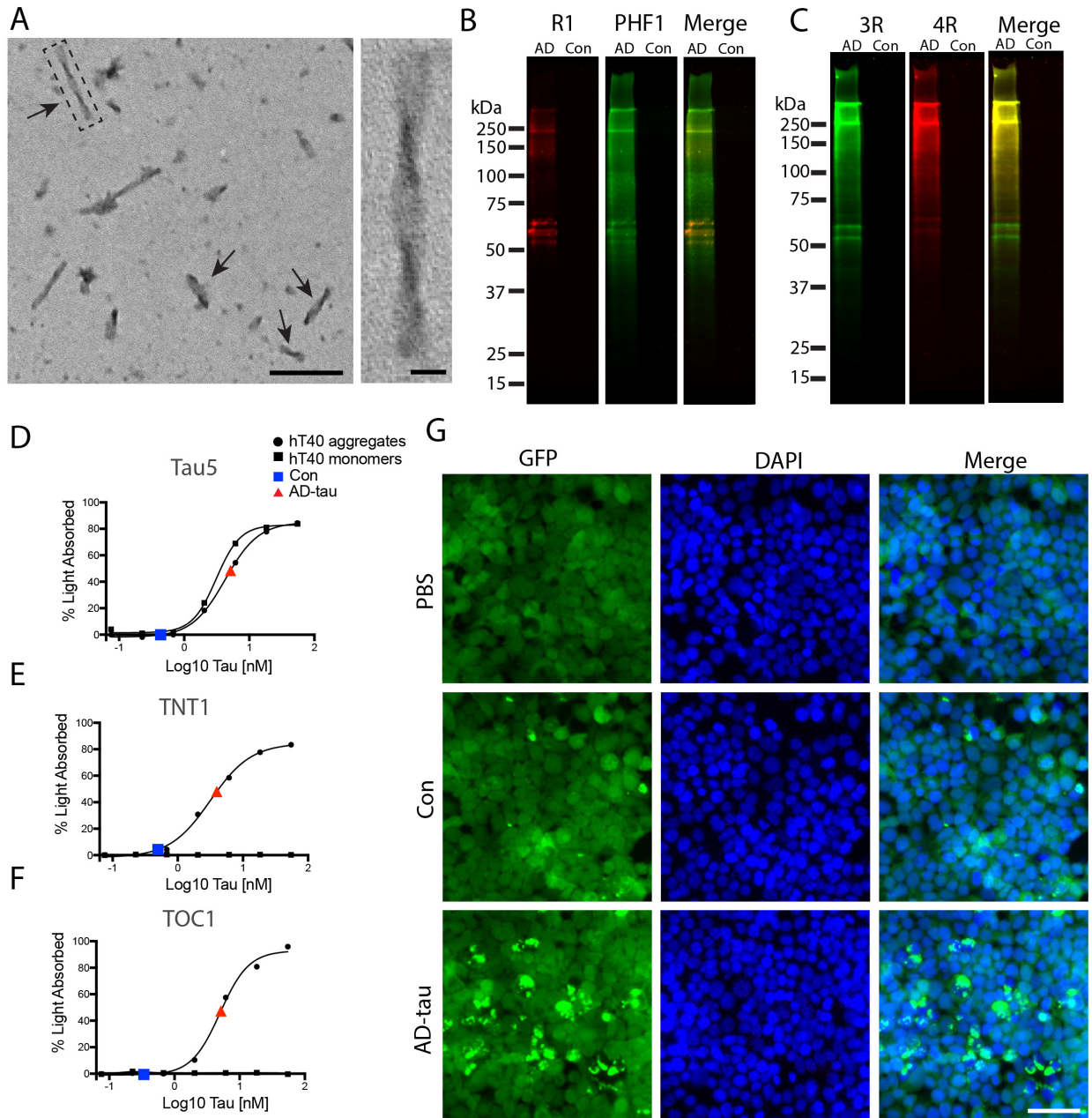


Figure 2.3. AD brain-derived tau samples contain known disease-associated pathological tau species and are seed-competent in Tau RD P301S Biosensor cells. A) Representative EM photomicrograph AD-tau before sonication. Paired helical filaments are visible samples (arrows). Scale bar = 200 nm; inset 25 nm.

Figure 2.3 (cont'd).

B) Western blot of AD-tau or Con samples probed with R1 (total tau; red) and PHF1 phospho-tau (green). C) Western blot of AD-tau or Con samples probed with 3R tau (green) and 4R tau (red) isoform-specific antibodies. D-F) Sandwich ELISAs of AD-tau or Con samples captured with Tau5 (total tau; D), TNT1 (PAD-exposed tau; E), or TOC1 (tau oligomeric complex 1; F) antibodies and detected with R1 (total tau) antibody. G) PBS, Con, or AD-tau (2.8 nM tau) was delivered via lipid-mediated transfection into Tau RD P301S Biosensor cells. Cells (green) were fixed after 48 hours, counterstained with DAPI (blue), and imaged to detect aggregated tau puncta. Scale bar = 50 μ m.

Treatment of MAPT-KI neurons with AD-tau results in the progressive formation of PAD-exposed tau inclusions

To determine whether treatment of MAPT-KI hippocampal cultures with AD-tau would seed PAD-exposed tau conformations, I conducted a time course in which cells were treated with PBS, Con or AD-tau (28 nM tau) on DIV5, then fixed 7, 14 or 28d post-treatment (corresponding to DIV 12, 19 and 33 at collection) and immunolabelled with TNT1 and Tuj1 antibodies (Figure 2.4). MeOH fixation was used to remove soluble tau. There was a time-dependent increase in TNT1+ tau inclusions in the AD-tau treated neurons (Figure 2.4F). The TNT1+ inclusion load increased ~5-fold from DIV14 to 22, and ~2-fold from DIV22 to 31. Some TNT1+ inclusions were observed in the Con group at 28d post-treatment, these also showed a time-dependent increase (Figure 2.4E). The TNT1+ inclusion load increased ~2-fold from DIV14 to 22, and ~8-fold from DIV22 to 31 in Con-treated neurons. At DIV31, the TNT1+ inclusion load in the AD-tau treated cells was ~16x that observed in the Con-treated cells.

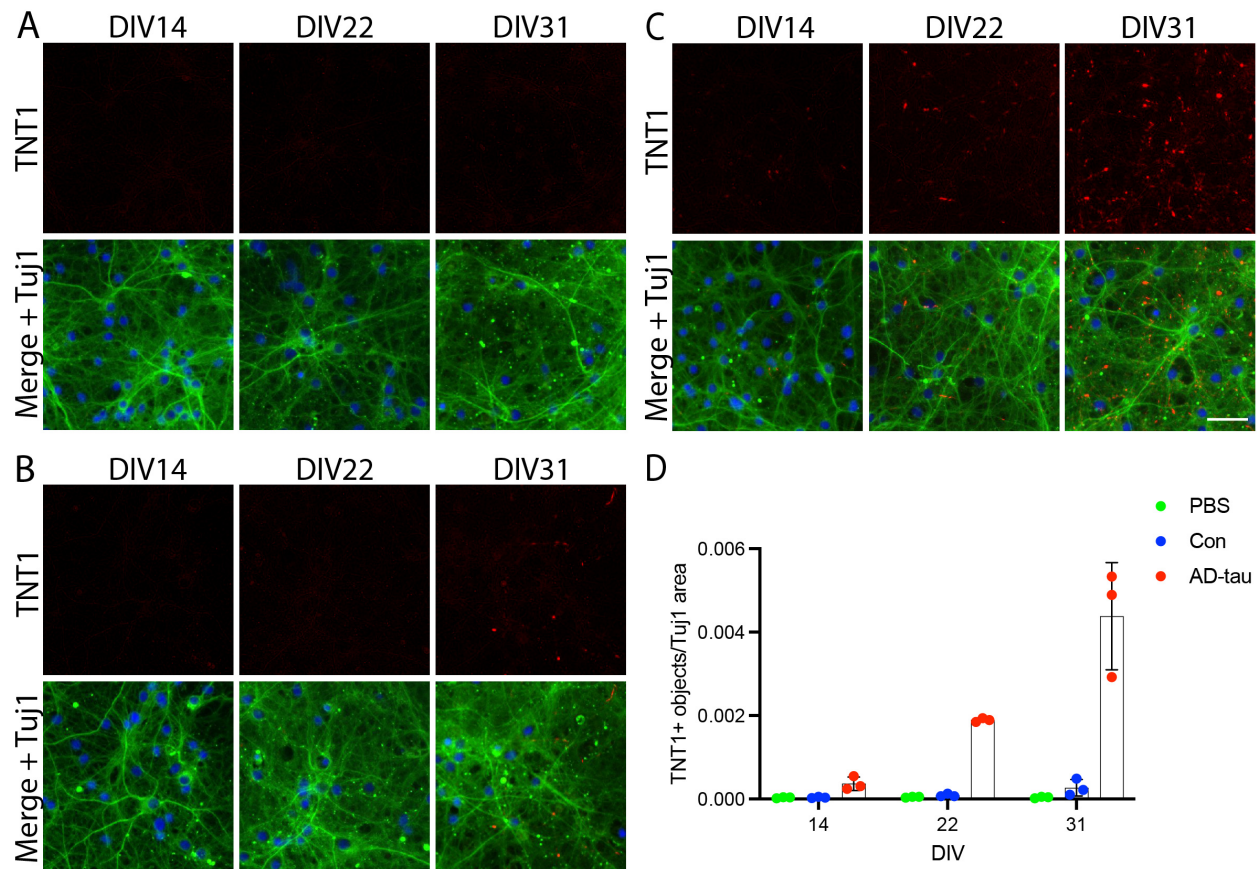


Figure 2.4. Progressive formation of PAD-exposed tau inclusions in MAPT-KI primary neurons treated with AD-tau. Scale bar = 50 μ m. MAPT-KI primary hippocampal neurons were treated with PBS (A), Con (B), or AD-tau (28 nM; C) on DIV5. Cultures were fixed with methanol on DIV14, 22, or 31 to remove soluble tau. Cells were immunolabelled with TNT1 (PAD-exposed tau; red) and β -III tubulin (Tuj1; green) antibodies, and counterstained with DAPI (blue). Cells were imaged using an automated microscope (A-C). Scale bar = 50 μ m. D) Quantitation of the number of TNT1+ aggregates normalized to Tuj1 surface area. N=3; Images are representative of findings in each independent experimental replicate which were derived from 3 separate neuron harvests from unique timed pregnant MAPT-KI females.

I treated Tau-KO primary neuron cultures with AD-tau to confirm that TNT1+ inclusions require endogenous tau expression. At 28d post-treatment (DIV33 at collection) the Tau-KO neurons showed no sign of TNT1+ tau pathology accumulation (Figure 2.5). Next, to confirm that the TNT1+ inclusions in the MAPT-KI neurons were intracellular, AD-tau-treated MAPT-KI cells 21d post-treatment (DIV26 at collection) were immunostained with and without permeabilizing the cells. (Figure 2.6A, B). Non-permeabilized cells showed no TNT1+ signal, confirming that the PAD-exposed tau was intracellular. Consistent with these findings, cells treated with trypsin prior to fixation and permeabilization to remove extracellular proteins showed positive TNT1 signal. Together, these data provide strong evidence that the inclusions observed in the MAPT-KI neurons are formed through the seeding of endogenous tau in neurons and that they adopt a known pathogenic conformation (i.e. TNT+ or PAD exposed conformation).

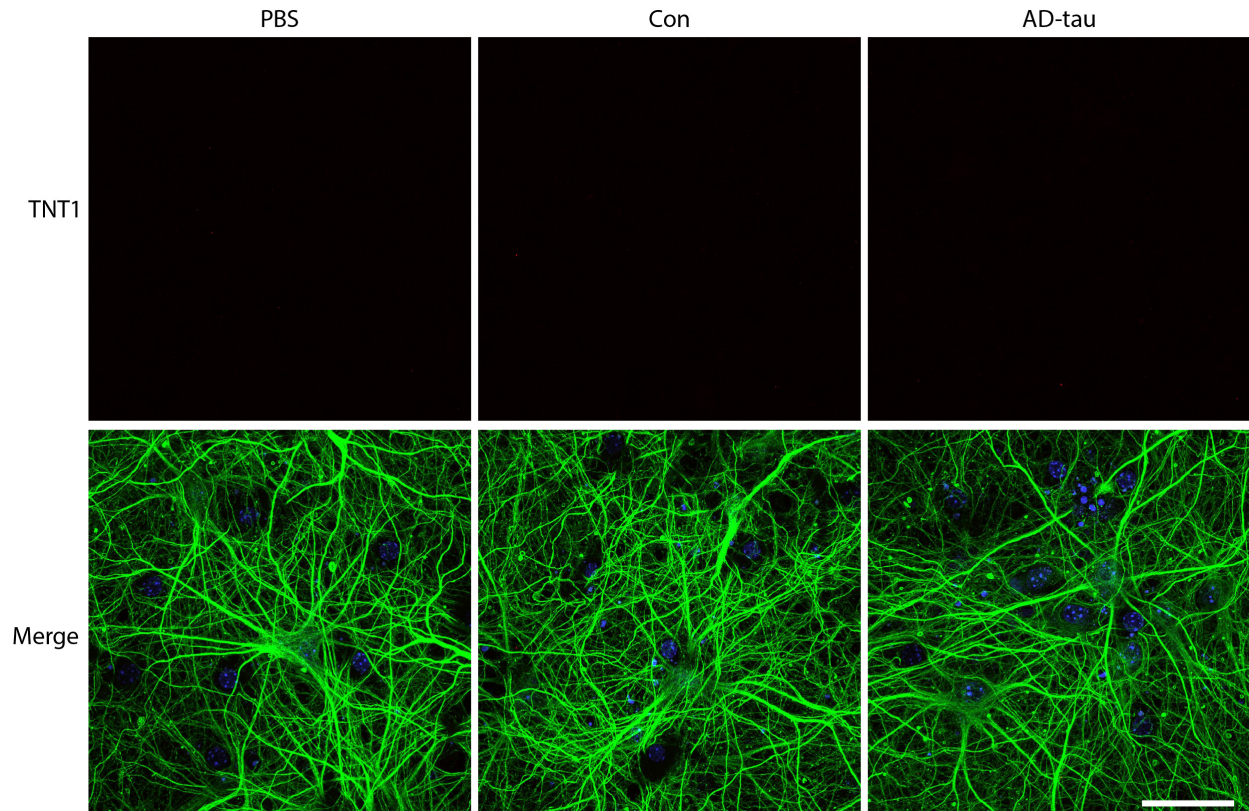


Figure 2.5. PAD-exposed tau inclusions are absent in AD-tau-treated Tau-KO primary neurons at 28d post-treatment. Primary neurons from Tau-KO mice were treated with PBS, Con or AD-tau (28 nM) on DIV5. Cells were fixed on DIV33 and immunolabelled with TNT1 (PAD-exposed tau; top panels) and β -III tubulin (Tuj1; green) antibodies, and nuclei were stained with DAPI. TNT1+ inclusions were not detected. Scale bar = 50 μ m. N=3; Images are representative of findings in each independent experimental replicate which were derived from separate neuron harvests from unique timed pregnant Tau-KO females.

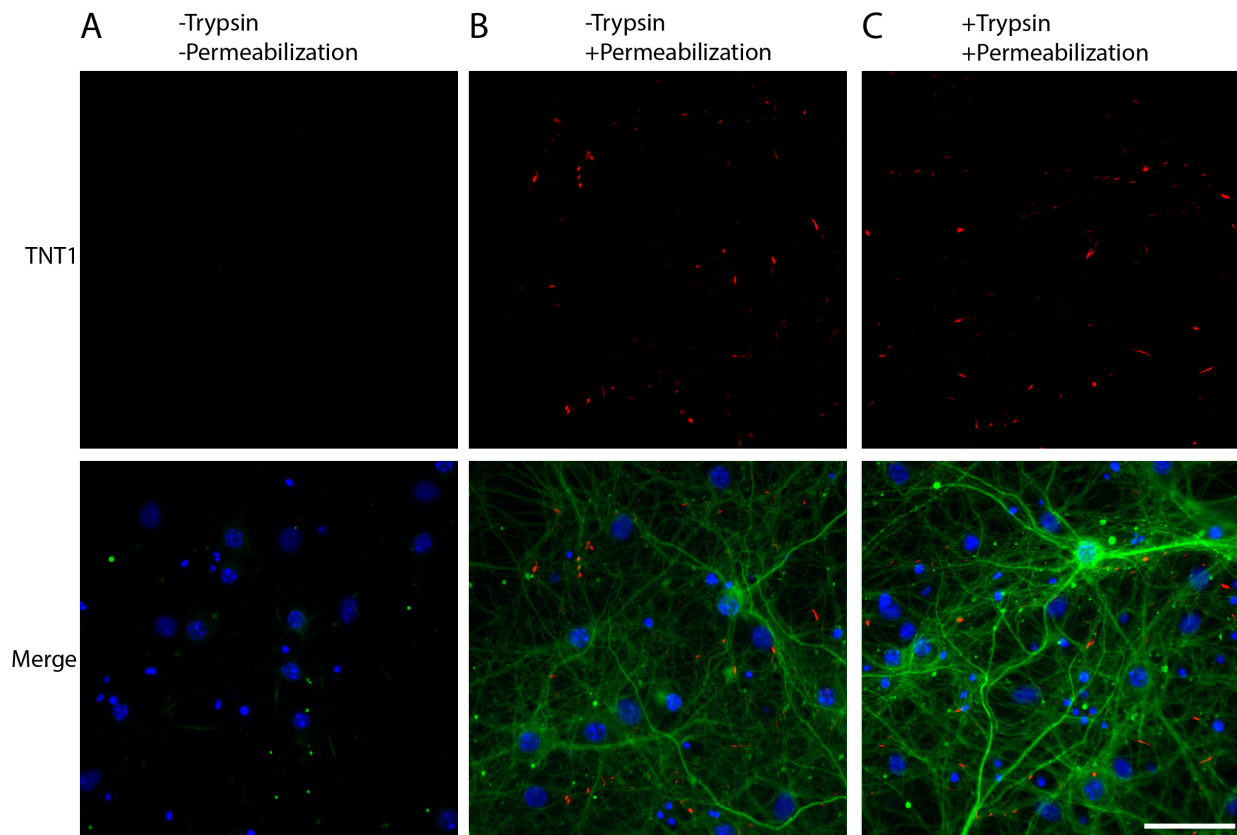


Figure 2.6. PAD-exposed tau inclusions are intracellular. MAPT-KI primary neurons were treated with AD-tau (28 nM tau) on DIV5 and collected 21d post-treatment (corresponding to DIV26). A) Non-permeabilized cells were immunolabelled alongside B) permeabilized cells with TNT1 (PAD-exposed tau; red) and β -III tubulin (Tuj1, green) antibodies, and nuclei were stained with DAPI (blue). Omission of the permeabilization step showed no TNT1 signal, indicating that the inclusions were intracellular. C) Prior to fixation and permeabilization, cells were treated with trypsin to remove extracellular proteins. Cells were immediately fixed, then permeabilized and immunolabelled as in A-B. TNT1+ signal was observed in the +Trypsin condition, confirming that the inclusions are intracellular. Scale bar = 50 μ m. N=3; Images are representative of findings in each independent experimental replicate which were derived from separate neuron harvests from unique timed pregnant MAPT-KI females.

Cellular distribution of seeded PAD-exposed tau inclusions

The tau pathology in AD is primarily restricted to neurons while other tauopathies present with both neuronal and glial tau pathology (Kovacs et al., 2018). These patterns of distribution are recapitulated in tau seeding studies *in vitro* and *in vivo* (Clavaguera et al., 2013; Kaufman et al., 2016; Narasimhan et al., 2017; Sanders et al., 2014). Astrocytes account for a substantial portion of the total cell population in the MAPT-KI primary hippocampal cultures. To determine whether the TNT1+ inclusions were restricted to neurons, the MAPT-KI cultures were treated with PBS, Con, or AD-tau on DIV5, fixed on 16 days post-treatment (i.e. DIV21 at collection), and immunolabeled with TNT1 and cell type-specific antibodies. Neurons were labelled with MAP2 (somatodendritic compartment) and Tuj1 (somatodendritic compartment and axons). TNT1+ inclusions were observed in neurons, primarily in axons (Tuj1+/MAP2- processes), with rare somatodendritic localization (Figure 2.7). TNT1+ inclusions were not observed in GFAP antibody-labelled astrocytes (Figure 2.8).

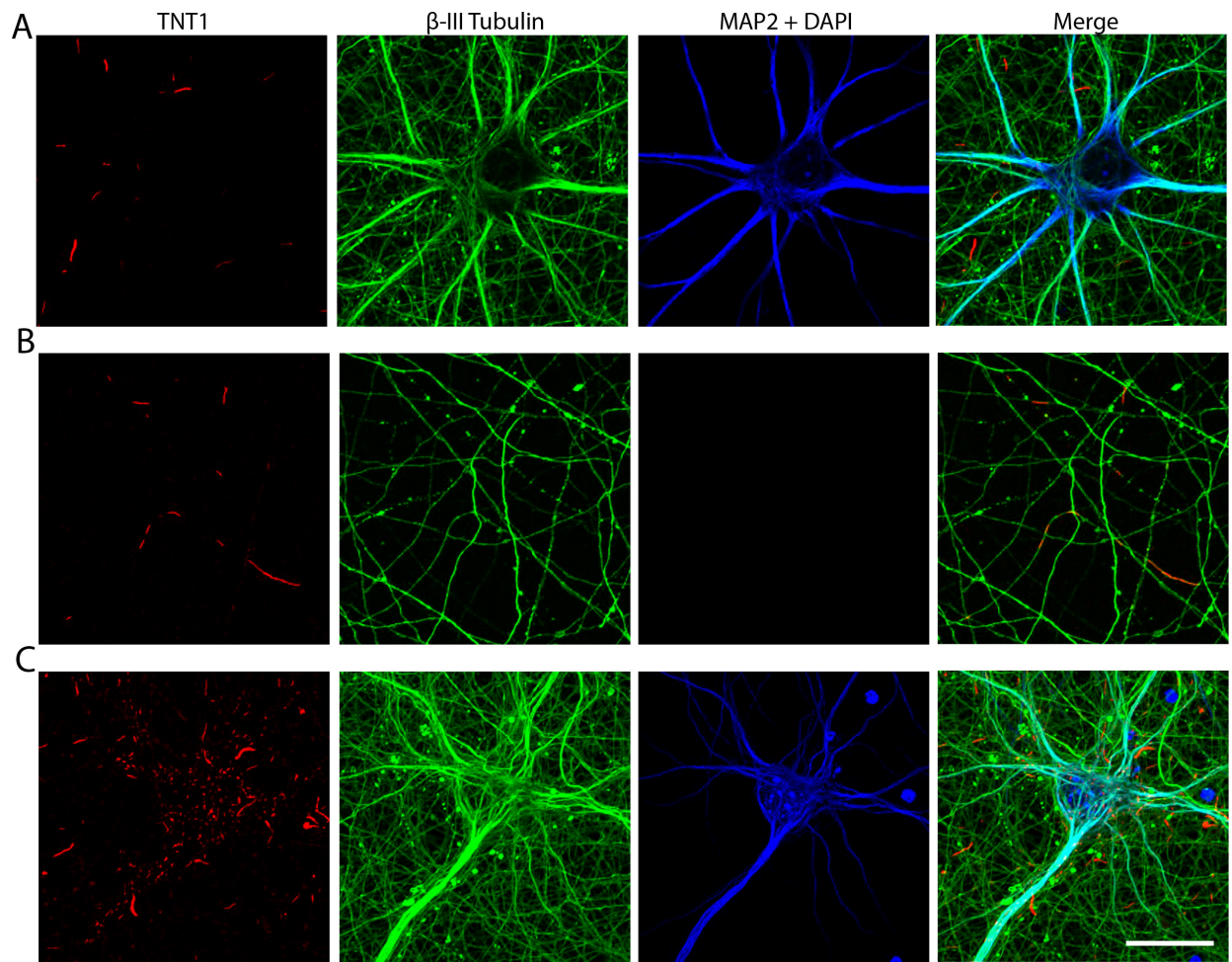


Figure 2.7. Tau inclusions are primarily neuritic with rare somatodendritic localization. MAPT-KI primary neurons were treated with PBS, Con, or AD-tau on DIV5 and fixed on DIV21. Cultures were immunolabeled with TNT1 (PAD-exposed tau; red), β -III tubulin (Tuj1; labels somatodendritic compartment and axons), and MAP2 (somatodendritic compartment only; blue) antibodies. A) The vast majority of neurons lacked TNT1+ inclusions in the somatodendritic compartment (MAP2+/ β -III tubulin+). B) TNT1+ inclusions formed primarily in axons (MAP2-/ β -III tubulin+). C) Rare somatodendritic localization of TNT1+ inclusions was observed. Scale bar = 25 μ m. N=3; Images are representative of findings in each independent experimental replicate which were derived from separate neuron harvests from unique timed pregnant MAPT-KI females.

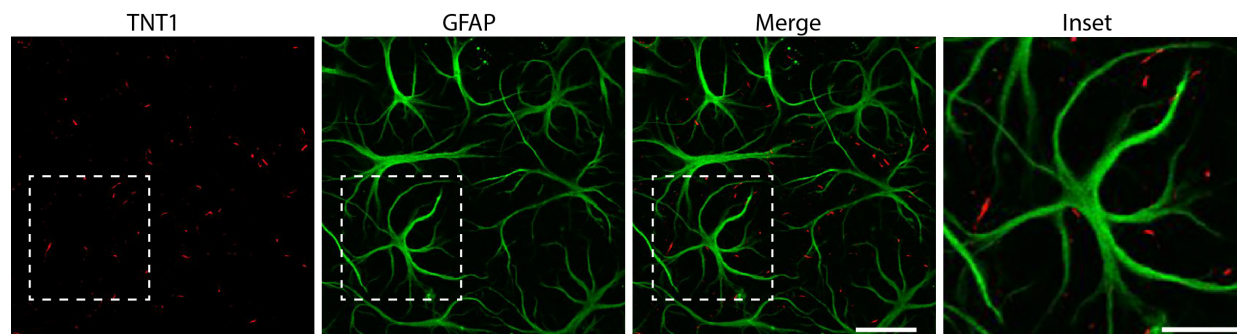


Figure 2.8. PAD-exposed tau inclusions are absent in astrocytes. MAPT-KI primary hippocampal cultures were treated on DIV5 with PBS, Con, or AD-tau and fixed on DIV21. Astrocytes were immunolabelled with glial fibrillary acid protein (GFAP; green) and TNT1 (PAD-exposed tau; red) antibodies. A representative image shows that TNT1+ inclusions were located outside of astrocytes. Scale bar = 50 μm ; inset scale bar = 25 μm . N=3; Images are representative of findings in each independent experimental replicate which were derived from separate neuron harvests from unique timed pregnant MAPT-KI females.

PAD-exposed tau inclusions co-localize with AD-associated phosphorylated and oligomeric tau species

We used conformation-specific TNT1 and TOC1 antibodies to detect PAD-exposed and oligomeric tau species, respectively, in the AD-tau treated cultures (Figure 2.9). ICF showed co-localization between TNT1 and TOC1 in AD-tau treated cultures (Figure 2.9B), and no TNT1 or TOC1 inclusions in the PBS treated cultures (Figure 2.9A). Lysates of PBS, Con, or AD-tau treated cultures were collected and sELISA was used to detect total tau, TNT1 and TOC1 tau. PBS, Con, and AD-tau cultures had similar levels of total tau (Tau5; Figure 2.9C) (one-way ANOVA; $F_{(2,15)} = 0.2749$, $p = 0.3180$). Small amounts of TNT1+ tau was observed in the Con culture lysates (Figure 2.9D). TNT1+ (Kruskal-Wallis ANOVA with Dunn's post hoc; $H = 15.16$, $p < 0.0001$;

PBS vs. AD-tau $p = 0.0003$) and TOC1+ (Kruskal-Wallis ANOVA with Dunn's post hoc; $H = 11.66$, $p = 0.0003$; PBS vs. AD-tau $p = 0.0043$; Con vs. AD-tau $p = 0.0242$) tau species were observed in the AD-tau treated culture lysates (Figure 2.9D, E, respectively).

To further characterize the pathological tau species formed in AD-tau-treated MAPT-KI hippocampal neurons, antibodies specific to several pathological modifications were assessed for their co-localization with TNT1. Multiple z-stack images were obtained using a confocal microscope at 60x magnification. There was nearly complete co-localization of TNT1 with AT8 (Figure 2.10) and pS422 (Figure 2.11). TNT1 immunoreactivity also co-localized PHF1 (Figure 2.11), albeit not as robustly as pS422 and AT8. Together, these findings show that treatment of MAPT-KI cultures with AD-tau results in the formation of several known pathological tau conformations and phosphorylated species associated with AD and other tauopathies.

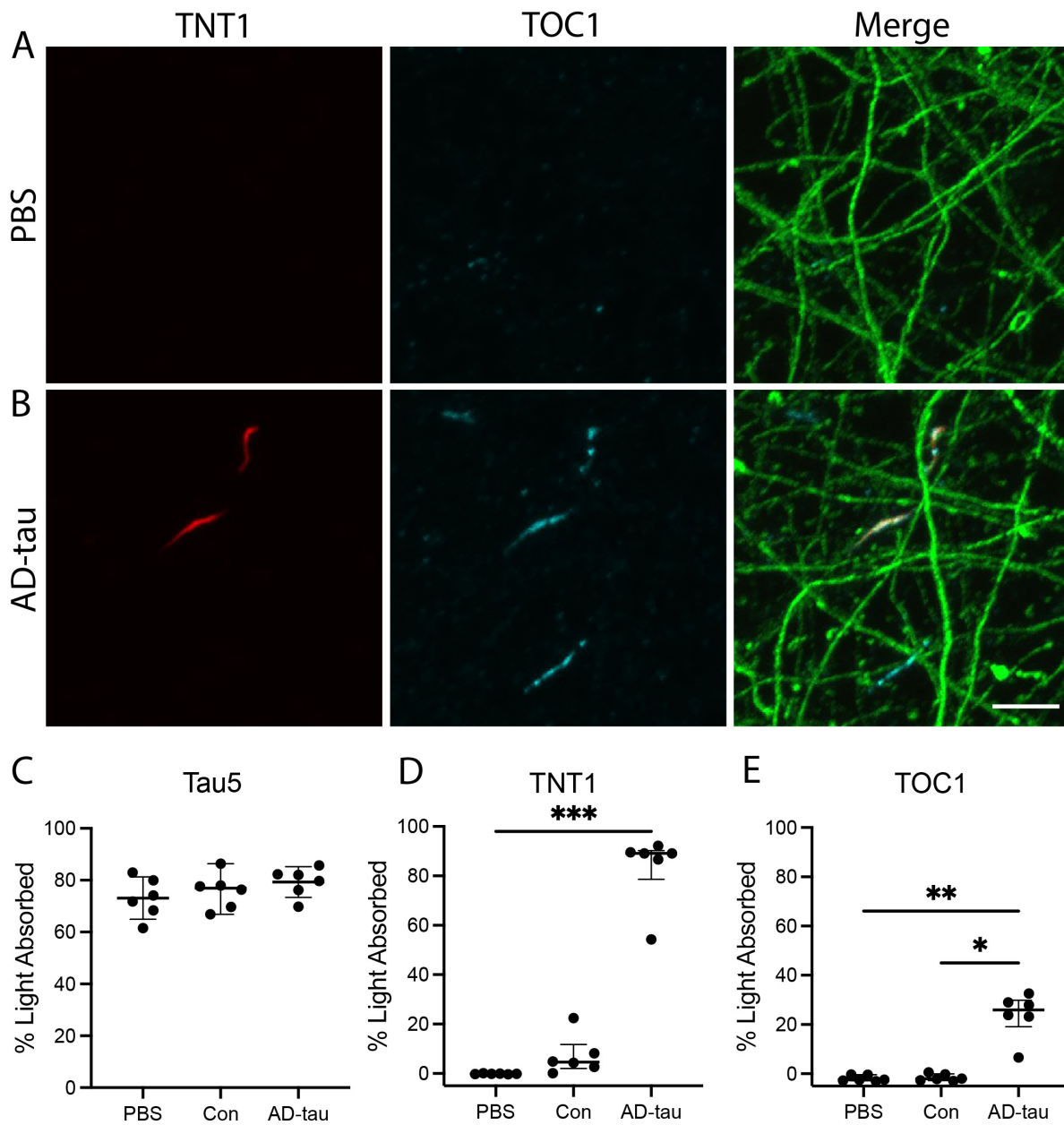


Figure 2.9. Seeded tau inclusions are comprised of PAD-exposed tau and AD-associated oligomeric species. MAPT-KI cells were treated with PBS, Con, or AD-tau (28 nM) on DIV5, treated briefly with trypsin, and fixed on DIV26. A-B) Cells were immunolabelled with TNT1 (PAD-exposed tau; red) and TOC1 (oligomeric tau; cyan) antibodies. A) No inclusions were observed in PBS-treated cells. B) TNT1 and TOC1 signal colocalize in the inclusions detected in AD-tau-treated cells. Some TOC1+/TNT1- inclusions were observed.

Figure 2.9 (cont'd).

Scale bar = 5 μm . C-E) Total tau, PAD-exposed tau, and oligomeric tau species were detected in lysates collected from AD-tau treated cultures at DIV31. Sandwich ELISAs were performed using Tau5 (total tau), TNT1, and TOC1 capture antibodies and the R1 (total tau) detection antibody. The data in C are mean \pm SD and were compared using one-way ANOVA with Tukey's multiple comparisons test. The data in D-E are median \pm interquartile range and were compared using Kruskal-Wallis ANOVA with Dunn's multiple comparisons test. Significance was defined as $p \leq 0.05$. ICF: representative images for N=3; sELISAs: N=6; each experimental replicate represent cultures derived from separate neuron harvests from unique timed pregnant MAPT-KI females.

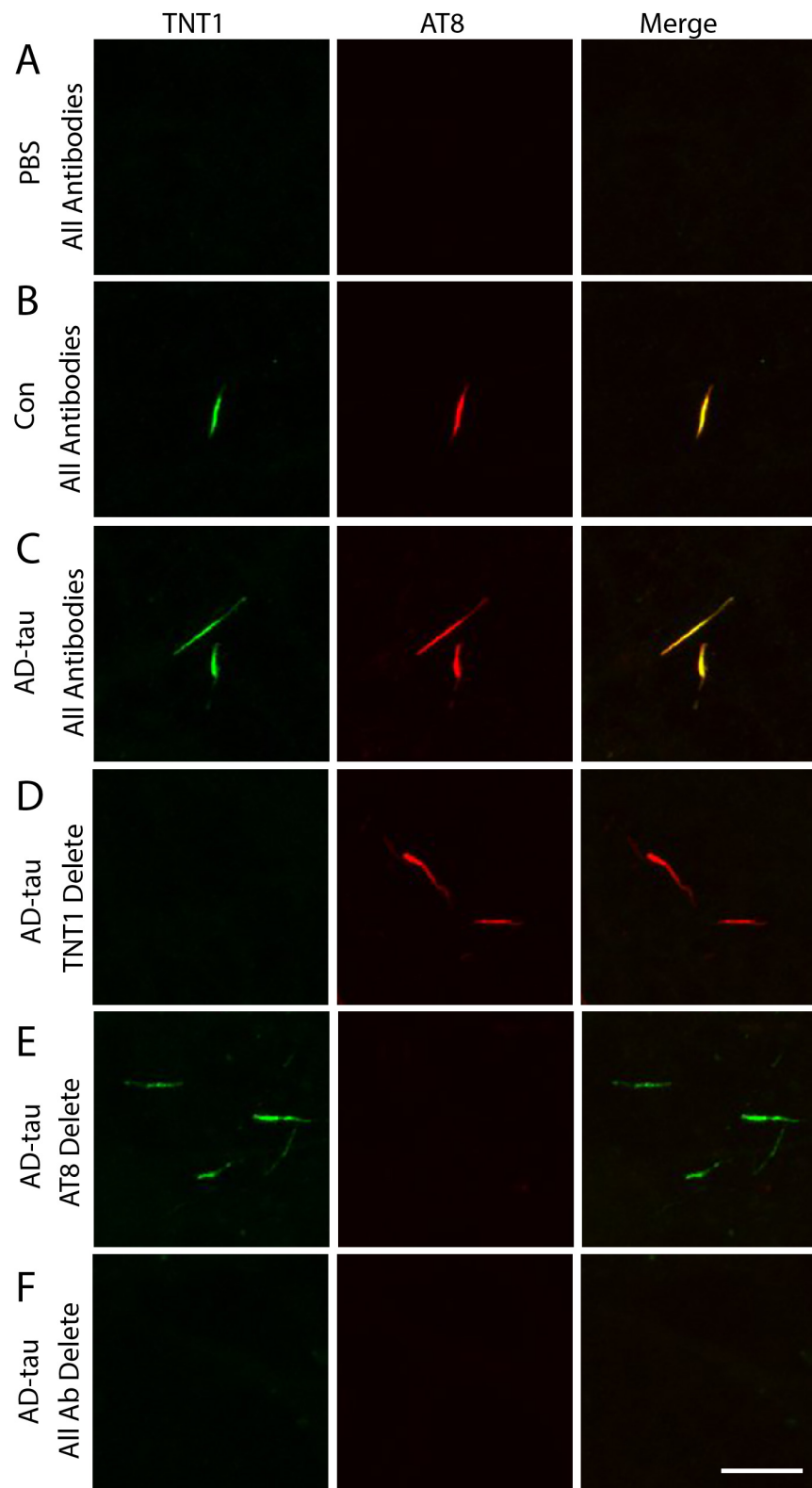


Figure 2.10. Seeded tau inclusions are comprised of AD-associated tau phosphorylated at the AT8 site.

Figure 2.10 (cont'd).

MAPT-KI cells were treated with PBS, Con, or AD-tau (28 nM) on DIV5 and fixed on DIV21. A-C) Cells were immunolabelled with TNT1 (PAD-exposed tau; green) and AT8 (red) antibodies. A) No inclusions were observed in PBS-treated cells. B-C) TNT1 and AT8 signal highly colocalize in the inclusions detected in Con and AD-tau-treated cells. D-F) Immunocytofluorescence (ICF) primary antibody delete control labeling was performed in AD-tau-treated neurons. D) Omission of the TNT1 primary antibody showed no TNT1 signal. E) Omission of the AT8 primary antibody showed no AT8 signal. F) Omission of all primary antibodies showed no TNT1 or AT8 signal. The lack of signal in the primary antibody deletes confirms that these ICF stains do not cross react with each other. Scale bar = 10 μ m. N=3; Images are representative of findings in each independent experimental replicate which were derived from separate neuron harvests from unique timed pregnant MAPT-KI females.

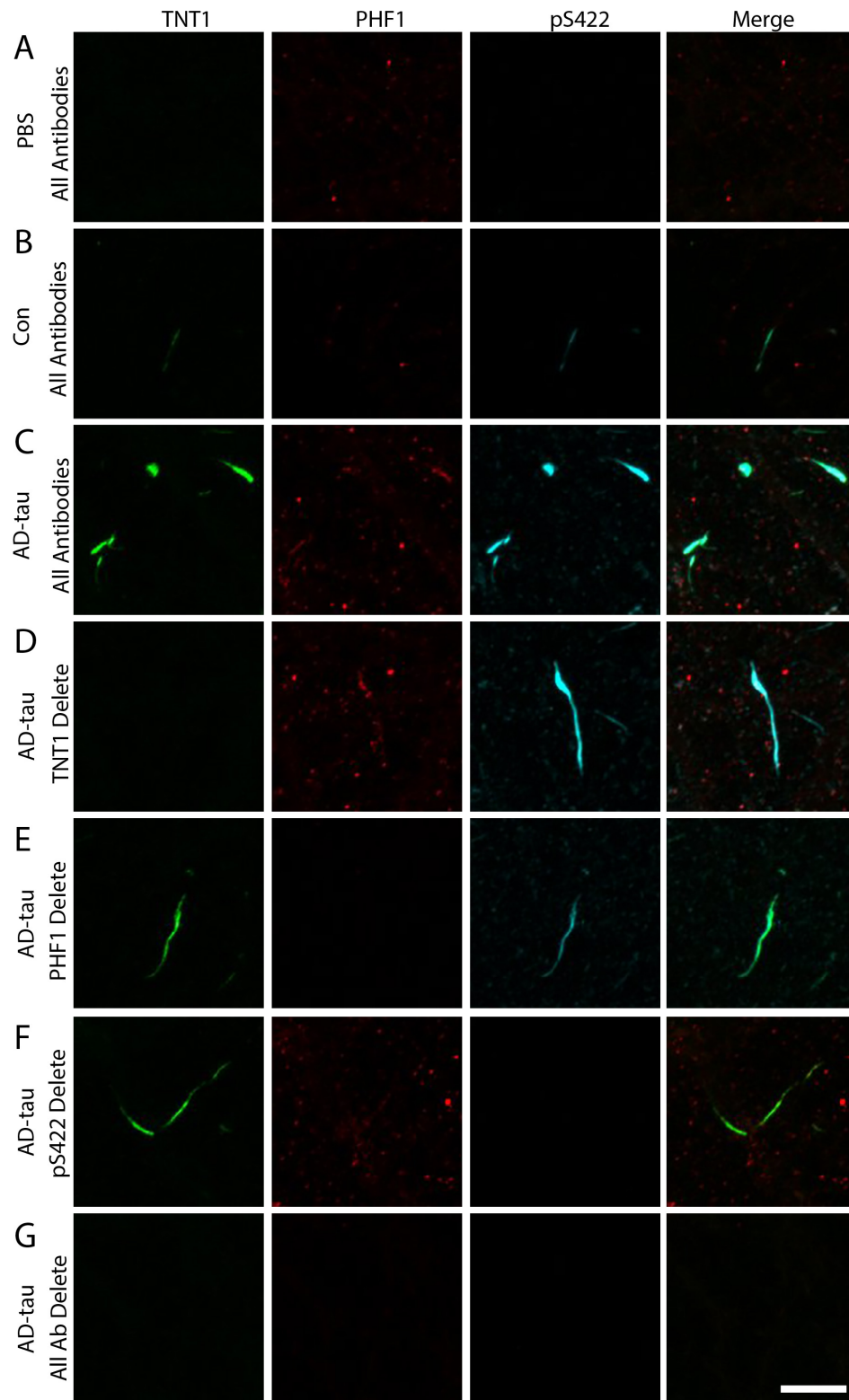


Figure 2.11. Seeded tau inclusions are comprised of AD-associated phosphorylated species PHF1 and pS422.

Figure 2.11 (cont'd).

MAPT-KI cells were treated with PBS, Con, or AD-tau (28 nM) on DIV5 and fixed on DIV21. A-C) Cells were immunolabelled with TNT1 (PAD-exposed tau; green), PHF1 (red), and pS422 (cyan) antibodies. A) No inclusions were observed PBS-treated cells. B) Relatively few tau inclusions were present in the Con-treated cells, but the inclusions present were TNT1+ and pS422+. C) Robust formation of seeded TNT1+ and pS422+ inclusions was detected in AD-tau-treated cells. D-G) Immunocytofluorescence (ICF) primary antibody delete control labeling was performed in AD-tau-treated neurons. D) Omission of the TNT1 primary antibody showed no TNT1 signal. E) Omission of the PHF1 primary antibody showed no PHF1 signal. F) Omission of the pS422 primary antibody showed no pS422 signal. G) Omission of all primary antibodies showed no TNT1, PHF1, or pS422 signal. The lack of signal in the primary antibody deletes confirms that these ICF stains do not cross react with each other. Scale bar = 10 μ m. N=3; Images are representative of findings in each independent experimental replicate which were derived from separate neuron harvests from unique timed pregnant MAPT-KI females.

Evidence of AD-associated truncated tau species in seeded neurons

Having observed early pretangle changes (PAD-exposure, oligomerization and specific phospho-epitopes), the presence of truncated tau species in the inclusions was assessed next. Evidence suggests that caspase 3 can cleave tau at D421 and that this modification likely occurs after filament formation during the intermediate stages of tau tangle evolution in AD (Guillozet-Bongaarts et al., 2005; De Calignon et al., 2010). The TauC3 antibody, an antibody specific to tau truncated at D421 (Gamblin et al., 2003), labeled relatively infrequent tau inclusions. The TauC3 pathology was primarily located in neurites, but also in some somatodendritic compartments of affected neurons. TauC3+ species did not typically colocalize with TNT1 (Figure 2.12). ThR is a

β -pleated sheet dye and was used to determine if the tau inclusions contained β -sheet structure (Combs et al., 2016; Mena et al., 1995; Luna-Munoz et al., 2008 Acta; Luna-Viramontes et al., 2020). There was no evidence that tau inclusions label with ThR (Figure 2.13). Collectively, these findings suggest that the majority of the seeded pathology exists in states associated with the earlier phases of tau pathology evolution in human disease, but a small subset of neurons develop more mature forms (e.g. TauC3+ pathology). Moreover, the data suggest that there is no evidence of some modifications associated with the latest stages of tangle evolution (e.g. ThR).

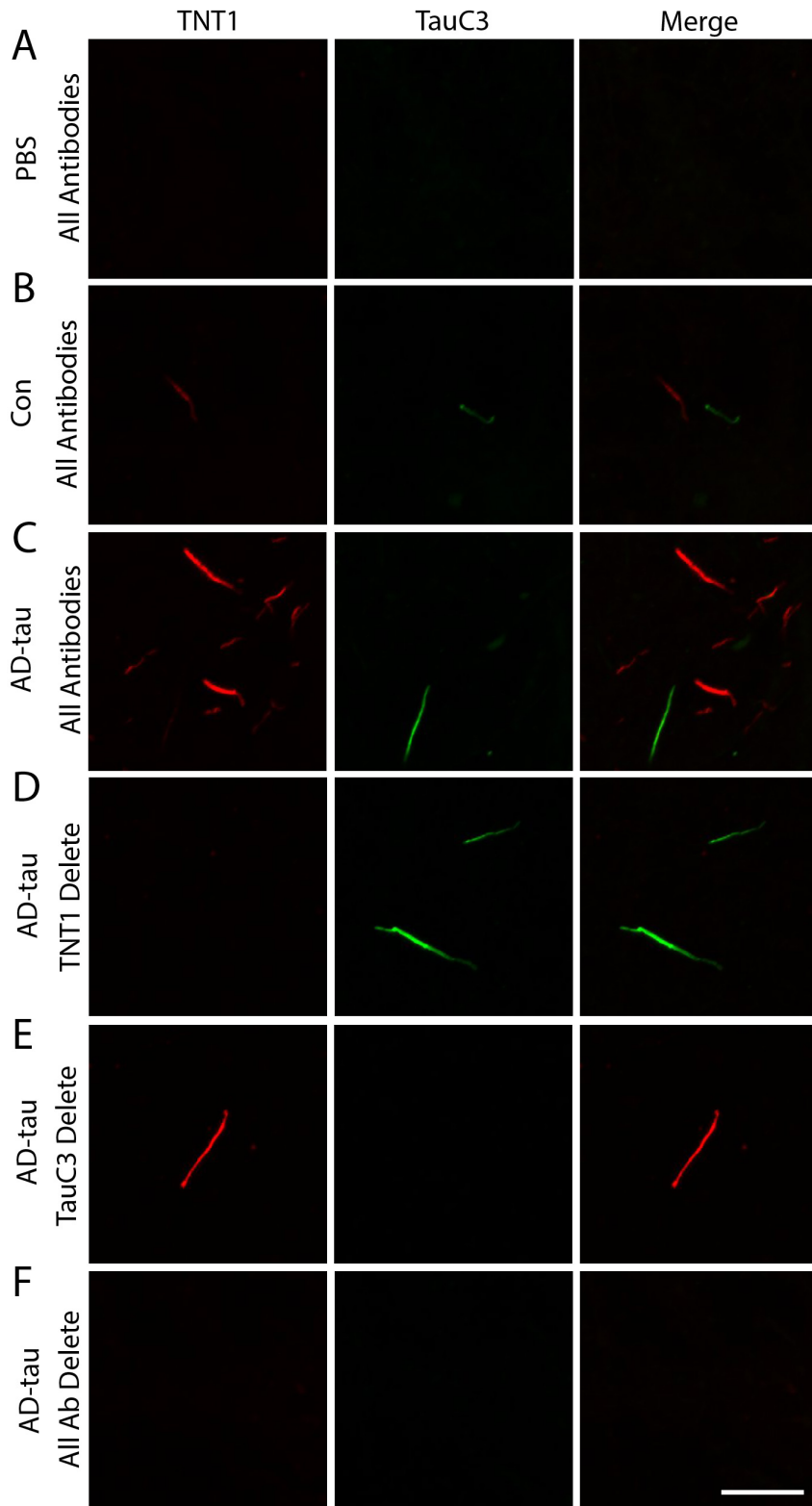


Figure 2.12. Seeded tau inclusions are comprised of AD-associated truncated tau. MAPT-KI cells were treated with PBS, Con, or AD-tau (28 nM) on DIV5 and fixed on DIV21.

Figure 2.12 (cont'd).

A-C) Cells were immunolabelled with TNT1 (PAD-exposed tau; green) and TauC3 (tau truncated at E391; red), antibodies. A) No inclusions were observed PBS-treated cells. B) Relatively few tau inclusions were present in the Con-treated cells and few were TNT1+ and TauC3+. C) Robust formation of seeded TNT1+ and TauC3+ inclusions was detected in AD-tau-treated cells. The TNT1+ and TauC3+ signals rarely colocalized. D-F) Immunocytofluorescence (ICF) primary delete control labeling was performed in AD-tau-treated neurons. D) Omission of the TNT1 primary antibody showed no TNT1 signal. E) Omission of the TauC3 primary antibody showed no TauC3 signal. F) Omission of all primary antibodies showed no TNT1 or TauC3 signal. The lack of signal in the primary antibody deletes confirms that these ICF stains do not cross react with each other. Scale bar = 10 μ m. N=3; Images are representative of findings in each independent experimental replicate which were derived from separate neuron harvests from unique timed pregnant MAPT-KI females.

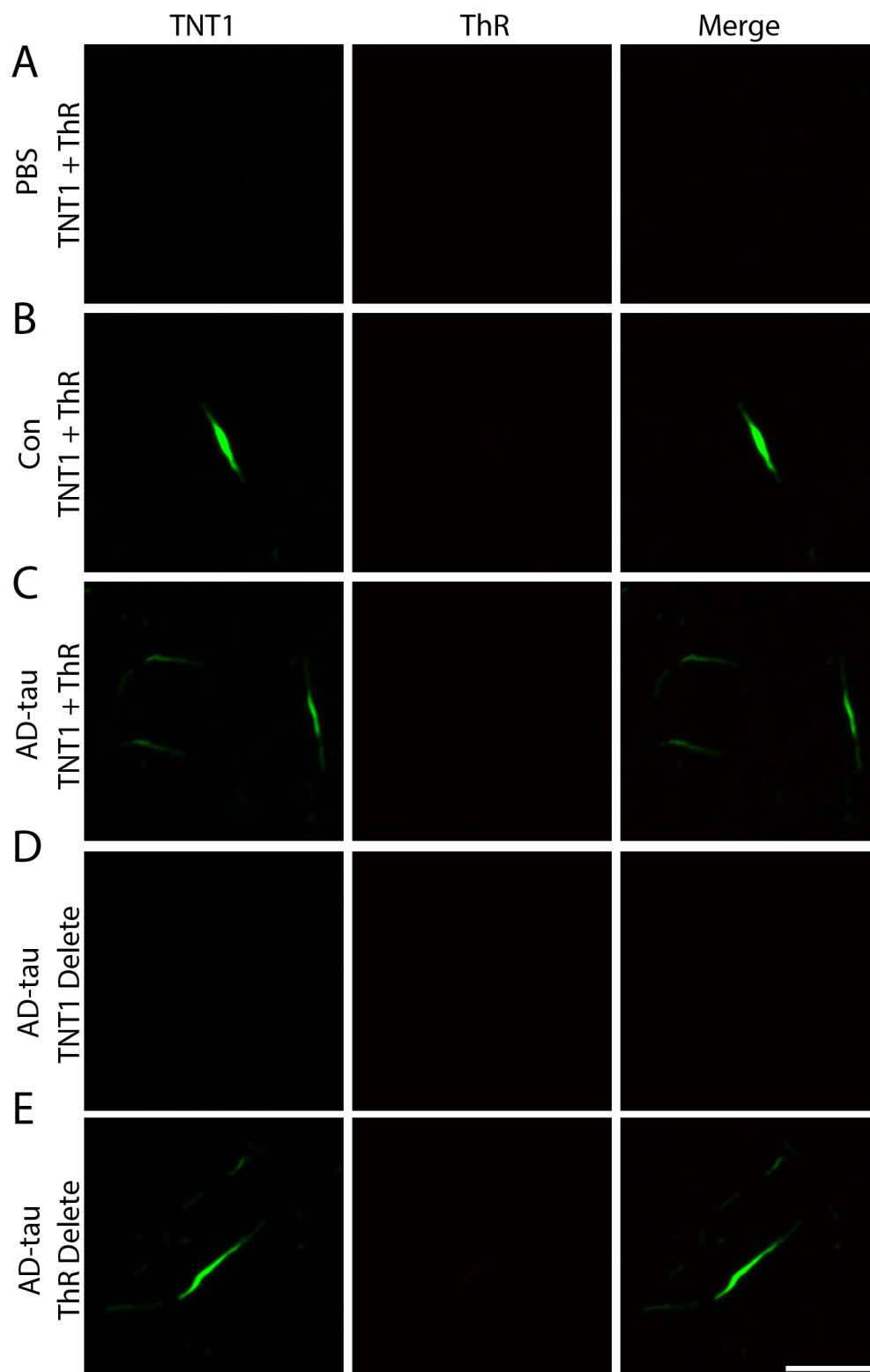


Figure 2.13. β -sheet structures are not detected in seeded tau inclusions. MAPT-KI cells were treated with PBS, Con, or AD-tau (28 nM) on DIV5 and fixed on DIV21. A-C) Cells were stained

Figure 2.13 (cont'd).

with thiazine red (ThR; a β -sheet dye; red), then immunolabelled with TNT1 (PAD-exposed tau; green). A) No inclusions were observed PBS-treated cells. B-C) No ThR signal was detected in Con or AD-tau-treated cells. E) Omission of the TNT1 primary antibody showed no TNT1 signal. F) Omission of the ThR dye showed no ThR signal. The lack of signal in the primary antibody and stain deletes confirms that these stains do not cross react with each other. Scale bar = 10 μ m. N=3; Images are representative of findings in each independent experimental replicate which were derived from separate neuron harvests from unique timed pregnant MAPT-KI females.

Seeding MAPT-KI cultures does not result in overt toxicity

To determine if the formation of pathological tau in the MAPT-KI neurons was toxic to the cells, two cell viability assays (CellTiter Glo and ApoTox-Glo) were used. The CellTiter-Glo cell viability assay (quantifies ATP) showed that ATP levels were similar across all treatment groups at 28d post-treatment (corresponding to DIV33; Figure 2.14 A; one-way ANOVA; $F_{(2,9)} = 0.04135$, $p = 0.9597$). Similarly, the ApoTox-Glo assay measures cell viability, cytotoxicity and caspase-3/7 activity and showed that there were no significant differences between treatment groups in viability (one-way ANOVA; $F_{(2,6)} = 0.1169$, $p = 0.8917$), cytotoxicity (one-way ANOVA; $F_{(2,6)} = 0.2899$, $p = 0.7583$) or caspase-3/7 activity (one-way ANOVA; $F_{(2,6)} = 0.2853$, $p = 0.7614$) at 26d post-treatment (corresponding to DIV31; Figure 2.14 B-D). Taken together, these results show that, despite the presence of multiple forms of tau pathology, tau seeding is not overtly toxic to MAPT-KI primary hippocampal neurons up to DIV28 days post-treatment.

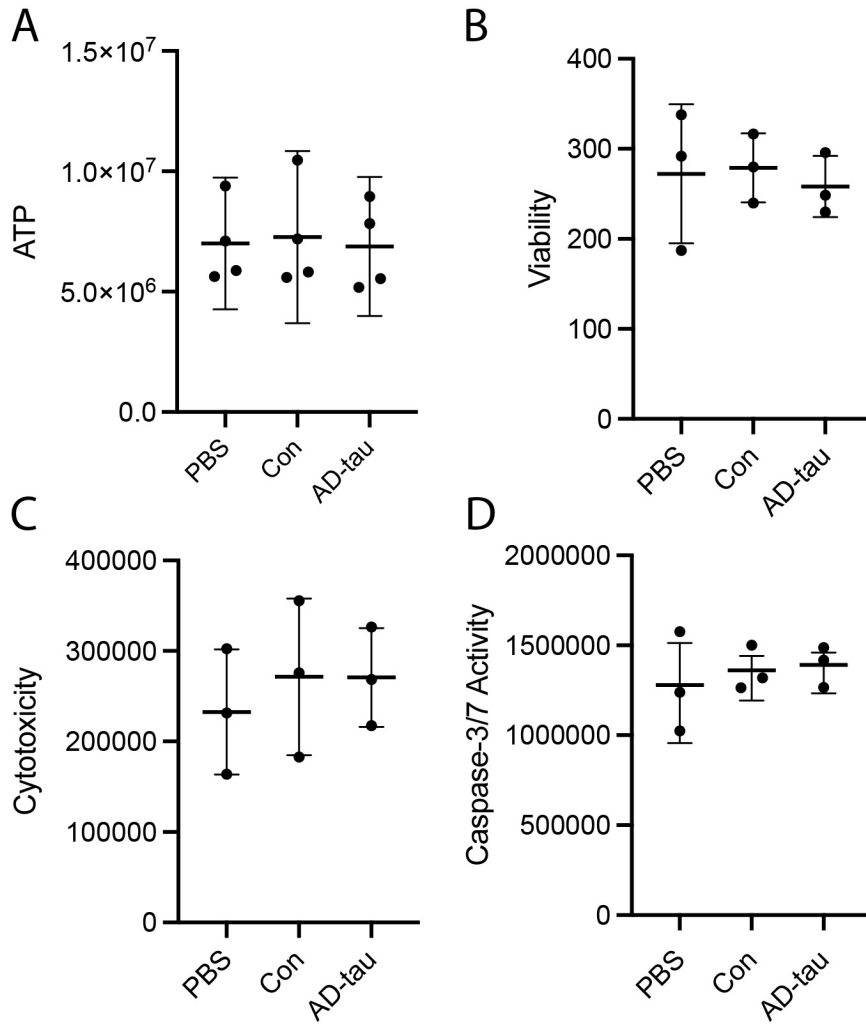


Figure 2.14. Tau seeding did not affect cell culture viability out to 28d post-treatment. Primary MAPT-KI hippocampal neurons were treated with PBS, Con, or AD-tau (28 nM) on DIV5. A) On DIV 33, cell viability was assessed using the CellTiter-Glo assay kit. ATP levels were quantified. ATP levels were the same across groups. B) On DIV 31, cell viability, toxicity and caspase activity were assessed using the ApoTox-Glo assay kit. No change in viability (B), cytotoxicity (C), or in caspase-3/7 activity was observed. The data are mean \pm SD and were compared using one-way ANOVA with Tukey's multiple comparisons test, significance was defined as $p \leq 0.05$. N=4 (A) or N=3 (B-D); each independent experimental replicate represents a separate primary neuron harvest from unique timed pregnant MAPT-KI females.

Seeding MAPT-KI cultures does not cause loss of neurons, astrocytes, or oligodendrocytes

To determine if the pathological tau had cell type-specific toxicity, the number of neurons, astrocytes, or oligodendrocytes were manually counted (Figure 2.15) and cell type-specific proteins were quantified in lysates using immunoblots (Figure 2.16). Cultures were immunolabeled with antibodies for MAP2, GFAP, and MBP to label neurons, astrocytes and oligodendrocytes, respectively. There were no statistically significant treatment effects in cell number neurons (Kruskal-Wallis ANOVA with Dunn's post hoc, $H = 0.2689$, $p = 0.9071$), astrocytes (one-way ANOVA; $F_{(2,3)} = 0.0711$, $p = 0.4655$) or oligodendrocytes (one-way ANOVA; $F_{(2,3)} = 3.257$, $p = 0.1102$) (Figure 2.15). There was a notable stability in the number of neurons across groups, but astrocytes were 7% lower in Con and 24% lower in AD-tau treated cells (Figure 2.15) and oligodendrocytes were 71% higher in Con and 176% higher in AD-tau treated cells when compared to PBS treated cultures, but due to high variability these differences were not statistically significant.

There were no significant treatment differences in β -III tubulin (neurons; one-way ANOVA; $F_{(2,15)} = 0.0771$, $p = 0.9262$) or GFAP (astrocytes; one-way ANOVA; $F_{(2,15)} = 0.2658$, $p = 0.7701$) protein expression (Figure 2.16). The mean GFAP protein levels in the Con and AD-tau-treated cultures were 24% and 26% increased compared to that observed in the PBS-treated cultures, respectively, though this was not statistically significant (Figure 2.16). MBP was undetectable on immunoblots because of the low number of cells in the cultures. Taken together, these results suggest that tau seeding does not cause cell death and may have a mild effect on glial cell composition in the cultures.

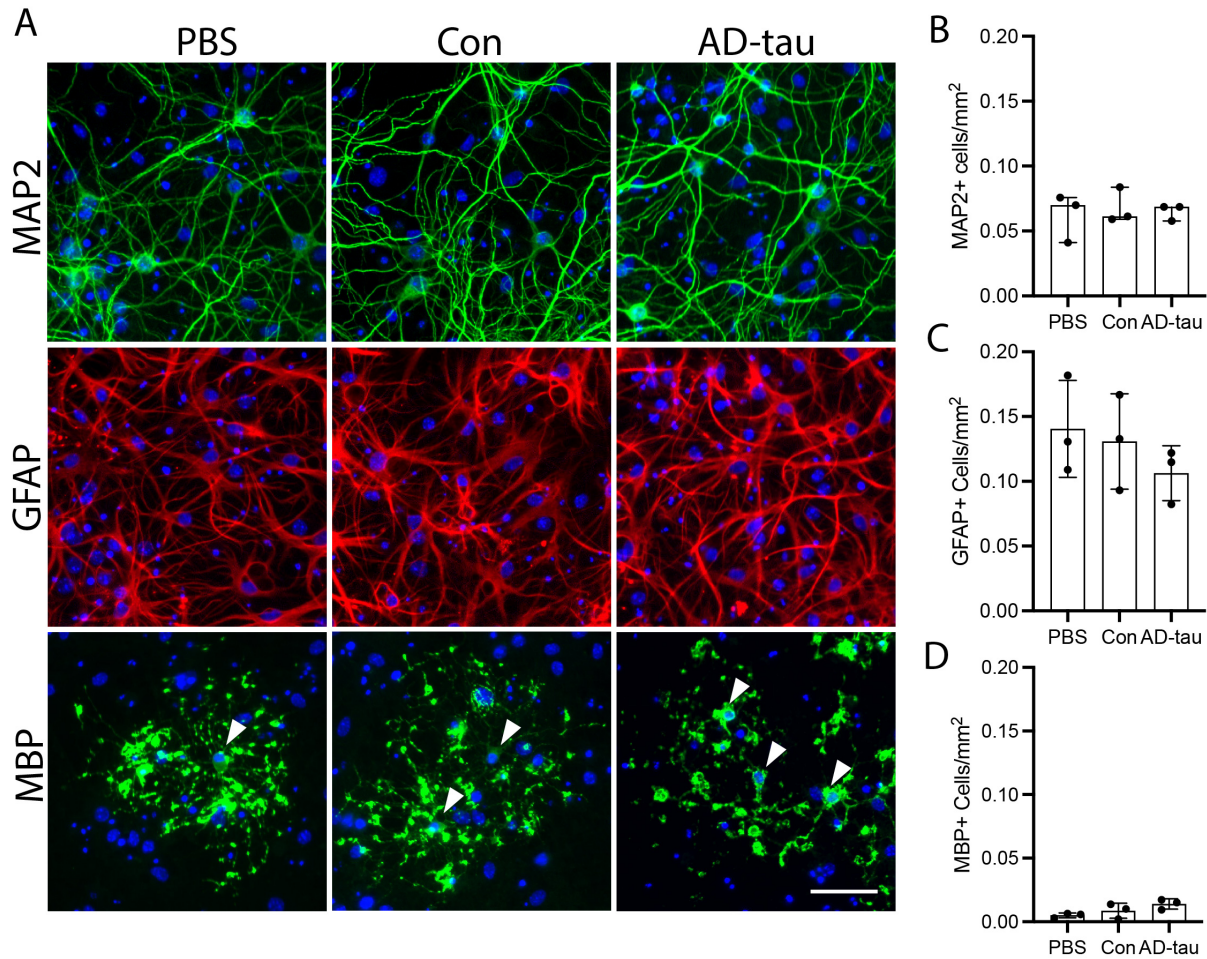


Figure 2.15. Tau seeding does not cause overt cell death. Primary MAPT-KI hippocampal cultures were treated with PBS, Con, or AD-tau on DIV5 and fixed on DIV 33. A) Neurons were immunolabelled with MAP2 (top row; green), astrocytes with glial fibrillary acidic protein (GFAP; red), and oligodendrocytes with myelin basic protein (MBP; bottom row; green). B-D) Cells were manually counted. B) The number of neurons is stable across treatment groups. The data are median \pm interquartile range and were compared using the nonparametric Kruskal-Wallis analysis of variance with Dunn's multiple comparisons test, significance was defined as $p \leq 0.05$. $N=3$; each experimental replicate represents a separate primary neuron harvest. C) No significant change in astrocyte number was observed. D) An increase in MBP was observed in the AD-tau group, this was not statistically significant. Scale bar = 50 μm .

Figure 2.15 (cont'd).

The data in C and D are mean \pm SD and were compared using one-way ANOVA with Tukey's multiple comparisons test, significance was defined as $p \leq 0.05$. N=3; Images are representative of findings in each independent experimental replicate which were derived from separate neuron harvests from unique timed pregnant MAPT-KI females.

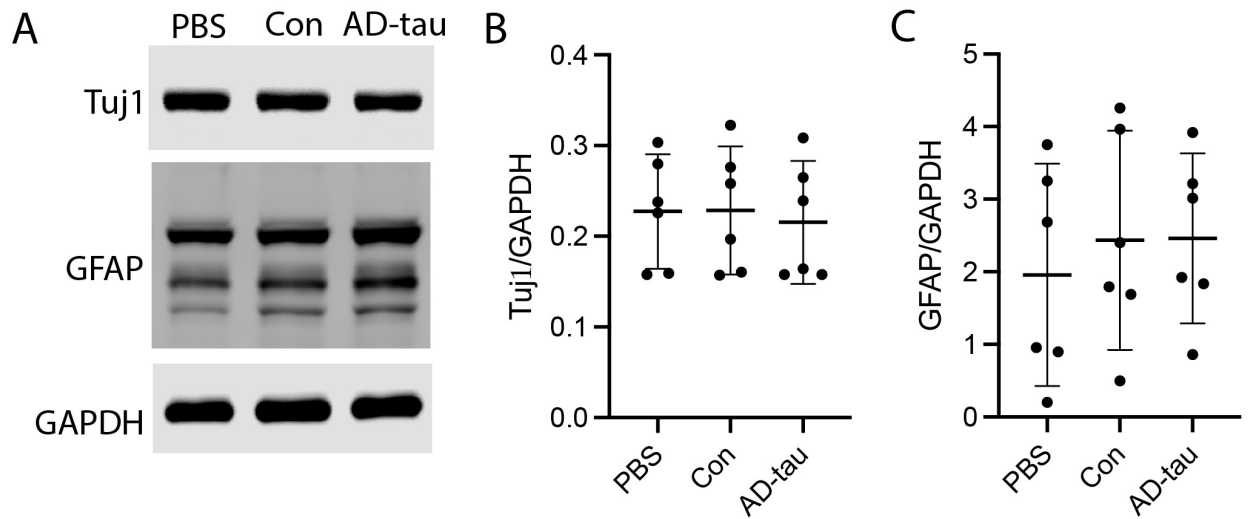


Figure 2.16. Tau seeding does not affect the expression of neuron or astrocyte markers. Primary MAPT-KI hippocampal cultures were treated with PBS, Con, or AD-tau (28 nM) on DIV5 and collected on DIV31. A) Western blot of cell lysates probed with β -III tubulin (TuJ1; neuronal), glial fibrillary acidic protein (GFAP; astrocytic), and GAPDH (loading control) antibodies. B-C) Quantitation of the signal of the β -III tubulin or GFAP protein bands normalized to GAPDH. B) The neuronal protein expression is the same across treatments. C) There is a small, non-statistically significant increase in GFAP in both the Con and AD-tau treated groups compared to PBS. The data are mean \pm SD and were compared using one-way ANOVA with Tukey's multiple comparisons test, significance was defined as $p \leq 0.05$.

Figure 2.16 (cont'd).

N=6; each independent experimental replicate represents a separate primary neuron harvest from unique timed pregnant MAPT-KI females.

DISCUSSION

A unique feature of our seeding model is the use of the MAPT-KI mouse model. Early tau seeding studies were conducted in transgenic animal models (e.g. PS19 mice, ALZ17 mice, rTg4510 mice) that typically overexpress a single tau isoform with or without a tau mutation (Boluda et al., 2015; Chakrabarty et al., 2015; Clavaguera et al., 2013; Clavaguera et al., 2009; Guo & Lee, 2013; Holmes et al., 2014; Iba et al., 2013; Iba et al., 2015; Perez-Rando et al., 2020). Sporadic AD accounts for over 95% of AD cases and is not associated with mutant tau or tau overexpression (Masters et al., 2015). Furthermore, the PHFs and SFs in NFTs are comprised of both 3R and 4R tau. Adult mice only express 4R tau isoforms, and the transgenic models used in earlier tau seeding models typically overexpressed a single isoform of 3R or 4R tau (i.e. mostly 4R tau) (de Calignon et al., 2012; Lewis et al., 2000; Probst et al., 2000; Santacruz et al., 2005; Terwel et al., 2005; Yoshiyama et al., 2007). More recently, tau seeding was studied in wildtype mice or in hTau transgenic mice that overexpress the six human tau isoforms and no mouse tau (Andres-Benito et al., 2022; Guo et al., 2016; He et al., 2020; Narasimhan et al., 2017; Zareba-Paslawska et al., 2020). In contrast, the MAPT-KI model expresses all six human tau isoforms at normal levels, and no tau pathology or cognitive deficits are observed in adult MAPT-KI mice (Benskey et al., 2023; Saito et al., 2019). In humans and mice, only the 0N3R isoform is expressed in fetal brain (Wang & Mandelkow, 2016). The tau isoform expression profile in primary hippocampal neurons harvested from E16 MAPT-KI mice was not known. All but the 2N4R isoforms were detected in culture lysates, albeit 0N3R remained the most prominent isoform

through DIV31. The 2N4R isoform is detected at very low levels in adult MAPT mice (Benskey et al., 2023; Saito et al., 2019) and may be expressed in the MAPT-KI primary cultures at levels below the limit of detection on Western blot. Our cultures are primarily a mix of neurons and astrocytes with a minor oligodendrocyte component (~1%). Furthermore, the expression of tau in neurons and astrocytes in our cultures is consistent with reports of tau expression in neurons and in glia in the brain. These features of the MAPT-KI cells make them an ideal model to study tau seeding.

Early tau seeding studies utilized recombinant tau aggregates or brain homogenates from AD mouse models harboring tau pathology (e.g. PS19 mice) to seed pathological tau (Clavaguera et al., 2009; Guo & Lee, 2013; Iba et al., 2013; Iba et al., 2015). More recently, sarkosyl-insoluble tau purified from human AD-brain tissue was used as seeding material (Andres-Benito et al., 2022; Gibbons et al., 2017; Guo et al., 2016; He et al., 2020; Miao et al., 2019; Narasimhan et al., 2017). The core structures of NFTs and SFs in AD are unique from the core structures of tau filaments in other tauopathies including CBD, PSP and CTE (Scheres et al., 2020). Furthermore, insoluble tau derived from different tauopathies propagate distinct pathological features that are unique to each disease (Narasimhan et al., 2017). Therefore, the best way to study AD-relevant tau species is to use AD-brain-derived tau. The AD-tau samples used here contained PHFs and both 3R and 4R tau isoforms were detected in the seed samples. Known AD-relevant tau species including PHF1, TNT1, and TOC1 were detected as well. Pathological tau was detected at low levels in the Con sample. This is consistent with studies that show pathological tau in cognitively healthy older people, albeit to a lesser extent compared to AD (Bennett et al., 2006; Davis et al., 1999; Ziontz et al., 2019). The amount of tau in the Con sample is relatively minimal compared to the AD-tau sample. For example, ten times the amount of total protein was needed in the Con sample compared

to the AD-sample to reach the detection limit on the tau sELISAs. The difference in the amount of pathological tau in the Con versus AD-tau samples was apparent in the RD Tau P301S seeding assay.

The progressive accumulation of PAD-exposed (TNT1+) tau inclusions in the MAPT-KI primary hippocampal neurons from 9 to 26d post-treatment with AD-tau suggested that tau seeding required endogenous tau. This was confirmed by the lack of TNT1+ tau inclusions in the AD-tau treated Tau-KO mouse primary neurons. The use of methanol for fixation in the time-course studies indicated that the tau inclusions are insoluble, as methanol extracts soluble proteins. Tau inclusions colocalized with β -III tubulin, were only detected when antibodies could enter permeabilized cells, and were present after trypsin digestion (prior to fixation and permeabilization) used to remove extracellular proteins. Together, the data confirm that the tau inclusions were intracellular. The tau inclusions were identified primarily in neurites and are reminiscent of the neuropil threads and dystrophic neurites seen in AD. Pathological tau was rarely observed in the somatodendritic compartment. This pattern of seeding is consistent with other seeding studies using AD-tau in wildtype or hTau mouse primary neurons (Gibbons et al., 2020; Guo et al., 2016; He et al., 2020; Narasimhan et al., 2017; Saito et al., 2019). Seeding in the somatodendritic compartment was relatively rare. Not all tau inclusions colocalized with β -III tubulin, though they shared the thread-like morphology that would suggest they were intraneuronal. Astrocytes are a substantial component in the primary cultures, and they express tau. Thus, I assessed tau seeding in astrocytes and did not find evidence of tau inclusions in astrocytes.

The colocalization of PAD-exposed tau with pS422, AT8 and TOC1 is consistent with human AD tissue studies (Christensen et al., 2019; Combs et al., 2016; Cox et al., 2016; Kanaan

et al., 2016; Kanaan et al., 2011; Tiernan et al., 2016). These are markers of pretangle pathology early in AD and persist through later stages of the disease.

I observed TauC3⁺ inclusions, albeit at a much lower frequency compared to the TNT1⁺ inclusions. TauC3⁺ is specific to tau truncated at D421. Caspase 3 cleaves tau at this site, D421 truncated tau is associated with toxicity (Conze et al., 2022; Zhang et al., 2009; Zhao et al., 2015), and increased caspase 3 activity is associated with AD (Gastard et al., 2003; Su et al., 2001). Due to the infrequent appearance of TauC3⁺ inclusions, caspase activation is not likely widespread in these cultures. The data showing that Caspase-3/7 levels were unchanged in the AD-tau-treated cultures supports a lack of overactive caspase. Truncation of tau at D421 is considered a mid to late change in the evolution of tangle formation (Guillozet-Bongaarts et al., 2006). The evidence presented here shows that most of the seeded tau inclusions are comprised of tau species associated with early pretangle stages. Consistent with this, I did not observe ThR⁺ inclusions, suggesting that tau inclusions have not developed into β -sheet structures at this point, a characteristic associated with later stages of tau aggregation into filaments.

Tau seeding did not affect cell viability or lead to overt loss of neurons, astrocytes or oligodendrocytes. There was a non-significant trend showing an increase in oligodendrocytes in the AD-tau treated cells, however oligodendrocyte numbers were highly variable between cultures. Oligodendrocytes support neurons through myelination and new oligodendrocytes and myelin can be generated to meet the needs of neurons (LoPresti, 2018). The increase in oligodendrocytes could be a compensatory response to early neuronal pathology in the seeded cultures. Another potential explanation could be the presence of growth factors present in or induced by the AD-tau material. Further studies are needed to determine what is driving the trend. Though not statistically significant, the mean GFAP protein levels in the Con and AD-tau-treated cultures were 24% and

26% increased compared to that observed in the PBS-treated cultures, respectively. The astrocyte number did not increase (ICF), and the increase in GFAP protein on Western blot could be due to enhanced expression, which is known to occur with astrocyte reactivity (Eng & Ghirnikar, 1994). The increase of GFAP protein was observed in the Con and AD-tau-treated groups, which suggests the addition of sarkosyl-insoluble human brain material, and not tau or tau seeding, likely drove this effect. Again, future studies are required to determine what is causing the mild change in astrocyte GFAP expression.

The lack of overt cell toxicity is consistent with the majority of *in vitro* and *in vivo* tau seeding studies and specifically in seeding studies using AD-tau seeds (Gibbons et al., 2017; Guo et al., 2016; Hayashi et al., 2021; He et al., 2020; Miao et al., 2019; Narasimhan et al., 2017; Saito et al., 2019). One study showed that treatment of primary cortical neurons from wildtype mice with AD-tau resulted in primarily neuritic tau pathology and no overt toxicity was reported (Guo et al., 2016). A separate study using primary neurons from transgenic mice expressing mutant tau (JNPL3 mice) showed increased LDH levels and decreased NeuN levels by 7d post-treatment with AD-tau. The toxicity observed was likely due to the overexpression of the pro-aggregant P301L tau (Congdon et al., 2016). The post-treatment interval (26-28d post-treatment) in these studies may be too short for overt toxicity to occur. A caveat of these experiments is that seeding did not occur in all neurons nor did it occur in the vast majority of somatodendritic compartments of neurons, therefore the effects of pathological tau within individual neurons or neuronal compartments could be “washed out” when looking at the culture-level. It is also possible that compensatory mechanisms (e.g. upregulation of other microtubule associated proteins, increased autophagy, altered glial activity) protect against overt toxicity. Age and AD-related cellular stressors may be required for tau-mediated toxicity (i.e., oxidative stress, autophagy pathway

dysfunction, mitochondrial dysfunction). Perhaps it would be useful to incorporate a second stressor in this model.

This novel seeding model recapitulates several forms of AD-associated tau pathology, mostly in the form of pretangle-associated tau species. The lack of overt toxicity suggests that this model may be used to study the effects of pathological tau on neurons in early stages of pathogenesis (i.e. axon and synaptic dysfunction). Furthermore, this model likely holds great potential for determining the effects of multiple hits in a model that displays early pretangle forms of pathogenic tau on the backdrop of cells that do not overexpress tau and express human tau isoforms (not murine tau).

REFERENCES

- 2024 Alzheimer's disease facts and figures. (2024, May). *Alzheimers Dement*, 20(5), 3708-3821. <https://doi.org/10.1002/alz.13809>
- Andres-Benito, P., Carmona, M., Jordan, M., Fernandez-Irigoyen, J., Santamaria, E., Del Rio, J. A., & Ferrer, I. (2022, Jan 10). Host Tau Genotype Specifically Designs and Regulates Tau Seeding and Spreading and Host Tau Transformation Following Intrahippocampal Injection of Identical Tau AD Inoculum. *Int J Mol Sci*, 23(2). <https://doi.org/10.3390/ijms23020718>
- Bennett, D. A., Schneider, J. A., Arvanitakis, Z., Kelly, J. F., Aggarwal, N. T., Shah, R. C., & Wilson, R. S. (2006, Jun 27). Neuropathology of older persons without cognitive impairment from two community-based studies. *Neurology*, 66(12), 1837-1844. <https://doi.org/10.1212/01.wnl.0000219668.47116.e6>
- Benskey, M. J., Panoushek, S., Saito, T., Saido, T. C., Grabinski, T., & Kanaan, N. M. (2023). Behavioral and neuropathological characterization over the adult lifespan of the human tau knock-in mouse. *Front Aging Neurosci*, 15, 1265151. <https://doi.org/10.3389/fnagi.2023.1265151>
- Berry, R. W., Sweet, A. P., Clark, F. A., Lagalwar, S., Lapin, B. R., Wang, T., Topgi, S., Guillozet-Bongaarts, A. L., Cochran, E. J., Bigio, E. H., & Binder, L. I. (2004, May). Tau epitope display in progressive supranuclear palsy and corticobasal degeneration. *J Neurocytol*, 33(3), 287-295. <https://doi.org/10.1023/B:NEUR.0000044190.96426.b9>
- Biernat, J., Mandelkow, E., Schröter, C., Lichtenberg-Kraag, B., Steiner, B., Berling, B., Meyer, H., Mercken, M., Vandermeeren, A., & Goedert, M. (1992). The switch of tau protein to an Alzheimer-like state includes the phosphorylation of two serine-proline motifs upstream of the microtubule binding region. *The EMBO journal*, 11(4), 1593-1597.
- Binder, L. I., Frankfurter, A., & Rebhun, L. I. (1986). Differential localization of MAP-2 and tau in mammalian neurons in situ. *Ann N Y Acad Sci*, 466, 145-166. <https://doi.org/10.1111/j.1749-6632.1986.tb38392.x>
- Boluda, S., Iba, M., Zhang, B., Raible, K. M., Lee, V. M., & Trojanowski, J. Q. (2015, Feb). Differential induction and spread of tau pathology in young PS19 tau transgenic mice following intracerebral injections of pathological tau from Alzheimer's disease or corticobasal degeneration brains. *Acta Neuropathol*, 129(2), 221-237. <https://doi.org/10.1007/s00401-014-1373-0>
- Braak, H., Alafuzoff, I., Arzberger, T., Kretschmar, H., & Del Tredici, K. (2006). Staging of Alzheimer disease-associated neurofibrillary pathology using paraffin sections and immunocytochemistry. *Acta neuropathologica*, 112(4), 389-404.

- Braak, H., & Braak, E. (1991). Neuropathological staging of Alzheimer-related changes. *Acta Neuropathol*, 82(4), 239-259. <https://doi.org/10.1007/BF00308809>
- Braak, H., Thal, D. R., Ghebremedhin, E., & Del Tredici, K. (2011, Nov). Stages of the pathologic process in Alzheimer disease: age categories from 1 to 100 years. *J Neuropathol Exp Neurol*, 70(11), 960-969. <https://doi.org/10.1097/NEN.0b013e318232a379>
- Caccamo, D., Katsetos, C. D., Herman, M. M., Frankfurter, A., Collins, V. P., & Rubinstein, L. J. (1989, Mar). Immunohistochemistry of a spontaneous murine ovarian teratoma with neuroepithelial differentiation. Neuron-associated beta-tubulin as a marker for primitive neuroepithelium. *Lab Invest*, 60(3), 390-398. <https://www.ncbi.nlm.nih.gov/pubmed/2467076>
- Caceres, A., Binder, L. I., Payne, M. R., Bender, P., Rebhun, L., & Steward, O. (1984, Feb). Differential subcellular localization of tubulin and the microtubule-associated protein MAP2 in brain tissue as revealed by immunocytochemistry with monoclonal hybridoma antibodies. *J Neurosci*, 4(2), 394-410. <https://doi.org/10.1523/JNEUROSCI.04-02-00394.1984>
- Carmel, G., Mager, E. M., Binder, L. I., & Kuret, J. (1996, Dec 20). The structural basis of monoclonal antibody Alz50's selectivity for Alzheimer's disease pathology. *J Biol Chem*, 271(51), 32789-32795. <https://doi.org/10.1074/jbc.271.51.32789>
- Chakrabarty, P., Hudson, V. J., III, Sacino, A. N., Brooks, M. M., D'Alton, S., Lewis, J., Golde, T. E., & Giasson, B. I. (2015, Aug). Inefficient induction and spread of seeded tau pathology in P301L mouse model of tauopathy suggests inherent physiological barriers to transmission. *Acta Neuropathol*, 130(2), 303-305. <https://doi.org/10.1007/s00401-015-1444-x>
- Christensen, K. R., Beach, T. G., Serrano, G. E., & Kanaan, N. M. (2019, Feb 28). Pathogenic tau modifications occur in axons before the somatodendritic compartment in mossy fiber and Schaffer collateral pathways. *Acta Neuropathol Commun*, 7(1), 29. <https://doi.org/10.1186/s40478-019-0675-9>
- Christensen, K. R., Beach, T. G., Serrano, G. E., & Kanaan, N. M. (2019). Pathogenic tau modifications occur in axons before the somatodendritic compartment in mossy fiber and Schaffer collateral pathways. *Acta neuropathologica communications*, 7, 1-21.
- Christensen, K. R., Combs, B., Richards, C., Grabinski, T., Alhadidy, M. M., & Kanaan, N. M. (2023). Phosphomimetics at Ser199/Ser202/Thr205 in tau impairs axonal transport in rat hippocampal neurons. *Molecular Neurobiology*, 60(6), 3423-3438.
- Clavaguera, F., Akatsu, H., Fraser, G., Crowther, R. A., Frank, S., Hench, J., Probst, A., Winkler, D. T., Reichwald, J., Staufenbiel, M., Ghetti, B., Goedert, M., & Tolnay, M. (2013, Jun 4). Brain homogenates from human tauopathies induce tau inclusions in mouse brain. *Proc Natl Acad Sci U S A*, 110(23), 9535-9540. <https://doi.org/10.1073/pnas.1301175110>

- Clavaguera, F., Bolmont, T., Crowther, R. A., Abramowski, D., Frank, S., Probst, A., Fraser, G., Stalder, A. K., Beibel, M., & Staufenbiel, M. (2009). Transmission and spreading of tauopathy in transgenic mouse brain. *Nature cell biology*, *11*(7), 909-913.
- Combs, B., Christensen, K. R., Richards, C., Kneynsberg, A., Mueller, R. L., Morris, S. L., Morfini, G. A., Brady, S. T., & Kanaan, N. M. (2021). Frontotemporal lobar dementia mutant tau impairs axonal transport through a protein phosphatase 1 γ -dependent mechanism. *Journal of neuroscience*, *41*(45), 9431-9451.
- Combs, B., Hamel, C., & Kanaan, N. M. (2016, Oct). Pathological conformations involving the amino terminus of tau occur early in Alzheimer's disease and are differentially detected by monoclonal antibodies. *Neurobiol Dis*, *94*, 18-31. <https://doi.org/10.1016/j.nbd.2016.05.016>
- Combs, B., Mueller, R. L., Morfini, G., Brady, S. T., & Kanaan, N. M. (2019). Tau and axonal transport misregulation in tauopathies. *Tau Biology*, 81-95.
- Combs, B., Tiernan, C. T., Hamel, C., & Kanaan, N. M. (2017). Production of recombinant tau oligomers in vitro. *Methods Cell Biol*, *141*, 45-64. <https://doi.org/10.1016/bs.mcb.2017.06.005>
- Conze, C., Rierola, M., Trushina, N. I., Peters, M., Janning, D., Holzer, M., Heinisch, J. J., Arendt, T., Bakota, L., & Brandt, R. (2022, Jul). Caspase-cleaved tau is senescence-associated and induces a toxic gain of function by putting a brake on axonal transport. *Mol Psychiatry*, *27*(7), 3010-3023. <https://doi.org/10.1038/s41380-022-01538-2>
- Cox, K., Combs, B., Abdelmesih, B., Morfini, G., Brady, S. T., & Kanaan, N. M. (2016). Analysis of isoform-specific tau aggregates suggests a common toxic mechanism involving similar pathological conformations and axonal transport inhibition. *Neurobiology of aging*, *47*, 113-126.
- Cox, K., Combs, B., Abdelmesih, B., Morfini, G., Brady, S. T., & Kanaan, N. M. (2016, Nov). Analysis of isoform-specific tau aggregates suggests a common toxic mechanism involving similar pathological conformations and axonal transport inhibition. *Neurobiol Aging*, *47*, 113-126. <https://doi.org/10.1016/j.neurobiolaging.2016.07.015>
- Crowther, R. (1991). Straight and paired helical filaments in Alzheimer disease have a common structural unit. *Proceedings of the National Academy of Sciences*, *88*(6), 2288-2292.
- Davis, D. G., Schmitt, F. A., Wekstein, D. R., & Markesbery, W. R. (1999, Apr). Alzheimer neuropathologic alterations in aged cognitively normal subjects. *J Neuropathol Exp Neurol*, *58*(4), 376-388. <https://doi.org/10.1097/00005072-199904000-00008>
- de Calignon, A., Polydoro, M., Suarez-Calvet, M., William, C., Adamowicz, D. H., Kopeikina, K. J., Pitstick, R., Sahara, N., Ashe, K. H., Carlson, G. A., Spires-Jones, T. L., & Hyman, B.

- T. (2012, Feb 23). Propagation of tau pathology in a model of early Alzheimer's disease. *Neuron*, 73(4), 685-697. <https://doi.org/10.1016/j.neuron.2011.11.033>
- Eng, L. F., & Ghirnikar, R. S. (1994, Jul). Gfap and Astrogliosis. *Brain Pathology*, 4(3), 229-237. <https://doi.org/DOI 10.1111/j.1750-3639.1994.tb00838.x>
- Fitzpatrick, A. W., Falcon, B., He, S., Murzin, A. G., Murshudov, G., Garringer, H. J., Crowther, R. A., Ghetti, B., Goedert, M., & Scheres, S. H. (2017). Cryo-EM structures of tau filaments from Alzheimer's disease. *Nature*, 547(7662), 185-190.
- Frost, B., Jacks, R. L., & Diamond, M. I. (2009). Propagation of tau misfolding from the outside to the inside of a cell. *Journal of biological chemistry*, 284(19), 12845-12852.
- Gamblin, T. C., Chen, F., Zambrano, A., Abraha, A., Lagalwar, S., Guillozet, A. L., Lu, M., Fu, Y., Garcia-Sierra, F., LaPointe, N., Miller, R., Berry, R. W., Binder, L. I., & Cryns, V. L. (2003, Aug 19). Caspase cleavage of tau: linking amyloid and neurofibrillary tangles in Alzheimer's disease. *Proc Natl Acad Sci U S A*, 100(17), 10032-10037. <https://doi.org/10.1073/pnas.1630428100>
- Gastard, M. C., Troncoso, J. C., & Koliatsos, V. E. (2003, Sep). Caspase activation in the limbic cortex of subjects with early Alzheimer's disease. *Ann Neurol*, 54(3), 393-398. <https://doi.org/10.1002/ana.10680>
- Gibbons, G. S., Banks, R. A., Kim, B., Xu, H., Changolkar, L., Leight, S. N., Riddle, D. M., Li, C., Gathagan, R. J., Brown, H. J., Zhang, B., Trojanowski, J. Q., & Lee, V. M. (2017, Nov 22). GFP-Mutant Human Tau Transgenic Mice Develop Tauopathy Following CNS Injections of Alzheimer's Brain-Derived Pathological Tau or Synthetic Mutant Human Tau Fibrils. *J Neurosci*, 37(47), 11485-11494. <https://doi.org/10.1523/JNEUROSCI.2393-17.2017>
- Gibbons, G. S., Kim, S. J., Wu, Q., Riddle, D. M., Leight, S. N., Changolkar, L., Xu, H., Meymand, E. S., O'Reilly, M., Zhang, B., Brunden, K. R., Trojanowski, J. Q., & Lee, V. M. Y. (2020, Nov 4). Conformation-selective tau monoclonal antibodies inhibit tau pathology in primary neurons and a mouse model of Alzheimer's disease. *Mol Neurodegener*, 15(1), 64. <https://doi.org/10.1186/s13024-020-00404-5>
- Gibbons, G. S., Lee, V. M., & Trojanowski, J. Q. (2019). Mechanisms of cell-to-cell transmission of pathological tau: a review. *JAMA neurology*, 76(1), 101-108.
- Goedert, M., Jakes, R., & Vanmechelen, E. (1995). Monoclonal antibody AT8 recognises tau protein phosphorylated at both serine 202 and threonine 205. *Neuroscience letters*, 189(3), 167-170.
- Greenberg, S., Davies, P., Schein, J., & Binder, L. (1992). Hydrofluoric acid-treated tau PHF proteins display the same biochemical properties as normal tau. *Journal of biological chemistry*, 267(1), 564-569.

- Guillozet-Bongaarts, A. L., Garcia-Sierra, F., Reynolds, M. R., Horowitz, P. M., Fu, Y., Wang, T., Cahill, M. E., Bigio, E. H., Berry, R. W., & Binder, L. I. (2005, Jul). Tau truncation during neurofibrillary tangle evolution in Alzheimer's disease. *Neurobiol Aging*, *26*(7), 1015-1022. <https://doi.org/10.1016/j.neurobiolaging.2004.09.019>
- Guillozet-Bongaarts, A. L., Cahill, M. E., Cryns, V. L., Reynolds, M. R., Berry, R. W., & Binder, L. I. (2006). Pseudophosphorylation of tau at serine 422 inhibits caspase cleavage: in vitro evidence and implications for tangle formation in vivo. *Journal of neurochemistry*, *97*(4), 1005-1014.
- Guo, J. L., & Lee, V. M. (2013, Mar 18). Neurofibrillary tangle-like tau pathology induced by synthetic tau fibrils in primary neurons over-expressing mutant tau. *FEBS Lett*, *587*(6), 717-723. <https://doi.org/10.1016/j.febslet.2013.01.051>
- Guo, J. L., & Lee, V. M.-Y. (2011). Seeding of normal Tau by pathological Tau conformers drives pathogenesis of Alzheimer-like tangles. *Journal of biological chemistry*, *286*(17), 15317-15331.
- Guo, J. L., Narasimhan, S., Changolkar, L., He, Z., Stieber, A., Zhang, B., Gathagan, R. J., Iba, M., McBride, J. D., & Trojanowski, J. Q. (2016). Unique pathological tau conformers from Alzheimer's brains transmit tau pathology in nontransgenic mice. *Journal of Experimental Medicine*, *213*(12), 2635-2654.
- Harrington, C. R., Mukaetova-Ladinska, E. B., Hills, R., Edwards, P. C., Montejo de Garcini, E., Novak, M., & Wischik, C. M. (1991, Jul 1). Measurement of distinct immunochemical presentations of tau protein in Alzheimer disease. *Proc Natl Acad Sci U S A*, *88*(13), 5842-5846. <https://doi.org/10.1073/pnas.88.13.5842>
- Hayashi, T., Shimonaka, S., Elahi, M., Matsumoto, S. E., Ishiguro, K., Takanashi, M., Hattori, N., & Motoi, Y. (2021). Learning Deficits Accompanied by Microglial Proliferation After the Long-Term Post-Injection of Alzheimer's Disease Brain Extract in Mouse Brains. *J Alzheimers Dis*, *79*(4), 1701-1711. <https://doi.org/10.3233/JAD-201002>
- He, Z., McBride, J. D., Xu, H., Changolkar, L., Kim, S.-j., Zhang, B., Narasimhan, S., Gibbons, G. S., Guo, J. L., & Kozak, M. (2020). Transmission of tauopathy strains is independent of their isoform composition. *Nature communications*, *11*(1), 7.
- Holmes, B. B., Furman, J. L., Mahan, T. E., Yamasaki, T. R., Mirbaha, H., Eades, W. C., Belaygorod, L., Cairns, N. J., Holtzman, D. M., & Diamond, M. I. (2014, Oct 14). Proteopathic tau seeding predicts tauopathy in vivo. *Proc Natl Acad Sci U S A*, *111*(41), E4376-4385. <https://doi.org/10.1073/pnas.1411649111>
- Horowitz, P. M., LaPointe, N., Guillozet-Bongaarts, A. L., Berry, R. W., & Binder, L. I. (2006, Oct 24). N-terminal fragments of tau inhibit full-length tau polymerization in vitro. *Biochemistry*, *45*(42), 12859-12866. <https://doi.org/10.1021/bi061325g>

- Iba, M., Guo, J. L., McBride, J. D., Zhang, B., Trojanowski, J. Q., & Lee, V. M. (2013, Jan 16). Synthetic tau fibrils mediate transmission of neurofibrillary tangles in a transgenic mouse model of Alzheimer's-like tauopathy. *J Neurosci*, *33*(3), 1024-1037. <https://doi.org/10.1523/JNEUROSCI.2642-12.2013>
- Iba, M., McBride, J. D., Guo, J. L., Zhang, B., Trojanowski, J. Q., & Lee, V. M.-Y. (2015). Tau pathology spread in PS19 tau transgenic mice following locus coeruleus (LC) injections of synthetic tau fibrils is determined by the LC's afferent and efferent connections. *Acta neuropathologica*, *130*, 349-362.
- Kalcheva, N., Albala, J. S., Binder, L. I., & Shafit-Zagardo, B. (1994, Dec). Localization of specific epitopes on human microtubule-associated protein 2. *J Neurochem*, *63*(6), 2336-2341. <https://doi.org/10.1046/j.1471-4159.1994.63062336.x>
- Kanaan, N. M., Cox, K., Alvarez, V. E., Stein, T. D., Poncil, S., & McKee, A. C. (2016, Jan). Characterization of Early Pathological Tau Conformations and Phosphorylation in Chronic Traumatic Encephalopathy. *J Neuropathol Exp Neurol*, *75*(1), 19-34. <https://doi.org/10.1093/jnen/nlv001>
- Kanaan, N. M., Morfini, G., Pigino, G., LaPointe, N. E., Andreadis, A., Song, Y., Leitman, E., Binder, L. I., & Brady, S. T. (2012). Phosphorylation in the amino terminus of tau prevents inhibition of anterograde axonal transport. *Neurobiology of aging*, *33*(4), 826. e815-826. e830.
- Kanaan, N. M., Morfini, G. A., LaPointe, N. E., Pigino, G. F., Patterson, K. R., Song, Y., Andreadis, A., Fu, Y., Brady, S. T., & Binder, L. I. (2011, Jul 6). Pathogenic forms of tau inhibit kinesin-dependent axonal transport through a mechanism involving activation of axonal phosphotransferases. *J Neurosci*, *31*(27), 9858-9868. <https://doi.org/10.1523/JNEUROSCI.0560-11.2011>
- Kanaan, N. M., Morfini, G. A., LaPointe, N. E., Pigino, G. F., Patterson, K. R., Song, Y., Andreadis, A., Fu, Y., Brady, S. T., & Binder, L. I. (2011). Pathogenic forms of tau inhibit kinesin-dependent axonal transport through a mechanism involving activation of axonal phosphotransferases. *Journal of neuroscience*, *31*(27), 9858-9868.
- Kimura, T., Ono, T., Takamatsu, J., Yamamoto, H., Ikegami, K., Kondo, A., Hasegawa, M., Ihara, Y., Miyamoto, E., & Miyakawa, T. (1996). Sequential changes of tau-site-specific phosphorylation during development of paired helical filaments. *Dementia and Geriatric Cognitive Disorders*, *7*(4), 177-181.
- LaPointe, N. E., Morfini, G., Pigino, G., Gaisina, I. N., Kozikowski, A. P., Binder, L. I., & Brady, S. T. (2009). The amino terminus of tau inhibits kinesin-dependent axonal transport: implications for filament toxicity. *Journal of neuroscience research*, *87*(2), 440-451.
- Lewis, J., McGowan, E., Rockwood, J., Melrose, H., Nacharaju, P., Van Slegtenhorst, M., Gwinn-Hardy, K., Paul Murphy, M., Baker, M., Yu, X., Duff, K., Hardy, J., Corral, A., Lin, W. L., Yen, S. H., Dickson, D. W., Davies, P., & Hutton, M. (2000, Aug). Neurofibrillary

- tangles, amyotrophy and progressive motor disturbance in mice expressing mutant (P301L) tau protein. *Nat Genet*, 25(4), 402-405. <https://doi.org/10.1038/78078>
- LoPresti, P. (2018, Aug 15). Tau in Oligodendrocytes Takes Neurons in Sickness and in Health. *Int J Mol Sci*, 19(8). <https://doi.org/10.3390/ijms19082408>
- LoPresti, P., Szuchet, S., Papasozomenos, S. C., Zinkowski, R. P., & Binder, L. I. (1995, Oct 24). Functional implications for the microtubule-associated protein tau: localization in oligodendrocytes. *Proc Natl Acad Sci U S A*, 92(22), 10369-10373. <https://doi.org/10.1073/pnas.92.22.10369>
- Luna-Munoz, J., Peralta-Ramirez, J., Chavez-Macias, L., Harrington, C. R., Wischik, C. M., & Mena, R. (2008, Nov). Thiazin red as a neuropathological tool for the rapid diagnosis of Alzheimer's disease in tissue imprints. *Acta Neuropathol*, 116(5), 507-515. <https://doi.org/10.1007/s00401-008-0431-x>
- Luna-Viramontes, N. I., Campa-Cordoba, B. B., Ontiveros-Torres, M. A., Harrington, C. R., Villanueva-Fierro, I., Guadarrama-Ortiz, P., Garces-Ramirez, L., de la Cruz, F., Hernandez-Alejandro, M., Martinez-Robles, S., Gonzalez-Ballesteros, E., Pacheco-Herrero, M., & Luna-Munoz, J. (2020). PHF-Core Tau as the Potential Initiating Event for Tau Pathology in Alzheimer's Disease. *Front Cell Neurosci*, 14, 247. <https://doi.org/10.3389/fncel.2020.00247>
- Malia, T. J., Teplyakov, A., Ernst, R., Wu, S. J., Lacy, E. R., Liu, X., Vandermeeren, M., Mercken, M., Luo, J., & Sweet, R. W. (2016). Epitope mapping and structural basis for the recognition of phosphorylated tau by the anti-tau antibody AT8. *Proteins: Structure, Function, and Bioinformatics*, 84(4), 427-434.
- Masters, C. L., Bateman, R., Blennow, K., Rowe, C. C., Sperling, R. A., & Cummings, J. L. (2015, Oct 15). Alzheimer's disease. *Nat Rev Dis Primers*, 1, 15056. <https://doi.org/10.1038/nrdp.2015.56>
- Mena, R., Edwards, P., Perez-Olvera, O., & Wischik, C. M. (1995). Monitoring pathological assembly of tau and beta-amyloid proteins in Alzheimer's disease. *Acta Neuropathol*, 89(1), 50-56. <https://doi.org/10.1007/BF00294259>
- Miao, J., Shi, R., Li, L., Chen, F., Zhou, Y., Tung, Y. C., Hu, W., Gong, C. X., Iqbal, K., & Liu, F. (2019). Pathological Tau From Alzheimer's Brain Induces Site-Specific Hyperphosphorylation and SDS- and Reducing Agent-Resistant Aggregation of Tau in vivo. *Front Aging Neurosci*, 11, 34. <https://doi.org/10.3389/fnagi.2019.00034>
- Morfini, G. A., Burns, M., Binder, L. I., Kanaan, N. M., LaPointe, N., Bosco, D. A., Brown, R. H., Brown, H., Tiwari, A., & Hayward, L. (2009). Axonal transport defects in neurodegenerative diseases. *Journal of neuroscience*, 29(41), 12776-12786.

- Mueller, R. L., Combs, B., Alhadidy, M. M., Brady, S. T., Morfini, G. A., & Kanaan, N. M. (2021). Tau: A Signaling Hub Protein. *Front Mol Neurosci*, *14*, 647054. <https://doi.org/10.3389/fnmol.2021.647054>
- Mueller, R. L., Kanaan, N. M., & Combs, B. (2023, Dec 22). Using Live-Cell Imaging to Measure the Effects of Pathological Proteins on Axonal Transport in Primary Hippocampal Neurons. *J Vis Exp*(202). <https://doi.org/10.3791/66156>
- Narasimhan, S., Guo, J. L., Changolkar, L., Stieber, A., McBride, J. D., Silva, L. V., He, Z., Zhang, B., Gathagan, R. J., & Trojanowski, J. Q. (2017). Pathological tau strains from human brains recapitulate the diversity of tauopathies in nontransgenic mouse brain. *Journal of neuroscience*, *37*(47), 11406-11423.
- Narasimhan, S., & Lee, V. M. (2017). The use of mouse models to study cell-to-cell transmission of pathological tau. In *Methods in cell biology* (Vol. 141, pp. 287-305). Elsevier.
- Novak, M., Wischik, C. M., Edwards, P., Pannell, R., & Milstein, C. (1989). Characterisation of the first monoclonal antibody against the pronase resistant core of the Alzheimer PHF. *Prog Clin Biol Res*, *317*, 755-761. <https://www.ncbi.nlm.nih.gov/pubmed/2602435>
- Otvos Jr, L., Feiner, L., Lang, E., Szendrei, G., Goedert, M., & Lee, V. M. Y. (1994). Monoclonal antibody PHF-1 recognizes tau protein phosphorylated at serine residues 396 and 404. *Journal of neuroscience research*, *39*(6), 669-673.
- Patterson, K. R., Remmers, C., Fu, Y., Brooker, S., Kanaan, N. M., Vana, L., Ward, S., Reyes, J. F., Philibert, K., Glucksman, M. J., & Binder, L. I. (2011, Jul 1). Characterization of prefibrillar Tau oligomers in vitro and in Alzheimer disease. *J Biol Chem*, *286*(26), 23063-23076. <https://doi.org/10.1074/jbc.M111.237974>
- Perez-Rando, M., Dujardin, S., Bennett, R. E., Commins, C., Nibhanupudy, T., & Hyman, B. T. (2020, Oct 19). Synaptic and metabolic gene expression alterations in neurons that are recipients of proteopathic tau seeds. *Acta Neuropathol Commun*, *8*(1), 168. <https://doi.org/10.1186/s40478-020-01049-7>
- Probst, A., Gotz, J., Wiederhold, K. H., Tolnay, M., Mistl, C., Jaton, A. L., Hong, M., Ishihara, T., Lee, V. M., Trojanowski, J. Q., Jakes, R., Crowther, R. A., Spillantini, M. G., Burki, K., & Goedert, M. (2000, May). Axonopathy and amyotrophy in mice transgenic for human four-repeat tau protein. *Acta Neuropathol*, *99*(5), 469-481. <https://doi.org/10.1007/s004010051148>
- Saito, T., Mihira, N., Matsuba, Y., Sasaguri, H., Hashimoto, S., Narasimhan, S., Zhang, B., Murayama, S., Higuchi, M., Lee, V. M. Y., Trojanowski, J. Q., & Saido, T. C. (2019, Aug 23). Humanization of the entire murine Mapt gene provides a murine model of pathological human tau propagation. *J Biol Chem*, *294*(34), 12754-12765. <https://doi.org/10.1074/jbc.RA119.009487>

- Santacruz, K., Lewis, J., Spires, T., Paulson, J., Kotilinek, L., Ingelsson, M., Guimaraes, A., DeTure, M., Ramsden, M., McGowan, E., Forster, C., Yue, M., Orne, J., Janus, C., Mariash, A., Kuskowski, M., Hyman, B., Hutton, M., & Ashe, K. H. (2005, Jul 15). Tau suppression in a neurodegenerative mouse model improves memory function. *Science*, *309*(5733), 476-481. <https://doi.org/10.1126/science.1113694>
- Scheres, S. H., Zhang, W., Falcon, B., & Goedert, M. (2020, Oct). Cryo-EM structures of tau filaments. *Curr Opin Struct Biol*, *64*, 17-25. <https://doi.org/10.1016/j.sbi.2020.05.011>
- Su, J. H., Zhao, M., Anderson, A. J., Srinivasan, A., & Cotman, C. W. (2001, Apr 20). Activated caspase-3 expression in Alzheimer's and aged control brain: correlation with Alzheimer pathology. *Brain Research*, *898*(2), 350-357. [https://doi.org/10.1016/S0006-8993\(01\)02018-2](https://doi.org/10.1016/S0006-8993(01)02018-2)
- Terwel, D., Lasrado, R., Snauwaert, J., Vandeweert, E., Van Haesendonck, C., Borghgraef, P., & Van Leuven, F. (2005, Feb 4). Changed conformation of mutant Tau-P301L underlies the moribund tauopathy, absent in progressive, nonlethal axonopathy of Tau-4R/2N transgenic mice. *J Biol Chem*, *280*(5), 3963-3973. <https://doi.org/10.1074/jbc.M409876200>
- Tiernan, C. T., Combs, B., Cox, K., Morfini, G., Brady, S. T., Counts, S. E., & Kanaan, N. M. (2016, Sep). Pseudophosphorylation of tau at S422 enhances SDS-stable dimer formation and impairs both anterograde and retrograde fast axonal transport. *Exp Neurol*, *283*(Pt A), 318-329. <https://doi.org/10.1016/j.expneurol.2016.06.030>
- Tiernan, C. T., Ginsberg, S. D., He, B., Ward, S. M., Guillozet-Bongaarts, A. L., Kanaan, N. M., Mufson, E. J., & Counts, S. E. (2018, Sep). Pretangle pathology within cholinergic nucleus basalis neurons coincides with neurotrophic and neurotransmitter receptor gene dysregulation during the progression of Alzheimer's disease. *Neurobiol Dis*, *117*, 125-136. <https://doi.org/10.1016/j.nbd.2018.05.021>
- Tiernan, C. T., Mufson, E. J., Kanaan, N. M., & Counts, S. E. (2018, Mar 1). Tau Oligomer Pathology in Nucleus Basalis Neurons During the Progression of Alzheimer Disease. *J Neuropathol Exp Neurol*, *77*(3), 246-259. <https://doi.org/10.1093/jnen/nlx120>
- Tucker, R. P., Binder, L. I., Viereck, C., Hemmings, B. A., & Matus, A. I. (1988, Dec). The sequential appearance of low- and high-molecular-weight forms of MAP2 in the developing cerebellum. *J Neurosci*, *8*(12), 4503-4512. <https://doi.org/10.1523/JNEUROSCI.08-12-04503.1988>
- Vana, L., Kanaan, N. M., Ugwu, I. C., Wu, J., Mufson, E. J., & Binder, L. I. (2011, Nov). Progression of tau pathology in cholinergic Basal forebrain neurons in mild cognitive impairment and Alzheimer's disease. *Am J Pathol*, *179*(5), 2533-2550. <https://doi.org/10.1016/j.ajpath.2011.07.044>
- Wang, Y., & Mandelkow, E. (2016). Tau in physiology and pathology. *Nature reviews neuroscience*, *17*(1), 22-35.

- Ward, S. M., Himmelstein, D. S., Lancia, J. K., Fu, Y., Patterson, K. R., & Binder, L. I. (2013). TOC1: characterization of a selective oligomeric tau antibody. *J Alzheimers Dis*, 37(3), 593-602. <https://doi.org/10.3233/JAD-131235>
- Ward, S. M., Himmelstein, D. S., Lancia, J. K., Fu, Y., Patterson, K. R., & Binder, L. I. (2013). TOC1: characterization of a selective oligomeric tau antibody. *Journal of Alzheimer's Disease*, 37(3), 593-602.
- Yoshiyama, Y., Higuchi, M., Zhang, B., Huang, S. M., Iwata, N., Saido, T. C., Maeda, J., Suhara, T., Trojanowski, J. Q., & Lee, V. M. (2007, Feb 1). Synapse loss and microglial activation precede tangles in a P301S tauopathy mouse model. *Neuron*, 53(3), 337-351. <https://doi.org/10.1016/j.neuron.2007.01.010>
- Zareba-Paslawska, J., Patra, K., Kluzer, L., Revesz, T., & Svenningsson, P. (2020). Tau Isoform-Driven CBD Pathology Transmission in Oligodendrocytes in Humanized Tau Mice. *Front Neurol*, 11, 589471. <https://doi.org/10.3389/fneur.2020.589471>
- Zhang, Q., Zhang, X., & Sun, A. (2009, Jun). Truncated tau at D421 is associated with neurodegeneration and tangle formation in the brain of Alzheimer transgenic models. *Acta Neuropathol*, 117(6), 687-697. <https://doi.org/10.1007/s00401-009-0491-6>
- Zhao, Y., Tseng, I. C., Heyser, C. J., Rockenstein, E., Mante, M., Adame, A., Zheng, Q., Huang, T., Wang, X., Arslan, P. E., Chakrabarty, P., Wu, C., Bu, G., Mobley, W. C., Zhang, Y. W., St George-Hyslop, P., Masliah, E., Fraser, P., & Xu, H. (2015, Sep 2). Apoptosis-Mediated Caspase Cleavage of Tau Contributes to Progressive Supranuclear Palsy Pathogenesis. *Neuron*, 87(5), 963-975. <https://doi.org/10.1016/j.neuron.2015.08.020>
- Ziontz, J., Bilgel, M., Shafer, A. T., Moghekar, A., Elkins, W., Helphrey, J., Gomez, G., June, D., McDonald, M. A., Dannals, R. F., Azad, B. B., Ferrucci, L., Wong, D. F., & Resnick, S. M. (2019, Dec). Tau pathology in cognitively normal older adults. *Alzheimers Dement (Amst)*, 11, 637-645. <https://doi.org/10.1016/j.dadm.2019.07.007>

CHAPTER 3

Early axonopathy in MAPT-KI primary neurons seeded with human brain derived AD-tau
without overt axonal degeneration

ABSTRACT

Axonal degeneration is a common feature several neurodegenerative diseases including AD and other tauopathies. Studies in tauopathy models suggest a link between pathological tau and axonal degeneration and dysfunction. Tau's role in these processes is a topic of active investigation. For example, several studies show that disease-associated tau species can impair axonal transport, an essential cellular process that maintains functional connectivity between neurons. The exposure of an N-terminal domain of tau (phosphatase activating domain, PAD) recruits and activates signaling molecules including protein phosphatase 1 and glycogen synthase kinase 3 β (GSK3 β) that play a role in regulating fast axonal transport. Aberrant PAD-exposure is associated with AD and other tauopathies. Here, insoluble tau derived from human AD-brains (AD-tau) was used to seed the formation of pathological tau inclusions in primary neurons from MAPT knock-in mice that express all six human tau isoforms. Overt axonal degeneration was measured using microscopy and biochemical approaches. Furthermore, the association between PAD-exposed tau inclusions and axonal transport cargo proteins (i.e. synaptophysin and amyloid precursor protein) or active GSK3 β (npGSK3 β) was assessed. Finally, axonal function was measured using multi-electrode arrays to measure action potential propagation. Overt axonal degeneration does not occur despite relatively abundant tau pathology. However, early signs of axonopathy including the accumulation of cargo proteins and npGSK3 β in association with discrete PAD-exposed tau inclusions were observed, which may suggest local impairment of axonal transport. There was no evidence of abnormal axonal action potential conductance velocity

in the seeded neurons, or changes in the lengths of axonal arbors (as measured by action potential propagation with MEAs). Together, these data suggest that this seeding model represents an early stage in the neurodegenerative process, and that axonal transport may be impaired. This model can be used to further elucidate the role of insoluble pathological tau inclusions in impairing axonal transport and may help to identify potential targets for early disease-modifying therapies.

INTRODUCTION

Pathological aggregation of the microtubule-associated protein, tau, is a hallmark of Alzheimer's disease (AD) (Braak et al., 2006; Braak et al., 2011; Grundke-Iqbal et al., 1986). Tau pathology accumulates in the brain following a stereotypical pattern in AD and correlates with neurodegeneration and cognitive decline (Braak et al., 2006; Braak & Braak, 1991; Giannakopoulos et al., 2003; Price et al., 1991; Price & Morris, 1999). Pathological tau may be a critical target for disease-modifying therapies, but we must first better understand its role in disease. Indeed, several lines of evidence suggest tau may exert toxicity through specific mechanisms, but this remains an active area of investigation.

Axonal degeneration is an early event in the pathogenesis of several neurodegenerative diseases, including AD and other tauopathies (Kneynsberg et al., 2017; Kovacs, 2015). In human tissue, a specific pattern of axonal degeneration is generally observed. First, axonal proteins begin to accumulate, forming enlargements known as swellings and/or spheroids in dystrophic neurites (Raff et al., 2002; Stokin et al., 2005). In AD, the dystrophic neurites often display an accumulation of axon cargos, pathological tau species, transport motor proteins and other cytoskeletal proteins (Coleman, 2005; Dessi et al., 1997; Stokin et al., 2005). The axonal segments between the spheroids become thin, and eventually degenerate (Stokin et al., 2005).

Axonal degeneration is a prominent feature in several tauopathies including AD, progressive supranuclear palsy (PSP), corticobasal degeneration (CBD), Pick's disease (PiD), and chronic traumatic encephalopathy (CTE) (reviewed in (Kneynsberg et al., 2017)). Furthermore, transgenic animal models that express mutant tau associated with familial frontotemporal dementia tauopathies exhibit axonal degeneration (Kneynsberg et al., 2017). These observations strongly suggest a role for pathological tau in axonal degeneration. Some mechanisms leading to axonal degeneration are known, but all the mechanisms involved are not yet fully understood. Nonetheless, it is generally believed that axonal transport deficits play a critical role because neurons rely on bidirectional transport of cargos along the axon to maintain functional synapses and neural connectivity (Berth & Lloyd, 2023; Millicamps & Julien, 2013; Roy et al., 2005). Furthermore, the delivery of ion channels to specific sites along the axon is important for axonal functions such as action potential propagation. The accumulation of transport cargos in dystrophic neurites supports the role of axonal transport impairments in axon degeneration (Praprotnik et al., 1996; Stokin & Goldstein, 2006). Our group previously identified one mechanism linking a specific conformation associated with pathological tau to axonal transport impairment (Combs et al., 2019).

Several studies in the squid giant axon, and more recently in rat primary hippocampal neurons, show that specific disease-associated pathological tau modifications (i.e., aggregation, pseudophosphorylation, and disease-causing tau mutations) disrupt fast axonal transport (Christensen et al., 2023; Combs et al., 2021; Combs et al., 2019; Cox et al., 2016; Kanaan et al., 2012; Kanaan et al., 2011; LaPointe et al., 2009; Patterson et al., 2011; Tiernan et al., 2016). This effect of tau on axonal transport is dependent on exposure of the tau's N-terminal phosphatase activating domain (PAD), and subsequent activation of a protein phosphatase 1 (PP1), which

dephosphorylates and activates glycogen synthase kinase 3 β (GSK3 β). Active GSK3 β phosphorylates kinesin light chains, causing cargo release (Kanaan et al., 2012; Kanaan et al., 2011; LaPointe et al., 2009; Morfini et al., 2002; Patterson et al., 2011; Tiernan et al., 2016). Notably, PAD-exposure is observed in AD, PSP, CBD, PiD and CTE (Christensen et al., 2019; Combs et al., 2016; Combs & Kanaan, 2017; Cox et al., 2016; Kanaan et al., 2016; Kanaan et al., 2011; Tiernan et al., 2016), highlighting the relevance of this mechanism to human disease. Amyloid precursor protein (APP) and synaptophysin are commonly used markers for axonal transport and the accumulation of these transport cargo markers occurs in axonal spheroids and dystrophic neurites (Coleman, 2005; Medana & Esiri, 2003). Both APP and synaptophysin cargo protein accumulations are thought to result from dysfunctional axonal transport mechanisms (Kamal et al., 2000; Koo et al., 1990; Medana & Esiri, 2003). Consistent with this, we recently showed impaired axonal transport of synaptophysin cargos in rat neurons expressing pathological forms of tau associated with PAD-exposure (Christensen et al., 2023; Combs et al., 2021).

Specific disease-associated tau pathology is recapitulated *in vitro* and *in vivo* by seeding with insoluble tau derived from brain tissue of AD and other tauopathies (Boluda et al., 2015; Clavaguera et al., 2013; Guo et al., 2016; Holmes et al., 2014; Narasimhan et al., 2017; Zareba-Paslawska et al., 2020). This phenomenon was leveraged as a tool to induce the formation of AD-associated pathological tau species, including PAD-exposed tau inclusions, in primary neurons and subsequently assess their role in axonal degeneration. A mouse model in which the entire murine *MAPT* gene was replaced with human *MAPT* (MAPT-KI) was used, resulting in expression of all six human tau isoforms at normal levels in the adult CNS (Benskey et al., 2023; Saito et al., 2019).

In this relatively novel tau seeding model, localized accumulations of cargo proteins and active GSK3 β at sites of neuritic PAD-exposed tau inclusions in the seeded neurons was observed. However, there was no evidence of overt axonal degeneration or dysfunction, suggesting that this is a model of early axonopathy associated with pathological tau.

METHODS

Animals

All studies were conducted in compliance with the approval of Michigan State University's Institutional Animal Care and Use Committee. Embryonic day 16 (E16) *MAPT* knock-in (MAPT-KI) mice were used for primary neuron experiments (Saito et al., 2019). Timed-pregnant MAPT-KI females were bred in-house; E0 refers to the day the vaginal plug was found. All mice were housed in 12h light/dark conditions with food and water provided *ad libitum*. On the day of primary neuron harvest, pregnant females were euthanized by sodium pentobarbital overdose (at least 100 mg/kg) administered via intraperitoneal injection.

Primary Neurons

Embryonic day 16 pups were obtained from timed pregnant MAPT-KI mice. Primary neurons were harvested and dissociated as described previously (Mueller et al., 2023). Briefly, hippocampi were dissected and placed in ice-cold calcium and magnesium free buffer [CMF; 1X Dulbecco's PBS (Gibco, 14200-075), 0.1% glucose (Sigma, G7528), 2.5 μ g/mL Amphotericin B (Gibco, 15290-026), and 50 μ g/mL Gentamicin (Gibco, 15710-072)] and incubated in warm 0.125% trypsin for 15 min at 37 °C. The tissue was washed 2x with cold CMF, then 3 mL of trypsin inactivating solution was added [Hank's Balanced Salt Solution (Gibco, 24020-117), 20% Newborn Calf Serum (Gibco, 16010-167) and 1X DNase I solution (10X stock: 5 mM sodium acetate (Sigma S5636), 1 μ M calcium chloride (Sigma, C7902), 0.5 mg/mL DNaseI (Fisher,

NC9185812)]. The cells were triturated using a 3 mL syringe with progressively smaller diameter needles then layered onto Fetal Bovine Serum (Invitrogen, 16000044) and centrifuged at 200 x g for 5 min at 4 °C. The cells were resuspended in 1 mL of warm Neurobasal Media Plus (Gibco, A3582901) supplemented with 2% B27 Plus (Gibco, A3582801), and 1% GlutaMAX (Gibco, 35050061), with antibiotics: 2.5 µg/mL Amphotericin B (Gibco, 15290-026), and 50 µg/mL Gentamicin (Gibco, 15710-072). Cells were maintained in a humidity-controlled incubator at 37 °C, and 5% CO₂.

Purification of AD-tau from human frontal cortex

Sarkosyl-insoluble tau was purified from human frontal cortical tissue obtained from the University of Michigan Brain Bank according to methods adapted from Narasimhan and Lee (Narasimhan & Lee, 2017). Briefly, tissue from six individuals who had Braak stage V-VI AD was pooled (3.5-4.5 g total). Concurrently, the same amount of frontal cortical tissue from five or six age-matched Braak stage I-II cognitively unimpaired individuals was pooled for use as a control sample throughout experiments (Con). Tissue was homogenized using a glass Dounce homogenizer in 9 volumes of ice-cold high-salt extraction buffer (10 mM Tris, pH 7.4, 10% sucrose, 0.8 M NaCl, 1 mM EDTA, 0.1% sarkosyl) supplemented on the day of use with protease (2 µg/mL pepstatin, 2 µg/mL bestatin, 2 µg/mL leupeptin, 4 mM phenylmethylsulfonyl fluoride, 10 µg/mL aprotinin) and phosphatase inhibitors (1 mM tetra-sodium pyrophosphate decahydrate, 10 mM β-glycerophosphate, 1 mM sodium orthovanadate, 1 M sodium fluoride). The homogenate was transferred to 50 mL conical tubes and centrifuged at 10,000 x g(max) for 10 min at 4 °C in a F14-14 x 50cy fixed angle rotor (Thermo Scientific, 096-145075) and Sorvall LYNX 4000 Superspeed centrifuge (Thermo Scientific, 75006581). The supernatant was filtered through a KimWipe into a 50 mL conical tube. The pellet was homogenized and centrifuged as above. The

2nd supernatant was filtered as above. This process was repeated one more time. The three supernatants were pooled into a glass beaker and the sarkosyl concentration was increased to 1%. The mixture was stirred with a stir bar on a stir plate for 1.5 h at room temperature, then the suspension was transferred to 36 mL ultracentrifuge tubes (Beckman Coulter 355618) and centrifuged at 300,000 x g(max) at 4 °C for 60 min in a T-865 fixed angle rotor (Thermo Scientific, 51411) and Sorvall WX+ Ultra centrifuge (Thermo Fisher, 75000100). The pellet was washed with 1X Dulbecco's Phosphate Buffered Saline (dPBS; Gibco, 14200-075), broken up with a pipet tip, transferred to a new 36 mL tube which was then filled with dPBS, and centrifuged at 250,000 x g(max) at 4 °C for 30 min in a T-865 8 x 36ml rotor and Sorvall WX+ Ultra centrifuge. The resulting pellet was broken up in dPBS (100 µl/g of original tissue, i.e., 450 µl dPBS for 4.5 g), transferred to a 1.5 mL tube, and incubated on a shaker at room temperature overnight. The next day the pellet was homogenized by passing the suspension through a 21G needle, followed by a 27G needle, then sonicated (20 x 1 sec pulses at power level 1.5; Misonix, XL-2000). The homogenate was transferred to a thickwall 0.5 mL tube (Thermo Scientific, 45235) and centrifuged at 100,000 x g(max) at 4 °C for 30 min in a S120-AT3 14 x 0.5 ml rotor (Thermo Scientific, 45584) and Sorvall MTX Micro-Ultra centrifuge (Thermo Scientific, 46960). The resulting pellet was resuspended in 150 µl – 200 µl dPBS, sonicated (60 x 1 sec pulses at power level 1.5), transferred to a thickwall 0.2 mL tube (Thermo Scientific, 45233) and centrifuged at 10,000 x g(max) for 30 min at 4 °C in a S100-AT3 fixed angle rotor (Thermo Scientific, 45585) and Sorvall MTX Micro-Ultra centrifuge. The resulting supernatant containing the sarkosyl-insoluble tau (or Con proteins) was sonicated (60 x 1 sec pulses at power level 1.5), then aliquoted and stored at -80 °C until use.

Treatment of primary hippocampal cultures

Primary hippocampal cultures were treated on DIV5 with 28 nM of AD-tau (based on the tau concentration determined by total tau sandwich ELISA), Con (matched to the total protein concentration of the AD-tau samples), or dPBS. Treatments were prepared in fresh NBM Plus media and prewarmed to 37 °C. The treatments were mixed briefly by vortex immediately before addition to cells. The treatments were added directly to the cell culture media in a spiral pattern, then the culture plate or slide was gently rocked to mix, and returned to the incubator.

Calpain-Glo Assay

Cells were plated in a PDL-coated 96-well plate (Corning, 354461) at 25,000 cells/well in 100 µl/well of NBM Plus. At 26d post-treatment (corresponding to DIV31), calpain activity was measured using a Calpain-Glo Assay kit (Promega, G8501) according to the manufacturer's instructions. Calpain-Glo reagent was added directly into the cell media at a 1:1 ratio. The reaction was mixed on a shaker at room temperature for 30 s, then developed for 30 min. Then, 50 µl each reaction was transferred to a solid white plate and luminescence was recorded using a Promega GloMax plate reader.

Western blotting of primary neuron lysates

Cells were collected in lysis buffer (20 mM Tris, 0.5 mM DTT, 150 mM NaCl, 0.5% Triton X-100, 2 µg/mL pepstatin, 2 µg/mL bestatin, 2 µg/mL leupeptin, 4 mM phenylmethylsulfonyl fluoride, 10 µg/mL aprotinin, 1 mM tetra-sodium pyrophosphate decahydrate, 10 mM β-glycerophosphate, 1 mM sodium orthovanadate, 1 M sodium fluoride, pH7.5) on 26d post-treatment (corresponding to DIV 31). Lysates were sonicated then the total protein concentration of each lysate was quantified using the Bio-Rad protein assay (Bio-Rad, 5000006) as directed. Then lysates were adjusted to 20 µg with TBS, then heated with Laemmli sample buffer (final 1X

composition: 20 mM Tris, pH 6.8, 2% SDS, 6% glycerol, 1% β -mercaptoethanol, 0.002% Bromophenol Blue) at 95 °C for 5 min. Lysates were loaded onto 12-well Criterion TGX Precast 4-20% gels (Bio-Rad, 567-1093) and proteins were separated via SDS-PAGE at 250V for 40 min. All Blue Precision Plus Protein Standards (Bio-Rad, 161-0373) were used. Proteins were transferred onto nitrocellulose membranes (Pall Life Sciences, Port Washington, NY, #66593) using a Bio-Rad transfer unit at 400 mA for 50 min. Membranes were blocked in 2% non-fat dry milk (NFDM) for 1 hour. Then, membranes were probed with primary antibodies overnight at 4 °C. Membranes were incubated with 12B2 nonphosphoSer9 GSK3 β antibody (npGSK3 β ; 1:1,000; mouse IgG; (Grabinski & Kanaan, 2016)) and GSK3 α/β total antibody (1:2,000; rabbit; Cell Signaling, 5679). Membranes were washed with 1X TBS-TWEEN 20 (TBST) 3 x 5 min, then incubated with fluorescently tagged secondary antibodies diluted in 2% NFDM for 1 hour. Membranes were incubated with IRDye 680LT goat anti-mouse IgG1 (LiCor, 926-68050) and IRDye 800CW goat anti-rabbit (LiCor, 926-32211). Membranes were washed 3 x 5 min in TBST then imaged using a Li-Cor Odyssey infrared imaging system and Li-Cor ImageStudioLite 5.2 software was used to quantify the signal intensity of the bands. The npGSK3 β signal was normalized to the GSK3 α/β total signal.

Axonal degeneration Assessment

First, 8-well glass bottom chamber slides (Ibidi, 80827) were coated with 0.5 mg/mL poly-D-lysine in borate buffer overnight at room temperature. Slides were washed 4x with sterile water and air dried. Slides were warmed prior to plating. Cells were plated as two micro-islands/well (1 island = 10 μ l drop of 15,000 cells/drop) arranged diagonally. Cells were allowed to settle for 12 min in the incubator. Then, the volume was raised to 250 μ l/well with NBM Plus. Cells were treated at DIV 5 with PBS, CO, or AD-tau. On DIV 21, cells were fixed with prewarmed 4%

paraformaldehyde in 1X cytoskeleton buffer (10 mM 2-(N-morpholino)ethanesulfonic acid, 138 mM KCl, 3 mM MgCl₂, and 4 mM EGTA, pH 6.1) for 20 min. The wells were washed 3 x 5 min with TBS on a shaker at room temperature. Cells were incubated with blocking buffer (5% goat serum, 1% BSA, 0.2% Triton-X in TBS) for 1 h at room temperature. Then, cells were incubated with MAP2 antibody (1:250; rabbit; Cell Signaling, 8707S), Tuj1 β -III tubulin antibody (1:5,000, mouse IgG2a; (Caccamo et al., 1989)), and TNT1 antibody (1:40,000; mouse IgG1; Kanaan Lab; (Combs et al., 2016; Kanaan et al., 2011)) in 2% goat serum-TBS overnight at 4°C. The next day, cells were washed 3 x 5 min with 1X TBS. Cells were incubated with Alexa Fluor goat anti-mouse IgG1 647 (Thermo, A21240), Alexa Fluor goat anti-mouse IgG2a 568 (Thermo, A21134), and Alexa Fluor goat anti-rabbit 488 (Thermo, A32731) secondary antibodies (all 1:500) in 2% goat serum-1X TBS for 1 h at room temperature. Then, cells were washed 3 x 5 min with TBS and stored at 4° C until analysis with microscopy.

Immunocytofluorescence

Cells were fixed 16d post-treatment (corresponding to DIV21) with prewarmed 4% paraformaldehyde in cytoskeleton buffer at room temperature for 20 min. Cells were incubated with blocking buffer as above for 1 h. Then, cells were incubated with primary antibodies in 2% goat serum-TBS overnight at 4° C. One set of cells was incubated with TNT1 antibody (1:40,000), Tuj1 antibody (1:5,000), and synaptophysin antibody (1:100; rabbit; Abcam, ab52636). A second set of cells was incubated with TNT1 antibody (1:40,000), Tuj1 antibody (1:5,000), and amyloid precursor protein antibody (APP; 1:100; rabbit; Abcam, ab32136). A third set of cells was incubated with Tuj1 antibody (1:5,000), 12B2 npGSK3 β antibody (1:100), and pS422 antibody (1:1000; rabbit; Abcam, 79415). Cells were washed 3 x 5 min with TBS, then incubated with secondary antibodies (all 1:500) in 2% goat serum-TBS for 1 h. The first two sets were incubated

with Alexa Fluor goat anti-mouse IgG1 488 (Thermo, A21121), Alexa Fluor goat anti-mouse IgG2a 647 (Thermo, A21241), and Alexa Fluor goat anti-rabbit 568 (Thermo, A11036) secondary antibodies. The third set was labelled with Alexa Fluor goat anti-rabbit 488, Alexa Fluor goat anti-mouse IgG2a 647, and Alexa Fluor goat anti-mouse IgG1 568 (Thermo, A21124) secondary antibodies. Then, cells were washed 3 x 5 min with TBS and stored at 4° C until imaging.

Confocal imaging

Images were acquired on a Nikon A1+ laser scanning confocal microscope system equipped with solid-state lasers (405, 488, 561, and 640 nm) and Nikon Elements AR software. For the axonal degeneration study, whole micro-islands were imaged by acquiring and stitching multiple 20x images. All other images were acquired with a 60x oil immersion lens. All images in an experiment were acquired using identical acquisition settings (i.e. gain, offset, laser intensity, pinhole size, resolution, scan speed, and step-size for z-stacks). Images were prepared using ImageJ (version 2.14.0/1.54f), Adobe Photoshop (version 25.9.0) and Adobe Illustrator (version 28.5).

Axonal degeneration assay analysis

For the axonal degeneration assay, cells were imaged at 20x with a Nikon A1+ laser scanning confocal microscope equipped with 405, 488, 561, and 640 solid state lasers and Nikon Elements AR software. For each condition, an entire micro-island was imaged by acquiring and stitching multiple fields of view using the Nikon Elements AR software. Images were analyzed using ImageJ software (FIJI; version 2.14.0/1.54f). First, the channels were split using the Split channels function. Next, a threshold mask was generated for the Tuj1 signal (red channel) using the Huang setting. Next, the poly line tool was used to outline the MAP2+ area (somatodendritic component) of each island, then I deleted the MAP2+ area so that the subsequent analysis was performed on Tuj1+/MAP2- axons. Using the polyline tool, I traced the outer perimeter of the axon growth area.

Next, the number of axonal segments were quantified using the Analyze Particles function (Size: 1-Infinity, Circularity 0.00 – 1.00).

High-density microelectrode arrays (MEAs)

For the MEA experiments, instead of using NBM Plus with B27 Plus Supplement as described above, I used a different formulation of neurobasal media that was optimized for electrophysiology experiments called NBM Electro (Gibco, A14098-01) with B27 Electro Supplement (Gibco, A14097-01) referred to from here as NBME. As above, I supplemented the NBME with 1% GlutaMAX and antibiotics: amphotericin B and Gentamicin. I used a high-density MEA system (MaxWell Biosystems) to measure action potential propagation in neurons at the single cell level. Two days prior to plating, MaxOne Chips (MaxWell Biosystems AG MaxOne Chip MX1-S/U-CHP) were treated with 1 mL/well of 1% Terg-a-zyme (Sigma-Aldrich, Z273287) for 2 h at room temperature. Chips were washed six times with ultra-pure diH₂O, then sterilized via immersion in 70% EtOH for 30 min at room temperature. Chips were washed 4x with sterile ultra-pure diH₂O and air dried. 600 µl of NBME was added to the well of each chip. A MaxOne Lid (autoclaved; MaxWell Biosystems AG MX1-LID-PSM) was placed over each well. To minimize evaporation, chips were arranged in a petri dish containing a cap (from 50 mL conical tube) full of sterile water. Then, chips were placed in a humidity-controlled 37 °C incubator with 5% CO₂ for two days. On the day of the primary neuron harvest, the NBME was removed and each well was washed 1x with sterile water. The electrode surface in the middle of the well was coated with 50 µl of 0.1 mg/mL poly-D-lysine (Sigma, P7886) in borate buffer (12.5 mM sodium borate decahydrate [VWR, MK745706] and 50 mM boric acid [Sigma, B6768-1KG]) for 2 h at 37 °C. Then, each well was washed 4x with sterile water and air dried for 45 min. Next, the electrode surface was coated with 50 µl of 0.02 mg/mL laminin (Thermo Fisher, 23017015) for 1 h at 37 °C. During the electrode-

coating steps, primary hippocampi neurons were obtained from E16 MAPT-KI mice as described above. After the 1 h incubation with laminin, the laminin was removed, and a 50 μ l droplet of 100,000 cells in NBME was plated onto the electrode chip. The cells settled onto the chip for 1 h at 37 °C. Then, 350 μ l of NBME/well was added to bring the total volume in each well to 400 μ l. Cells received 80 μ l of fresh NBME to each well 3x per week. Cells were treated at DIV 5 with PBS, CO or 28 nM AD-tau.

Neurons were recorded 23d post-treatment (corresponding to DIV28). All cells were fed 80 μ l of fresh NBME 1 h prior to the first activity recording. The chip was placed into the recording unit and allowed to equilibrate for 10 min. Then, the activity scan analysis was selected from the assay gallery. The assay was set up to use a checkerboard configuration to record to record from every other electrode (12,980 electrodes recorded). Immediately following the activity scan, the axon tracking assay was selected. The selection preference was set to firing rate, and the number of units (neurons to be recorded) was set to 60. The minimum spacing between units was set to 175 μ m. The scanning mode was set to Full Array. The activity was recorded (approximately 1 h and 30 min) and then the axon tracking analysis was run. For the analysis, the number of spikes threshold was set to 20, the footprint threshold was set to 0.75, the latency threshold was set to 0 ms, and the radius was set to 3 pixels.

Statistical analyses

Independent experimental replicates (N) represent a single primary cell culture from a unique timed pregnant MAPT-KI female. Each primary cell culture was produced by dissecting the hippocampi from multiple E16 fetuses from a single timed-pregnant female and pooling them. Experiments each had three treatment groups (PBS, Con, and AD-tau), and in each experiment $N \geq 3$ (as indicated in the figure legends). The data were assessed for normality and equal variance

assumptions using the Shapiro-Wilk test normality test and the Brown-Forsythe variance test. When both were not met, nonparametric statistical tests were used to analyze the data. Experiments that met the normality and equal variance assumptions were analyzed with a one-way analysis of variance test followed by Tukey's post hoc test when overall significance was achieved. For nonparametric analyses, the Kruskal-Wallis test was used followed by the Dunn's post hoc test when overall significance was achieved. Significance was defined as $p \leq 0.05$. Data are shown as mean \pm standard deviation for parametric tests or as median \pm interquartile range for nonparametric tests. Analyses were performed using GraphPad Prism 10 software (version 10.2.3).

RESULTS

Overt axonal degeneration is not observed in seeded MAPT-KI cultures

Multi-label ICF was used to assess axonal degeneration in PBS, Con, and AD-tau-treated cultures at 16d post-treatment (corresponding to DIV21). To isolate axons for analysis, cells were plated in micro-islands. MAP2 is restricted to the somatodendritic compartment whereas Tuj1 (β -III tubulin) is distributed throughout the somatodendritic and axonal compartments of neurons. In our ICF study, the MAP2+ signal was limited to the center of the micro-islands, and MAP2-/Tuj1+ processes (axons) extended outward (Figure 3.1A-C). To assess axonal degeneration, two outcome measures were performed: 1) the number of axonal objects/total axon area, and 2) the average axonal object size. A degenerated axon is expected to have a greater number of objects, and a smaller average size compared to an intact neuron. No treatment effects were observed for number of objects/total axon area (one-way ANOVA; $F_{(2,9)} = 1.219$, $p = 0.3400$; Figure 3.1D) or for the mean object size (one-way ANOVA; $F_{(2,9)} = 0.9936$, $p = 0.4075$; Figure 3.1E).

Next, calpain activity was measured as an indirect measure of axonal degeneration (Adamec et al., 2002; Rao et al., 2014; Yin et al., 2016) in PBS, Con, and AD-tau-treated cultures

at 26d post-treatment (corresponding to DIV31). On DIV31, Calpain-Glo reagent was added to the live cells, then luminescence was measured (Figure 3.1F). No significant effects on calpain activity were observed when comparing PBS, Con or AD-tau-treated groups (one-way ANOVA; $F_{(2,6)} = 0.5674, p = 0.5947$) (Figure 3.1F).

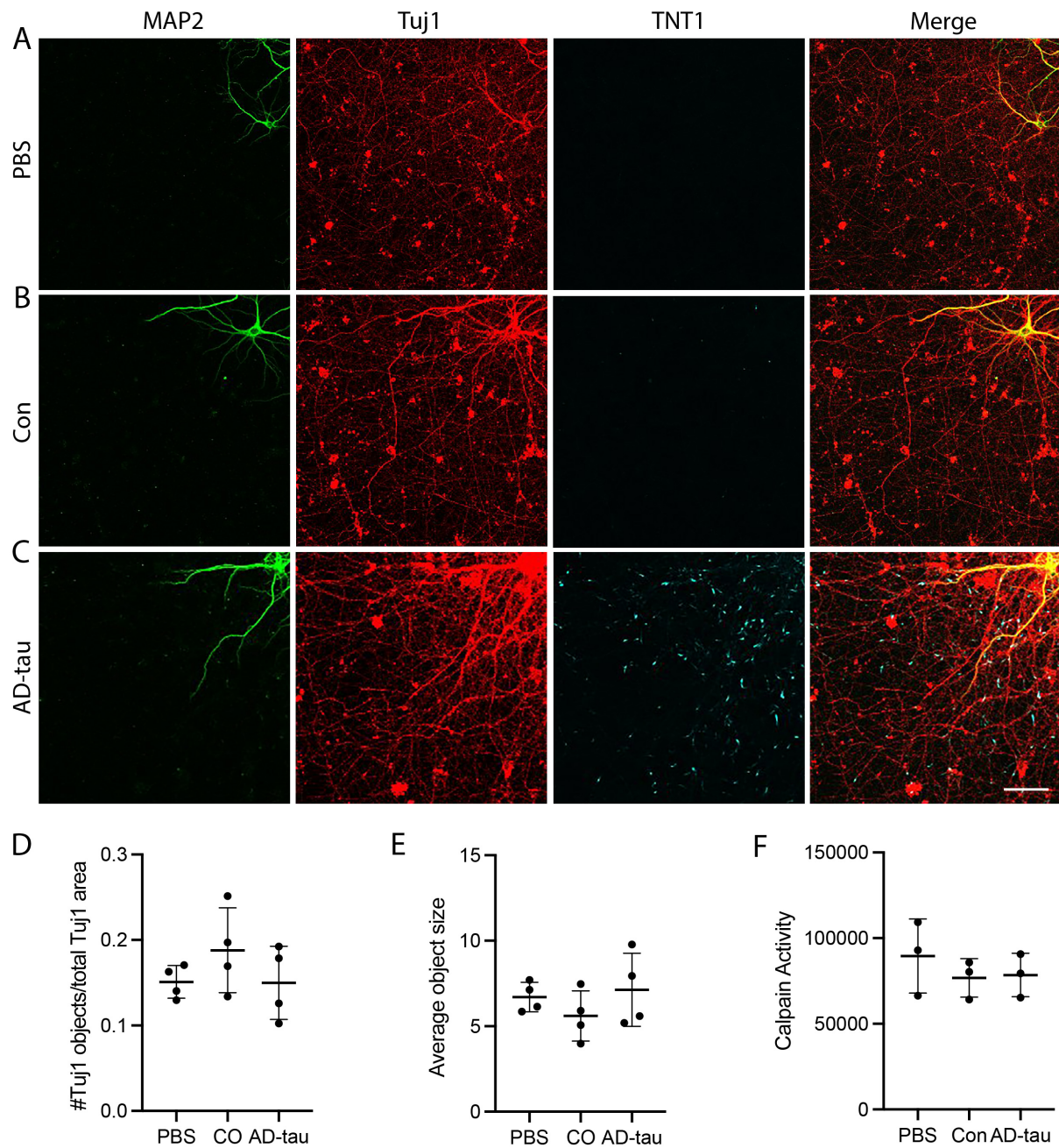


Figure 3.1. Overt axonal degeneration was not observed in AD-tau-treated MAPT-KI primary neurons 16d post-treatment. A-C) Representative images of the axon outgrowth in PBS, Con, and AD-tau-treated neurons immunolabelled with MAP2 (green), Tuj1 (β -III tubulin; red), and TNT1 (cyan) antibodies. D) Quantification of the number of Tuj1+ objects normalized to Tuj1+ surface area showed no treatment effects.

Figure 3.1 (cont'd).

E) Quantification of the mean object size showed similar sizes across groups. F) Quantification of calpain activity in PBS, Con, or AD-tau-treated cultures at 26d post-treatment (corresponding to DIV31) showed similar activity across groups. Scale bar = 50 μ m. The data are mean \pm SD and were compared using one-way ANOVA with Tukey's multiple comparisons test, significance was defined as $p \leq 0.05$. A-E) N=4. F) N=3.

Cargo proteins accumulate in discrete regions of neurites with PAD-exposed tau

To determine if cargo proteins accumulate along neurites in regions of PAD-exposed tau pathology, ICF was performed on seeded cells fixed on DIV21 (16d post-treatment) using TNT1 antibody with synaptophysin (bidirectionally transported; Figures 3.2 and 3.3) or amyloid precursor protein (APP; transported primarily anterogradely; Figures 3.4 and 3.5) antibodies. Synaptophysin signal frequently colocalized with the thread-like TNT1+ inclusions in Con and AD-tau treated cultures (Figure 3.4B, C). Interestingly, APP+/TNT1+/Tuj1+ neurite swellings were present that are reminiscent of the axonal spheroid bodies observed in AD (Figure 3.4C). APP rarely accumulated with thread-like neuritic TNT1+ inclusions (e.g. TNT1+/APP- example inclusion in Figure 3.4B). However, small accumulations of APP were observed at the tips of short TNT1+ segments (Figure 3.5C). Primary delete controls for each of the ICF primary antibodies are shown in Figures 3.3 and 3.5, no non-specific signal was detected.

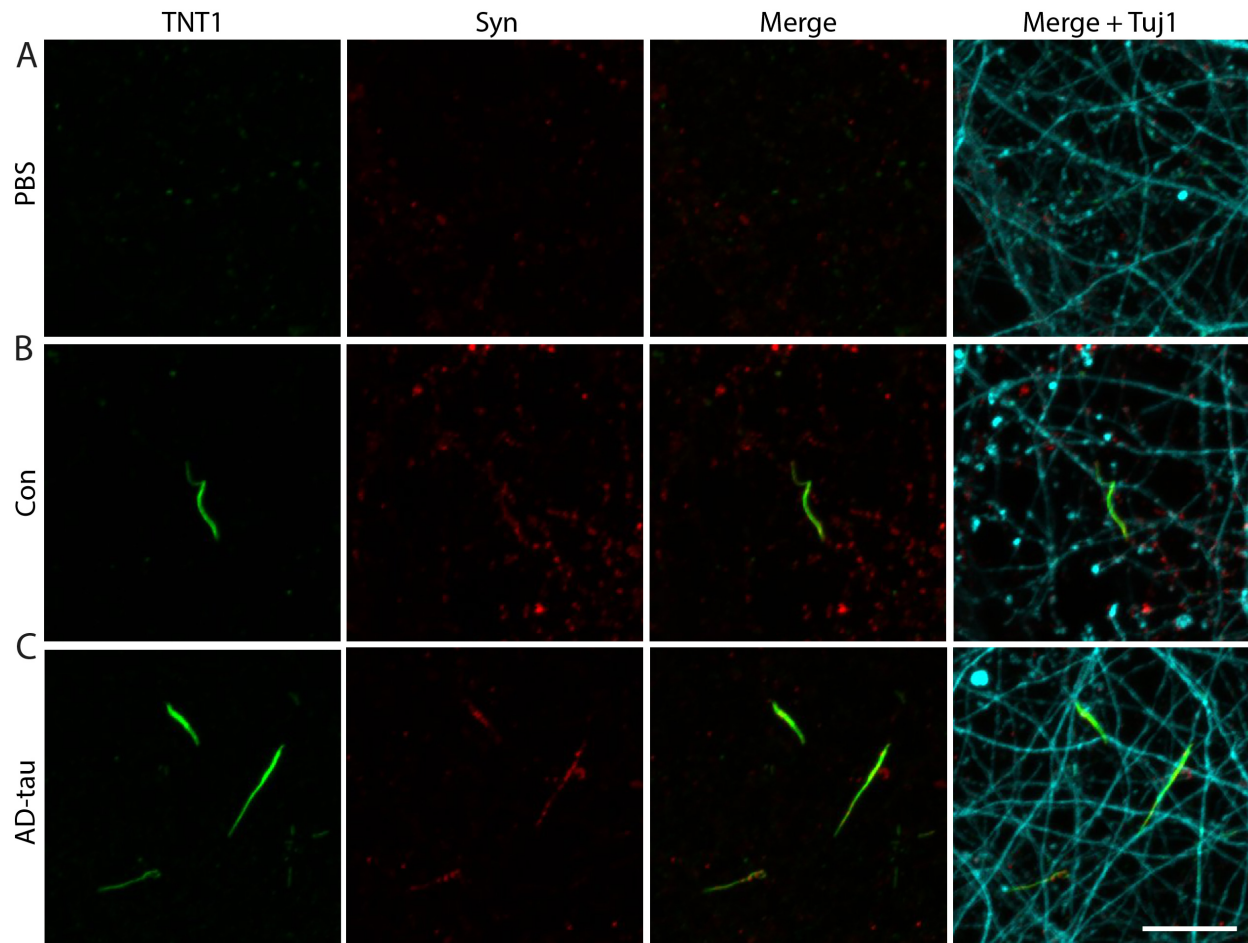


Figure 3.2. Synaptophysin cargos colocalize with PAD-exposed tau inclusions. A-C) Cells were treated on DIV5 with PBS, Con, or AD-tau and fixed at 16d post-treatment (corresponding to DIV21). Immunocytofluorescence indicates β -III tubulin (Tuj1; cyan) and synaptophysin signal (Syn; red) was observed in A) PBS, B) Con, and C) AD-tau treated cultures. Synaptophysin appeared to accumulate at sites of PAD-exposed tau inclusions (TNT1; green) in B) Con and C) AD-tau-treated cultures. Scale bar = 10 μ m. N=3; Images are representative of findings in each independent experimental replicate which were derived from separate neuron harvests from unique timed pregnant MAPT-KI females.

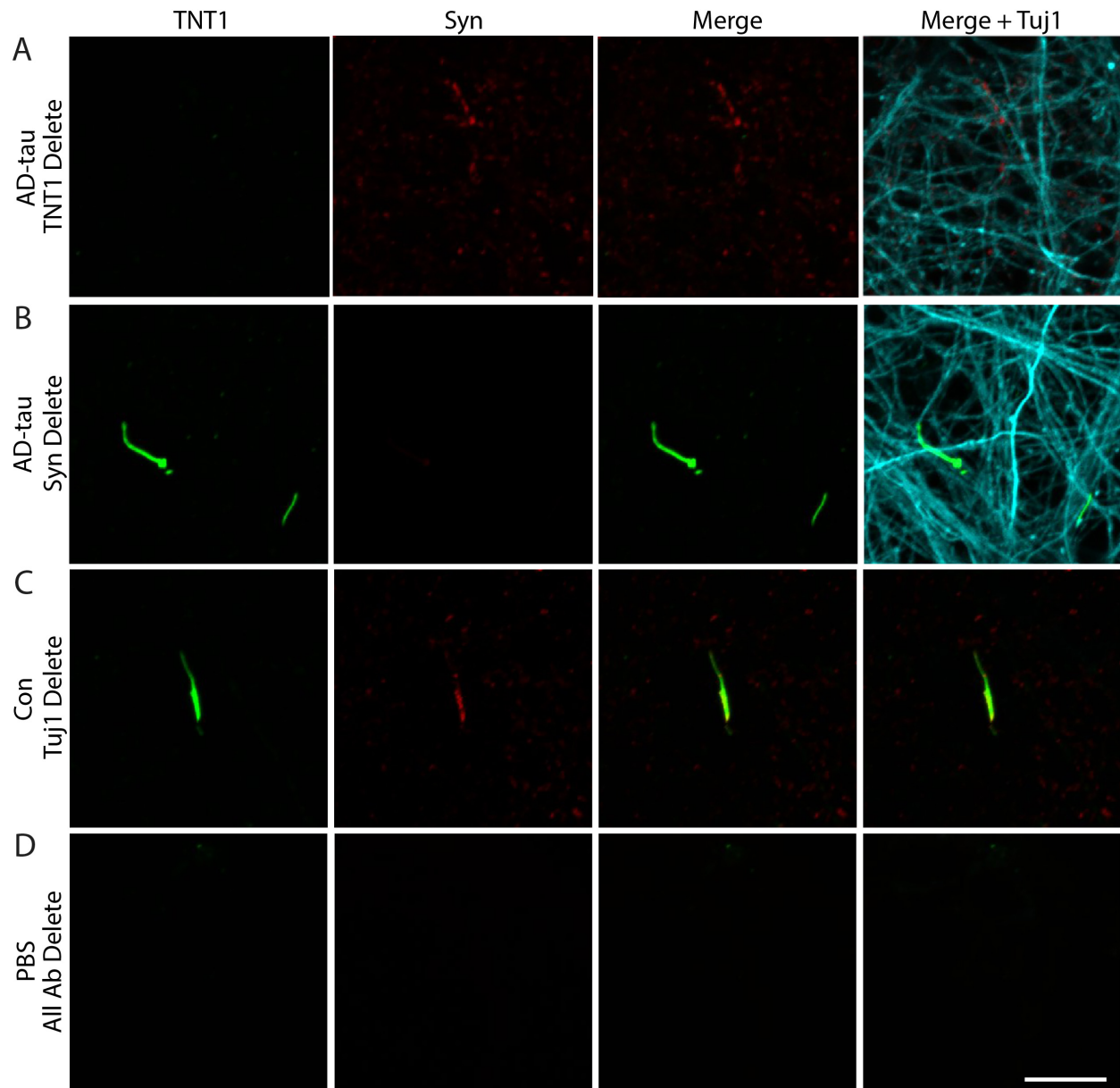


Figure 3.3. Synaptophysin Immunocytofluorescence (ICF) primary delete control labeling. ICF primary antibody delete control labeling was performed in A-B) AD-tau-treated neurons, C) Con treated neurons, or D) PBS treated neurons. A) Omission of the TNT1 primary antibody (green) showed no TNT1 signal. B) Omission of the synaptophysin primary antibody (Syn; red) showed no synaptophysin signal. C) Omission of the Tuj1 primary antibody (cyan) showed no Tuj1 signal. D) Omission of all primary antibodies showed no TNT1, synaptophysin or Tuj1 signal.

Figure 3.3 (cont'd).

The lack of signal in the primary antibody deletes confirms that these ICF stains do not cross react with each other. Scale bar = 10 μm . N=3; Images are representative of findings in each independent experimental replicate which were derived from separate neuron harvests from unique timed pregnant MAPT-KI females.

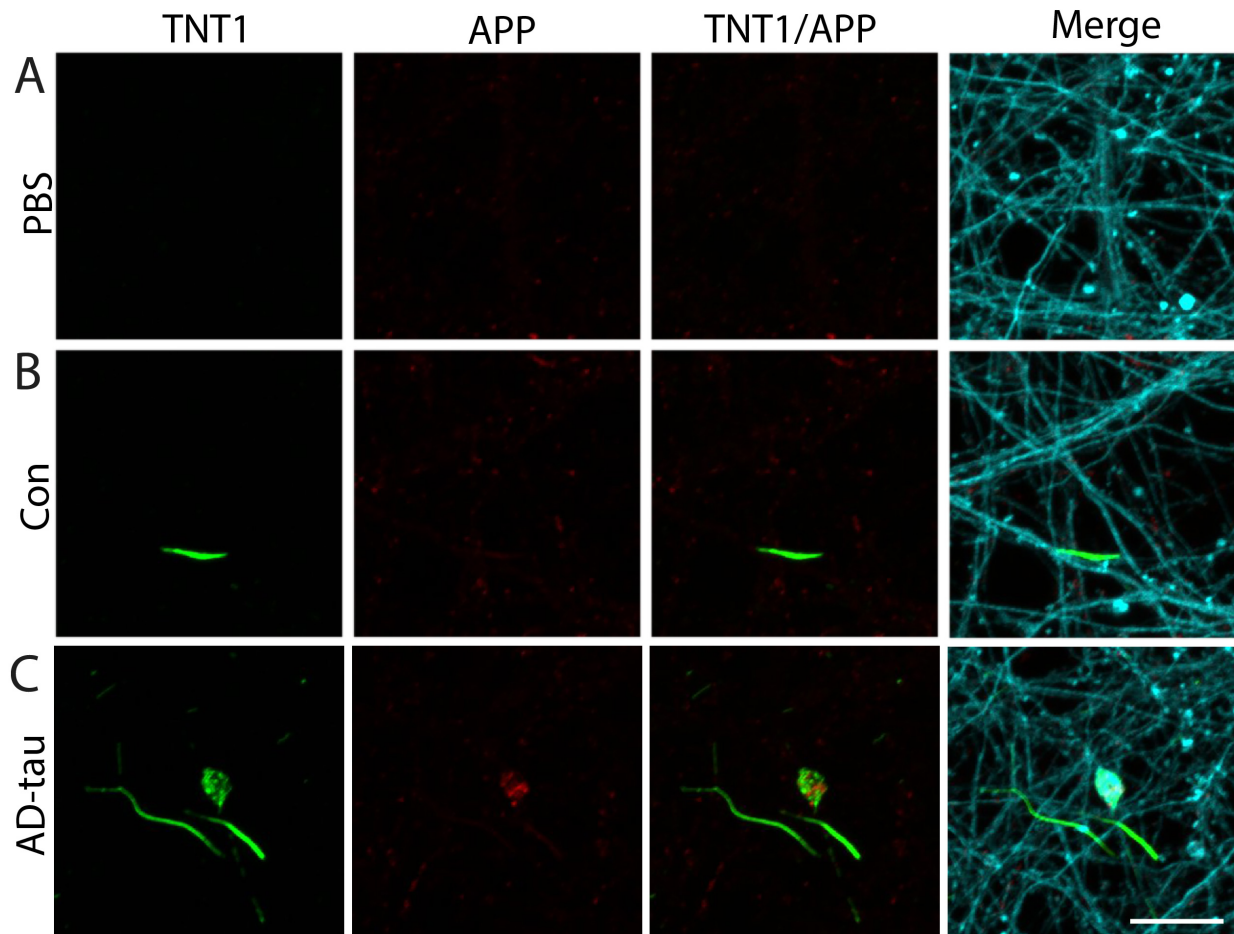


Figure 3.4. APP cargos accumulate with PAD-exposed tau in axonal swellings. A-C) Cells were treated on DIV5 with PBS, Con, or AD-tau and fixed at 16d post-treatment (corresponding to DIV21). Immunocytofluorescence indicates that APP co-localized with TNT1+ tau inclusions (green) in axonal swellings in C) AD-tau-treated cultures. Scale bar = 10 μ m. N=3; Images are representative of findings in each independent experimental replicate which were derived from separate neuron harvests from unique timed pregnant MAPT-KI females.

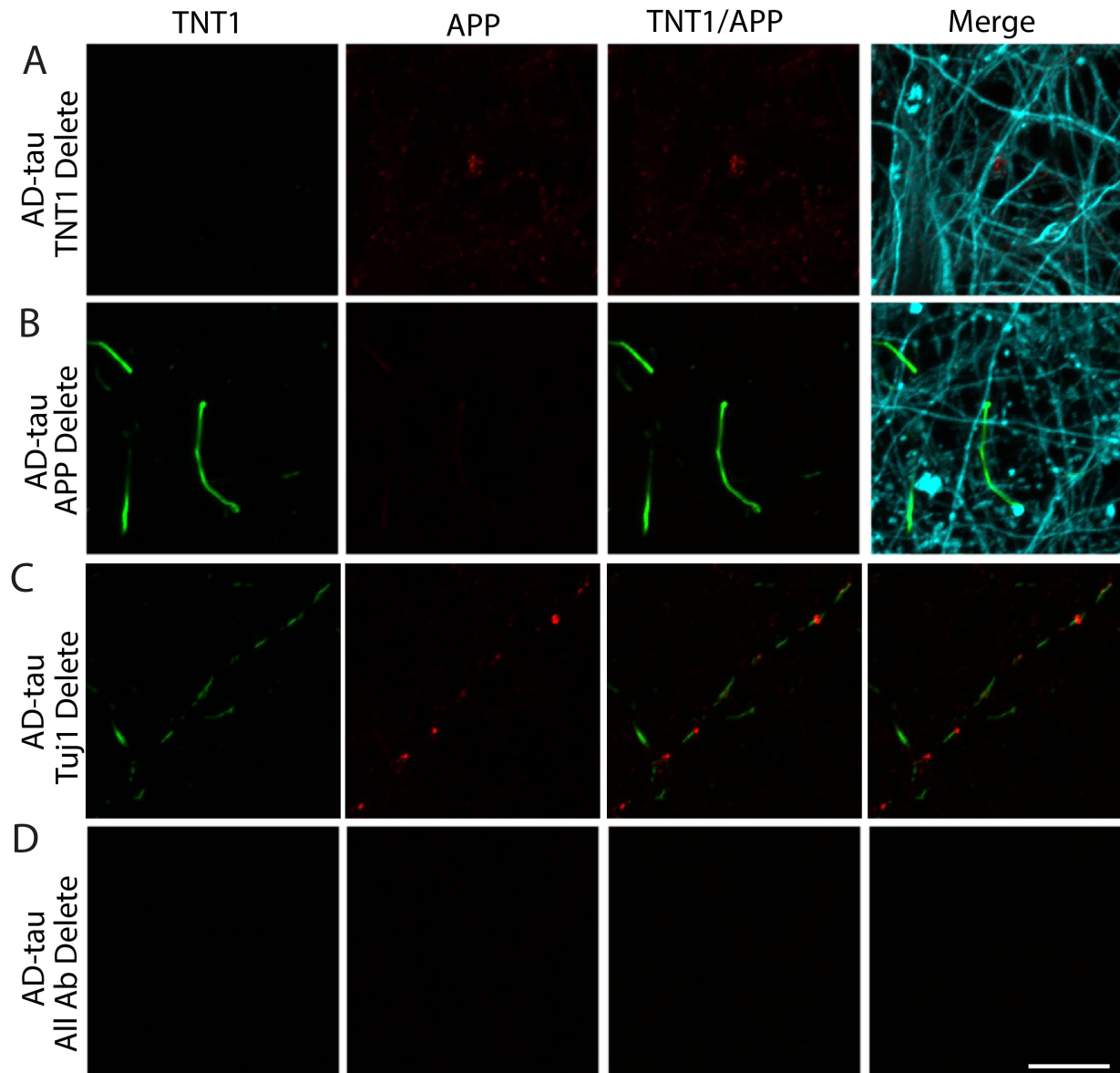


Figure 3.5. APP Immunocytofluorescence (ICF) primary delete control labeling. A-D) ICF primary antibody delete control labeling was performed in AD-tau-treated neurons. A) Omission of the TNT1 primary antibody (green) showed no TNT1 signal. B) Omission of the APP primary antibody (red) showed no APP signal. C) Omission of the Tuj1 primary antibody (cyan) showed no Tuj1 signal. D) Omission of all primary antibodies showed no TNT1, APP, or Tuj1 signal. The lack of signal in the primary antibody deletes confirms that these ICF stains do not cross react with each other. Scale bar = 10 μ m.

Figure 3.5 (cont'd).

N=3; Images are representative of findings in each independent experimental replicate which were derived from separate neuron harvests from unique timed pregnant MAPT-KI females.

Localization of active GSK3 β with pathological tau inclusions

To determine if there is aberrant PAD-pathway signaling (Figure 3.4A) in the AD-tau treated neurons, levels of active GSK3 β were assessed in culture lysates. Cells were treated with PBS, Con, or AD-tau (28 nM tau) on DIV5 and cell lysates were collected 26d post-treatment (corresponding to DIV31). Immunoblotting was performed for active and total GSK3 β using npGSK3 β (active) and total GSK3 α/β antibodies, respectively (Figure 3.4B). The active npGSK3 β signal was normalized to the signal of the β -isoform band of total GSK3 α/β (Figure 3.4C). No significant differences in normalized active GSK3 β signals were observed in the whole culture lysates (one-way ANOVA; $F_{(2,15)} = 0.9203$, $p = 0.4198$). Seeded pathology forms discrete inclusions, therefore, colocalization between active GSK3 β and the sites of pathological tau inclusions was evaluated. Neurons were treated with PBS, Con, or AD-tau, fixed on DIV21 and multi-label ICF was to visualize pS422 (tau inclusions), active npGSK3 β , and Tuj1 β -III tubulin antibodies (Figure 3.6D). Numerous examples of npGSK3 β accumulations localized to pS422+ inclusions. This was true for tau inclusions in the Con and in the AD-tau-treated neurons (Figure 3.6D). However, not all pS422+ tau inclusions were associated with npGSK3 β accumulation. It is noteworthy, that pS422 is extensively colocalized with TNT1+ inclusions, and thus, was used as a surrogate for TNT1+ pathology (TNT1 and npGSK3 β are the same mouse antibody isotype).

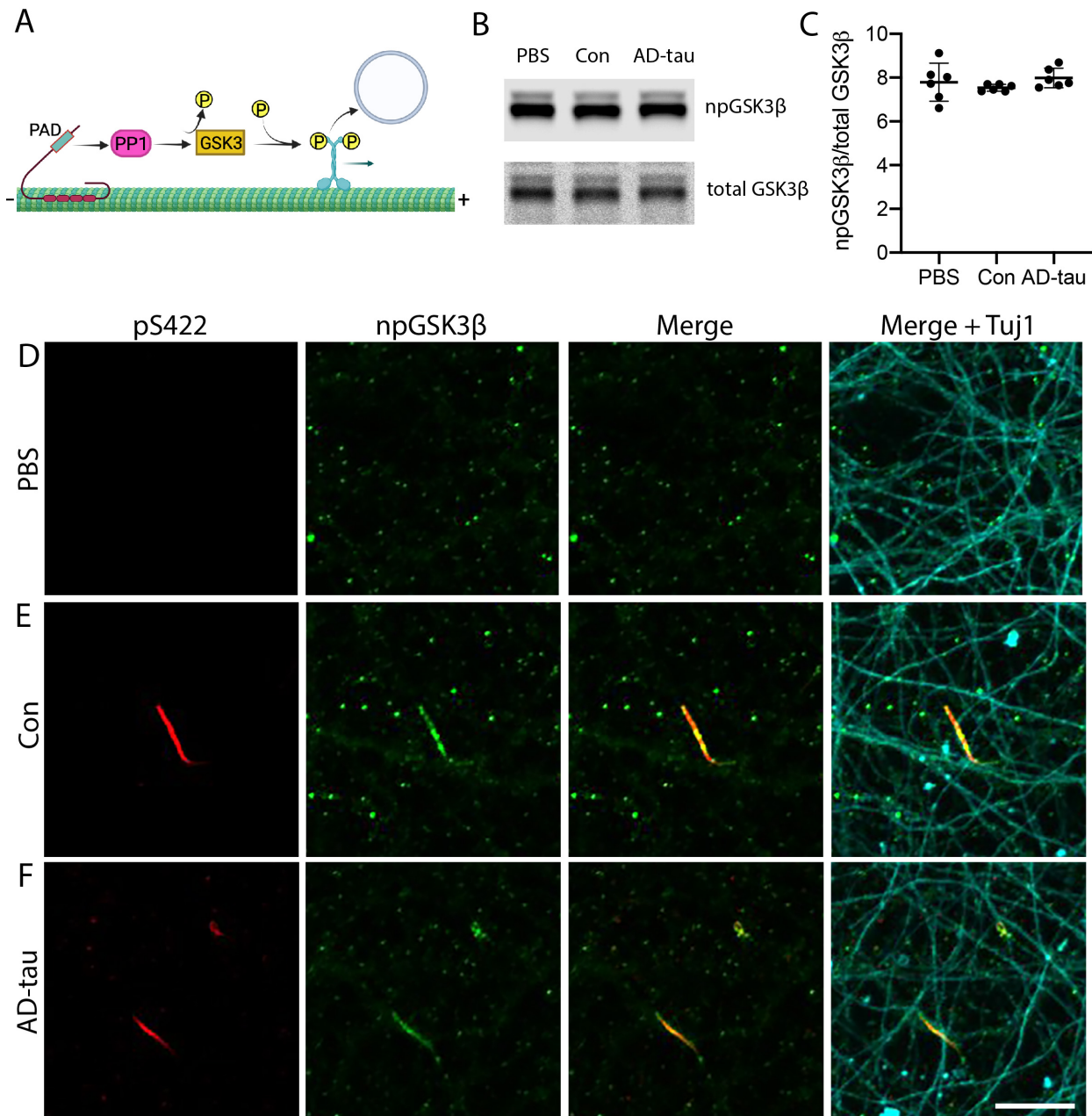


Figure 3.6. Active GSK3 β accumulates with pS422-positive tau inclusions. A) Schematic of the PAD-PP1-GSK3 signaling cascade. B) Immunoblot of cell lysates from PBS, Con, or AD-tau-treated cells probed with npGSK3 β (active) and total GSK3 α/β antibodies. C) Quantification of npGSK3 β normalized to the β -isoform of total GSK3 indicated similar levels of active GSK3 β across groups.

Figure 3.6 (cont'd).

D) ICF of PBS, Con, or AD-tau-treated cells fixed 16d post-treatment (corresponding to DIV21) using pS422 tau (red, seeded tau pathology marker), npGSK3 β (green, active GSK3 β marker), and Tuj1 (cyan, β -III tubulin) antibodies. I observed accumulations of npGSK3 β localized to pS422+ pathological tau inclusions in both the Con and AD-tau conditions. Images are representative of findings in each independent experimental replicate which were derived from separate neuron harvests from unique timed pregnant MAPT-KI females. Scale bar = 10 μ m. The data are mean \pm SD and were compared using one-way ANOVA with Tukey's multiple comparisons test, significance was defined as $p \leq 0.05$.

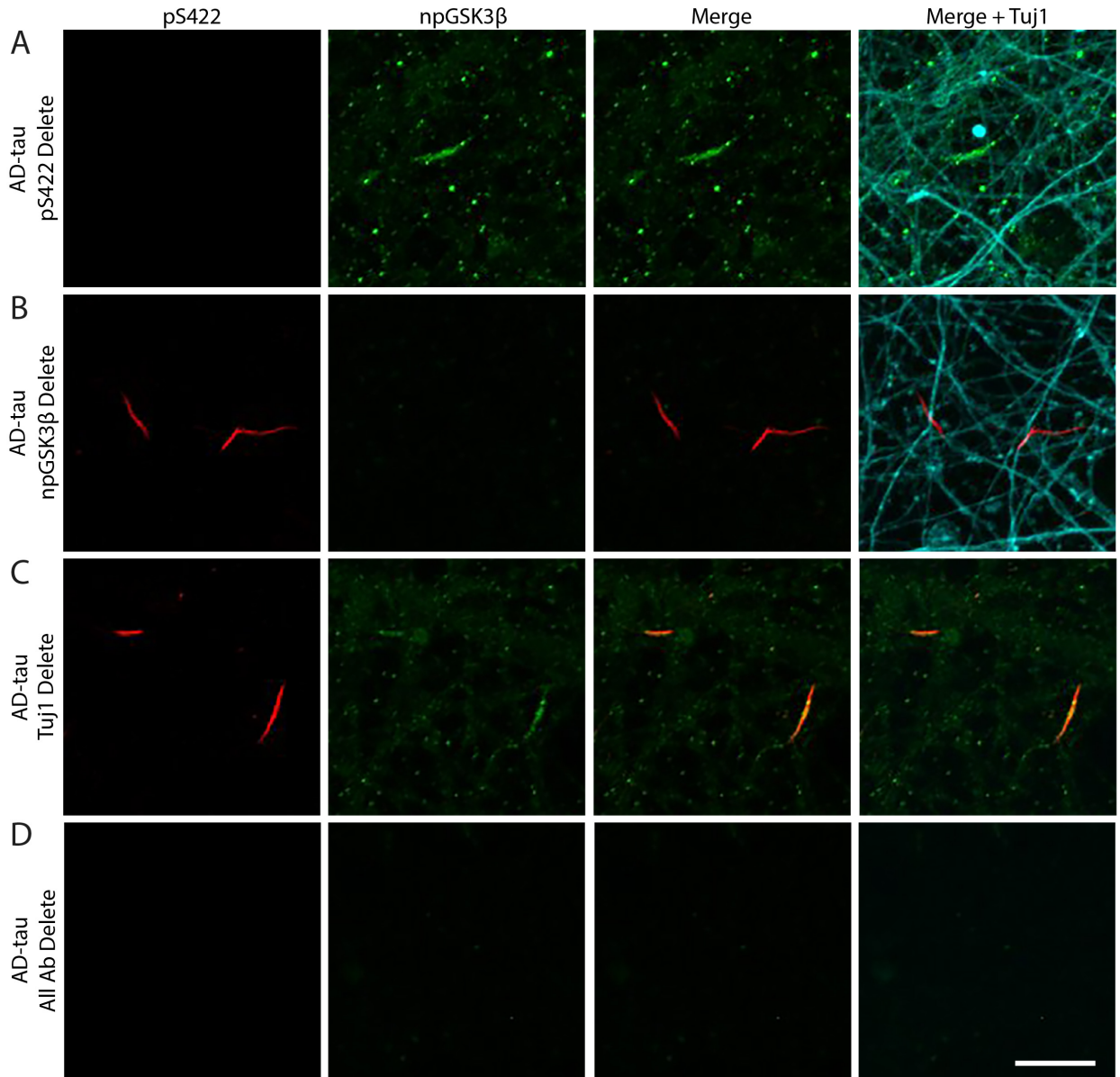


Figure 3.7. npGSK3 Immunocytofluorescence (ICF) primary delete control labeling. A-D) ICF primary antibody delete control labeling was performed in AD-tau-treated neurons. A) Omission of the pS422 primary antibody (red) showed no pS422 signal. B) Omission of the npGSK3 β primary antibody (green) showed no npGSK3 β signal. C) Omission of the Tuj1 primary antibody showed no Tuj1 signal. D) Omission of all primary antibodies showed no pS422, npGSK3 β , or Tuj1 signal.

Figure 3.7 (cont'd).

The lack of signal in the primary antibody deletes confirms that these ICF stains do not cross react with each other. Scale bar = 10 μm . N=3; Images are representative of findings in each independent experimental replicate which were derived from separate neuron harvests from unique timed pregnant MAPT-KI females.

Assessing axonal action potential conduction velocity and axon length using high-density multi-electrode arrays

High-density multielectrode arrays (MEAs) were used to track the action potential propagation along the axonal arborizations of individual cells (Figure 3.8A). An object tracking algorithm was used that detects propagating action potentials from the initiation site to distal branches of individual neurons. Primary MAPT-KI neurons were plated onto MEA chips, then treated with PBS, Con, or AD-tau on DIV5 and recorded on DIV28. I recorded from 60 cells per MEA chip, and only the neurons with branches (i.e. an axon) were included in the analyses. The number of cells with branches used for analyses was similar across groups (Kruskal-Wallis ANOVA with Dunn's post hoc; $H = 1.099$, $p = 0.5964$; Figure 3.8B). The mean action potential conduction velocity was similar across groups (Kruskal-Wallis ANOVA with Dunn's post hoc; $H = 0.1089$, $p = 0.9453$; Figure 3.8C). No differences were observed in the mean total axonal length (Kruskal-Wallis ANOVA with Dunn's post hoc; $H = 0.1520$, $p = 0.9379$; Figure 3.8D) or in the length of the longest axonal branch (one-way ANOVA; $F_{(2,15)} = 0.03201$, $p = 0.9686$; Figure 3.8E).

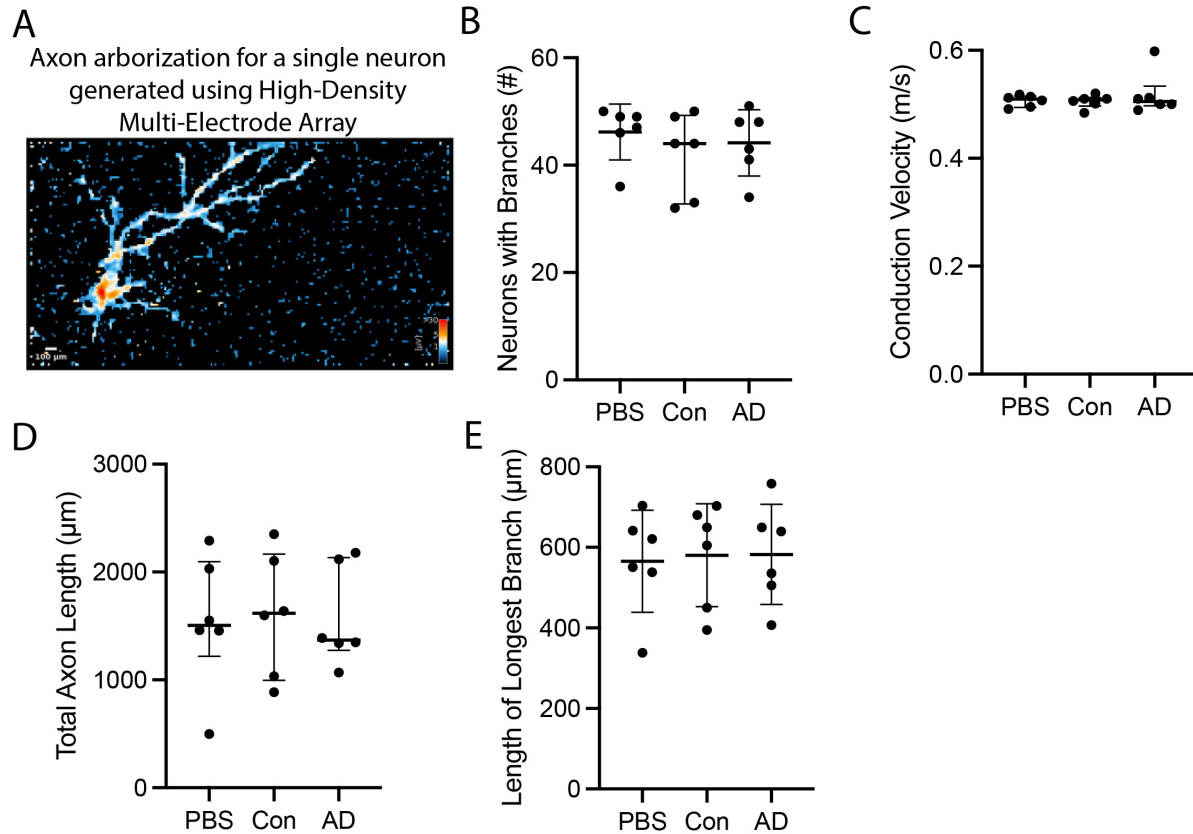


Figure 3.8. Multi-electrode array experiments reveal normal axonal properties in neurons from PBS, Con, or AD-tau treated MAPT-KI cultures. A) PBS, Con, or AD-tau treated cultures were recorded using MEAs on DIV28 (23d post-treatment). Axonal arborizations were tracked using the Axonal Tracking Assay. A representative arborization for a single neuron is shown. B) The number of neurons with branches used for downstream analysis was similar between groups. C) No significant treatment effect on action potential conduction velocity was observed. D) The total axonal length is the sum of the length of all branches per neuron. No treatment effect was observed. E) The length of the longest branch was similar between groups. N=6; each N represents a separate primary neuron harvest from unique timed pregnant MAPT-KI females. Each data point represents the mean for the cells analyzed on a single MEA chip. The data in B-D are median \pm interquartile range and were compared using Kruskal-Wallis ANOVA with Dunn's multiple comparisons test.

Figure 3.8 (cont'd).

The data in E are mean \pm SD and were compared using one-way ANOVA with Tukey's multiple comparisons test. Significance was defined as $p \leq 0.05$.

DISCUSSION

Axonal degeneration is a common event in the pathogenesis of neurodegenerative diseases including AD and other tauopathies (reviewed in (Kneynsberg et al., 2017)). The observations of axonal degeneration in tauopathy animal models (e.g. mice overexpressing tau, often with an FTD-tau mutation) provided a link between pathological tau and axonal degeneration (Lewis et al., 2000; Lin et al., 2003; Lin et al., 2005; Ludvigson et al., 2011; Mayford et al., 1996; Spire et al., 2006). Here, MAPT-KI primary hippocampal neurons were seeded with AD-tau to study the effects of AD-associated pathological tau species on axon degeneration and/or dysfunction. Signs of overt axonal degeneration in the AD-tau treated cultures were not seen using the calpain activity assay and the axon degeneration assays. During neurodegeneration, increased Ca^{2+} levels lead to increased activation of calcium-activated proteases including calpain. Increased calpain activation can result in aberrant proteolysis of axonal cytoskeletal proteins (Yin et al., 2016). Enhanced calpain activity was observed in AD and other tauopathy brains (Adamec et al., 2002). Furthermore, inhibition of calcium-activated proteases in transgenic mice expressing mutant P301L tau reduced axonal degeneration (Rao et al., 2014). In our seeding model, the calpain activity was similar in all groups, suggesting that overt axonal degeneration was not occurring in the AD-tau treated cells. Consistent with this, the analysis of axon degeneration using immunocytofluorescence did not show significant changes in the number of axonal segments or mean axonal segment size (i.e. axonal fragmentation).

Next, earlier signs of axonopathy were measured, including cargo protein accumulations and spheroid bodies, which are observed in human AD brain and could suggest that axon transport mechanism may be impaired. Axonal enlargements containing APP and TNT1+ tau in the AD-tau-treated neurons were present and these were reminiscent of spheroid bodies observed in post-mortem AD brain (Dessi et al., 1997; Stokin et al., 2005). This is consistent with multiple reports of spheroid bodies in animal models of tauopathy (Andorfer et al., 2003; Caillierez et al., 2013; Duff et al., 2000; Hebron et al., 2014; Lewis et al., 2000; Lin et al., 2003; Lin et al., 2005; Ludvigson et al., 2011; Mayford et al., 1996; Santacruz et al., 2005; Spires et al., 2006). Furthermore, synaptophysin accumulations were localized to TNT1+ inclusions in neurites. Accumulation of APP and synaptophysin is observed in AD and thought to result from impaired axonal transport mechanisms (Coleman, 2005; Kamal et al., 2000; Koo et al., 1990). This is consistent with previous work by our group that showed impaired axonal transport of synaptophysin cargos in rat primary neurons expressing FTD-mutant tau or AT8 phosphomimetic tau, which are associated with PAD-exposure and activation of the PP1-GSK3 pathway (Christensen et al., 2023; Combs et al., 2021).

In our seeding model, treatment of neurons with AD-tau resulted in the recruitment of endogenous tau into insoluble inclusions with several disease-associated characteristics including PAD-exposure, oligomerization, and phosphorylation at pS422 and AT8 epitopes (Chapter 2). Each of these tau modifications is mechanistically linked to axonal transport dysfunction (Combs et al., 2021; Combs et al., 2019; Cox et al., 2016; Kanaan et al., 2012; Kanaan et al., 2011; LaPointe et al., 2009). Previous work using isolated axoplasm from the squid giant axon established that tau aggregates, but not wild-type monomer, inhibited fast anterograde transport (FAT) through PP1-GSK3 β signaling, and that the effect was dependent on PAD-exposure (Combs et al., 2021; Combs

et al., 2019; Cox et al., 2016; Kanaan et al., 2012; Kanaan et al., 2011; LaPointe et al., 2009; Morfini et al., 2002; Morfini et al., 2009). Furthermore, monomeric tau with AD-associated modifications (pseudophosphorylation at AT8 and pS422 sites) that are associated with PAD-exposure also inhibited FAT in the squid axoplasm (Kanaan et al., 2011; Tiernan et al., 2016). Expression of monomeric AT8 phosphomimetic tau in rat primary neurons resulted in axonal transport dysfunction. (Christensen et al., 2023). Specifically, there was a significant increase in the pausing frequency of synaptophysin cargoes in AT8-tau expressing neurons (Christensen et al., 2023). Notably, AT8 is one of the primary markers for pathological tau in human tissue, is a modification associated with early pretangle inclusions and is used for Braak staging in AD (Braak et al., 2006; Braak et al., 2011). The pS422+, TOC1+ and TNT1+ tau species are also observed in AD and other tauopathies (Combs & Kanaan, 2017), highlighting their relevance to human disease.

In addition to the presence of synaptophysin accumulation localized to TNT1+ tau inclusions, the observation of local accumulations of active GSK3 β at sites of tau inclusions supports the occurrence of local increases in the PAD-pathway signaling. Technical issues prevented us from performing ICF with TNT1 and npGSK3 β (active) antibodies together (both are mouse IgG1 antibodies). Instead, I used npGSK3 β and pS422 (rabbit) antibodies together. In our model, pS422 and TNT1 were highly colocalized (Chapter 2, Figure 2.11). Furthermore, pS422 and TNT1 immunoreactivity were highly co-localized in human tissue in early through late-stage AD (Tiernan et al., 2016). Therefore, it is reasonable to suggest that PAD-exposure is present at the sites of pS422-immunoreactive tau inclusions. Together, our findings that npGSK3 β (active) and cargo proteins accumulate with pS422 or TNT1 immunoreactivity, respectively, provide indirect evidence of axonal transport dysregulation due to aberrant PAD-exposure and GSK3 β activation.

Recently, another group reported axonal transport dysfunction in primary hippocampal neurons from WT mice transfected with a tau phosphomimetic in which 14 disease-relevant serine/threonine residues were mutated to glutamate to mimic phosphorylation (tau^{E14}; (Hallinan et al., 2019)). Tau accumulations were observed in the distal axon and transport of bidirectionally transported lysosomes was measured. The pool of moving lysosomes was significantly reduced by 50%. PAD-exposure was not assessed in these studies, though the findings support a model of increased cargo pausing, similar to what our group reported in the WT rat neurons transfected with AT8-tau or with FTD-mutant tau (Christensen et al., 2023; Combs et al., 2021). These data suggest that the current findings likely reflect impaired axonal transport in the primary MAPT-KI neurons harboring AD-associated tau pathology. Future studies aimed at assessing live-cell axonal transport at or near TNT1+ inclusions would provide a more direct measure of potential axonal transport impairments.

Axonal transport dysfunction could impair the delivery of ion channels along the axon and alter action potential conduction velocity. Interestingly, disrupted conduction velocity was observed in the CA1 area of the hippocampus in the rTg4510 tauopathy mouse model (Gelman et al., 2020). MEAs were used to assess axonal action potential conduction velocity as a measure of axonal function, but the conduction velocity was not affected in the AD-tau-treated cultures. The MEAs were also used to track the axon arborization of neurons based on electrical activity and quantify axonal length. Consistent with the axon degeneration assay, no change in axonal length in the AD-tau-treated cultures was observed using this measurement. Notably, it was feasible to record 60 neurons per chip (6 chips per treatment). A potential caveat in these studies was that pathological tau was not present in all axons and it is possible that only a portion of the recorded neurons contained tau inclusions. Thus, the effects of pathological tau were potentially washed out

in the measures used here assessing culture-wide effects (e.g. MEA, lysate immunoblotting). This was evident in the GSK3 activity experiments in which an increase in GSK3 β activity was not observed in cell lysates, however, clear accumulations of npGSK3 β were present at sites of PAD-exposed tau inclusions. Local changes in the cell may not be reflected in assays like the indirect calpain activity or even the more direct immunocytofluorescence axonal degeneration assays in which all the neurons were included in the analysis.

The lack of widespread overt axonal degeneration in our model is consistent with findings from other tau seeding models. Most tau seeding studies focus primarily on demonstrating the spread of pathological tau and identifying the mechanisms underlying the spread. However, there are a few studies assessing axonal degeneration in tau seeding models. In one such study, no axonal degeneration was observed in mice expressing human 2N4R tau that were injected with brain homogenate from mice expressing human 0N4R P301S mutant tau out to 15 months post-injection despite the progressive formation of extensive tau pathology (Clavaguera et al., 2009). Three *in vivo* tau propagation studies provide evidence of axonal degeneration. In the first model, expression of mutant P301L tau was restricted to layer II of the entorhinal cortex, and the tau pathology spread to functionally connected sites (i.e. the dentate gyrus and beyond; (de Calignon et al., 2012)). An initial increase in tau pathology in the EC neurons terminating in the dentate gyrus from 3 to 12 months was followed by a decrease in pathology at 18 months. The authors suggested that the loss of pathology was due to axonal degeneration. In a separate study, expression of phosphomimetic tau (pseudophosphorylated at 14 disease-relevant sites) was restricted to the locus coeruleus, and the tau pathology spread to functionally connected regions including the olfactory bulb. Similarly, a reduction of LC noradrenergic fibers in the olfactory cortex was observed at 15 months (Omoluabi et al., 2021). In a third study, atrophy of the dentate gyrus

(molecular layer, granule cell layer and hilus) was observed in WT and THY-Tau22 mice 2 months after injection with human AD-tau into the dentate gyrus (Audouard et al., 2016). The authors suggested that the pattern of atrophy was consistent with loss of dendritic and axonal processes of granule cells (Audouard et al., 2016). Together, these studies suggest that if axonal degeneration occurs, it is observed months after the presence of tau pathology. This could explain why overt axonal degeneration was not observed despite the presence of tau pathology in our seeding model up to 28d post-treatment (corresponding to DIV33). Indeed, signs of *early* axonopathy were present in this model, including axonal swellings reminiscent of the axonal spheroid bodies in human AD brain, and accumulations of cargos and active GSK3 β , suggesting that transport may be impaired.

While signs of early axonopathy were observed, the pathological tau inclusions do not appear to be acutely toxic. Neurons harboring neurofibrillary tangles can survive for decades in the human brain (Morsch et al., 1999). There is growing consensus in the field that soluble tau in the form of modified monomers or oligomers are the toxic species, and that insoluble tau filaments are inert or possibly neuroprotective (Cowan & Mudher, 2013; Ward et al., 2012). Consistent with this idea, overt cell loss is absent in most tau seeding models that use insoluble tau seeds (Baker et al., 2016; Clavaguera et al., 2009; Hallinan et al., 2019; Jackson et al., 2016; McCarthy et al., 2021; Miller et al., 2021; Verheyen et al., 2015) and there are only a few reports of modest axonal degeneration (Audouard et al., 2016; de Calignon et al., 2012; Omoluabi et al., 2021). Furthermore, it was not clear whether the axonal degeneration observed in those studies was due to soluble or insoluble tau pathology.

Here, the evidence supports an accumulation of active GSK3 β , synaptophysin, and APP at the sites of tau inclusions associated with increased PAD-exposure. Together, these findings

suggest that axonal transport may be disrupted in these regions. Experiments that directly measure fast axonal transport in and around the tau inclusions would help elucidate the mechanisms involved. Despite the accumulations of cargo proteins, evidence of overt axonal degeneration or impaired action potential propagation were not seen. An important caveat of these studies is that not all axons contained pathological tau. Therefore, the pathological “load” may not be sufficient to detect widespread axonal degeneration in the assays used. Indeed, perhaps a so-called “second hit” or additional stressor (e.g. amyloid- β , oxidative stress, neuroinflammation, etc.) may be necessary to breach the threshold of degeneration. Future studies should focus on overcoming the challenges with this modeling approach and analyze individual seeded neurons, as this is likely critical to elucidating effects of pathological tau species in the axon.

REFERENCES

- Adamec, E., Mohan, P., Vonsattel, J. P., & Nixon, R. A. (2002, Jul). Calpain activation in neurodegenerative diseases: confocal immunofluorescence study with antibodies specifically recognizing the active form of calpain 2. *Acta Neuropathol*, *104*(1), 92-104. <https://doi.org/10.1007/s00401-002-0528-6>
- Andorfer, C., Kress, Y., Espinoza, M., de Silva, R., Tucker, K. L., Barde, Y. A., Duff, K., & Davies, P. (2003, Aug). Hyperphosphorylation and aggregation of tau in mice expressing normal human tau isoforms. *J Neurochem*, *86*(3), 582-590. <https://doi.org/10.1046/j.1471-4159.2003.01879.x>
- Audouard, E., Houben, S., Masaracchia, C., Yilmaz, Z., Suain, V., Authelet, M., De Decker, R., Buee, L., Boom, A., Leroy, K., Ando, K., & Brion, J. P. (2016, Oct). High-Molecular-Weight Paired Helical Filaments from Alzheimer Brain Induces Seeding of Wild-Type Mouse Tau into an Argyrophilic 4R Tau Pathology in Vivo. *Am J Pathol*, *186*(10), 2709-2722. <https://doi.org/10.1016/j.ajpath.2016.06.008>
- Baker, S., Polanco, J. C., & Gotz, J. (2016, Oct 4). Extracellular Vesicles Containing P301L Mutant Tau Accelerate Pathological Tau Phosphorylation and Oligomer Formation but Do Not Seed Mature Neurofibrillary Tangles in ALZ17 Mice. *J Alzheimers Dis*, *54*(3), 1207-1217. <https://doi.org/10.3233/JAD-160371>
- Benskey, M. J., Panoushek, S., Saito, T., Saido, T. C., Grabinski, T., & Kanaan, N. M. (2023). Behavioral and neuropathological characterization over the adult lifespan of the human tau knock-in mouse. *Front Aging Neurosci*, *15*, 1265151. <https://doi.org/10.3389/fnagi.2023.1265151>
- Berth, S. H., & Lloyd, T. E. (2023, Jun 1). Disruption of axonal transport in neurodegeneration. *J Clin Invest*, *133*(11). <https://doi.org/10.1172/JCI168554>
- Boluda, S., Iba, M., Zhang, B., Raible, K. M., Lee, V. M., & Trojanowski, J. Q. (2015, Feb). Differential induction and spread of tau pathology in young PS19 tau transgenic mice following intracerebral injections of pathological tau from Alzheimer's disease or corticobasal degeneration brains. *Acta Neuropathol*, *129*(2), 221-237. <https://doi.org/10.1007/s00401-014-1373-0>
- Braak, H., Alafuzoff, I., Arzberger, T., Kretschmar, H., & Del Tredici, K. (2006). Staging of Alzheimer disease-associated neurofibrillary pathology using paraffin sections and immunocytochemistry. *Acta neuropathologica*, *112*(4), 389-404.
- Braak, H., & Braak, E. (1991). Neuropathological staging of Alzheimer-related changes. *Acta Neuropathol*, *82*(4), 239-259. <https://doi.org/10.1007/BF00308809>

- Braak, H., Thal, D. R., Ghebremedhin, E., & Del Tredici, K. (2011, Nov). Stages of the pathologic process in Alzheimer disease: age categories from 1 to 100 years. *J Neuropathol Exp Neurol*, 70(11), 960-969. <https://doi.org/10.1097/NEN.0b013e318232a379>
- Caccamo, D., Katsetos, C. D., Herman, M. M., Frankfurter, A., Collins, V. P., & Rubinstein, L. J. (1989, Mar). Immunohistochemistry of a spontaneous murine ovarian teratoma with neuroepithelial differentiation. Neuron-associated beta-tubulin as a marker for primitive neuroepithelium. *Lab Invest*, 60(3), 390-398. <https://www.ncbi.nlm.nih.gov/pubmed/2467076>
- Caillierez, R., Begard, S., Lecolle, K., Deramecourt, V., Zommer, N., Dujardin, S., Loyens, A., Dufour, N., Auregan, G., Winderickx, J., Hantraye, P., Deglon, N., Buee, L., & Colin, M. (2013, Jul). Lentiviral delivery of the human wild-type tau protein mediates a slow and progressive neurodegenerative tau pathology in the rat brain. *Mol Ther*, 21(7), 1358-1368. <https://doi.org/10.1038/mt.2013.66>
- Christensen, K. R., Beach, T. G., Serrano, G. E., & Kanaan, N. M. (2019). Pathogenic tau modifications occur in axons before the somatodendritic compartment in mossy fiber and Schaffer collateral pathways. *Acta neuropathologica communications*, 7, 1-21.
- Christensen, K. R., Combs, B., Richards, C., Grabinski, T., Alhadidy, M. M., & Kanaan, N. M. (2023). Phosphomimetics at Ser199/Ser202/Thr205 in tau impairs axonal transport in rat hippocampal neurons. *Molecular Neurobiology*, 60(6), 3423-3438.
- Clavaguera, F., Akatsu, H., Fraser, G., Crowther, R. A., Frank, S., Hench, J., Probst, A., Winkler, D. T., Reichwald, J., Staufenbiel, M., Ghetti, B., Goedert, M., & Tolnay, M. (2013, Jun 4). Brain homogenates from human tauopathies induce tau inclusions in mouse brain. *Proc Natl Acad Sci U S A*, 110(23), 9535-9540. <https://doi.org/10.1073/pnas.1301175110>
- Clavaguera, F., Bolmont, T., Crowther, R. A., Abramowski, D., Frank, S., Probst, A., Fraser, G., Stalder, A. K., Beibel, M., & Staufenbiel, M. (2009). Transmission and spreading of tauopathy in transgenic mouse brain. *Nature cell biology*, 11(7), 909-913.
- Coleman, M. (2005, Nov). Axon degeneration mechanisms: commonality amid diversity. *Nat Rev Neurosci*, 6(11), 889-898. <https://doi.org/10.1038/nrn1788>
- Combs, B., Christensen, K. R., Richards, C., Kneynsberg, A., Mueller, R. L., Morris, S. L., Morfini, G. A., Brady, S. T., & Kanaan, N. M. (2021). Frontotemporal lobar dementia mutant tau impairs axonal transport through a protein phosphatase 1 γ -dependent mechanism. *Journal of neuroscience*, 41(45), 9431-9451.
- Combs, B., Hamel, C., & Kanaan, N. M. (2016, Oct). Pathological conformations involving the amino terminus of tau occur early in Alzheimer's disease and are differentially detected by monoclonal antibodies. *Neurobiol Dis*, 94, 18-31. <https://doi.org/10.1016/j.nbd.2016.05.016>

- Combs, B., & Kanaan, N. M. (2017, Jun). Exposure of the Amino Terminus of Tau Is a Pathological Event in Multiple Tauopathies. *Am J Pathol*, 187(6), 1222-1229. <https://doi.org/10.1016/j.ajpath.2017.01.019>
- Combs, B., Mueller, R. L., Morfini, G., Brady, S. T., & Kanaan, N. M. (2019). Tau and axonal transport misregulation in tauopathies. *Tau Biology*, 81-95.
- Cowan, C. M., & Mudher, A. (2013). Are tau aggregates toxic or protective in tauopathies? *Front Neurol*, 4, 114. <https://doi.org/10.3389/fneur.2013.00114>
- Cox, K., Combs, B., Abdelmesih, B., Morfini, G., Brady, S. T., & Kanaan, N. M. (2016). Analysis of isoform-specific tau aggregates suggests a common toxic mechanism involving similar pathological conformations and axonal transport inhibition. *Neurobiology of aging*, 47, 113-126.
- Cox, K., Combs, B., Abdelmesih, B., Morfini, G., Brady, S. T., & Kanaan, N. M. (2016, Nov). Analysis of isoform-specific tau aggregates suggests a common toxic mechanism involving similar pathological conformations and axonal transport inhibition. *Neurobiol Aging*, 47, 113-126. <https://doi.org/10.1016/j.neurobiolaging.2016.07.015>
- de Calignon, A., Polydoro, M., Suarez-Calvet, M., William, C., Adamowicz, D. H., Kopeikina, K. J., Pitstick, R., Sahara, N., Ashe, K. H., Carlson, G. A., Spires-Jones, T. L., & Hyman, B. T. (2012, Feb 23). Propagation of tau pathology in a model of early Alzheimer's disease. *Neuron*, 73(4), 685-697. <https://doi.org/10.1016/j.neuron.2011.11.033>
- Dessi, F., Colle, M. A., Haw, J. J., & Duyckaerts, C. (1997, Dec 1). Accumulation of SNAP-25 immunoreactive material in axons of Alzheimer's disease. *Neuroreport*, 8(17), 3685-3689. <https://doi.org/10.1097/00001756-199712010-00006>
- Duff, K., Knight, H., Refolo, L. M., Sanders, S., Yu, X., Picciano, M., Malester, B., Hutton, M., Adamson, J., Goedert, M., Burki, K., & Davies, P. (2000, Apr). Characterization of pathology in transgenic mice over-expressing human genomic and cDNA tau transgenes. *Neurobiol Dis*, 7(2), 87-98. <https://doi.org/10.1006/nbdi.1999.0279>
- Gelman, S., Palma, J., & Ghavami, A. (2020). Axonal Conduction Velocity in CA1 Area of Hippocampus is Reduced in Mouse Models of Alzheimer's Disease. *J Alzheimers Dis*, 77(4), 1383-1388. <https://doi.org/10.3233/JAD-200661>
- Giannakopoulos, P., Herrmann, F. R., Bussiere, T., Bouras, C., Kovari, E., Perl, D. P., Morrison, J. H., Gold, G., & Hof, P. R. (2003, May 13). Tangle and neuron numbers, but not amyloid load, predict cognitive status in Alzheimer's disease. *Neurology*, 60(9), 1495-1500. <https://doi.org/10.1212/01.wnl.0000063311.58879.01>
- Grabinski, T., & Kanaan, N. M. (2016). Novel Non-phosphorylated Serine 9/21 GSK3beta/alpha Antibodies: Expanding the Tools for Studying GSK3 Regulation. *Front Mol Neurosci*, 9, 123. <https://doi.org/10.3389/fnmol.2016.00123>

- Grundke-Iqbal, I., Iqbal, K., Quinlan, M., Tung, Y. C., Zaidi, M. S., & Wisniewski, H. M. (1986, May 5). Microtubule-associated protein tau. A component of Alzheimer paired helical filaments. *J Biol Chem*, *261*(13), 6084-6089. <https://www.ncbi.nlm.nih.gov/pubmed/3084478>
- Guo, J. L., Narasimhan, S., Changolkar, L., He, Z., Stieber, A., Zhang, B., Gathagan, R. J., Iba, M., McBride, J. D., & Trojanowski, J. Q. (2016). Unique pathological tau conformers from Alzheimer's brains transmit tau pathology in nontransgenic mice. *Journal of Experimental Medicine*, *213*(12), 2635-2654.
- Hallinan, G. I., Vargas-Caballero, M., West, J., & Deinhardt, K. (2019, Nov 27). Tau Misfolding Efficiently Propagates between Individual Intact Hippocampal Neurons. *J Neurosci*, *39*(48), 9623-9632. <https://doi.org/10.1523/JNEUROSCI.1590-19.2019>
- Hebron, M. L., Algarzae, N. K., Lonskaya, I., & Moussa, C. (2014, Jan). Fractalkine signaling and Tau hyper-phosphorylation are associated with autophagic alterations in lentiviral Tau and Abeta1-42 gene transfer models. *Exp Neurol*, *251*, 127-138. <https://doi.org/10.1016/j.expneurol.2013.01.009>
- Holmes, B. B., Furman, J. L., Mahan, T. E., Yamasaki, T. R., Mirbaha, H., Eades, W. C., Belaygorod, L., Cairns, N. J., Holtzman, D. M., & Diamond, M. I. (2014, Oct 14). Proteopathic tau seeding predicts tauopathy in vivo. *Proc Natl Acad Sci U S A*, *111*(41), E4376-4385. <https://doi.org/10.1073/pnas.1411649111>
- Jackson, S. J., Kerridge, C., Cooper, J., Cavallini, A., Falcon, B., Cella, C. V., Landi, A., Szekeres, P. G., Murray, T. K., Ahmed, Z., Goedert, M., Hutton, M., O'Neill, M. J., & Bose, S. (2016, Jan 20). Short Fibrils Constitute the Major Species of Seed-Competent Tau in the Brains of Mice Transgenic for Human P301S Tau. *J Neurosci*, *36*(3), 762-772. <https://doi.org/10.1523/JNEUROSCI.3542-15.2016>
- Kamal, A., Stokin, G. B., Yang, Z., Xia, C. H., & Goldstein, L. S. (2000, Nov). Axonal transport of amyloid precursor protein is mediated by direct binding to the kinesin light chain subunit of kinesin-I. *Neuron*, *28*(2), 449-459. [https://doi.org/10.1016/s0896-6273\(00\)00124-0](https://doi.org/10.1016/s0896-6273(00)00124-0)
- Kanaan, N. M., Cox, K., Alvarez, V. E., Stein, T. D., Poncil, S., & McKee, A. C. (2016). Characterization of early pathological tau conformations and phosphorylation in chronic traumatic encephalopathy. *Journal of Neuropathology & Experimental Neurology*, *75*(1), 19-34.
- Kanaan, N. M., Morfini, G., Pigino, G., LaPointe, N. E., Andreadis, A., Song, Y., Leitman, E., Binder, L. I., & Brady, S. T. (2012). Phosphorylation in the amino terminus of tau prevents inhibition of anterograde axonal transport. *Neurobiology of aging*, *33*(4), 826. e815-826. e830.
- Kanaan, N. M., Morfini, G. A., LaPointe, N. E., Pigino, G. F., Patterson, K. R., Song, Y., Andreadis, A., Fu, Y., Brady, S. T., & Binder, L. I. (2011). Pathogenic forms of tau inhibit

- kinesin-dependent axonal transport through a mechanism involving activation of axonal phosphotransferases. *Journal of neuroscience*, 31(27), 9858-9868.
- Kanaan, N. M., Morfini, G. A., LaPointe, N. E., Pigino, G. F., Patterson, K. R., Song, Y., Andreadis, A., Fu, Y., Brady, S. T., & Binder, L. I. (2011, Jul 6). Pathogenic forms of tau inhibit kinesin-dependent axonal transport through a mechanism involving activation of axonal phosphotransferases. *J Neurosci*, 31(27), 9858-9868. <https://doi.org/10.1523/JNEUROSCI.0560-11.2011>
- Kneysberg, A., Combs, B., Christensen, K., Morfini, G., & Kanaan, N. M. (2017). Axonal Degeneration in Tauopathies: Disease Relevance and Underlying Mechanisms. *Front Neurosci*, 11, 572. <https://doi.org/10.3389/fnins.2017.00572>
- Koo, E. H., Sisodia, S. S., Archer, D. R., Martin, L. J., Weidemann, A., Beyreuther, K., Fischer, P., Masters, C. L., & Price, D. L. (1990, Feb). Precursor of amyloid protein in Alzheimer disease undergoes fast anterograde axonal transport. *Proc Natl Acad Sci U S A*, 87(4), 1561-1565. <https://doi.org/10.1073/pnas.87.4.1561>
- Kovacs, G. G. (2015, Feb). Invited review: Neuropathology of tauopathies: principles and practice. *Neuropathol Appl Neurobiol*, 41(1), 3-23. <https://doi.org/10.1111/nan.12208>
- LaPointe, N. E., Morfini, G., Pigino, G., Gaisina, I. N., Kozikowski, A. P., Binder, L. I., & Brady, S. T. (2009). The amino terminus of tau inhibits kinesin-dependent axonal transport: implications for filament toxicity. *Journal of neuroscience research*, 87(2), 440-451.
- Lewis, J., McGowan, E., Rockwood, J., Melrose, H., Nacharaju, P., Van Slegtenhorst, M., Gwinn-Hardy, K., Paul Murphy, M., Baker, M., Yu, X., Duff, K., Hardy, J., Corral, A., Lin, W. L., Yen, S. H., Dickson, D. W., Davies, P., & Hutton, M. (2000, Aug). Neurofibrillary tangles, amyotrophy and progressive motor disturbance in mice expressing mutant (P301L) tau protein. *Nat Genet*, 25(4), 402-405. <https://doi.org/10.1038/78078>
- Lin, W. L., Lewis, J., Yen, S. H., Hutton, M., & Dickson, D. W. (2003, Nov). Ultrastructural neuronal pathology in transgenic mice expressing mutant (P301L) human tau. *J Neurocytol*, 32(9), 1091-1105. <https://doi.org/10.1023/B:NEUR.0000021904.61387.95>
- Lin, W. L., Zehr, C., Lewis, J., Hutton, M., Yen, S. H., & Dickson, D. W. (2005, Dec). Progressive white matter pathology in the spinal cord of transgenic mice expressing mutant (P301L) human tau. *J Neurocytol*, 34(6), 397-410. <https://doi.org/10.1007/s11068-006-8726-0>
- Ludvigson, A. E., Luebke, J. I., Lewis, J., & Peters, A. (2011, Mar). Structural abnormalities in the cortex of the rTg4510 mouse model of tauopathy: a light and electron microscopy study. *Brain Struct Funct*, 216(1), 31-42. <https://doi.org/10.1007/s00429-010-0295-4>
- Mayford, M., Bach, M. E., Huang, Y. Y., Wang, L., Hawkins, R. D., & Kandel, E. R. (1996, Dec 6). Control of memory formation through regulated expression of a CaMKII transgene. *Science*, 274(5293), 1678-1683. <https://doi.org/10.1126/science.274.5293.1678>

- McCarthy, J. M., Virdee, J., Brown, J., Ursu, D., Ahmed, Z., Cavallini, A., & Nuthall, H. N. (2021, May 13). Development of P301S tau seeded organotypic hippocampal slice cultures to study potential therapeutics. *Sci Rep*, *11*(1), 10309. <https://doi.org/10.1038/s41598-021-89230-3>
- Medana, I. M., & Esiri, M. M. (2003, Mar). Axonal damage: a key predictor of outcome in human CNS diseases. *Brain*, *126*(Pt 3), 515-530. <https://doi.org/10.1093/brain/awg061>
- Millecamps, S., & Julien, J. P. (2013, Mar). Axonal transport deficits and neurodegenerative diseases. *Nat Rev Neurosci*, *14*(3), 161-176. <https://doi.org/10.1038/nrn3380>
- Miller, L. V. C., Mukadam, A. S., Durrant, C. S., Vaysburd, M. J., Katsinelos, T., Tuck, B. J., Sanford, S., Sheppard, O., Knox, C., Cheng, S., James, L. C., Coleman, M. P., & McEwan, W. A. (2021, Mar 12). Tau assemblies do not behave like independently acting prion-like particles in mouse neural tissue. *Acta Neuropathol Commun*, *9*(1), 41. <https://doi.org/10.1186/s40478-021-01141-6>
- Morfini, G., Szebenyi, G., Elluru, R., Ratner, N., & Brady, S. T. (2002, Feb 1). Glycogen synthase kinase 3 phosphorylates kinesin light chains and negatively regulates kinesin-based motility. *EMBO J*, *21*(3), 281-293. <https://doi.org/10.1093/emboj/21.3.281>
- Morfini, G. A., Burns, M., Binder, L. I., Kanaan, N. M., LaPointe, N., Bosco, D. A., Brown, R. H., Brown, H., Tiwari, A., & Hayward, L. (2009). Axonal transport defects in neurodegenerative diseases. *Journal of neuroscience*, *29*(41), 12776-12786.
- Morsch, R., Simon, W., & Coleman, P. D. (1999, Feb). Neurons may live for decades with neurofibrillary tangles. *J Neuropathol Exp Neurol*, *58*(2), 188-197. <https://doi.org/10.1097/00005072-199902000-00008>
- Mueller, R. L., Kanaan, N. M., & Combs, B. (2023, Dec 22). Using Live-Cell Imaging to Measure the Effects of Pathological Proteins on Axonal Transport in Primary Hippocampal Neurons. *J Vis Exp*(202). <https://doi.org/10.3791/66156>
- Narasimhan, S., Guo, J. L., Changolkar, L., Stieber, A., McBride, J. D., Silva, L. V., He, Z., Zhang, B., Gathagan, R. J., & Trojanowski, J. Q. (2017). Pathological tau strains from human brains recapitulate the diversity of tauopathies in nontransgenic mouse brain. *Journal of neuroscience*, *37*(47), 11406-11423.
- Narasimhan, S., & Lee, V. M. (2017). The use of mouse models to study cell-to-cell transmission of pathological tau. In *Methods in cell biology* (Vol. 141, pp. 287-305). Elsevier.
- Omoluabi, T., Torraville, S. E., Maziar, A., Ghosh, A., Power, K. D., Reinhardt, C., Harley, C. W., & Yuan, Q. (2021). Novelty-like activation of locus coeruleus protects against deleterious human pretangle tau effects while stress-inducing activation worsens its effects. *Alzheimers Dement (N Y)*, *7*(1), e12231. <https://doi.org/10.1002/trc2.12231>

- Patterson, K. R., Remmers, C., Fu, Y., Brooker, S., Kanaan, N. M., Vana, L., Ward, S., Reyes, J. F., Philibert, K., Glucksman, M. J., & Binder, L. I. (2011, Jul 1). Characterization of prefibrillar Tau oligomers in vitro and in Alzheimer disease. *J Biol Chem*, *286*(26), 23063-23076. <https://doi.org/10.1074/jbc.M111.237974>
- Praprotnik, D., Smith, M. A., Richey, P. L., Vinters, H. V., & Perry, G. (1996). Filament heterogeneity within the dystrophic neurites of senile plaques suggests blockage of fast axonal transport in Alzheimer's disease. *Acta Neuropathol*, *91*(3), 226-235. <https://doi.org/10.1007/s004010050420>
- Price, J. L., Davis, P. B., Morris, J. C., & White, D. L. (1991, Jul-Aug). The distribution of tangles, plaques and related immunohistochemical markers in healthy aging and Alzheimer's disease. *Neurobiol Aging*, *12*(4), 295-312. [https://doi.org/10.1016/0197-4580\(91\)90006-6](https://doi.org/10.1016/0197-4580(91)90006-6)
- Price, J. L., & Morris, J. C. (1999, Mar). Tangles and plaques in nondemented aging and "preclinical" Alzheimer's disease. *Ann Neurol*, *45*(3), 358-368. [https://doi.org/10.1002/1531-8249\(199903\)45:3<358::aid-ana12>3.0.co;2-x](https://doi.org/10.1002/1531-8249(199903)45:3<358::aid-ana12>3.0.co;2-x)
- Raff, M. C., Whitmore, A. V., & Finn, J. T. (2002, May 3). Axonal self-destruction and neurodegeneration. *Science*, *296*(5569), 868-871. <https://doi.org/10.1126/science.1068613>
- Rao, M. V., McBrayer, M. K., Campbell, J., Kumar, A., Hashim, A., Sershen, H., Stavrides, P. H., Ohno, M., Hutton, M., & Nixon, R. A. (2014, Jul 9). Specific calpain inhibition by calpastatin prevents tauopathy and neurodegeneration and restores normal lifespan in tau P301L mice. *J Neurosci*, *34*(28), 9222-9234. <https://doi.org/10.1523/JNEUROSCI.1132-14.2014>
- Roy, S., Zhang, B., Lee, V. M., & Trojanowski, J. Q. (2005, Jan). Axonal transport defects: a common theme in neurodegenerative diseases. *Acta Neuropathol*, *109*(1), 5-13. <https://doi.org/10.1007/s00401-004-0952-x>
- Saito, T., Mihira, N., Matsuba, Y., Sasaguri, H., Hashimoto, S., Narasimhan, S., Zhang, B., Murayama, S., Higuchi, M., Lee, V. M. Y., Trojanowski, J. Q., & Saido, T. C. (2019, Aug 23). Humanization of the entire murine Mapt gene provides a murine model of pathological human tau propagation. *J Biol Chem*, *294*(34), 12754-12765. <https://doi.org/10.1074/jbc.RA119.009487>
- Santacruz, K., Lewis, J., Spires, T., Paulson, J., Kotilinek, L., Ingelsson, M., Guimaraes, A., DeTure, M., Ramsden, M., McGowan, E., Forster, C., Yue, M., Orne, J., Janus, C., Mariash, A., Kuskowski, M., Hyman, B., Hutton, M., & Ashe, K. H. (2005, Jul 15). Tau suppression in a neurodegenerative mouse model improves memory function. *Science*, *309*(5733), 476-481. <https://doi.org/10.1126/science.1113694>
- Spires, T. L., Orne, J. D., SantaCruz, K., Pitstick, R., Carlson, G. A., Ashe, K. H., & Hyman, B. T. (2006, May). Region-specific dissociation of neuronal loss and neurofibrillary

- pathology in a mouse model of tauopathy. *Am J Pathol*, 168(5), 1598-1607. <https://doi.org/10.2353/ajpath.2006.050840>
- Stokin, G. B., & Goldstein, L. S. (2006). Axonal transport and Alzheimer's disease. *Annu Rev Biochem*, 75, 607-627. <https://doi.org/10.1146/annurev.biochem.75.103004.142637>
- Stokin, G. B., Lillo, C., Falzone, T. L., Bruschi, R. G., Rockenstein, E., Mount, S. L., Raman, R., Davies, P., Masliah, E., Williams, D. S., & Goldstein, L. S. (2005, Feb 25). Axonopathy and transport deficits early in the pathogenesis of Alzheimer's disease. *Science*, 307(5713), 1282-1288. <https://doi.org/10.1126/science.1105681>
- Tiernan, C. T., Combs, B., Cox, K., Morfini, G., Brady, S. T., Counts, S. E., & Kanaan, N. M. (2016, Sep). Pseudophosphorylation of tau at S422 enhances SDS-stable dimer formation and impairs both anterograde and retrograde fast axonal transport. *Exp Neurol*, 283(Pt A), 318-329. <https://doi.org/10.1016/j.expneurol.2016.06.030>
- Verheyen, A., Diels, A., Dijkmans, J., Oyelami, T., Meneghello, G., Mertens, L., Versweyveld, S., Borgers, M., Buist, A., Peeters, P., & Cik, M. (2015). Using Human iPSC-Derived Neurons to Model TAU Aggregation. *PLoS One*, 10(12), e0146127. <https://doi.org/10.1371/journal.pone.0146127>
- Ward, S. M., Himmelstein, D. S., Lancia, J. K., & Binder, L. I. (2012, Aug). Tau oligomers and tau toxicity in neurodegenerative disease. *Biochem Soc Trans*, 40(4), 667-671. <https://doi.org/10.1042/BST20120134>
- Yin, Y., Wang, Y., Gao, D., Ye, J., Wang, X., Fang, L., Wu, D., Pi, G., Lu, C., Zhou, X. W., Yang, Y., & Wang, J. Z. (2016, Jun 9). Accumulation of human full-length tau induces degradation of nicotinic acetylcholine receptor alpha4 via activating calpain-2. *Sci Rep*, 6, 27283. <https://doi.org/10.1038/srep27283>
- Zareba-Paslawska, J., Patra, K., Kluzer, L., Revesz, T., & Svenningsson, P. (2020). Tau Isoform-Driven CBD Pathology Transmission in Oligodendrocytes in Humanized Tau Mice. *Front Neurol*, 11, 589471. <https://doi.org/10.3389/fneur.2020.589471>

CHAPTER 4

Primary neurons seeded with human AD brain-derived tau exhibit altered NMDAR-mediated synaptic activity and loss of excitatory synapses

ABSTRACT

Synapse loss is one of the earliest and strongest structural correlates of cognitive decline in AD. The burden of tau pathology negatively correlates with synapse density, and tau is mechanistically linked to synapse dysfunction in AD models. Tau is linked to hyperexcitability and epilepsy. Furthermore, neuronal hyperexcitability, network hypersynchrony (e.g. epileptiform activity), and hyperactivity of specific brain regions have each been implicated in early AD. The precise mechanisms underlying these dysfunctions are not fully known, however, NMDA receptors are thought to play a role. Evidence suggests a role for tau in regulating NMDARs through Fyn kinase and pathological tau can cause dysregulation that can lead to excitotoxicity. The precise mechanisms through which tau exerts toxic effects on the synapse are still being investigated. Here, AD brain-derived tau (AD-tau) was used to seed the formation of AD-associated pathological tau inclusions in human tau knock-in primary neurons (MAPT-KI), then the effects of these pathological tau species on synapse integrity and function were investigated. Synaptic integrity was assessed by quantifying pre- and postsynaptic proteins in cell lysates of AD-tau treated cells, and proximity ligation assays were used to quantify the number of intact excitatory synapses in fixed cells. Next, synaptic function was measured using multielectrode arrays. Basal firing rate, network burst frequency, and glutamate-evoked changes in these measures were assessed. There was a significant reduction in the number of excitatory synapses in the seeded neurons compared to controls. The basal activity of the seeded cultures was normal, however, the magnitude of the glutamate-evoked response on network burst frequency was significantly greater

compared to controls. Upon addition of an NMDAR antagonist, AP5, the network hypersynchrony was decreased, and in most cases, abolished, suggesting that the response was NMDAR-mediated. These data demonstrate that this seeding model exhibits aspects of neuronal dysfunction associated with early stages of disease. Understanding the specific mechanisms involved in the earliest stages of AD could help guide the development of treatments that could prevent downstream overt neurodegeneration and neuronal loss.

INTRODUCTION

Alzheimer's disease (AD) is defined by the postmortem identification of intracellular neurofibrillary tangles and extracellular plaques comprised of filamentous tau or amyloid- β proteins, respectively. The spatiotemporal distribution of tau pathology correlates with cognitive decline and disease progression in AD, therefore, there is great interest in identifying the specific mechanisms whereby pathological tau exerts toxic effects on neurons in AD (Arriagada et al., 1992; Braak et al., 2006; Braak & Braak, 1991; Cho et al., 2016; Giannakopoulos et al., 2003; Lagarde et al., 2022; Nelson et al., 2012; Price et al., 1991; Price & Morris, 1999; Scholl et al., 2016). The strongest and one of the earliest structural correlates in the brain for cognitive decline in AD is the loss of synapses (DeKosky & Scheff, 1990; Masliah et al., 1994; Scheff et al., 2007; Serrano-Pozo et al., 2011). Pathological tau burden correlates with synaptic density in postmortem tissue analyses and more recently in longitudinal positron emission tomography studies using pathological tau-specific tracers (Heinonen et al., 1995; Scheff & Price, 1993; Scheff et al., 1993; Terry et al., 1991; Wang et al., 2024). Furthermore, synaptic dysfunction resulting in neuronal hyperexcitability is an early phenotype of AD, as demonstrated in humans and in animal models of AD (Targa Dias Anastacio et al., 2022). Determining the role of tau in synaptic dysfunction and loss is an area of active investigation.

Evidence from *in vitro* and *in vivo* animal models of AD showed an increase in action potential firing rate, and a lower threshold for firing (Targa Dias Anastacio et al., 2022). Studies consistently show that early stages of AD involve hyperexcitability at the single neuron level, the neural network level, and at the brain region level (Targa Dias Anastacio et al., 2022). Tau is experimentally linked to neuronal hyperexcitability. In animal models of epilepsy, tau knockdown or knockout ameliorates seizure activity (Targa Dias Anastacio et al., 2022). Tau also has a role in LTP, the molecular substrate of learning and memory. Recombinant tau oligomers were shown to acutely impair LTP in the rat hippocampus *in vivo*, and in mouse hippocampal slices (Fa et al., 2016; Ondrejcek et al., 2019; Ondrejcek et al., 2018).

Over the past decade, a growing body of research used tau seeding models to study the impact of pathological tau on neuron dysfunction and degeneration. In both *in vitro* and *in vivo* modeling systems, the application of exogenous sources of pathological tau (e.g. recombinant or human tissue-derived) leads to its uptake in neurons and templating of endogenous tau proteins into pathological species. This modeling approach provides an excellent means to study the downstream consequences of pathogenic forms of tau. Several groups demonstrated that tau pathology is propagated via tau seeding *in vitro* and *in vivo*. Interestingly, relatively few have reported functional or structural evidence of neurodegeneration. The few studies documenting synaptic dysfunction, axon degeneration or overt cell loss typically utilize recombinant tau modified to harbor mutations or phosphomimetics at specific disease-relevant residues as the seeding material (de Calignon et al., 2012; Hallinan et al., 2019; Reilly et al., 2017; Shrivastava et al., 2019; Stancu et al., 2015; Usenovic et al., 2015; Zhu et al., 2022). Nevertheless, these studies provide evidence of a role for tau in impairing spontaneous neuronal network activity, affecting Ca^{2+} homeostasis at the presynapse, and decreases in presynaptic or postsynaptic markers (e.g.

synaptophysin, synapsin-1 and PSD95). Furthermore, these studies employed pharmacological methods to determine key players in the affected pathways (i.e. agonists and antagonists targeting GABA, AMPA or NMDA receptors) (Stancu et al., 2015; Usenovic et al., 2015).

The structure of tau fibril cores are unique in various tauopathies, as highlighted by cryoEM analyses (Falcon, Zhang, Murzin, et al., 2018; Falcon, Zhang, Schweighauser, et al., 2018; Falcon et al., 2019; Fitzpatrick et al., 2017; Scheres et al., 2020; Zhang et al., 2019; Zhang et al., 2020). This highlights the importance of using human brain-derived tau as the seeding material in AD models to recapitulate the structural features of human disease tau aggregates. Acute synaptic dysfunction was observed in wild-type primary neurons treated with human AD brain-derived tau (Fa et al., 2016; Saroja et al., 2022), however, long term effects of seeding were not explored. Notably, APP/PS1 mice injected with AD brain-derived tau exhibited epileptiform activity and network excitability five months post-injection (Tok et al., 2022). The effects were not observed in APP-KI mice (Tok et al., 2022). Here, a mouse model in which the entire mouse *MAPT* gene was replaced with human *MAPT* (MAPT-KI) was used (Saito et al., 2019)). I seeded MAPT-KI mouse primary hippocampal neurons with human AD brain-derived tau and investigated the effects of seeding on synaptic density, as well as spontaneous and evoked neuron activity. I report that the AD-tau seeded primary neuron cultures exhibited NMDAR-mediated network hyperexcitability in response to glutamate.

METHODS

Animals

Timed-pregnant female *MAPT* knock-in (MAPT-KI (Saito et al., 2019)) mice were bred in-house. Animals were housed in 12 h light/dark cycle and had access to food and water *ad libitum*. Pregnant females were euthanized with a lethal dose of sodium pentobarbital (at least 100 mg/kg) delivered

by intraperitoneal injection. These studies were conducted in compliance with federal, state, and institutional guidelines and all procedures were approved by Michigan State University's Institutional Animal Care and Use Committee.

Primary Neurons

Glass-bottom 18-well chamber slides (Ibidi, 81817) were coated with 0.5 mg/mL poly-D-lysine (Sigma P7886-100MG) in borate buffer [12.5 mM sodium borate decahydrate (VWR, MK745706) and 50 mM boric acid (Sigma, B6768-1KG)] overnight at room temperature. Slides were washed 4x with sterile deionized water and air dried. Primary neurons were obtained from E16 MAPT-KI mice as previously described (Mueller et al., 2023). Briefly, the hippocampi were dissected from each pup and pooled in ice-cold calcium and magnesium-free buffer [CMF; 1X Dulbecco's PBS (Gibco, 14200-075), 0.1% glucose (Sigma, G7528), 2.5 µg/mL amphotericin B (Gibco, 15290-026), and 50 µg/mL gentamicin (Gibco, 15710-072)]. The tissue was washed twice with CMF then incubated with 0.125% trypsin/CMF for 15 min at 37 °C. Then, the tissue was washed twice with CMF, followed by the addition of 3 mL trypsin inactivation solution [Hank's Balanced Salt Solution (Gibco, 24020-117), 20% newborn calf serum (Gibco, 16010-167) and 1X DNase I solution (10X stock: 5 mM sodium acetate (Sigma, S5636), 1 µM calcium chloride (Sigma, C7902), 0.5 mg/mL DNaseI (Fisher, NC9185812)]. Tissue was immediately dissociated into a single-cell suspension by trituration with a 3 mL syringe and a series of progressively smaller diameter needles. Cells were centrifuged over Fetal Bovine Serum (FBS; Invitrogen, 16000044) at 200 x g for 5 min. The FBS was discarded and the cells were resuspended in warm neurobasal media plus (Gibco, A3582901) supplemented with 2% B27 Plus (Gibco, A3582801), and 1% GlutaMAX (Gibco, 35050061), with antibiotics: 2.5 µg/mL amphotericin B and 50 µg/mL gentamicin. Cells were plated in poly-D-lysine coated 24-well plates (150,000 cells/well in 500

μl/well NBM Plus; Fisher, 08-774-124) for biochemistry or in poly-D-lysine coated 18-well chamber slides (25,000 cells/well in 100 μl/well NBM Plus) for microscopy. Cells were maintained in a humidity-controlled 37 °C incubator with 5% CO₂. Cells received fresh NBM Plus every other day: 5 μl (18-well chamber slides) or 75 μl (24-well plates) per well.

Purification of AD-tau from human frontal cortex

Sarkosyl-insoluble tau was purified from human AD brain frontal cortical tissue obtained from the University of Michigan Brain Bank according to methods adapted from Narasimhan and Lee (Narasimhan & Lee, 2017). Briefly, frontal cortical tissue from six post-mortem cases of advanced AD, Braak stage V-VI, was pooled (3.5-4.5 g total). The same amount of post-mortem frontal cortical tissue from five or six age-matched cognitively unimpaired individuals, Braak stage I-II, was pooled and processed in parallel with the AD tissue to be used as a control throughout experiments (Con). Tissue was homogenized in 9 volumes of ice-cold high-salt extraction buffer (10 mM Tris, pH 7.4, 10% sucrose, 0.8 M NaCl, 1 mM EDTA, 0.1% sarkosyl) supplemented on the day of use with protease (2 μg/mL pepstatin, 2 μg/mL bestatin, 2 μg/mL leupeptin, 4 mM phenylmethylsulfonyl fluoride, 10 μg/mL aprotinin) and phosphatase inhibitors (1 mM tetrasodium pyrophosphate decahydrate, 10 mM β-glycerophosphate, 1 mM sodium orthovanadate, 1 M sodium fluoride) using a glass Dounce homogenizer. The homogenate was transferred to 50 mL conical tubes and centrifuged at 10,000 x g(max) for 10 min at 4 °C in a F14-14 x 50cy fixed angle rotor (Thermo Scientific, 096-145075) and Sorvall LYNX 4000 Superspeed centrifuge (Thermo Scientific, 75006581). The supernatant was filtered through a KimWipe into a new 50 mL conical tube. The pellet was homogenized and centrifuged as above. The 2nd supernatant was filtered as above. This process was repeated once more. The supernatants were pooled into a glass beaker and the concentration of sarkosyl was increased to 1%. The mixture was stirred with a stir bar on

a stir plate for 1.5 h at room temperature, then transferred to 36 mL ultracentrifuge tubes (Beckman Coulter 355618) and centrifuged at 300,000 x g(max) at 4 °C for 60 min in a T-865 fixed angle rotor (Thermo Scientific, 51411) and Sorvall WX+ Ultra centrifuge (Thermo Fisher, 75000100). The resulting pellet was washed with 1X Dulbecco's Phosphate Buffered Saline (dPBS; Gibco, 14200-075), broken up with a pipet tip, then transferred to a new 36 mL tube which was then filled with dPBS, and centrifuged at 250,000 x g(max) at 4 °C for 30 min in a T-865 8 x 36ml rotor and Sorvall WX+ Ultra centrifuge. The resulting pellet was broken up in dPBS (100 µl/g of original tissue, i.e., 450 µl dPBS for 4.5 g) and transferred to a 1.5 mL tube, then incubated on a shaker at room temperature overnight. The following day the pellet was homogenized by passing the suspension through a 21G needle, followed by a 27G needle, and sonicated (20 x 1 sec pulses at power level 1.5; Misonix, XL-2000). The homogenate was transferred to a thick wall 0.5 mL tube (Thermo Scientific, 45235) tube and centrifuged at 100,000 x g(max) at 4 °C for 30 min in a S120-AT3 14 x 0.5 ml rotor (Thermo Scientific, 45584) and Sorvall MTX Micro-Ultra centrifuge (Thermo Scientific, 46960). The resulting pellet was resuspended in 150 µl – 200 µl dPBS, sonicated (60 x 1 sec pulses at power level 1.5), transferred to a thick wall 0.2 mL tube (Thermo Scientific, 45233) and centrifuged at 10,000 x g(max) for 30 min at 4 °C in a S100-AT3 fixed angle rotor (Thermo Scientific, 45585) and Sorvall MTX Micro-Ultra centrifuge. The resulting supernatant contained the sarkosyl-insoluble tau (or Con proteins) and was sonicated (60 x 1 sec pulses at power level 1.5), then aliquoted and stored at -80 °C until use.

Treatment of primary hippocampal cultures

Primary hippocampal cultures were treated on DIV5 with 28 nM of AD-tau (based on the tau concentration determined by total tau sandwich ELISA), Con (matched to the total protein concentration of the AD-tau samples), or dPBS. Treatments were prepared in fresh NBM Plus

media and prewarmed to 37 °C. The treatments were mixed briefly by vortex immediately before addition to cells. The treatments were added directly to the cell culture media in a spiral pattern, then the culture plate or slide or MEA device was gently rocked to mix, and returned to the incubator.

Western blotting

Cell lysates were collected 26d post-treatment (corresponding to DIV31) in cell lysis buffer (20 mM Tris, 0.5 mM DTT, 150 mM NaCl, 0.5% Triton X-100, pH7.5) supplemented with protease inhibitors (2 µg/mL pepstatin, 2 µg/mL bestatin, 2 µg/mL leupeptin, 4 mM phenylmethylsulfonyl fluoride, 10 µg/mL aprotinin) and phosphatase inhibitors (1 mM tetra-sodium pyrophosphate decahydrate, 10 mM β-glycerophosphate, 1 mM sodium orthovanadate, 1 M sodium fluoride). Lysates were sonicated and total protein was quantified using the Bradford protein assay (Bio-Rad, 5000006) as directed. Then, 40 µg of each lysate was prepared in TBS with Laemmli sample buffer (final 1X composition: 20 mM Tris, pH 6.8, 2% SDS, 6% glycerol, 1% β-mercaptoethanol, 0.002% Bromophenol Blue) and heated to 95 °C for 5 min. Samples were loaded onto 12-well Criterion TGX Precast 4-20% gels (Bio-Rad, 567-1093) alongside All Blue Precision Plus Protein Standards (Bio-Rad 161-0373) and run at 250V until the dye front reached the bottom of the gel (32 min). Proteins were transferred onto nitrocellulose membranes using a Bio-Rad transfer unit at 400 mA for 50 min. Membranes were blocked in 2% Non-Fat Dry Milk (NFDM) for 1 hour. Membranes were cut horizontally just above the 50 kDa marker. The top half was probed with PSD95 antibody (1:1,000; rabbit; Cell Signaling Technology, 3450), and the bottom half of the membrane was incubated with synaptophysin antibody (1:1,000; mouse IgG1; Sigma, MAB5258) and GAPDH antibody (used as a loading control, 1:2,000; rabbit; Cell Signaling Technology, 5174) in 2% NFDM overnight at 4 °C. Membranes were washed with TBS/0.1% TWEEN 20

(TBST) 3 x 5 min, then incubated with secondary antibodies (all 1:20,000) in 2% NFDM for 1 hour. The top portion of the blot was incubated with IRDye 680LT goat anti-rabbit (LiCor, 926-68021) and the bottom portion was incubated with IRDye 680LT goat anti-mouse IgG1 (LiCor, 926-68050) and IRDye 800CW goat anti-rabbit (LiCor, 926-32211). Membranes were washed 3 x 5 min in TBST then imaged using a Li-Cor Odyssey infrared imaging system and Li-Cor ImageStudioLite 5.2 software was used to quantify the signal intensity of the bands. Synaptophysin and PSD95 signals were normalized to GAPDH signal.

Proximity ligation assay (PLA)

Primary MAPT-KI neurons were plated in PDL-coated 18-well glass-bottom chamber slides at a density of 25,000 cells/well in 100 μ l of NBM Plus media. Cultures were treated on DIV 5 with PBS, CO, or 56 nM AD-tau. Cells were fixed on DIV 33 (16- or 28-d post-treatment) with warm 4% paraformaldehyde in cytoskeleton buffer (10 mM MES, 138 mM KCl, 3 mM MgCl₂, and 4 mM EGTA, pH 6.1) for 20 min, then washed 3 x 5 min with 1X TBS. Cells were blocked (5% goat serum, 1% BSA, and 0.2% triton-X in TBS) for 1 h at room temperature. Then cells treated with PBS, CO or AD-tau were incubated overnight at 4 °C with homer 1 antibody (2 ng/ μ L; rabbit; Synaptic Systems, 160003) and bassoon antibody (2 ng/ μ L; mouse IgG2b; NeuroMab, 73-491) diluted in 2% goat serum. Untreated cells were incubated with either homer (bassoon primary delete) or bassoon (homer primary delete), or no antibody (both primaries omitted) as controls for the PLA method. The next day, I used a Duolink PLA kit (Sigma-Aldrich, DUO96020) to identify intact synapses in which homer and bassoon were in close association. The cells were washed 4 x 5 min in Buffer A, then incubated with anti-mouse PLUS and anti-rabbit MINUS secondary antibody probes (each diluted 1:15 in 2% goat serum) for 1 h at 37 °C. Cells were washed 4 x 5 min in Buffer A, then incubated in ligase (diluted 1:40 in 1X ligation buffer) for 30 min at 37 °C.

Cells were washed again 4 x 5 min in Buffer A, then incubated in polymerase (diluted 1:80 in 1X amplification buffer) for 100 min at 37 °C. Then, cells were washed 2 x 10 min in Wash Buffer B at room temperature. Next, cells were incubated in blocking buffer as above for 1 h at room temperature and then incubated overnight at 4 °C with TNT1 (25 ng/mL; mouse IgG1; Kanaan Lab; (Combs et al., 2016; Kanaan et al., 2011)) and Tuj1, a β -III tubulin antibody, (100 ng/mL; mouse IgG2a; (Caccamo et al., 1989)) in 2% goat serum. Individual and double antibody-deletes were included as controls in untreated and AD-tau-treated neurons that had also undergone the PLA assay as described above. The cells were washed 3 x 5 min with 1X TBS, then incubated with secondary antibodies Alexa Fluor goat anti-mouse IgG2a 568 (Thermo, A21134) and goat anti-mouse IgG1 647 (Thermo Fisher, A21240) each diluted 1:500 in 2% goat serum for 1 h at room temperature. Cells were washed 3 x 5 min in 1X TBS. DAPI stain (1:10,000; Thermo, D1306) was included in the first wash to label nuclei.

Cells were imaged with a Nikon A1+ laser scanning confocal microscope equipped with 405, 488, 561, and 640 solid state lasers and Nikon Elements AR software. Z-stack images were acquired using a 60x/1.40 NA oil-immersion objective with a step size of 0.25 μ m (21 images/stack). Z-stack images for analysis (0.5 μ m step sizes and 11 images/stack) were collected using a 40x/1.3 NA objective; 4 representative images were acquired. Maximum Projection images of the Z-stacks were generated in NIS-Elements. The channels were split in FIJI ImageJ for data quantitation. A threshold mask was generated for the PLA puncta (green channel) using the default threshold setting and the number of puncta per image were counted using the Analyze Particles function (Size: 0-infinity, Circularity: 0.00-1.00). A separate threshold mask was generated for the Tuj1 immunolabelling (red channel) using the Huang setting and the total area of the mask was calculated using the Measure function. The number of puncta/total Tuj1 area (μ m²) were calculated

for each image. Individual data points represent the mean of the results from all analyzed images within an individual experimental replicate and the experiment was repeated four independent times (N=4). Representative images were prepared for publication using ImageJ (version 2.14.0/1.54f), Adobe Photoshop (version 25.9.1), and Adobe Illustrator (version 28.5).

High-density microelectrode arrays (MEAs)

High-density MEA system (MaxWell Biosystems) were used to measure the activity of live MAPT-KI neurons. MaxOne Chips (MaxWell Biosystems AG MaxOne Chip MX1-S/U-CHP) were treated with 1 mL/well of 1% Terg-a-zyme (Sigma-Aldrich, Z273287) for 2 h at room temperature. Chips were washed six times with ultra-pure diH₂O, then immersed in 70% EtOH for 30 min at room temperature. Chips were washed 4x with sterile ultra-pure diH₂O and air dried. Then, 600 µl of Neurobasal Media, Electro (NBM Electro, Gibco, A14098-01) supplemented with B-27 Supplement, Electro (Gibco, A14097-01), 1% GlutaMAX (Gibco, 35050061), and antibiotics: 2.5 µg/mL amphotericin B (Gibco 15290-026), and 50 µg/mL Gentamicin (Gibco 15710-072). A MaxOne Lid (autoclaved; MaxWell Biosystems AG MX1-LID-PSM) was placed over each well. Chips were arranged in a petri dish containing a cap (from 50 mL conical tube) full of sterile water. Then, chips were placed in a humidity-controlled 37 °C incubator with 5% CO₂ for two days. On the day of the primary neuron harvest, the NBME was removed and each well was washed 1x with sterile water. The electrode surface in the center of the chip was coated with 50 µl of 0.1 mg/mL poly-D-lysine (Sigma, P7886) in borate buffer (12.5 mM sodium borate decahydrate [VWR, MK745706] and 50 mM boric acid [Sigma, B6768-1KG]) for 2 h at 37 °C. Next, each well was washed 4x with sterile water and air dried for 45 min. Then, the electrode surface was coated with 50 µl of 0.02 mg/mL laminin (Thermo Fisher, 23017015) for 1 h at 37 °C. During the poly-D-lysine and laminin coating steps, primary hippocampi neurons were

obtained from E16 MAPT-KI mice as described above. After the 1 h incubation with laminin, the laminin was removed, and a 50 μ l droplet of 100,000 cells in NBME was plated onto the chip. The cells settled onto the chip for 1 h at 37 °C. Then, 350 μ l of NBME/well was added. Cells were maintained by adding 80 μ l of fresh NBME to each well 3x per week. Cells were treated at DIV 5 with PBS, CO or 28 nM AD-tau.

Basal MEA activity scan and network assays

Basal neuron activity was recorded on DIV 28 (23d post-treatment). All cells were fed 80 μ l of fresh NBME 1 h prior to the first activity recording. The chip was placed into the recording unit and allowed to equilibrate for 10 min. Then, the activity scan analysis was selected from the assay gallery. The assay was set up to use a checkerboard configuration to record from every other electrode (12,980 electrodes recorded). Immediately following the activity scan, a network activity analysis was performed. The recording configuration was based on the corresponding activity scan. The recording parameters were set to network selection, random, and 5 min. These settings create a configuration in which recorded electrodes were assigned randomly to active electrodes as determined by the activity scan and where the electrodes were recorded for 5 min.

Glutamate and NMDA receptor antagonist evoked MEA activity and network analyses

On DIV 28 (23d post-treatment), baseline activity and network assays were performed as above. Immediately following the baseline network activity recording, 50 μ l of the media from an MEA chip was transferred to a 1.5 mL Eppendorf tube and 1 μ l of an 8 mM stock L-glutamic acid (Glu; Sigma, G1251-1G) was mixed with the conditioned media (final concentration of 20 μ M Glu). The 51 μ l of media + drug was returned to the well, the chip was gently rocked 5x to mix, and then returned to the recording unit. A 5 min network recording was immediately obtained using the same parameters as above. Then, 50 μ l of media from the chip was removed, mixed with 1 μ l of

a 2 mM stock D-2-Amino-5-phosphonopentanoic acid (AP5; Tocris, 0106), then returned to the well (final concentration of 5 μ M AP5), the chip was gently rocked 5x, and returned to the recording unit. A final 5 min network recording was obtained using the same parameters as above. After the recordings were complete, the cells were collected in 100 μ l of cell lysis buffer (20 mM Tris, 0.5 mM DTT, 150 mM NaCl, 0.5% Triton X-100, 2 μ g/mL pepstatin, 2 μ g/mL bestatin, 2 μ g/mL leupeptin, 4 mM phenylmethylsulfonyl fluoride, 10 μ g/mL aprotinin, 1 mM tetra-sodium pyrophosphate decahydrate, 10 mM β -glycerophosphate, 1 mM sodium orthovanadate, 1 M sodium fluoride, pH7.5). Lysates were sonicated (Misonix XL-200) with 3 pulses at power = 2 and the total protein concentration was quantified using the Bio-Rad protein assay as directed.

Preparation of recombinant human 2N4R monomers and aggregates

Recombinant hT40 (2N4R) tau with a C-terminal 6x histidine tag was made as previously described (Combs et al., 2017). Briefly, T7 Express Competent *E. coli* cells (New England Biosciences, Ipswich, MA, C2566) were transformed with pT7C hT40 C-His DNA plasmids. Cells were grown in Luria broth and expression of the tau protein was induced using IPTG. Cells were pelleted, then lysed, and tau was purified through a sequence of heavy metal affinity, size exclusion, and anion exchange chromatography steps using an AKTA fast protein liquid chromatography system. First, the cell lysate was run over a HiTrap TALON crude column (Cytiva, 28953767), which binds the polyhistidine tag on tau, to eliminate the majority of non-target proteins. Next, a HiPrep 16/60 Sephacryl S500 HR size exclusion column (Cytiva, 28935606) was used to further purify tau proteins. Finally, a HiTrap Q anion exchange column (Cytiva, 17115401) was used to separate tau from fractions containing DnaK protein, a bacterial Hsp70 homologue that coelutes with recombinant tau from bacteria. Tau was concentrated within

the range of 1.5 – 5 mg/mL, then 1 mM of dithiothreitol (DTT) was added to reduce disulfide bonds. Single use aliquots were prepared and stored at -80 °C until use.

Recombinant hT40 monomer and aggregate samples were prepared for use as standard curves in sandwich enzyme-linked immunosorbent assays (sELISAs) as described previously (Combs et al., 2017). Briefly, stocks of 250 mM DTT, 1 M NaCl, 250 mM HEPES (pH7.6) and 1 mM EDTA were diluted in filtered ultrapure water to 5 mM DTT, 100 mM NaCl, 10 mM HEPES and 0.1 mM EDTA (adding each reagent in that order). Next, tau was added to a final concentration of 4 µM. An arachidonic acid stock was made immediately prior to use by diluting arachidonic acid (peroxide-free, Cayman Chemicals, Ann Arbor, MI 90010.1) to 2 mM in 100% ethanol (Sigma, 459836-100ML). Arachidonic acid was added to the tau reaction to a final concentration of 150 µM. Ethanol vehicle alone was added to the monomer reactions. Reactions were gently rocked by hand to mix. Tau monomers were immediately aliquoted and frozen at -80 °C until use. The aggregation reactions were allowed to proceed overnight at room temperature. Aggregate reactions were aliquoted and stored at -80 °C until use.

Total tau, TNT1 and TOC1 sELISAs

Plates (Corning 3590) were coated with 50 µl/well of capture antibody (2 ng/µl) in borate saline buffer (100 mM boric acid, 25 mM sodium tetraborate decahydrate, 75 mM NaCl, 250 µM thimerosal) for 1 h. Tau5 (mouse IgM; Kanaan Lab; (Carmel et al., 1996; LoPresti et al., 1995)), TNT1 or TOC1 (mouse IgM; Kanaan Lab; (Patterson et al., 2011; Ward et al., 2013)) were used as capture antibodies. Plates were washed 2x with 200 µl/well of ELISA wash solution (100 mM boric acid, 25 mM sodium tetraborate decahydrate, 75 mM NaCl, 250 µM thimerosal, 0.4% BSA and 0.1% tween-20, pH 9.0) then blocked with 200 µl/well of 5% non-fat dry milk made in ELISA wash solution for 1 h. Recombinant 2N4R tau monomer and aggregate standard curves were

prepared by diluting 80 nM 1:3 to 0.137 nM (Tau5 assay) or diluting 200 nM 1:3 to 0.137 nM (TNT1 and TOC1 assays). Plates were washed 2x then 50 μ l/well of each sample [5 μ g (Tau5 assay) or 20 μ g (TNT and TOC1 assays) total protein diluted to 50 μ l in 1X TBS] was applied to the plate for 1.5 h. Plates were washed 4x, then incubated with 50 μ l/well of total tau detection antibody (R1; 1:10,000; rabbit polyclonal; Kanaan Lab; (Berry et al., 2004)) in blocking buffer for 1.5 h. Plates were washed 4x then 50 μ l/well secondary antibody (Goat anti-rabbit HRP; 1:5,000 in blocking buffer) was added for 1 h. Plates were washed 4x and reactivity was detected by adding 50 μ l/well of 3,3',5,5' tetramethylbenzidine substrate (Sigma, T0440). The reactions were quenched with 50 μ l/well of 3.6% H₂SO₄ and absorbance read at 450 nm. The Tau5-R1 reactions were quenched after 10 min, the TNT1-R1 reactions at after 10 min, and the TOC1-R1 reactions after 45 min. Absorbance data were converted to percent absorbed light using the following equation %Absorbance = $(1 - 10^{-x}) * 100$, where x is absorbance.

Experimental design and statistical analyses

For all the western blot and PLA experiments, each experimental replicate (N) represents a single primary cell culture from a unique timed pregnant MAPT-KI female. Each primary cell culture was generated by pooling the hippocampi from multiple E16 fetuses from a single timed-pregnant female. For the MEA experiments, each experimental replicate (N) represents a single MaxOne MEA chip. Primary MAPT-KI neurons from a single harvest (one timed pregnant MAPT-KI female) were plated onto 18 MaxOne chips (6 per treatment group). Experiments that underwent data and statistical analysis each had three treatment groups (PBS, Con, and AD-tau), and each experiment had a sample size of three or more (as indicated in the figure legends). The data were assessed for normality and equal variance assumptions using the Shapiro-Wilk test normality test and the Brown-Forsythe variance test. When both were not met, nonparametric statistical tests

were used to analyze the data. Experiments that met the normality and equal variance assumptions were analyzed with a one-way, or two-way repeated measures, analysis of variance test followed by Tukey's post hoc test when overall significance was achieved. For nonparametric analyses, the Kruskal-Wallis test was used followed by the Dunn's post hoc test when overall significance was achieved. Significance was defined as $p \leq 0.05$. Data are shown as mean \pm standard deviation for parametric tests or as median \pm interquartile range for nonparametric tests. Analyses were performed using GraphPad Prism 10 software.

RESULTS

AD-tau treatment does not alter overall synaptic protein levels

To determine if tau seeding caused widespread synapse loss (as indicated by synaptic protein levels), lysates from PBS, Con, or AD-tau treated cultures at 26 days post-treatment (corresponding to DIV31) were collected. Western blots were used and the levels of the presynaptic marker synaptophysin and the postsynaptic protein PSD95 were quantified (Figure 4.1). I did not observe a significant change in PSD95 (one-way ANOVA; $F_{(2,15)} = 0.1206$, $p = 0.8873$) or synaptophysin (one-way ANOVA; $F_{(2,15)} = 0.1805$, $p = 0.8366$) total protein levels, which were normalized to GAPDH as a loading control.

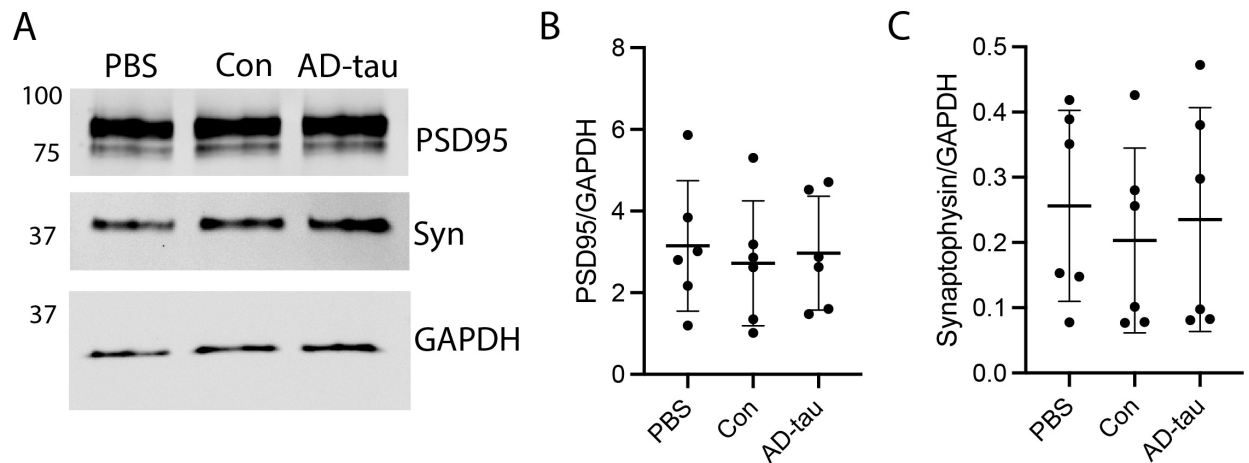


Figure 4.1. Western blots of AD-tau-treated MAPT-KI primary hippocampal cultures show no change in synaptophysin or PSD95 synaptic protein levels. A) Lysates from PBS, Con, or AD-tau-treated primary MAPT-KI neurons collected at 26d post-treatment (corresponding to DIV31) were immunoblotted for synaptic markers, including PSD95 (postsynaptic marker), synaptophysin (presynaptic marker) and GAPDH (a loading control). B) Quantification of PSD95 normalized to GAPDH indicated similar levels of PSD95 across groups. C) Quantification of synaptophysin normalized to GAPDH showed similar levels of synaptophysin across groups. The data are mean \pm SD and were compared using one-way ANOVA with Tukey's multiple comparisons test, significance was defined as $p \leq 0.05$. N=6; independent experimental replicates (i.e. separate primary neuron harvests from unique timed pregnant MAPT-KI females).

AD-tau treatment significantly reduces the density of intact synapses

Next, synaptic PLA was used as a complementary method to quantify the density of intact synapses (Verstraelen et al., 2020). Antibody probes for presynaptic homer 1 protein and postsynaptic bassoon protein were used. If the two proteins are in close proximity (<40 nm), then fluorescent green puncta are detected (Figure 4.2A). Primary hippocampal MAPT-KI cultures were treated with PBS, Con, or AD-tau (56 nM tau) on DIV5 and collected for PLA 28 days post-

treatment (corresponding to DIV 33). After PLA staining, cells were stained using ICF for TNT1 and β -III tubulin (Caccamo et al., 1989) (Figure 4.2B-E). Quantification of the PLA signal, normalized to β -III tubulin area (i.e. total neuronal area), showed a significant reduction in PLA puncta per β -III tubulin area in the AD-tau-treated cultures compared to the PBS-treated control group (one-way ANOVA; $F_{(2,9)} = 4.312$, $p = 0.0486$; PBS vs AD-tau $p = 0.0424$). Primary delete controls for each of the PLA probes are shown in Figure 4.3 and as expected little to no non-specific signal was detected. Untreated cells were used for these controls, and as expected, no TNT1+ inclusions were observed (Figure 4.3).

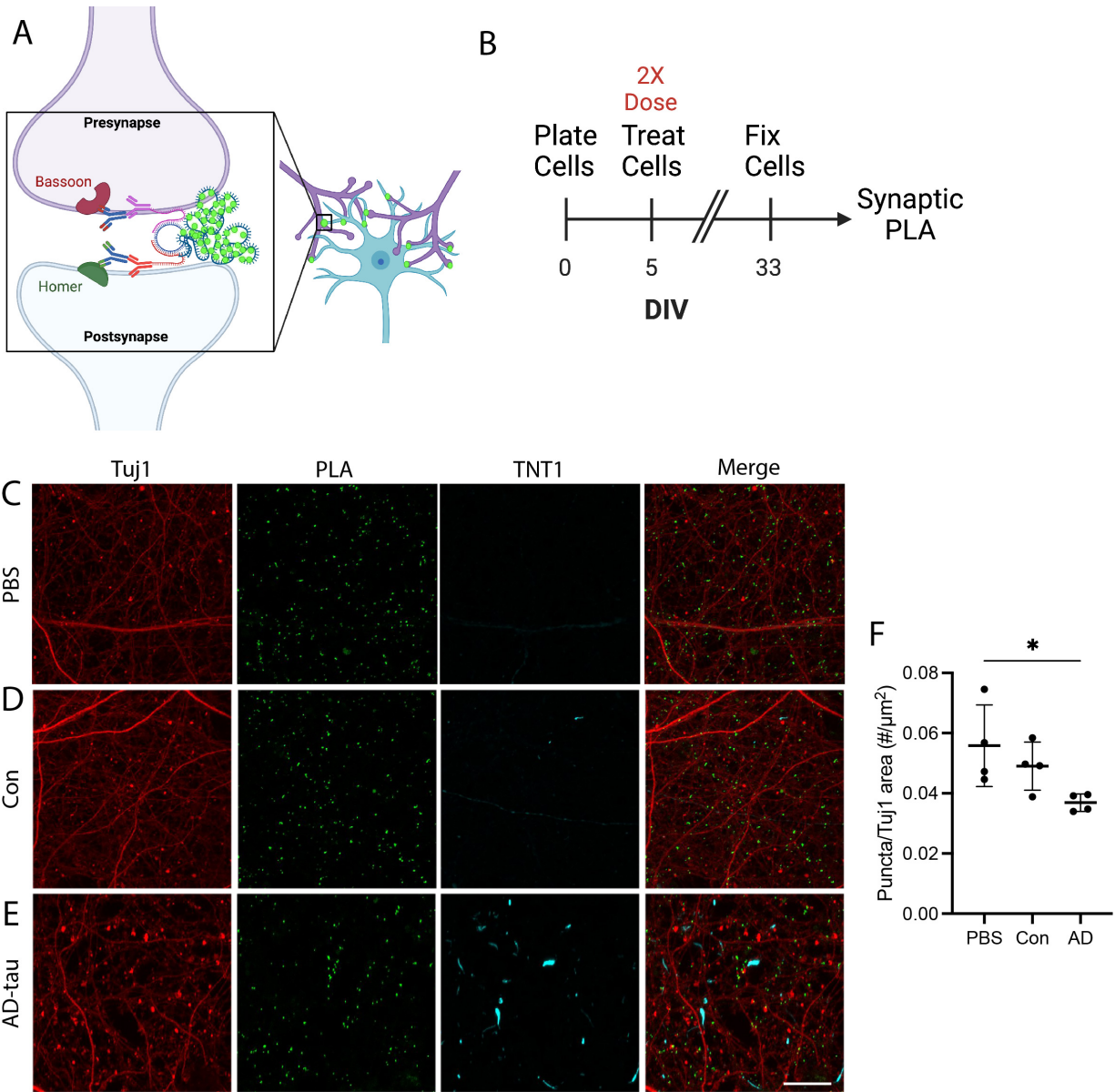


Figure 4.2. Proximity ligation assays show decreased density of intact excitatory synapses in AD-tau-treated cultures at 28d post-treatment. A) Cells were treated with PBS, Con, or AD-tau (56 nM tau) at DIV5 and fixed on 28d post-treatment (corresponding to DIV33). The proximity ligation assay (PLA) was performed to identify intact synapses in which homer 1 and bassoon proteins were in close association (<40 nm), indicated by green fluorescent puncta. Following PLA, cells were immunolabelled with TNT1 (cyan) and Tuj1 (red). B) Experimental timeline for PLA and ICF analysis of cells at 28d post-treatment.

Figure 4.2 (cont'd).

C-E) Representative images of PBS, Con, and AD-tau-treated cultures after PLA staining (green) and immunolabelling with β -III tubulin (red) and TNT1 (cyan) antibodies. F) Quantification of the number of PLA puncta normalized to Tuj1 area indicates a significant decrease in the AD-tau-treated cells compared to the PBS-treated cells. The data are mean \pm SD and were compared using one-way ANOVA with Tukey's multiple comparisons test, significance was defined as $p \leq 0.05$. N=4; each experimental replicate represents a separate primary neuron harvest from unique timed pregnant MAPT-KI females. Scale bar = 20 μ m.

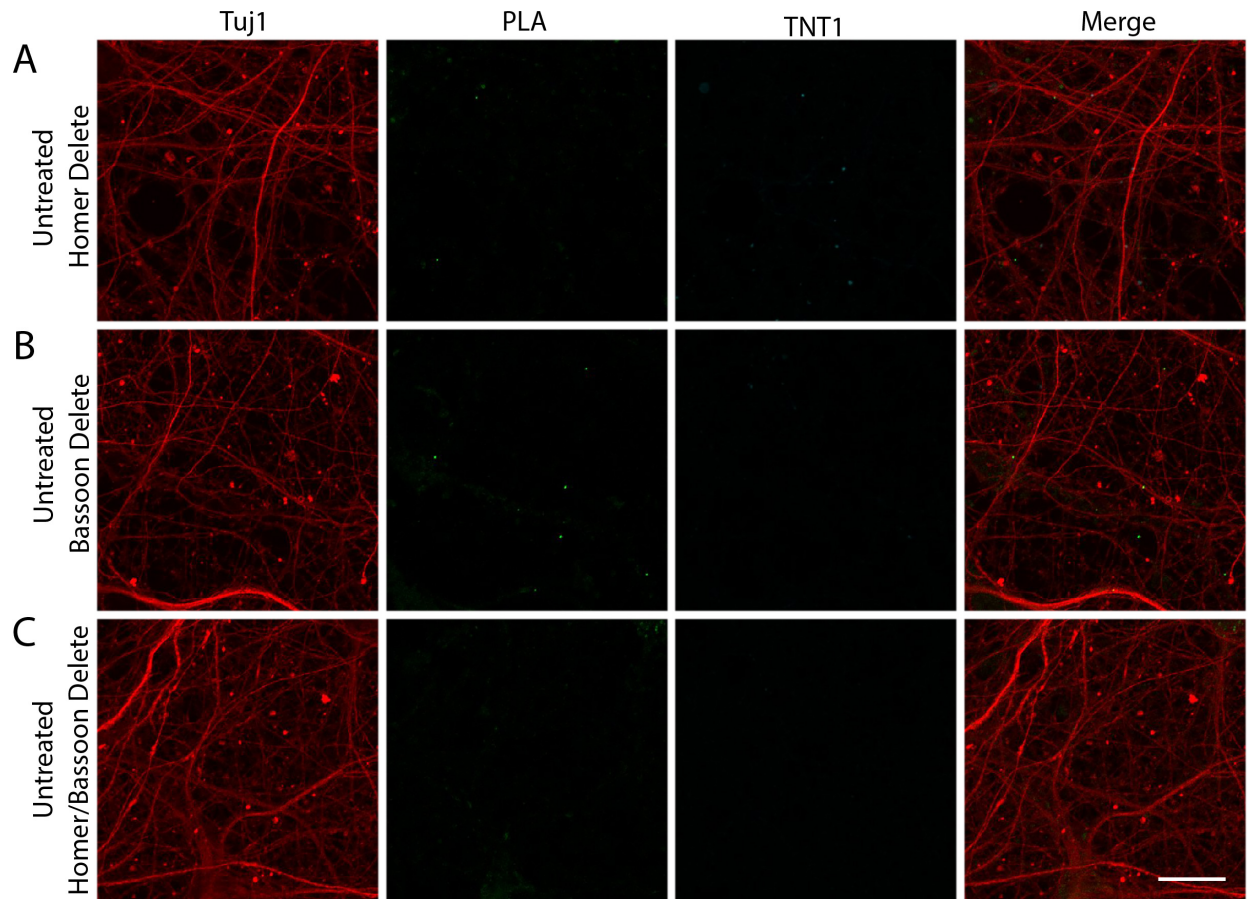


Figure 4.3. Proximity ligation assay (PLA) primary delete control labeling. Untreated cells were used for the primary delete control labeling. PLA was followed by ICF with Tuj1 (red) and TNT1 antibodies (cyan). A-C) Omission of the homer primary antibody (A), the bassoon primary antibody (B), or both (C) showed very low PLA signal (green). A-C) TNT1 signal was not observed in the untreated cell. Scale bar = 20 μm .

AD-tau-treated cultures show normal basal activity, but exhibit a greater response to glutamate and a NMDA receptor antagonist

The effect of tau seeding on neuronal function was measured using high-density multi-electrode arrays (MEAs). Cells were plated onto MEA chips on DIV0 and treated with PBS, Con, or AD-tau on DIV5. For each chip, ~1,020 electrodes selected randomly were assigned for the consecutive 5 minute recordings. Activity at the same electrodes was recorded after the Glu and AP5 treatments

(Figure 4.4A). This allowed us to calculate changes in the firing rate of action potentials at individual electrodes at baseline and in response to Glu or AP5 treatment.

First, action potential firing rate was measured. For each electrode recorded (~1,020), the firing rate is calculated as the number of detected spikes divided by the recording time (5 min). Basal neuron activity recordings were acquired on DIV28, and there was no significant differences in the baseline firing rate across PBS, Con and AD-tau treated neurons (Figure 4.4B; two-way repeated measures ANOVA; Recording (BL, +Glu, or +AP5) $F_{(2, 45)} = 2.104$ $p < 0.0001$; Treatment (PBS, Con, or AD-tau) $F_{(2, 45)} = 1.677$ $p = 0.2201$; Interaction $F_{(4, 45)} = 2.104$ $p = 0.1050$; PBS +Glu vs. +AP5 $p = 0.0031$; Con BL vs. +Glu $p = 0.0426$, +Glu vs. +AP5 $p = 0.0485$; AD-tau BL vs. +Glu $p = 0.0016$, +Glu vs. +AP5 $p = 0.0059$). Immediately after the basal recording for each culture, 20 μ M L-glutamic acid (Glu) was added and a second activity recording was acquired. The evoked firing rate following Glu treatment (+Glu) was not significantly different between PBS, Con and AD-tau treated neurons (Figure 4.4C; Kruskal-Wallis ANOVA with Dunn's post hoc, $H = 3.696$, $p = 0.1596$). Immediately following Glu treatment, cells were treated with an addition of 5 μ M AP5 (NMDA receptor antagonist) and a third activity recording was performed. There were no statistical differences between PBS, Con and AD-tau treated neurons in response to NMDAR antagonism (Figure 4.4D; one-way ANOVA; $F_{(2, 15)} = 1.560$, $p = 0.2424$).

Noting the variability in firing rate activity within and across groups, the response to Glu was normalized to baseline activity and the response to AP5 was normalized to Glu-evoked activity for each replicate. The magnitude of the Glu-evoked response (fold-change from baseline to +Glu) was not significantly different between PBS, Con and AD-tau treated neurons (Figure 4.4C, D; Kruskal-Wallis ANOVA with Dunn's post hoc, $H = 1.766$, $p = 0.4317$). The magnitude of the AP5-evoked response (fold-change from +Glu to +AP5) was not statistically different

between PBS, Con and AD-tau treated neurons (Figure 4.4C, E; Kruskal-Wallis ANOVA with Dunn's post hoc, $H = 5.632$, $p = 0.0537$). However, a trend was observed in which AD-tau treated cells showed stronger inhibition with AP5 treatment (Figure 4.4K; $p = 0.06$).

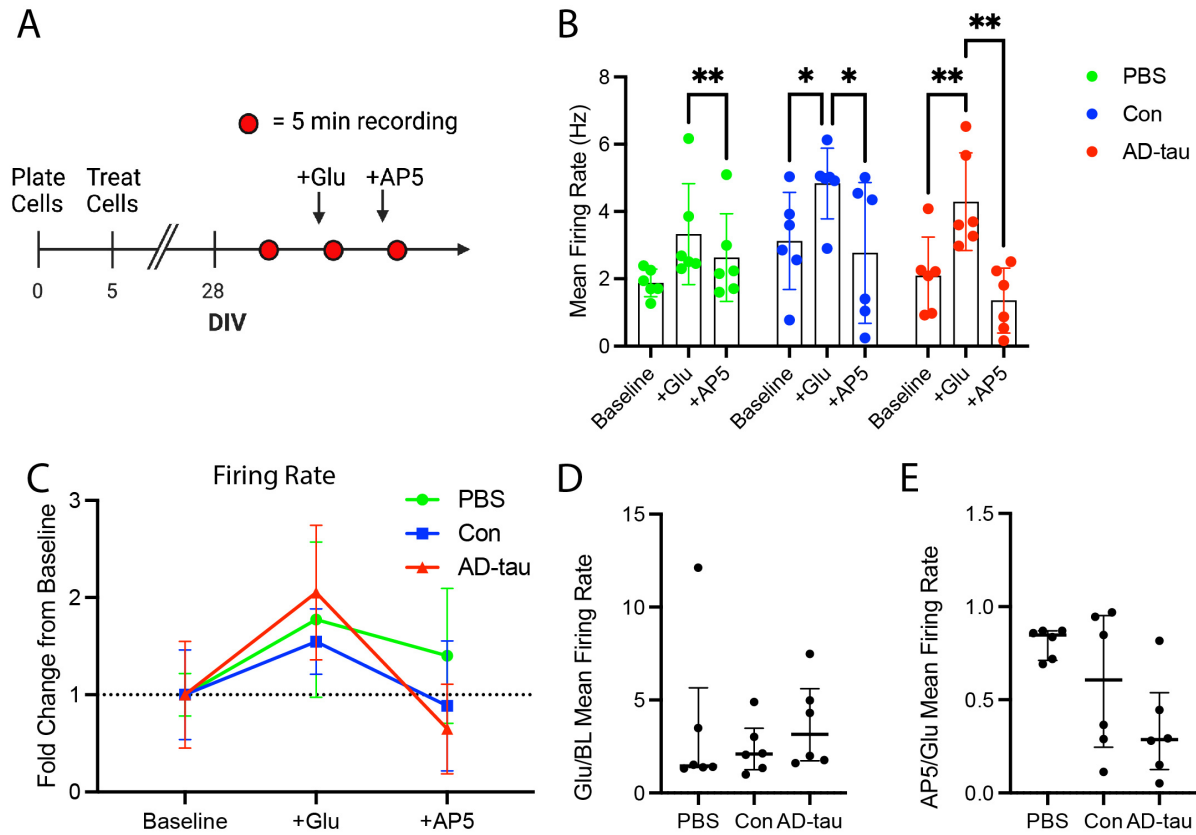


Figure 4.4. AD-tau treated cultures do not exhibit significant changes in action potential firing rate.

A) Primary hippocampal MAPT-KI cultures were plated on MEA chips on DIV0. Cells were treated with PBS, Con, or AD-tau on DIV5. On DIV28, three consecutive 5-minute neuronal activity recordings (red circles) were acquired: basal activity, after addition of glutamate (Glu; 20 μ M final concentration) and after addition of NMDAR antagonist (AP5; 5 μ M final concentration).

B) There were no AD-tau treatment effects on the mean firing rate across multiple electrodes at baseline, after the addition of Glu, or after the addition of AP5.

Figure 4.4 (cont'd).

C-E) The fold-change from baseline to +Glu and from +Glu to +AP5 were calculated. F) There was no significant treatment effect on the response to Glu or G) the response to AP5. However, there was a trend showing a greater fold change from +Glu to +AP5 in the AD-tau-treated cultures compared to the PBS controls ($p = 0.06$). $N=6$, each experimental replicate is defined as a separate MEA chip. For each chip, $\sim 1,020$ electrodes were randomly selected for recording. The same $\sim 1,020$ electrodes per chip were recorded from in the +Glu and +AP5 recordings. Only electrodes with a firing rate ≥ 0.1 Hz and with a spike amplitude ≥ 100 mA at baseline were used for analysis. The data in B are mean \pm standard deviation and were compared using two-way repeated measures ANOVA with Tukey's multiple comparisons test, significance was defined as $p \leq 0.05$. The data in D and E are median \pm interquartile range and were compared using Kruskal-Wallis ANOVA with Dunn's post hoc test, significance was defined as $p \leq 0.05$. * ≤ 0.05 , ** ≤ 0.01 .

Next, synchronous activity of the recorded neurons (i.e. periods of simultaneous firing followed by sparse activity, referred to as a network burst) was measured. To determine the effect of tau seeding on spontaneous and evoked network activity, the number of synchronous action potential firing events (bursts) were analyzed using the recordings described above (Figure 4.5B). There were no significant treatment effects on burst frequency at baseline, in response to glutamate addition, or NMDAR antagonism (Figure 4.5B; two-way repeated measures ANOVA; Recording (BL, +Glu, or +AP5) $F_{(2, 45)} = 20.07$ $p = 0.0021$; Treatment (PBS, Con, or AD-tau) $F_{(2, 45)} = 3.476$ $p = 0.0921$; Interaction $F_{(4, 45)} = 3.260$ $p = 0.0937$; PBS +Glu vs. +AP5 $p = 0.0041$; Con BL vs. +Glu $p = 0.0037$, +Glu vs. +AP5 $p = 0.0252$; AD-tau BL vs. +Glu $p = 0.0068$, +Glu vs. +AP5 $p = 0.0111$).

Again, noting the variability in network bursting activity within and across groups, the response to Glu was normalized to baseline activity and the response to AP5 was normalized to Glu-evoked activity for each replicate. The magnitude of the Glu-evoked response (fold-change from baseline to +Glu) was significantly greater in the AD-tau treated cells (Figure 4.5C, D; Kruskal-Wallis ANOVA with Dunn's post hoc, $H = 7.638$, $p = 0.0150$; PBS vs AD-tau $p = 0.0172$). The magnitude of the AP5-evoked response (fold-change from +Glu to +AP5) was also significantly greater in the AD-tau treated cells (Figure 4.5C, E; Kruskal-Wallis ANOVA with Dunn's post hoc, $H = 6.334$, $p = 0.0350$; PBS vs AD-tau $p = 0.0385$).

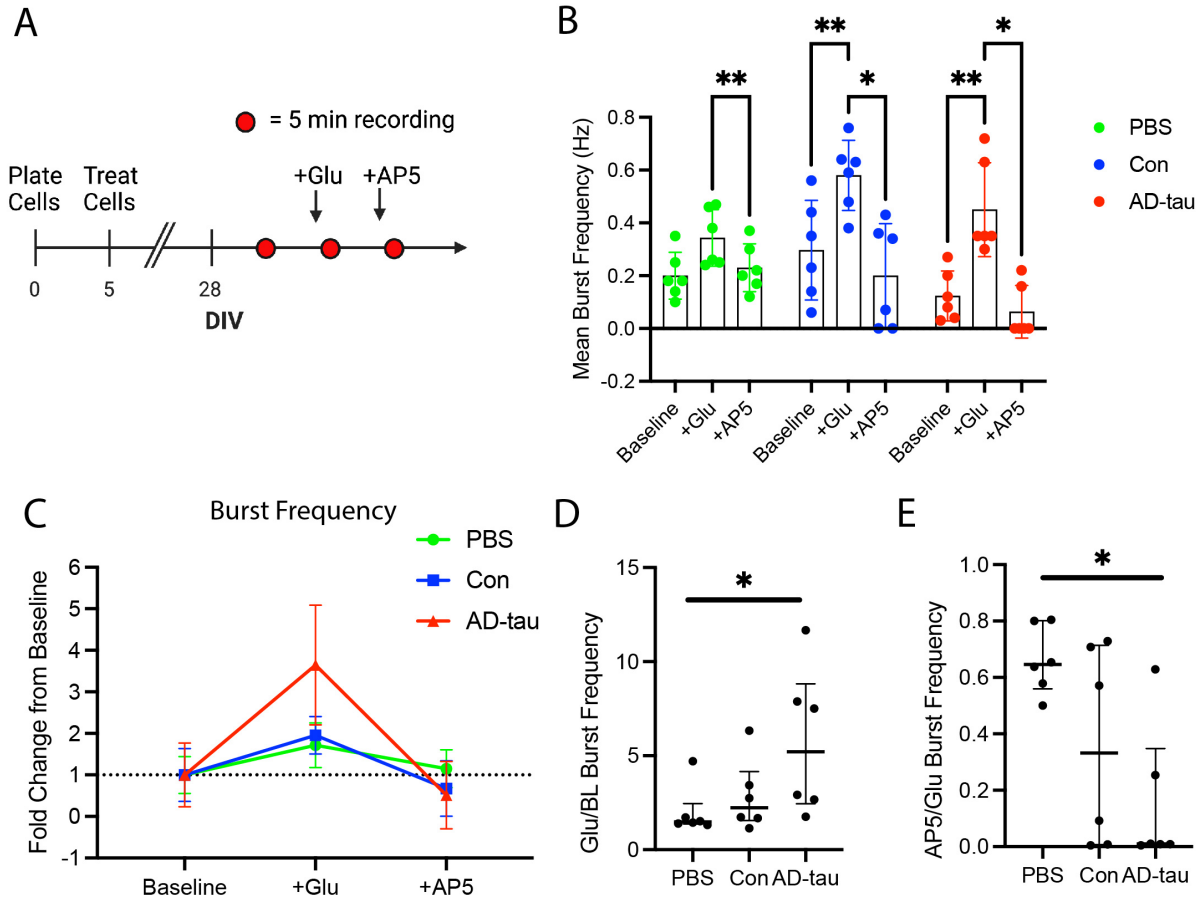


Figure 4.5. AD-tau treated cultures exhibit network hypersynchrony in response to glutamate. A) Primary hippocampal MAPT-KI cultures were plated on MEA chips on DIV0. Cells were treated with PBS, Con, or AD-tau on DIV5. On DIV28, three consecutive 5-minute neuronal activity recordings (red circles) were acquired: basal activity, after addition of glutamate (Glu; 20 μ M final concentration) and after addition of NMDAR antagonist (AP5; 5 μ M final concentration). B) There were no AD-tau treatment effects on mean burst frequency at baseline, after the addition of Glu, or after the addition of AP5. C-E) The fold-change from baseline to +Glu and from +Glu to +AP5 were calculated. D) The AD-tau-treated cultures exhibited a significantly greater change from baseline to +Glu, and E) from +Glu to +AP5 compared to the PBS-treated cultures. N=6, each experimental replicate is defined as a separate MEA chip.

Figure 4.5 (cont'd).

For each chip, ~1,020 electrodes were randomly selected for recording. The same ~1,020 electrodes per chip were recorded from in the +Glu and +AP5 recordings. The data in B are mean \pm standard deviation and were compared using two-way repeated measures ANOVA with Tukey's multiple comparisons test, significance was defined as $p \leq 0.05$. The data in D and E are median \pm interquartile range and were compared using Kruskal-Wallis ANOVA with Dunn's post hoc test, significance was defined as $p \leq 0.05$. * ≤ 0.05 , ** ≤ 0.01 .

To validate tau seeding in the MEA cultures, the cells were collected after the final recording and Tau5, TNT1, and TOC1 species were detected using sELISAs (Figure 4.6). There was not a significant difference in total tau (Tau5 sELISA) between the PBS and AD-tau treated neurons, though there was a statistically significant increase in total tau in the AD-tau treated neurons compared to Con treated neurons (Figure 4.6B; one-way ANOVA; $F_{(2,15)} = 3.616$, $p = 0.0523$; Con vs AD-tau $p = 0.0145$). There was a significant increase in TNT1+ tau species in the AD-tau treated cells compared to the PBS and Con treated cells (Figure 4.6D; Kruskal-Wallis ANOVA with Dunn's post hoc, $H = 11.46$, $p = 0.0005$; PBS vs AD-tau $p = 0.0072$; Con vs AD-tau $p = 0.0145$). There was also a significant increase in TOC1+ tau species in the AD-tau treated cells compared to the PBS and Con treated cells (Figure 4.6F; one-way ANOVA; $F_{(2,15)} = 168.4$, $p < 0.0001$; PBS vs AD-tau $p < 0.0001$; Con vs AD-tau $p < 0.0001$).

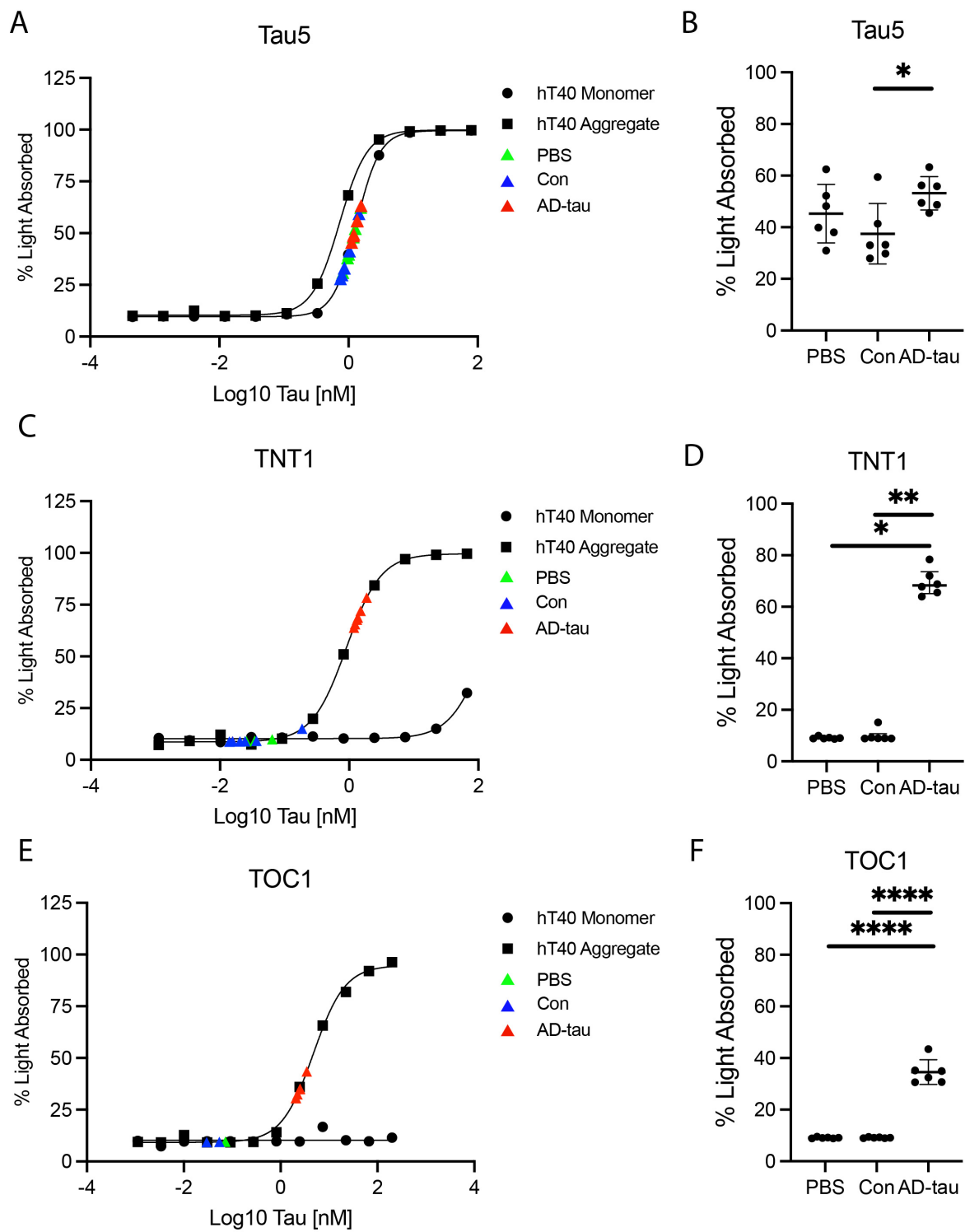


Figure 4.6. AD-tau treated cultures used in MEA experiments contain pathological tau species.

Figure 4.6 (cont'd).

After collecting baseline, glutamate-evoked, and AP5-evoked activity recordings, lysates were collected, and the presence of pathological tau species was quantified using sELISA. Samples were captured with Tau5 (total tau; A-B), TNT1 (PAD exposed tau; C-D), or TOC1 (tau oligomers; E-F) and detected with R1 (total tau) antibody. Recombinant hT40 monomer and aggregate standard curves were included for each assay (A, C, E). Tau5+ species were detected in all neuron cultures (A-B). TNT1+ and TOC1+ tau species were detected in all AD-tau treated cultures, and in some Con treated cultures at low levels. In B and F, the data are mean \pm SD and were compared using one-way ANOVA with Tukey's multiple comparisons test, significance was defined as $p < 0.05$. In D, the data are median with interquartile range and were compared using the nonparametric Kruskal-Wallis analysis of variance with Dunn's multiple comparisons test, significance was defined as $p < 0.05$. N=6; each experimental replicate represents a single MaxOne MEA chip. Primary neurons from a single harvest were plated onto 18 MaxOne chips (6 chips per treatment).

DISCUSSION

Synapse loss is the best correlate of cognitive decline in AD, and synaptic dysfunction is an early event in the pathogenesis of AD ("2024 Alzheimer's disease facts and figures," 2024; DeKosky & Scheff, 1990; DeKosky et al., 1996; Masliah et al., 2001; Masliah et al., 1994; Scheff et al., 2007; Scheff et al., 2006; Scheff et al., 1993; Selkoe, 2002; Serrano-Pozo et al., 2011; Terry et al., 1991). Tau pathology burden correlates with synaptic loss in neurodegenerative disease (Masliah et al., 1994). Therefore, understanding the mechanisms linking tau pathology to synaptic dysfunction and loss is an area of active investigation. Pathological tau can acutely impair LTP and LTD, disrupt neuronal network activity, alter Ca^{2+} homeostasis and neurotransmitter release, and affect neuron excitability (reviewed in (Mueller et al., 2021)). Furthermore, loss of presynaptic

and postsynaptic markers is observed in tauopathy models (de Calignon et al., 2012; Katsuse et al., 2006; Kopeikina et al., 2013; Reilly et al., 2017; Sydow et al., 2011; Van der Jeugd et al., 2011; Yoshiyama et al., 2007). A major limitation of those studies is that most used models of tau overexpression, often with mutations associated with inherited tauopathies. Here, I treated MAPT-KI primary hippocampal neurons with AD-tau to seed the formation of intracellular AD-associated pathological tau species. This provides a more relevant model to study the effects of AD-associated pathological tau species on synaptic impairment in the context of AD.

Hyperexcitability and hypersynchrony are neuronal phenotypes associated with AD (Targa Dias Anastacio et al., 2022). Functional magnetic resonance imaging (fMRI) studies in humans show hyperactivity in the hippocampus in early stages of MCI during memory-related tasks (Celone et al., 2006; Dickerson et al., 2005). Interestingly, hypoactivity is observed in later stage MCI and in AD, suggesting that hyperactivity is transient and represents one of the earliest physiological changes in the brain in individuals at risk of developing AD (Celone et al., 2006; Dickerson et al., 2005). Similarly, neuronal hypersynchrony is also observed in models of AD (Palop & Mucke, 2016; Ranasinghe et al., 2022). Hypersynchrony can manifest as clinical or subclinical epilepsy, which is observed during the early stages of AD (Horvath et al., 2018; Horvath et al., 2021; Lam et al., 2017; Lam et al., 2020; Smailovic et al., 2018; Vossel et al., 2013; Vossel et al., 2016). The exact mechanisms underlying hyperexcitability and hypersynchrony are still being investigated, however, it is apparent that both are NMDA-dependent phenomena (Fellin et al., 2004; Molina et al., 2014; Wagatsuma et al., 2016). The current findings are consistent with these studies. Indeed, seeding MAPT-KI neurons with insoluble AD brain-derived tau resulted in NMDA-mediated synaptic dysfunction 23d post-treatment (corresponding to DIV28). Specifically, I show evidence of network hypersynchrony in the AD-tau seeded neurons, which

exhibited a significantly greater glutamate-evoked increase in network bursting frequency compared to the response observed in PBS treated neurons. Furthermore, the AP5-evoked change in network burst frequency was significantly greater in the AD-tau seeded neurons. Together, these data suggest that tau seeding results in NMDA-mediated hypersynchrony. The above network activity results integrated all of the recorded electrodes (~1020) into the analysis. Changes in firing rate activity at the electrode level were also assessed. For activity at a particular electrode to be considered in the firing rate analysis, the amplitude of the action potential spike had to be ≥ 100 mV, and the firing rate had to be ≥ 0.1 Hz. The Glu-evoked increase in the mean firing rate was ~2x that of the Glu-evoked increase observed in the PBS treated cells, albeit a statistically non-significant difference. Furthermore, the AP5-evoked decrease in firing rate was ~3x that of the AP5-evoked response observed in the PBS treated cells, but again this was not statistically significant. A likely explanation for the difficulty in measuring significant changes at the electrode level is that not all the AD-tau treated neurons in my model develop intracellular tau pathology. The unavoidable inclusion of neurons lacking tau pathology in my MEA analyses may have “washed out” more robust effects specifically in tau affected neurons at the electrode level.

Most of the tau seeding studies using insoluble AD-tau did not assess synaptic density (Guo et al., 2016; He et al., 2020; Leyns et al., 2019; Narasimhan et al., 2017). A significant reduction in excitatory synapses was observed in this model at 28d post-treatment (corresponding to DIV33) with a high-dose of AD-tau (56 nM vs. 28 nM AD-tau used in other experiments). These findings are consistent with a tau seeding study that showed significant reductions in synaptophysin and PSD95 in WT mice injected with AD-tau at least 4.5 months post-injection (Bassil et al., 2021). Similar to this model, synapse loss was observed in the absence of a reduction in neuron number, suggesting that synaptic loss preceded overt cell loss in the model. In a separate study, synaptic

dysfunction was observed in primary neurons from P301S transgenic mice (overexpress mutant P301S human tau) with heparin-induced recombinant tau filaments comprised of the repeat domain harboring the P301L mutation (Stancu et al., 2015). Specifically, the authors reported disrupted spontaneous neuronal network activity and GABA_A antagonist-induced neuronal network activity. Despite these functional changes, no changes in presynaptic markers were observed (Stancu et al., 2015). Importantly, this model approach is substantively more aggressive (mutant transgenic neurons treated with mutant repeat domain seeding material) than the approach used here (physiological expression of WT human tau). Notably, there is evidence that GABAergic neurons are differentially affected in tauopathies (Levenga et al., 2013; Targa Dias Anastacio et al., 2022; Usenovic et al., 2015; Witton et al., 2016). Therefore, it is worth performing a PLA using an antibody pair specific to inhibitory synapses like Neurexin 1b and Neuroligin 2 (Verstraelen et al., 2020) and challenging AD-tau treated cultures with GABA agonists and antagonists.

The tau seeding studies discussed thus far used insoluble, fibrillar tau as the seeding material. It is worth mentioning the numerous studies that showed acute synaptic impairment following application of soluble tau oligomers. Abnormal forms of tau (i.e. modified monomers and oligomers) are likely more toxic than insoluble filamentous forms of tau. In line with this, treatment of primary cortical neurons from WT mice with soluble AD brain-derived tau species resulted in significant decreases in homer and bassoon only 3 days post-treatment (Saroja et al., 2022). In a separate study, tau oligomers immunoprecipitated from AD brain using the oligomer-specific T22 antibody were injected into the brain of WT mice (Lasagna-Reeves et al., 2012). Acute and transient object recognition impairment was observed just 3d post-injection. Application of the T22+ oligomers onto WT hippocampal slices resulted in acute LTP inhibition (Lasagna-Reeves et al., 2012). Furthermore, WT human iPSCs treated with recombinant heparin-

induced soluble tau oligomers resulted in significant decreases in synaptophysin and synapsin-1 puncta along with increased intracellular Ca^{2+} levels, decreased neurite length, and cell loss, 14d post-treatment (Usenovic et al., 2015). Various tau oligomers were sufficient to cause synaptic dysfunction in WT mice (Lasagna-Reeves et al., 2011) and impair LTP in tau-expressing cells and in tau knockout neurons (Fa et al., 2016; Hill et al., 2019; Puzzo et al., 2020). Most tau seeding studies use short, insoluble tau fibrils to seed robust aggregation (Audouard et al., 2016; Boluda et al., 2015; Gibbons et al., 2017; Guo et al., 2016). Studies on the seeding efficiency of soluble tau oligomers have yielded mixed results. Several studies show that soluble tau oligomers do not effectively seed aggregation, while others show that they do (Dujardin et al., 2020; Gerson & Kaye, 2013; Lasagna-Reeves et al., 2012; Mate De Gerando et al., 2023; Sengupta & Kaye, 2024; Takeda et al., 2015). The ability of various tau oligomers to seed aggregation probably depends on their conformation and whether they are “on-pathway” or “off-pathway” for filament formation (Alhadidy & Kanaan, 2024). The toxicity and seeding-efficiency of specific disease-relevant tau species warrants further investigation, and this model can be used to test both.

The current study suggests that the network hypersynchrony observed in the seeded neurons was NMDAR-mediated. Several studies found that 10-50 μM AP5 significantly reduces neuronal activity in cultured neurons (Edwards et al., 2017; Lam et al., 2023; Miyamoto et al., 2017; Jackel et al., 2017). Using a low dose of 5 μM AP5 allowed us to detect differential effects of the antagonist without completely abolishing neuron activity in the PBS-treated controls. I found that 5 μM AP5 did not abolish neuron firing or synchronous bursting activity in the PBS-treated cultures, however, bursting activity was completely abolished in 66% of the AD-tau-treated cultures. Furthermore, the AD-tau-treated cultures exhibited significantly greater response to AP5 in terms of spike firing rate compared to the PBS controls. These data suggest that NMDA

signaling is altered in the AD-tau seeded cultures. These studies cannot determine whether the effect is directly or indirectly attributed to tau, or whether the effect is due to intracellular or extracellular tau. Tau's role in modulating NMDARs at the postsynapse through interactions with Fyn kinase is well known. Tau directs Fyn into from the dendritic shaft into the spines where it phosphorylates NMDAR 2B subunits, stabilizing the NMDARs in the postsynaptic membrane. Tau knockdown results in increased Fyn localization in the dendritic shafts. Tau overexpression leads to hyperexcitability, possibly through increased NMDAR localization in the postsynaptic membrane. If tau levels were in fact increased in the somatodendritic compartment in AD-tau-treated cultures, this could result in increased localization of Fyn to the postsynapse and increased NMDARs. An important follow-up study would be to determine if there is a decrease in NMDARs in the postsynaptic membrane in the AD-tau-treated neurons. These mechanisms depend on direct interactions with tau, therefore, it is necessary to determine if pathological tau is discretely localized in synapses.

Pathological tau does not have to be present in the synaptic compartment to impact NMDA signaling. Instead, the role of tau could be more indirect. Deficits in axon transport could impair the delivery of important presynaptic components like synaptic vesicles and mitochondria which are critical for meeting the ATP production and Ca^{2+} buffering demands at the presynapse. Indeed, there was an apparent accumulation of synaptic vesicle cargoes (i.e. APP and synaptophysin) in discrete TNT1+ inclusions within neurites (mostly axonal) suggesting synaptic vesicle trafficking impairments in AD-tau seeded neurons (see Chapter 3, Figures 3.2-3.5). One could postulate that impaired presynaptic activity could result in increased NMDAR insertion into the postsynaptic membrane as a compensatory mechanism. If the maintenance of normal firing rate is dependent

on a compensatory increase in NMDARs, you would expect to see a significantly greater effect on activity when NMDARs are inhibited, which is what was observed in AD-tau seeded cultures.

Thus far, overt toxicity or evidence of axonal degeneration was not seen in this tau seeding model (see Chapter 2). This may be due to the lack of a “second hit” or an additional factor in facilitating tau-mediated toxicity (e.g. amyloid- β and/or neuroinflammatory pathways). The differential response to glutamate and AP5 may represent an impairment in NMDAR-related signaling that is a very early pathological event in neurons harboring tau aggregates. However, there are many outstanding questions about the precise drivers of the glutamate and AP5 response, and how this may be relevant to seeding mechanisms *in vivo*. It is evident that this seeding model may be best suited for studying the early mechanisms of neuronal dysfunction that precede overt axonal and neuronal degeneration.

REFERENCES

- 2024 Alzheimer's disease facts and figures. (2024, May). *Alzheimers Dement*, 20(5), 3708-3821. <https://doi.org/10.1002/alz.13809>
- Alhadidy, M. M., & Kanaan, N. M. (2024, Feb 28). Biochemical approaches to assess the impact of post-translational modifications on pathogenic tau conformations using recombinant protein. *Biochem Soc Trans*, 52(1), 301-318. <https://doi.org/10.1042/BST20230596>
- Arriagada, P. V., Growdon, J. H., Hedley-Whyte, E. T., & Hyman, B. T. (1992, Mar). Neurofibrillary tangles but not senile plaques parallel duration and severity of Alzheimer's disease. *Neurology*, 42(3 Pt 1), 631-639. <https://doi.org/10.1212/wnl.42.3.631>
- Audouard, E., Houben, S., Masaracchia, C., Yilmaz, Z., Suain, V., Authelet, M., De Decker, R., Buee, L., Boom, A., Leroy, K., Ando, K., & Brion, J. P. (2016, Oct). High-Molecular-Weight Paired Helical Filaments from Alzheimer Brain Induces Seeding of Wild-Type Mouse Tau into an Argyrophilic 4R Tau Pathology in Vivo. *Am J Pathol*, 186(10), 2709-2722. <https://doi.org/10.1016/j.ajpath.2016.06.008>
- Bassil, F., Meymand, E. S., Brown, H. J., Xu, H., Cox, T. O., Pattabhiraman, S., Maghames, C. M., Wu, Q., Zhang, B., Trojanowski, J. Q., & Lee, V. M. (2021, Jan 4). alpha-Synuclein modulates tau spreading in mouse brains. *J Exp Med*, 218(1). <https://doi.org/10.1084/jem.20192193>
- Berry, R. W., Sweet, A. P., Clark, F. A., Lagalwar, S., Lapin, B. R., Wang, T., Topgi, S., Guillozet-Bongaarts, A. L., Cochran, E. J., Bigio, E. H., & Binder, L. I. (2004, May). Tau epitope display in progressive supranuclear palsy and corticobasal degeneration. *J Neurocytol*, 33(3), 287-295. <https://doi.org/10.1023/B:NEUR.0000044190.96426.b9>
- Boluda, S., Iba, M., Zhang, B., Raible, K. M., Lee, V. M., & Trojanowski, J. Q. (2015, Feb). Differential induction and spread of tau pathology in young PS19 tau transgenic mice following intracerebral injections of pathological tau from Alzheimer's disease or corticobasal degeneration brains. *Acta Neuropathol*, 129(2), 221-237. <https://doi.org/10.1007/s00401-014-1373-0>
- Braak, H., Alafuzoff, I., Arzberger, T., Kretschmar, H., & Del Tredici, K. (2006). Staging of Alzheimer disease-associated neurofibrillary pathology using paraffin sections and immunocytochemistry. *Acta neuropathologica*, 112(4), 389-404.
- Braak, H., & Braak, E. (1991). Neuropathological staging of Alzheimer-related changes. *Acta Neuropathol*, 82(4), 239-259. <https://doi.org/10.1007/BF00308809>
- Caccamo, D., Katsetos, C. D., Herman, M. M., Frankfurter, A., Collins, V. P., & Rubinstein, L. J. (1989, Mar). Immunohistochemistry of a spontaneous murine ovarian teratoma with neuroepithelial differentiation. Neuron-associated beta-tubulin as a marker for primitive

neuroepithelium. *Lab Invest*, 60(3), 390-398.
<https://www.ncbi.nlm.nih.gov/pubmed/2467076>

- Carmel, G., Mager, E. M., Binder, L. I., & Kuret, J. (1996, Dec 20). The structural basis of monoclonal antibody Alz50's selectivity for Alzheimer's disease pathology. *J Biol Chem*, 271(51), 32789-32795. <https://doi.org/10.1074/jbc.271.51.32789>
- Celone, K. A., Calhoun, V. D., Dickerson, B. C., Atri, A., Chua, E. F., Miller, S. L., DePeau, K., Rentz, D. M., Selkoe, D. J., Blacker, D., Albert, M. S., & Sperling, R. A. (2006, Oct 4). Alterations in memory networks in mild cognitive impairment and Alzheimer's disease: an independent component analysis. *J Neurosci*, 26(40), 10222-10231. <https://doi.org/10.1523/JNEUROSCI.2250-06.2006>
- Cho, H., Choi, J. Y., Hwang, M. S., Lee, J. H., Kim, Y. J., Lee, H. M., Lyoo, C. H., Ryu, Y. H., & Lee, M. S. (2016, Jul 26). Tau PET in Alzheimer disease and mild cognitive impairment. *Neurology*, 87(4), 375-383. <https://doi.org/10.1212/WNL.0000000000002892>
- Combs, B., Hamel, C., & Kanaan, N. M. (2016, Oct). Pathological conformations involving the amino terminus of tau occur early in Alzheimer's disease and are differentially detected by monoclonal antibodies. *Neurobiol Dis*, 94, 18-31. <https://doi.org/10.1016/j.nbd.2016.05.016>
- de Calignon, A., Polydoro, M., Suarez-Calvet, M., William, C., Adamowicz, D. H., Kopeikina, K. J., Pitstick, R., Sahara, N., Ashe, K. H., Carlson, G. A., Spires-Jones, T. L., & Hyman, B. T. (2012, Feb 23). Propagation of tau pathology in a model of early Alzheimer's disease. *Neuron*, 73(4), 685-697. <https://doi.org/10.1016/j.neuron.2011.11.033>
- DeKosky, S. T., & Scheff, S. W. (1990, May). Synapse loss in frontal cortex biopsies in Alzheimer's disease: correlation with cognitive severity. *Ann Neurol*, 27(5), 457-464. <https://doi.org/10.1002/ana.410270502>
- DeKosky, S. T., Scheff, S. W., & Styren, S. D. (1996, Dec). Structural correlates of cognition in dementia: quantification and assessment of synapse change. *Neurodegeneration*, 5(4), 417-421. <https://doi.org/10.1006/neur.1996.0056>
- Dickerson, B. C., Salat, D. H., Greve, D. N., Chua, E. F., Rand-Giovannetti, E., Rentz, D. M., Bertram, L., Mullin, K., Tanzi, R. E., Blacker, D., Albert, M. S., & Sperling, R. A. (2005, Aug 9). Increased hippocampal activation in mild cognitive impairment compared to normal aging and AD. *Neurology*, 65(3), 404-411. <https://doi.org/10.1212/01.wnl.0000171450.97464.49>
- Dujardin, S., Commins, C., Lathuiliere, A., Beerepoot, P., Fernandes, A. R., Kamath, T. V., De Los Santos, M. B., Klickstein, N., Corjuc, D. L., Corjuc, B. T., Dooley, P. M., Viode, A., Oakley, D. H., Moore, B. D., Mullin, K., Jean-Gilles, D., Clark, R., Atchison, K., Moore, R., Chibnik, L. B., Tanzi, R. E., Frosch, M. P., Serrano-Pozo, A., Elwood, F., Steen, J. A., Kennedy, M. E., & Hyman, B. T. (2020, Aug). Tau molecular diversity contributes to

- clinical heterogeneity in Alzheimer's disease. *Nat Med*, 26(8), 1256-1263. <https://doi.org/10.1038/s41591-020-0938-9>
- Fa, M., Puzzo, D., Piacentini, R., Staniszewski, A., Zhang, H., Baltrons, M. A., Li Puma, D. D., Chatterjee, I., Li, J., Saeed, F., Berman, H. L., Ripoli, C., Gulisano, W., Gonzalez, J., Tian, H., Costa, J. A., Lopez, P., Davidowitz, E., Yu, W. H., Haroutunian, V., Brown, L. M., Palmeri, A., Sigurdsson, E. M., Duff, K. E., Teich, A. F., Honig, L. S., Sierks, M., Moe, J. G., D'Adamio, L., Grassi, C., Kanaan, N. M., Fraser, P. E., & Arancio, O. (2016, Jan 20). Extracellular Tau Oligomers Produce An Immediate Impairment of LTP and Memory. *Sci Rep*, 6, 19393. <https://doi.org/10.1038/srep19393>
- Falcon, B., Zhang, W., Murzin, A. G., Murshudov, G., Garringer, H. J., Vidal, R., Crowther, R. A., Ghetti, B., Scheres, S. H. W., & Goedert, M. (2018, Sep). Structures of filaments from Pick's disease reveal a novel tau protein fold. *Nature*, 561(7721), 137-140. <https://doi.org/10.1038/s41586-018-0454-y>
- Falcon, B., Zhang, W., Schweighauser, M., Murzin, A. G., Vidal, R., Garringer, H. J., Ghetti, B., Scheres, S. H. W., & Goedert, M. (2018, Nov). Tau filaments from multiple cases of sporadic and inherited Alzheimer's disease adopt a common fold. *Acta Neuropathol*, 136(5), 699-708. <https://doi.org/10.1007/s00401-018-1914-z>
- Falcon, B., Zivanov, J., Zhang, W., Murzin, A. G., Garringer, H. J., Vidal, R., Crowther, R. A., Newell, K. L., Ghetti, B., Goedert, M., & Scheres, S. H. W. (2019, Apr). Novel tau filament fold in chronic traumatic encephalopathy encloses hydrophobic molecules. *Nature*, 568(7752), 420-423. <https://doi.org/10.1038/s41586-019-1026-5>
- Fellin, T., Pascual, O., Gobbo, S., Pozzan, T., Haydon, P. G., & Carmignoto, G. (2004, Sep 2). Neuronal synchrony mediated by astrocytic glutamate through activation of extrasynaptic NMDA receptors. *Neuron*, 43(5), 729-743. <https://doi.org/10.1016/j.neuron.2004.08.011>
- Fitzpatrick, A. W., Falcon, B., He, S., Murzin, A. G., Murshudov, G., Garringer, H. J., Crowther, R. A., Ghetti, B., Goedert, M., & Scheres, S. H. (2017). Cryo-EM structures of tau filaments from Alzheimer's disease. *Nature*, 547(7662), 185-190.
- Gerson, J. E., & Kaye, R. (2013). Formation and propagation of tau oligomeric seeds. *Front Neurol*, 4, 93. <https://doi.org/10.3389/fneur.2013.00093>
- Giannakopoulos, P., Herrmann, F. R., Bussiere, T., Bouras, C., Kovari, E., Perl, D. P., Morrison, J. H., Gold, G., & Hof, P. R. (2003, May 13). Tangle and neuron numbers, but not amyloid load, predict cognitive status in Alzheimer's disease. *Neurology*, 60(9), 1495-1500. <https://doi.org/10.1212/01.wnl.0000063311.58879.01>
- Gibbons, G. S., Banks, R. A., Kim, B., Xu, H., Changolkar, L., Leight, S. N., Riddle, D. M., Li, C., Gathagan, R. J., Brown, H. J., Zhang, B., Trojanowski, J. Q., & Lee, V. M. (2017, Nov 22). GFP-Mutant Human Tau Transgenic Mice Develop Tauopathy Following CNS Injections of Alzheimer's Brain-Derived Pathological Tau or Synthetic Mutant Human Tau

- Fibrils. *J Neurosci*, 37(47), 11485-11494. <https://doi.org/10.1523/JNEUROSCI.2393-17.2017>
- Guo, J. L., Narasimhan, S., Changolkar, L., He, Z., Stieber, A., Zhang, B., Gathagan, R. J., Iba, M., McBride, J. D., & Trojanowski, J. Q. (2016). Unique pathological tau conformers from Alzheimer's brains transmit tau pathology in nontransgenic mice. *Journal of Experimental Medicine*, 213(12), 2635-2654.
- Hallinan, G. I., Vargas-Caballero, M., West, J., & Deinhardt, K. (2019, Nov 27). Tau Misfolding Efficiently Propagates between Individual Intact Hippocampal Neurons. *J Neurosci*, 39(48), 9623-9632. <https://doi.org/10.1523/JNEUROSCI.1590-19.2019>
- He, Z., McBride, J. D., Xu, H., Changolkar, L., Kim, S.-j., Zhang, B., Narasimhan, S., Gibbons, G. S., Guo, J. L., & Kozak, M. (2020). Transmission of tauopathy strains is independent of their isoform composition. *Nature communications*, 11(1), 7.
- Heinonen, O., Soininen, H., Sorvari, H., Kosunen, O., Paljarvi, L., Koivisto, E., & Riekkinen, P. J., Sr. (1995, Jan). Loss of synaptophysin-like immunoreactivity in the hippocampal formation is an early phenomenon in Alzheimer's disease. *Neuroscience*, 64(2), 375-384. [https://doi.org/10.1016/0306-4522\(94\)00422-2](https://doi.org/10.1016/0306-4522(94)00422-2)
- Hill, E., Karikari, T. K., Moffat, K. G., Richardson, M. J. E., & Wall, M. J. (2019, Sep/Oct). Introduction of Tau Oligomers into Cortical Neurons Alters Action Potential Dynamics and Disrupts Synaptic Transmission and Plasticity. *eNeuro*, 6(5). <https://doi.org/10.1523/ENEURO.0166-19.2019>
- Horvath, A., Szucs, A., Hidasi, Z., Csukly, G., Barcs, G., & Kamondi, A. (2018). Prevalence, Semiology, and Risk Factors of Epilepsy in Alzheimer's Disease: An Ambulatory EEG Study. *J Alzheimers Dis*, 63(3), 1045-1054. <https://doi.org/10.3233/JAD-170925>
- Horvath, A. A., Papp, A., Zsuffa, J., Szucs, A., Luckl, J., Radai, F., Nagy, F., Hidasi, Z., Csukly, G., Barcs, G., & Kamondi, A. (2021, Aug). Subclinical epileptiform activity accelerates the progression of Alzheimer's disease: A long-term EEG study. *Clin Neurophysiol*, 132(8), 1982-1989. <https://doi.org/10.1016/j.clinph.2021.03.050>
- Kanaan, N. M., Morfini, G. A., LaPointe, N. E., Pigino, G. F., Patterson, K. R., Song, Y., Andreadis, A., Fu, Y., Brady, S. T., & Binder, L. I. (2011). Pathogenic forms of tau inhibit kinesin-dependent axonal transport through a mechanism involving activation of axonal phosphotransferases. *Journal of neuroscience*, 31(27), 9858-9868.
- Katsuse, O., Lin, W. L., Lewis, J., Hutton, M. L., & Dickson, D. W. (2006, Dec 1). Neurofibrillary tangle-related synaptic alterations of spinal motor neurons of P301L tau transgenic mice. *Neurosci Lett*, 409(2), 95-99. <https://doi.org/10.1016/j.neulet.2006.09.021>

- Kopeikina, K. J., Polydoro, M., Tai, H. C., Yaeger, E., Carlson, G. A., Pitstick, R., Hyman, B. T., & Spires-Jones, T. L. (2013, Apr 15). Synaptic alterations in the rTg4510 mouse model of tauopathy. *J Comp Neurol*, *521*(6), 1334-1353. <https://doi.org/10.1002/cne.23234>
- Lagarde, J., Olivieri, P., Tonietto, M., Tissot, C., Rivals, I., Gervais, P., Caille, F., Moussion, M., Bottlaender, M., & Sarazin, M. (2022, May). Tau-PET imaging predicts cognitive decline and brain atrophy progression in early Alzheimer's disease. *J Neurol Neurosurg Psychiatry*, *93*(5), 459-467. <https://doi.org/10.1136/jnnp-2021-328623>
- Lam, A. D., Deck, G., Goldman, A., Eskandar, E. N., Noebels, J., & Cole, A. J. (2017, Jun). Silent hippocampal seizures and spikes identified by foramen ovale electrodes in Alzheimer's disease. *Nat Med*, *23*(6), 678-680. <https://doi.org/10.1038/nm.4330>
- Lam, A. D., Sarkis, R. A., Pellerin, K. R., Jing, J., Dworetzky, B. A., Hoch, D. B., Jacobs, C. S., Lee, J. W., Weisholtz, D. S., Zepeda, R., Westover, M. B., Cole, A. J., & Cash, S. S. (2020, Oct 20). Association of epileptiform abnormalities and seizures in Alzheimer disease. *Neurology*, *95*(16), e2259-e2270. <https://doi.org/10.1212/WNL.0000000000010612>
- Lasagna-Reeves, C. A., Castillo-Carranza, D. L., Sengupta, U., Clos, A. L., Jackson, G. R., & Kaye, R. (2011, Jun 6). Tau oligomers impair memory and induce synaptic and mitochondrial dysfunction in wild-type mice. *Mol Neurodegener*, *6*, 39. <https://doi.org/10.1186/1750-1326-6-39>
- Lasagna-Reeves, C. A., Castillo-Carranza, D. L., Sengupta, U., Guerrero-Munoz, M. J., Kiritoshi, T., Neugebauer, V., Jackson, G. R., & Kaye, R. (2012). Alzheimer brain-derived tau oligomers propagate pathology from endogenous tau. *Sci Rep*, *2*, 700. <https://doi.org/10.1038/srep00700>
- Levenga, J., Krishnamurthy, P., Rajamohamedsait, H., Wong, H., Franke, T. F., Cain, P., Sigurdsson, E. M., & Hoeffler, C. A. (2013, Jul 11). Tau pathology induces loss of GABAergic interneurons leading to altered synaptic plasticity and behavioral impairments. *Acta Neuropathol Commun*, *1*, 34. <https://doi.org/10.1186/2051-5960-1-34>
- Leyns, C. E. G., Gratuze, M., Narasimhan, S., Jain, N., Koscal, L. J., Jiang, H., Manis, M., Colonna, M., Lee, V. M. Y., Ulrich, J. D., & Holtzman, D. M. (2019, Aug). TREM2 function impedes tau seeding in neuritic plaques. *Nat Neurosci*, *22*(8), 1217-1222. <https://doi.org/10.1038/s41593-019-0433-0>
- LoPresti, P., Szuchet, S., Papasozomenos, S. C., Zinkowski, R. P., & Binder, L. I. (1995, Oct 24). Functional implications for the microtubule-associated protein tau: localization in oligodendrocytes. *Proc Natl Acad Sci U S A*, *92*(22), 10369-10373. <https://doi.org/10.1073/pnas.92.22.10369>
- Masliah, E., Mallory, M., Alford, M., DeTeresa, R., Hansen, L. A., McKeel, D. W., Jr., & Morris, J. C. (2001, Jan 9). Altered expression of synaptic proteins occurs early during progression of Alzheimer's disease. *Neurology*, *56*(1), 127-129. <https://doi.org/10.1212/wnl.56.1.127>

- Masliah, E., Mallory, M., Hansen, L., DeTeresa, R., Alford, M., & Terry, R. (1994, Jun 6). Synaptic and neuritic alterations during the progression of Alzheimer's disease. *Neurosci Lett*, *174*(1), 67-72. [https://doi.org/10.1016/0304-3940\(94\)90121-x](https://doi.org/10.1016/0304-3940(94)90121-x)
- Mate De Gerando, A., Welikovitch, L. A., Khasnavis, A., Commins, C., Glynn, C., Chun, J. E., Perbet, R., & Hyman, B. T. (2023, Aug). Tau seeding and spreading in vivo is supported by both AD-derived fibrillar and oligomeric tau. *Acta Neuropathol*, *146*(2), 191-210. <https://doi.org/10.1007/s00401-023-02600-1>
- Molina, L. A., Skelin, I., & Gruber, A. J. (2014). Acute NMDA receptor antagonism disrupts synchronization of action potential firing in rat prefrontal cortex. *PLoS One*, *9*(1), e85842. <https://doi.org/10.1371/journal.pone.0085842>
- Mueller, R. L., Combs, B., Alhadidy, M. M., Brady, S. T., Morfini, G. A., & Kanaan, N. M. (2021). Tau: A Signaling Hub Protein. *Front Mol Neurosci*, *14*, 647054. <https://doi.org/10.3389/fnmol.2021.647054>
- Mueller, R. L., Kanaan, N. M., & Combs, B. (2023, Dec 22). Using Live-Cell Imaging to Measure the Effects of Pathological Proteins on Axonal Transport in Primary Hippocampal Neurons. *J Vis Exp*(202). <https://doi.org/10.3791/66156>
- Narasimhan, S., Guo, J. L., Changolkar, L., Stieber, A., McBride, J. D., Silva, L. V., He, Z., Zhang, B., Gathagan, R. J., & Trojanowski, J. Q. (2017). Pathological tau strains from human brains recapitulate the diversity of tauopathies in nontransgenic mouse brain. *Journal of neuroscience*, *37*(47), 11406-11423.
- Narasimhan, S., & Lee, V. M. (2017). The use of mouse models to study cell-to-cell transmission of pathological tau. In *Methods in cell biology* (Vol. 141, pp. 287-305). Elsevier.
- Nelson, P. T., Alafuzoff, I., Bigio, E. H., Bouras, C., Braak, H., Cairns, N. J., Castellani, R. J., Crain, B. J., Davies, P., Del Tredici, K., Duyckaerts, C., Frosch, M. P., Haroutunian, V., Hof, P. R., Hulette, C. M., Hyman, B. T., Iwatsubo, T., Jellinger, K. A., Jicha, G. A., Kovari, E., Kukull, W. A., Leverenz, J. B., Love, S., Mackenzie, I. R., Mann, D. M., Masliah, E., McKee, A. C., Montine, T. J., Morris, J. C., Schneider, J. A., Sonnen, J. A., Thal, D. R., Trojanowski, J. Q., Troncoso, J. C., Wisniewski, T., Woltjer, R. L., & Beach, T. G. (2012, May). Correlation of Alzheimer disease neuropathologic changes with cognitive status: a review of the literature. *J Neuropathol Exp Neurol*, *71*(5), 362-381. <https://doi.org/10.1097/NEN.0b013e31825018f7>
- Ondrejcek, T., Hu, N. W., Qi, Y., Klyubin, I., Corbett, G. T., Fraser, G., Perkinson, M. S., Walsh, D. M., Billinton, A., & Rowan, M. J. (2019, Jul). Soluble tau aggregates inhibit synaptic long-term depression and amyloid beta-facilitated LTD in vivo. *Neurobiol Dis*, *127*, 582-590. <https://doi.org/10.1016/j.nbd.2019.03.022>
- Ondrejcek, T., Klyubin, I., Corbett, G. T., Fraser, G., Hong, W., Mably, A. J., Gardener, M., Hammersley, J., Perkinson, M. S., Billinton, A., Walsh, D. M., & Rowan, M. J. (2018, Dec

- 12). Cellular Prion Protein Mediates the Disruption of Hippocampal Synaptic Plasticity by Soluble Tau In Vivo. *J Neurosci*, 38(50), 10595-10606. <https://doi.org/10.1523/JNEUROSCI.1700-18.2018>
- Palop, J. J., & Mucke, L. (2016, Dec). Network abnormalities and interneuron dysfunction in Alzheimer disease. *Nat Rev Neurosci*, 17(12), 777-792. <https://doi.org/10.1038/nrn.2016.141>
- Patterson, K. R., Remmers, C., Fu, Y., Brooker, S., Kanaan, N. M., Vana, L., Ward, S., Reyes, J. F., Philibert, K., Glucksman, M. J., & Binder, L. I. (2011, Jul 1). Characterization of prefibrillar Tau oligomers in vitro and in Alzheimer disease. *J Biol Chem*, 286(26), 23063-23076. <https://doi.org/10.1074/jbc.M111.237974>
- Price, J. L., Davis, P. B., Morris, J. C., & White, D. L. (1991, Jul-Aug). The distribution of tangles, plaques and related immunohistochemical markers in healthy aging and Alzheimer's disease. *Neurobiol Aging*, 12(4), 295-312. [https://doi.org/10.1016/0197-4580\(91\)90006-6](https://doi.org/10.1016/0197-4580(91)90006-6)
- Price, J. L., & Morris, J. C. (1999, Mar). Tangles and plaques in nondemented aging and "preclinical" Alzheimer's disease. *Ann Neurol*, 45(3), 358-368. [https://doi.org/10.1002/1531-8249\(199903\)45:3<358::aid-ana12>3.0.co;2-x](https://doi.org/10.1002/1531-8249(199903)45:3<358::aid-ana12>3.0.co;2-x)
- Puzzo, D., Argyrousi, E. K., Staniszewski, A., Zhang, H., Calcagno, E., Zuccarello, E., Acquarone, E., Fa, M., Li Puma, D. D., Grassi, C., D'Adamio, L., Kanaan, N. M., Fraser, P. E., & Arancio, O. (2020, Sep 1). Tau is not necessary for amyloid-beta-induced synaptic and memory impairments. *J Clin Invest*, 130(9), 4831-4844. <https://doi.org/10.1172/JCI137040>
- Ranasinghe, K. G., Kudo, K., Hinkley, L., Beagle, A., Lerner, H., Mizuiri, D., Findlay, A., Miller, B. L., Kramer, J. H., Gorno-Tempini, M. L., Rabinovici, G. D., Rankin, K. P., Garcia, P. A., Kirsch, H. E., Vessel, K., & Nagarajan, S. S. (2022, Apr 18). Neuronal synchrony abnormalities associated with subclinical epileptiform activity in early-onset Alzheimer's disease. *Brain*, 145(2), 744-753. <https://doi.org/10.1093/brain/awab442>
- Reilly, P., Winston, C. N., Baron, K. R., Trejo, M., Rockenstein, E. M., Akers, J. C., Kfoury, N., Diamond, M., Masliah, E., Rissman, R. A., & Yuan, S. H. (2017, Oct). Novel human neuronal tau model exhibiting neurofibrillary tangles and transcellular propagation. *Neurobiol Dis*, 106, 222-234. <https://doi.org/10.1016/j.nbd.2017.06.005>
- Saito, T., Mihira, N., Matsuba, Y., Sasaguri, H., Hashimoto, S., Narasimhan, S., Zhang, B., Murayama, S., Higuchi, M., Lee, V. M. Y., Trojanowski, J. Q., & Saido, T. C. (2019, Aug 23). Humanization of the entire murine Mapt gene provides a murine model of pathological human tau propagation. *J Biol Chem*, 294(34), 12754-12765. <https://doi.org/10.1074/jbc.RA119.009487>

- Saroja, S. R., Sharma, A., Hof, P. R., & Pereira, A. C. (2022, Sep). Differential expression of tau species and the association with cognitive decline and synaptic loss in Alzheimer's disease. *Alzheimers Dement*, *18*(9), 1602-1615. <https://doi.org/10.1002/alz.12518>
- Scheff, S. W., & Price, D. A. (1993, Feb). Synapse loss in the temporal lobe in Alzheimer's disease. *Ann Neurol*, *33*(2), 190-199. <https://doi.org/10.1002/ana.410330209>
- Scheff, S. W., Price, D. A., Schmitt, F. A., DeKosky, S. T., & Mufson, E. J. (2007, May 1). Synaptic alterations in CA1 in mild Alzheimer disease and mild cognitive impairment. *Neurology*, *68*(18), 1501-1508. <https://doi.org/10.1212/01.wnl.0000260698.46517.8f>
- Scheff, S. W., Price, D. A., Schmitt, F. A., & Mufson, E. J. (2006, Oct). Hippocampal synaptic loss in early Alzheimer's disease and mild cognitive impairment. *Neurobiol Aging*, *27*(10), 1372-1384. <https://doi.org/10.1016/j.neurobiolaging.2005.09.012>
- Scheff, S. W., Sparks, L., & Price, D. A. (1993, Sep). Quantitative assessment of synaptic density in the entorhinal cortex in Alzheimer's disease. *Ann Neurol*, *34*(3), 356-361. <https://doi.org/10.1002/ana.410340309>
- Scheres, S. H., Zhang, W., Falcon, B., & Goedert, M. (2020, Oct). Cryo-EM structures of tau filaments. *Curr Opin Struct Biol*, *64*, 17-25. <https://doi.org/10.1016/j.sbi.2020.05.011>
- Scholl, M., Lockhart, S. N., Schonhaut, D. R., O'Neil, J. P., Janabi, M., Ossenkoppele, R., Baker, S. L., Vogel, J. W., Faria, J., Schwimmer, H. D., Rabinovici, G. D., & Jagust, W. J. (2016, Mar 2). PET Imaging of Tau Deposition in the Aging Human Brain. *Neuron*, *89*(5), 971-982. <https://doi.org/10.1016/j.neuron.2016.01.028>
- Selkoe, D. J. (2002, Oct 25). Alzheimer's disease is a synaptic failure. *Science*, *298*(5594), 789-791. <https://doi.org/10.1126/science.1074069>
- Sengupta, U., & Kaye, R. (2024). Tau Oligomers as Pathogenic Seeds: Preparation, Characterization, and Propagation In Vitro and In Vivo. *Methods Mol Biol*, *2754*, 147-183. https://doi.org/10.1007/978-1-0716-3629-9_9
- Serrano-Pozo, A., Frosch, M. P., Masliah, E., & Hyman, B. T. (2011, Sep). Neuropathological alterations in Alzheimer disease. *Cold Spring Harb Perspect Med*, *1*(1), a006189. <https://doi.org/10.1101/cshperspect.a006189>
- Shrivastava, A. N., Redeker, V., Pieri, L., Bousset, L., Renner, M., Madiona, K., Mailhes-Hamon, C., Coens, A., Buee, L., Hantraye, P., Triller, A., & Melki, R. (2019, Feb 1). Clustering of Tau fibrils impairs the synaptic composition of alpha3-Na(+)/K(+)-ATPase and AMPA receptors. *EMBO J*, *38*(3). <https://doi.org/10.15252/embj.201899871>
- Smailovic, U., Koenig, T., Kareholt, I., Andersson, T., Kramberger, M. G., Winblad, B., & Jelic, V. (2018, Mar). Quantitative EEG power and synchronization correlate with Alzheimer's

disease CSF biomarkers. *Neurobiol Aging*, 63, 88-95.
<https://doi.org/10.1016/j.neurobiolaging.2017.11.005>

- Stancu, I. C., Vasconcelos, B., Ris, L., Wang, P., Villers, A., Peeraer, E., Buist, A., Terwel, D., Baatsen, P., Oyelami, T., Pierrot, N., Casteels, C., Bormans, G., Kienlen-Campard, P., Octave, J. N., Moechars, D., & Dewachter, I. (2015, Jun). Templated misfolding of Tau by prion-like seeding along neuronal connections impairs neuronal network function and associated behavioral outcomes in Tau transgenic mice. *Acta Neuropathol*, 129(6), 875-894. <https://doi.org/10.1007/s00401-015-1413-4>
- Sydow, A., Van der Jeugd, A., Zheng, F., Ahmed, T., Balschun, D., Petrova, O., Drexler, D., Zhou, L., Rune, G., Mandelkow, E., D'Hooge, R., Alzheimer, C., & Mandelkow, E. M. (2011, Feb 16). Tau-induced defects in synaptic plasticity, learning, and memory are reversible in transgenic mice after switching off the toxic Tau mutant. *J Neurosci*, 31(7), 2511-2525. <https://doi.org/10.1523/JNEUROSCI.5245-10.2011>
- Takeda, S., Wegmann, S., Cho, H., DeVos, S. L., Commins, C., Roe, A. D., Nicholls, S. B., Carlson, G. A., Pitstick, R., Nobuhara, C. K., Costantino, I., Frosch, M. P., Muller, D. J., Irimia, D., & Hyman, B. T. (2015, Oct 13). Neuronal uptake and propagation of a rare phosphorylated high-molecular-weight tau derived from Alzheimer's disease brain. *Nat Commun*, 6, 8490. <https://doi.org/10.1038/ncomms9490>
- Targa Dias Anastacio, H., Matosin, N., & Ooi, L. (2022, Jun 22). Neuronal hyperexcitability in Alzheimer's disease: what are the drivers behind this aberrant phenotype? *Transl Psychiatry*, 12(1), 257. <https://doi.org/10.1038/s41398-022-02024-7>
- Terry, R. D., Masliah, E., Salmon, D. P., Butters, N., DeTeresa, R., Hill, R., Hansen, L. A., & Katzman, R. (1991, Oct). Physical basis of cognitive alterations in Alzheimer's disease: synapse loss is the major correlate of cognitive impairment. *Ann Neurol*, 30(4), 572-580. <https://doi.org/10.1002/ana.410300410>
- Tok, S., Crauwels, D., & Drinkenburg, W. (2022). A Characterization of Epileptiform Activity Associated with TAU Seeding and Amyloid Pathology in the APPKM670/671NL. PS1/L166P and APP-KI Animal Models. *J Neurol Exp Neurosci*, 8(2), 18-31.
- Usenovic, M., Niroomand, S., Drolet, R. E., Yao, L., Gaspar, R. C., Hatcher, N. G., Schachter, J., Renger, J. J., & Parmentier-Batteur, S. (2015, Oct 21). Internalized Tau Oligomers Cause Neurodegeneration by Inducing Accumulation of Pathogenic Tau in Human Neurons Derived from Induced Pluripotent Stem Cells. *J Neurosci*, 35(42), 14234-14250. <https://doi.org/10.1523/JNEUROSCI.1523-15.2015>
- Van der Jeugd, A., Ahmed, T., Burnouf, S., Belarbi, K., Hamdame, M., Grosjean, M. E., Humez, S., Balschun, D., Blum, D., Buee, L., & D'Hooge, R. (2011, Mar). Hippocampal tauopathy in tau transgenic mice coincides with impaired hippocampus-dependent learning and memory, and attenuated late-phase long-term depression of synaptic transmission. *Neurobiol Learn Mem*, 95(3), 296-304. <https://doi.org/10.1016/j.nlm.2010.12.005>

- Verstraelen, P., Garcia-Diaz Barriga, G., Verschuuren, M., Asselbergh, B., Nuydens, R., Larsen, P. H., Timmermans, J. P., & De Vos, W. H. (2020, Sep 25). Systematic Quantification of Synapses in Primary Neuronal Culture. *iScience*, 23(9), 101542. <https://doi.org/10.1016/j.isci.2020.101542>
- Vossel, K. A., Beagle, A. J., Rabinovici, G. D., Shu, H., Lee, S. E., Naasan, G., Hegde, M., Cornes, S. B., Henry, M. L., Nelson, A. B., Seeley, W. W., Geschwind, M. D., Gorno-Tempini, M. L., Shih, T., Kirsch, H. E., Garcia, P. A., Miller, B. L., & Mucke, L. (2013, Sep 1). Seizures and epileptiform activity in the early stages of Alzheimer disease. *JAMA Neurol*, 70(9), 1158-1166. <https://doi.org/10.1001/jamaneurol.2013.136>
- Vossel, K. A., Ranasinghe, K. G., Beagle, A. J., Mizuiri, D., Honma, S. M., Dowling, A. F., Darwish, S. M., Van Berlo, V., Barnes, D. E., Mantle, M., Karydas, A. M., Coppola, G., Roberson, E. D., Miller, B. L., Garcia, P. A., Kirsch, H. E., Mucke, L., & Nagarajan, S. S. (2016, Dec). Incidence and impact of subclinical epileptiform activity in Alzheimer's disease. *Ann Neurol*, 80(6), 858-870. <https://doi.org/10.1002/ana.24794>
- Wagatsuma, N., von der Heydt, R., & Niebur, E. (2016, Sep 1). Spike synchrony generated by modulatory common input through NMDA-type synapses. *J Neurophysiol*, 116(3), 1418-1433. <https://doi.org/10.1152/jn.01142.2015>
- Wang, J., Huang, Q., Chen, X., You, Z., He, K., Guo, Q., Huang, Y., Yang, Y., Lin, Z., Guo, T., Zhao, J., Guan, Y., Li, B., & Xie, F. (2024, Apr 8). Tau pathology is associated with synaptic density and longitudinal synaptic loss in Alzheimer's disease. *Mol Psychiatry*. <https://doi.org/10.1038/s41380-024-02501-z>
- Ward, S. M., Himmelstein, D. S., Lancia, J. K., Fu, Y., Patterson, K. R., & Binder, L. I. (2013). TOC1: characterization of a selective oligomeric tau antibody. *Journal of Alzheimer's Disease*, 37(3), 593-602.
- Witton, J., Staniaszek, L. E., Bartsch, U., Randall, A. D., Jones, M. W., & Brown, J. T. (2016, Aug 15). Disrupted hippocampal sharp-wave ripple-associated spike dynamics in a transgenic mouse model of dementia. *J Physiol*, 594(16), 4615-4630. <https://doi.org/10.1113/jphysiol.2014.282889>
- Yoshiyama, Y., Higuchi, M., Zhang, B., Huang, S. M., Iwata, N., Saido, T. C., Maeda, J., Suhara, T., Trojanowski, J. Q., & Lee, V. M. (2007, Feb 1). Synapse loss and microglial activation precede tangles in a P301S tauopathy mouse model. *Neuron*, 53(3), 337-351. <https://doi.org/10.1016/j.neuron.2007.01.010>
- Zhang, W., Falcon, B., Murzin, A. G., Fan, J., Crowther, R. A., Goedert, M., & Scheres, S. H. (2019, Feb 5). Heparin-induced tau filaments are polymorphic and differ from those in Alzheimer's and Pick's diseases. *Elife*, 8. <https://doi.org/10.7554/eLife.43584>
- Zhang, W., Tarutani, A., Newell, K. L., Murzin, A. G., Matsubara, T., Falcon, B., Vidal, R., Garringer, H. J., Shi, Y., Ikeuchi, T., Murayama, S., Ghetti, B., Hasegawa, M., Goedert,

- M., & Scheres, S. H. W. (2020, Apr). Novel tau filament fold in corticobasal degeneration. *Nature*, *580*(7802), 283-287. <https://doi.org/10.1038/s41586-020-2043-0>
- Zhu, B., Liu, Y., Hwang, S., Archuleta, K., Huang, H., Campos, A., Murad, R., Pina-Crespo, J., Xu, H., & Huang, T. Y. (2022, Sep 2). Trem2 deletion enhances tau dispersion and pathology through microglia exosomes. *Mol Neurodegener*, *17*(1), 58. <https://doi.org/10.1186/s13024-022-00562-8>

CHAPTER 5

Overall Discussion

DISCUSSION

Summary of key findings

I developed an *in vitro* tau seeding model by treating MAPT-KI primary hippocampal neurons with sarkosyl-insoluble tau purified from human AD brains. Seeding resulted in the progressive formation of AD-associated tau pathology in neurons. The seeded inclusions were localized primarily in neurites and had characteristics of early modifications associated with pentangle tau pathology. Seeding did not affect overall culture viability or cause overt cell death out to 28d post-treatment (corresponding to DIV33). While overt degeneration of axons was not found, there was evidence of axonal dysfunction in the form of dystrophic axons with accumulations of pathological tau conformations, active GSK3 β and axonal transport cargoes in AD-tau seeded neurons. AD-tau-treated neurons also exhibited signs of hyperexcitability in response to glutamate treatment and exacerbated inhibition following treatment with an NMDA-antagonist at 23d post-treatment (corresponding to DIV28). In addition, there was significant synapse loss at 28d post-treatment (corresponding to DIV33). This model recapitulates some of the earliest changes associated with AD, such as adoption of pathogenic tau conformations and synaptic toxicity. Future studies using this model may provide key insights into the early mechanisms involved in the pathogenesis of AD.

Tau inclusions in AD-tau-seeded MAPT-KI primary neurons are associated with pretangle pathology

Early modifications of tau include phosphorylation at AT8, PHF1 and pS422 epitopes and conformational changes such as oligomerization and PAD-exposure (Christensen et al., 2019;

Combs et al., 2016; Cox et al., 2016; Kanaan et al., 2011; Tiernan et al., 2016). These modifications are observed in human AD tissue (early through late stage) beginning in the pretangle stage of tau inclusion formation, which is thought to represent the earliest accumulations of pathogenic tau in neurons (Christensen et al., 2019; Combs et al., 2016; Cox et al., 2016; Kanaan et al., 2011; Tiernan et al., 2016). Tau inclusions in the AD-tau-seeded MAPT-KI primary hippocampal neurons exhibited immunoreactivity with each of the pretangle-associated markers used here. Furthermore, PAD-exposed tau (TNT1+) inclusions co-localized with AT8, pS422 and TOC1, and PHF1 to a lesser extent. This is consistent with observations in human AD tissue and other tauopathies (Christensen et al., 2019; Combs et al., 2016; Combs & Kanaan, 2017; Cox et al., 2016; Kanaan et al., 2016; Kanaan et al., 2011; Tiernan et al., 2016). Another modification that occurs at intermediate stages of tau pathology evolution in AD is truncation at D421, which is recognized by the TauC3 antibody (Gamblin et al., 2003). A relatively small number of TauC3+ inclusions were observed which often did not colocalize with TNT1. In general, the tau inclusions were primarily neuritic with rare somatodendritic localization. These inclusions are reminiscent of neuropil threads observed in dystrophic neuronal processes in AD (Christensen et al., 2019; Combs et al., 2019). Multiple studies show that neuropil threads precede NFTs in cell bodies (Christensen et al., 2019; Ghoshal et al., 2002; Su et al., 1997; Vana et al., 2011). NFTs are comprised of tau filaments with β -pleated sheet structures that are labelled with β -sheet dyes such as Thiazine Red (ThR) (Combs et al., 2016; Luna-Munoz et al., 2008; Luna-Viramontes et al., 2020; Mena et al., 1995). The tau inclusions in our model were ThR-negative. Taken together, I show that seeding MAPT-KI primary neurons with sarkosyl-insoluble AD-tau results in the formation of tau inclusions associated with early pretangle modifications.

Synaptic Dysfunction

In AD, affected neurons follow a dying-back pattern of degeneration that begins with synapse dysfunction and loss, followed by axon degeneration and eventually cell death. (Kanaan et al., 2013; Kneynsberg et al., 2017). I observed synaptic dysfunction and loss in our model. Furthermore, I observed early signs of axon degeneration including the accumulation of proteins in axonal swellings. I did not detect significant axonal fragmentation or overt neuron loss. These findings suggest that the neuronal changes observed in our model are associated with early changes in the neurodegenerative process.

Seeded MAPT-KI primary neurons exhibited a significantly greater response to glutamate compared to cultures treated with PBS or Con. Specifically, the frequency of network bursts (many neurons firing in synchrony) increased 3.6x from baseline, while PBS and Con-treated cultures increased 2x and 1.7x, from their respective baselines. Subsequent treatment with AP5, a NMDAR antagonist, resulted in the mean burst frequency returning to levels at or below baseline, suggesting that the glutamate-evoked hypersynchronicity was NMDAR-dependent. Further experiments are needed to identify the specific mechanisms underlying these changes.

Hypersynchrony is a feature of epileptic activity. Notably, epileptic activity is frequently associated with AD and can occur in the early stages of AD (Cretin et al., 2016; Palop & Mucke, 2010; Vossel et al., 2013; Vossel et al., 2016; Vossel et al., 2017). Similarly, clinical studies showed that hyperactivity in the hippocampus occurs early in AD, while hypoactivity is associated with later stages of disease (Targa Dias Anastacio et al., 2022). Interestingly, AD patients exhibit neuron hyperexcitability during a memory-encoding task (Celone et al., 2006; Dickerson et al., 2005; Hamalainen et al., 2007). Furthermore, activity recordings of single neurons, networks or

entire brain regions consistently show hyperexcitability in human with early AD and animal models (Balez et al., 2016; Busche et al., 2008; Ghatak et al., 2019; Siskova et al., 2014; Targa Dias Anastacio et al., 2022).

Aberrant NMDAR activity is linked to hyperexcitability. AD mice given the activity-dependent NMDAR blocker MK801 showed reduced neuronal firing rate in hyperactive neurons (Lerdkrai et al., 2018). Furthermore, one of the primary drugs used to treat AD is the NMDAR antagonist, Memantine. Tau is also linked to neuronal hyperexcitability that is ameliorated with tau reduction. Tau reduction or knockout improves cortical and hippocampal neuronal hyperexcitability in mouse and *Drosophila* models of epilepsy. Furthermore, tau reduction in AD mouse models was protective against hyperexcitability and reversed NMDAR dysfunction (Roberson et al., 2011).

At the electrode level, the glutamate-evoked increase in firing rate in the AD-tau treated cultures was not significantly greater compared to PBS and Con-treated cultures. This could be because not all neurons are seeded therefore the effects of seeded cells are “washed out” when randomly assessing the neuronal activity within the culture. In contrast, a small number of seeded cells may be sufficient to disrupt network-wide patterns.

This is the first report of impaired synaptic activity resulting from tau seeding using AD-brain derived tau in a model in which human tau is not overexpressed or mutated. Most seeding studies using AD-tau did not assess synaptic function or density (Guo et al., 2016; He et al., 2020; Narasimhan et al., 2017). One *in vivo* study showed significant reductions in PSD95 and synaptophysin in WT mice at least 4.5 months post-injection with AD-tau (Bassil et al., 2021). Consistent with our findings, the synaptic pathology was observed in the absence of cell loss, suggesting that synaptic loss preceded overt cell loss (Bassil et al., 2021). Synaptic dysfunction

was reported only in a substantively more aggressive model incorporating FTDP-17 tau mutations into the animal model and seeding material (Stancu et al., 2015). Primary neurons from PS19 transgenic mice (overexpress mutant P301S human tau) treated with recombinant preformed fibrils comprised of the repeat domain of P301L mutant tau disrupted spontaneous neuronal network activity and GABA_A antagonist-induced neuronal network activity (Stancu et al., 2015). The dysfunction was not accompanied by synapse loss.

Acute synaptic dysfunction is observed in neurons treated with soluble tau oligomers. Primary cortical neurons from WT mice treated with soluble AD-brain derived tau oligomers exhibited significant reductions in homer and bassoon just 3 days post-treatment (Saroja et al., 2022). Furthermore, WT human iPSCs treated with recombinant heparin-induced soluble tau oligomers (WT 2N4R tau) resulted in significant decreases in synaptophysin and synapsin-1 puncta 14d post-treatment, accompanied by increased intracellular Ca²⁺ levels, neurite degeneration and cell loss (Usenovic et al., 2015). These findings are consistent with reports that soluble oligomers are one of the toxic tau species (Guerrero-Munoz et al., 2015; Ward et al., 2012). It is reasonable to suggest that treating cells with insoluble tau oligomers derived from human AD-brain may better mimic what occurs in human disease. Indeed, Mate De Gerando and coworkers compared two separate pools of AD-derived tau: sarkosyl insoluble AD-tau (prepared similar to our approach) and high-molecular weight tau (HMW; prepared using size exclusion chromatography) (Mate De Gerando et al., 2023). The two different preparations were injected into the hippocampus of PS19 mice and found that both populations seeded tau aggregation and neither induced overt neuron loss or altered levels of bassoon or PSD95 up to 3 months post-injection (Mate De Gerando et al., 2023). In a separate study, the authors isolated tau oligomers from AD brains by immunoprecipitation techniques using the oligomer-specific T22 antibody

(Lasagna-Reeves et al., 2012). T22-oligomers, but not sarkosyl-insoluble PHFs, acutely inhibited LTP in hippocampal brain slices and impaired object recognition in WT mice 3d post-injection. The memory impairments were no longer observed at 11m post-injection despite the presence of tau pathology that propagated to functionally connected sites (Lasagna-Reeves et al., 2012). Soluble tau oligomers appear to be highly toxic and induce acute synaptic dysfunction. However, in AD, neuron loss occurs over decades and there appears to be a temporal progression in which synaptic dysfunction and loss is followed by axonopathy and then overt neuron death. Our seeding model aligns better with a progressive phenotype in which the pathological tau is not overtly toxic but induces network hyperexcitability and mild synapse loss without obvious axon degeneration or cell death.

Early signs of axonopathy

I did not observe axon degeneration in AD-tau treated cultures. In fact, total β -III tubulin protein levels were unchanged on Western blot and axon outgrowth was not affected in two separate but complementary assays (ICF and MEA). However, I observed pathological changes associated with early stages of axon degeneration. Namely, I identified dystrophic neurites and axonal spheroids enriched in PAD-exposed tau, amyloid precursor protein (APP), and synaptophysin. The accumulation of APP and synaptophysin is observed in AD and thought to result from dysfunctional axonal transport mechanisms (Coleman, 2005; Kamal et al., 2000; Koo et al., 1990). Our group identified a mechanism through which PAD-exposure inhibits axon transport through the initiation of a signaling cascade that ultimately causes anterograde-directed kinesin motor proteins to release cargos. Specifically, PAD-exposure activates protein phosphatase 1 (PP1), which activates glycogen synthase kinase 3 β which in turn phosphorylates kinesin light chains, resulting in cargo release. The total levels of active GSK3 β protein were not significantly

different in AD-tau treated cultures. However, using ICF, I found local “hot-spots” of active GSK3 β that colocalize with PAD-exposed pathological tau inclusions. These are the same tau inclusion sites where APP and synaptophysin appeared to accumulate, suggesting axonal transport deficits may be induced by PAD-exposed tau inclusions in dystrophic neurites. This hypothesis warrants further investigation, ideally using a live-cell axonal transport models in which transport is measured at the site of PAD-exposed tau inclusions as well as at sites directly proximal and distal to the inclusion. Our group showed that WT rat neurons transfected with mutant (P301L tau) tau or pseudophosphorylated tau (AT8 tau) results in significant increases in pausing frequency of mApple-tagged synaptophysin cargos (Christensen et al., 2023; Combs et al., 2021). Adapting the live-cell axon transport to long-term cultures and identifying specific sites of tau inclusions to measure transport are technically challenging, but future studies will need to be overcome these hurdles to confirm whether axonal transport is impaired. If achieved, this would be a very powerful tool to study the local effects of specific AD-associated tau conformations on axon transport, and then delineate the mechanisms involved. The accumulation of synaptophysin and APP proteins in axons, without overt axon degeneration, further suggests that this is a model of early pathological changes.

Studies assessing axon degeneration in tau seeding models are limited. One group showed the absence of axon degeneration in ALZ17 mice (overexpress 2N4R tau) injected with brain homogenates from PS19 mice (overexpress 0N4R P301S mutant tau) out to 15 months post-injection (Clavaguera et al., 2009). Two tau propagation studies report atrophy of functionally connected brain regions, and the authors suggest that this is the result of axonal degeneration, though they do not provide direct evidence of axonal loss (Arriagada et al., 1992; de Calignon et al., 2012). The lack of overt axon degeneration is consistent with the current seeding models. Ours

is the first report of early signs of axonopathy in human MAPT-KI mouse primary hippocampal neurons seeded with sarkosyl-insoluble AD-tau.

Caveats to consider

While this model provides an approach to study the potential early synaptic and axonal mechanisms of tau toxicity there are important caveats one must consider. First, in the human brain, the ratio of 3R and 4R isoforms is approximately equal with the 1N isoforms being the most abundant, followed by the 0N, and then the 2N isoforms (Wang & Mandelkow, 2016). The MAPT-KI hippocampal neurons primarily express the 0N3R isoform throughout the time-course of the experiments performed here (i.e. up to 31 days). Five out of the six primary CNS tau isoforms (1N4R, 0N4R, 2N3R, 1N3R and 0N3R, not 2N4R) were detectable on Western blot by DIV14 and progressively increased over time in culture. However, the difference in the 3R/4R tau isoform ratio between the adult human brain and the primary MAPT-KI hippocampal neurons could impact the effects of AD-tau seeding in the culture model.

Another caveat is that not all cells develop pathological tau inclusions. This phenomenon creates some difficulty in detecting culture-wide changes because the effects of pathological tau in discrete neuronal compartments may be washed out by unaffected neurons. Indeed, some of the findings reported here support this caveat. For example, total levels of active GSK3 β were unchanged, but upon inspection with immunostaining a clear pattern of accumulated active GSK3 β was observed in discrete axonal areas containing PAD-exposed tau pathology. Many of the findings reported here showed remarkably similar group means suggesting that these outcomes are unchanged. However, considering that subsets of neurons are affected by tau pathology I may have missed some important effects specifically in those neurons containing tau pathology. Though

technically challenging, narrowing in on the effects of pathological tau in seeded neurons could substantively improve the sensitivity for detecting changes in those neurons.

A caveat of primary neuron experiments in general is that the cells are collected at early developmental time periods and are not integrated into an adult CNS context. For example, our hippocampal primary neuron cultures likely have the excitatory and inhibitory neurons that make up the hippocampus, but they lack the highly ordered connectivity patterns present in the hippocampus *in situ*. Furthermore, microglia, which are known to contribute to the pathogenesis of AD (Hansen et al., 2018), are absent in most primary neuron cultures. Astrocytes also regulate synaptic activity and tau seeding (Chung et al., 2015; Mothes et al., 2023; Perea et al., 2009). As noted in Chapter 2, astrocytes are the second most abundant cell population in our MAPT-KI cultures. Oligodendrocytes were present in our cultures, albeit at low levels (accounting for ~1 % of the total population). Oligodendrocytes, astrocytes and microglia all contribute to neuronal function and disease pathogenesis, and these aspects of glial functions in the human brain cannot be fully recapitulated in primary neuron cultures. Nevertheless, primary neurons are extremely useful for identifying mechanisms of tau toxicity. The seeding assay I developed could be useful in identifying mechanisms underlying the role of tau in synaptic dysfunction and neuronal hyperexcitability. Furthermore, this model could be used to test pharmacological agents aimed at rescuing dysfunction associated with early stages of tau pathology in AD.

Future directions

Some key follow-up studies are needed to determine the specific effects of AD-tau-treatment on neuron activity. To confirm that the effect is due to tau, immunodepleting tau from the AD-tau seeding material should ameliorate the glutamate-evoked/NMDAR-mediated hyperexcitable phenotype. Furthermore, to determine if the intracellular seeded pathological tau

aggregates were responsible for the effect (and not the exogenously added AD-tau seeds), experiments could be repeated in conditions that prevent tau seeding. Heparan sulfate proteoglycans mediate tau seed uptake and propagation, therefore blocking the binding to HSPGs should ameliorate the effects if they are due to the intraneuronal seeded tau aggregates (Holmes et al., 2013).

The significant increase in neuronal network burst frequency (i.e. frequency of synchronized firing events) identified in the MEA experiments is especially intriguing. The effect appears to be NMDAR-mediated, however, the specific mechanisms are unknown. Is the impairment driven by pre- or post-synaptic changes, or both? At the postsynapse, tau modulates long term potentiation (LTP), the molecular substrate of learning and memory (Mueller et al., 2021). Tau transports Fyn kinase to the postsynapse where Fyn stabilizes NMDARs in the synaptic membrane (Ittner et al., 2010). Mice overexpressing Fyn showed NMDAR overactivation and excitotoxicity (Ittner et al., 2010; Xia et al., 2015). Mutant P301L tau was found to trap Fyn in the postsynaptic compartment (Padmanabhan et al., 2019). P301L tau is associated with PAD-exposure, and PAD-exposure is observed in the inclusions formed in our seeding model. Pathological tau is also linked to presynaptic impairment through regulation of protein phosphatase 1 that results in decreased neurotransmitter release (Moreno et al., 2016; Mueller et al., 2021). Tau may have effects on synaptic functionality by actions of tau within synapses or potentially via indirect routes. Indirectly, tau may cause synaptic dysfunction through impairment of axonal transport. Presynaptic function relies on the delivery of healthy mitochondria to provide ATP and for Ca²⁺ buffering (Devine & Kittler, 2018). It is also important to remove dysfunctional mitochondria from the synapse (Cai & Tammineni, 2017; Devine & Kittler, 2018; Han et al., 2020). Transport of other materials including synaptic vesicles, receptors, and neurotransmitters is

also important to maintain functional healthy synapses (Combs et al., 2019; Kneynsberg et al., 2017). Aberrant PAD-exposure, as seen in the tau inclusions formed in this model, may impair axon transport (Combs et al., 2019), and lead to synaptic deficits. Yet another way pathological tau could impair synaptic activity in this model is by changing the excitatory/inhibitory ratio. GABAergic neurons are differentially affected in tauopathies (Levenga et al., 2013; Targa Dias Anastacio et al., 2022; Usenovic et al., 2015; Witton et al., 2016). A loss of inhibitory input could drive hyperexcitability. It would be interesting to use excitatory and inhibitory neuron-specific markers to determine if either type is differentially seeded or affected in this model system. Furthermore, PLA experiments with an inhibitory synaptic pair of antibodies could identify whether inhibitory synapses are affected. Clearly, a number of avenues should be explored to determine what is driving the neuronal network excitability observed in the AD-tau-treated MAPT-KI cells.

Interestingly, overt cell loss is absent in the vast majority of seeding models, including ours (Gibbons et al., 2017; Guo et al., 2016; Hayashi et al., 2021; He et al., 2020; Miao et al., 2019; Narasimhan et al., 2017; Saito et al., 2019). Aging is the primary risk factor for AD ("2024 Alzheimer's disease facts and figures," 2024), and many features of human aging are not fully recapitulated using *in vivo* or *in vitro* model systems. Some age-related changes include chronic inflammation, mitochondrial dysfunction and oxidative stress, loss of proteostasis, disabled macroautophagy, and cellular senescence (Lopez-Otin et al., 2023). Furthermore, A β may exacerbate tau pathology and toxicity. Incorporating one or more of these additional stressors into a so-called "second-hit" modeling approach may be necessary to produce neurodegenerative effects.

Two *in vivo* studies showed that A β accelerated tau pathology and toxicity in AD animal models. In one study, 5xFAD mice (APP/PS1 mice with 5 familial AD mutations) were crossed with PS19 mice which resulted in ~10x the amount of tau pathology compared to PS19 mice (Stancu et al., 2014). The 5xFAD x PS19 mice exhibited impaired hippocampus-dependent spatial navigation tasks, these cognitive impairments are not observed in PS19 mice. Furthermore, only the 5xFAD x PS19 mice showed hippocampal atrophy (Stancu et al., 2014). In a separate study, APP/PS1 mice (harboring the Swedish *APP* mutation and the PSEN1dE9 mutation) were crossed with rTgTauEC. The rTgTauEC x APP/PS1 mice which exhibited accelerated propagation of tau pathology and neuronal loss (Pooler et al., 2015). Notably, these studies used aggressive models of A β and tauopathy. More recently, MAPT-KI mice were crossed with APP-knock-in mice (human *APP* gene knocked in) (Saito et al., 2019). The double-knock-in mice exhibited accelerated tau pathology propagation after seeding with AD-tau (Saito et al., 2019). Increased dystrophic neurites with pathological tau were observed near A β plaques (Saito et al., 2019). Thus, it would be interesting to test whether pathological A β would exacerbate the MAPT-KI seeding model described here. A logical next step would be to treat AD-tau seeded and unseeded neurons with A β oligomers and assess overt toxicity, axonal degeneration and synaptic function. Multiple studies showed that A β oligomers exert toxicity through mechanisms including axonal transport dysfunction (Decker et al., 2010; Pigino et al., 2009; Poon et al., 2013) and synaptic impairment (Li et al., 2011; Shankar et al., 2007; Wu et al., 2010). Notably, impaired axonal transport of dense-core vesicles and mitochondria in A β oligomer-treated primary neurons was prevented by GSK3 β inhibition (Decker et al., 2010). Furthermore, multiple studies showed A β oligomer-induced synaptic toxicity was NMDAR-mediated (Shankar et al., 2007; Shankar et al., 2008). Therefore, one would predict that addition of A β oligomers would result in significantly greater axonal

degeneration and synaptic impairment in the tau seeded neurons compared to the unseeded neurons. To determine if axonopathy and synaptic impairment are dependent on the PAD-PP1-GSK3 pathway, a complementary set of experiments could be performed in seeded and unseeded cells (+/- A β oligomers) using genetic deletion of the PAD. Such studies could help gain further understanding of the interplay between tau and A β , and the role of PAD in neuronal toxicity.

I have developed a model that allows us to study the effects of AD-associated pathological tau species on neuron function. The specific tau species formed, and the dysfunction observed, are likely most representative of changes occurring in the early phases of AD. It is critical to understand the mechanisms involved in early AD, so that we may prevent overt toxicity and neuron death. This model seems well positioned to serve as a tool to understand the contribution of additional stressors needed for neurodegeneration to occur. From a novel therapeutic development perspective, this model may prove useful in testing inhibitors of tau aggregation, spreading and early mechanisms of tau-mediated toxicity (e.g. immunotherapies with TNT1 or other tau-specific antibodies). Overall, this model has the potential to help investigators gain key insights into the pathogenesis of AD, with the ultimate goal of identifying critical therapeutic targets that prevent or at least slow the disease.

REFERENCES

- 2024 Alzheimer's disease facts and figures. (2024, May). *Alzheimers Dement*, 20(5), 3708-3821. <https://doi.org/10.1002/alz.13809>
- Arriagada, P. V., Growdon, J. H., Hedley-Whyte, E. T., & Hyman, B. T. (1992, Mar). Neurofibrillary tangles but not senile plaques parallel duration and severity of Alzheimer's disease. *Neurology*, 42(3 Pt 1), 631-639. <https://doi.org/10.1212/wnl.42.3.631>
- Balez, R., Steiner, N., Engel, M., Munoz, S. S., Lum, J. S., Wu, Y., Wang, D., Vallotton, P., Sachdev, P., O'Connor, M., Sidhu, K., Munch, G., & Ooi, L. (2016, Aug 12). Neuroprotective effects of apigenin against inflammation, neuronal excitability and apoptosis in an induced pluripotent stem cell model of Alzheimer's disease. *Sci Rep*, 6, 31450. <https://doi.org/10.1038/srep31450>
- Bassil, F., Meymand, E. S., Brown, H. J., Xu, H., Cox, T. O., Pattabhiraman, S., Maghames, C. M., Wu, Q., Zhang, B., Trojanowski, J. Q., & Lee, V. M. (2021, Jan 4). alpha-Synuclein modulates tau spreading in mouse brains. *J Exp Med*, 218(1). <https://doi.org/10.1084/jem.20192193>
- Busche, M. A., Eichhoff, G., Adelsberger, H., Abramowski, D., Wiederhold, K. H., Haass, C., Staufenbiel, M., Konnerth, A., & Garaschuk, O. (2008, Sep 19). Clusters of hyperactive neurons near amyloid plaques in a mouse model of Alzheimer's disease. *Science*, 321(5896), 1686-1689. <https://doi.org/10.1126/science.1162844>
- Cai, Q., & Tammineni, P. (2017). Mitochondrial Aspects of Synaptic Dysfunction in Alzheimer's Disease. *J Alzheimers Dis*, 57(4), 1087-1103. <https://doi.org/10.3233/JAD-160726>
- Celone, K. A., Calhoun, V. D., Dickerson, B. C., Atri, A., Chua, E. F., Miller, S. L., DePeau, K., Rentz, D. M., Selkoe, D. J., Blacker, D., Albert, M. S., & Sperling, R. A. (2006, Oct 4). Alterations in memory networks in mild cognitive impairment and Alzheimer's disease: an independent component analysis. *J Neurosci*, 26(40), 10222-10231. <https://doi.org/10.1523/JNEUROSCI.2250-06.2006>
- Christensen, K. R., Beach, T. G., Serrano, G. E., & Kanaan, N. M. (2019, Feb 28). Pathogenic tau modifications occur in axons before the somatodendritic compartment in mossy fiber and Schaffer collateral pathways. *Acta Neuropathol Commun*, 7(1), 29. <https://doi.org/10.1186/s40478-019-0675-9>
- Christensen, K. R., Combs, B., Richards, C., Grabinski, T., Alhadidy, M. M., & Kanaan, N. M. (2023). Phosphomimetics at Ser199/Ser202/Thr205 in tau impairs axonal transport in rat hippocampal neurons. *Molecular Neurobiology*, 60(6), 3423-3438.
- Chung, W. S., Allen, N. J., & Eroglu, C. (2015, Feb 6). Astrocytes Control Synapse Formation, Function, and Elimination. *Cold Spring Harb Perspect Biol*, 7(9), a020370. <https://doi.org/10.1101/cshperspect.a020370>

- Clavaguera, F., Bolmont, T., Crowther, R. A., Abramowski, D., Frank, S., Probst, A., Fraser, G., Stalder, A. K., Beibel, M., & Staufenbiel, M. (2009). Transmission and spreading of tauopathy in transgenic mouse brain. *Nature cell biology*, *11*(7), 909-913.
- Coleman, M. (2005, Nov). Axon degeneration mechanisms: commonality amid diversity. *Nat Rev Neurosci*, *6*(11), 889-898. <https://doi.org/10.1038/nrn1788>
- Combs, B., Christensen, K. R., Richards, C., Kneynsberg, A., Mueller, R. L., Morris, S. L., Morfini, G. A., Brady, S. T., & Kanaan, N. M. (2021). Frontotemporal lobar dementia mutant tau impairs axonal transport through a protein phosphatase 1 γ -dependent mechanism. *Journal of neuroscience*, *41*(45), 9431-9451.
- Combs, B., Hamel, C., & Kanaan, N. M. (2016, Oct). Pathological conformations involving the amino terminus of tau occur early in Alzheimer's disease and are differentially detected by monoclonal antibodies. *Neurobiol Dis*, *94*, 18-31. <https://doi.org/10.1016/j.nbd.2016.05.016>
- Combs, B., & Kanaan, N. M. (2017, Jun). Exposure of the Amino Terminus of Tau Is a Pathological Event in Multiple Tauopathies. *Am J Pathol*, *187*(6), 1222-1229. <https://doi.org/10.1016/j.ajpath.2017.01.019>
- Combs, B., Mueller, R. L., Morfini, G., Brady, S. T., & Kanaan, N. M. (2019). Tau and axonal transport misregulation in tauopathies. *Tau Biology*, 81-95.
- Cox, K., Combs, B., Abdelmesih, B., Morfini, G., Brady, S. T., & Kanaan, N. M. (2016, Nov). Analysis of isoform-specific tau aggregates suggests a common toxic mechanism involving similar pathological conformations and axonal transport inhibition. *Neurobiol Aging*, *47*, 113-126. <https://doi.org/10.1016/j.neurobiolaging.2016.07.015>
- Cretin, B., Sellal, F., Philippi, N., Bousiges, O., Di Bitonto, L., Martin-Hunyadi, C., & Blanc, F. (2016, Apr 18). Epileptic Prodromal Alzheimer's Disease, a Retrospective Study of 13 New Cases: Expanding the Spectrum of Alzheimer's Disease to an Epileptic Variant? *J Alzheimers Dis*, *52*(3), 1125-1133. <https://doi.org/10.3233/JAD-150096>
- de Calignon, A., Polydoro, M., Suarez-Calvet, M., William, C., Adamowicz, D. H., Kopeikina, K. J., Pitstick, R., Sahara, N., Ashe, K. H., Carlson, G. A., Spires-Jones, T. L., & Hyman, B. T. (2012, Feb 23). Propagation of tau pathology in a model of early Alzheimer's disease. *Neuron*, *73*(4), 685-697. <https://doi.org/10.1016/j.neuron.2011.11.033>
- Decker, H., Lo, K. Y., Unger, S. M., Ferreira, S. T., & Silverman, M. A. (2010, Jul 7). Amyloid-beta peptide oligomers disrupt axonal transport through an NMDA receptor-dependent mechanism that is mediated by glycogen synthase kinase 3 β in primary cultured hippocampal neurons. *J Neurosci*, *30*(27), 9166-9171. <https://doi.org/10.1523/JNEUROSCI.1074-10.2010>

- Devine, M. J., & Kittler, J. T. (2018, Jan 19). Mitochondria at the neuronal presynapse in health and disease. *Nat Rev Neurosci*, *19*(2), 63-80. <https://doi.org/10.1038/nrn.2017.170>
- Dickerson, B. C., Salat, D. H., Greve, D. N., Chua, E. F., Rand-Giovannetti, E., Rentz, D. M., Bertram, L., Mullin, K., Tanzi, R. E., Blacker, D., Albert, M. S., & Sperling, R. A. (2005, Aug 9). Increased hippocampal activation in mild cognitive impairment compared to normal aging and AD. *Neurology*, *65*(3), 404-411. <https://doi.org/10.1212/01.wnl.0000171450.97464.49>
- Gamblin, T. C., Chen, F., Zambrano, A., Abraha, A., Lagalwar, S., Guillozet, A. L., Lu, M., Fu, Y., Garcia-Sierra, F., LaPointe, N., Miller, R., Berry, R. W., Binder, L. I., & Cryns, V. L. (2003, Aug 19). Caspase cleavage of tau: linking amyloid and neurofibrillary tangles in Alzheimer's disease. *Proc Natl Acad Sci U S A*, *100*(17), 10032-10037. <https://doi.org/10.1073/pnas.1630428100>
- Ghatak, S., Dolatabadi, N., Trudler, D., Zhang, X., Wu, Y., Mohata, M., Ambasudhan, R., Talantova, M., & Lipton, S. A. (2019, Nov 29). Mechanisms of hyperexcitability in Alzheimer's disease hiPSC-derived neurons and cerebral organoids vs isogenic controls. *Elife*, *8*. <https://doi.org/10.7554/eLife.50333>
- Ghoshal, N., Garcia-Sierra, F., Wu, J., Leurgans, S., Bennett, D. A., Berry, R. W., & Binder, L. I. (2002, Oct). Tau conformational changes correspond to impairments of episodic memory in mild cognitive impairment and Alzheimer's disease. *Exp Neurol*, *177*(2), 475-493. <https://doi.org/10.1006/exnr.2002.8014>
- Gibbons, G. S., Banks, R. A., Kim, B., Xu, H., Changolkar, L., Leight, S. N., Riddle, D. M., Li, C., Gathagan, R. J., Brown, H. J., Zhang, B., Trojanowski, J. Q., & Lee, V. M. (2017, Nov 22). GFP-Mutant Human Tau Transgenic Mice Develop Tauopathy Following CNS Injections of Alzheimer's Brain-Derived Pathological Tau or Synthetic Mutant Human Tau Fibrils. *J Neurosci*, *37*(47), 11485-11494. <https://doi.org/10.1523/JNEUROSCI.2393-17.2017>
- Guerrero-Munoz, M. J., Gerson, J., & Castillo-Carranza, D. L. (2015). Tau Oligomers: The Toxic Player at Synapses in Alzheimer's Disease. *Front Cell Neurosci*, *9*, 464. <https://doi.org/10.3389/fncel.2015.00464>
- Guillozet-Bongaarts, A. L., Garcia-Sierra, F., Reynolds, M. R., Horowitz, P. M., Fu, Y., Wang, T., Cahill, M. E., Bigio, E. H., Berry, R. W., & Binder, L. I. (2005). Tau truncation during neurofibrillary tangle evolution in Alzheimer's disease. *Neurobiology of aging*, *26*(7), 1015-1022.
- Guo, J. L., Narasimhan, S., Changolkar, L., He, Z., Stieber, A., Zhang, B., Gathagan, R. J., Iba, M., McBride, J. D., & Trojanowski, J. Q. (2016). Unique pathological tau conformers from Alzheimer's brains transmit tau pathology in nontransgenic mice. *Journal of Experimental Medicine*, *213*(12), 2635-2654.

- Hamalainen, A., Pihlajamaki, M., Tanila, H., Hanninen, T., Niskanen, E., Tervo, S., Karjalainen, P. A., Vanninen, R. L., & Soininen, H. (2007, Dec). Increased fMRI responses during encoding in mild cognitive impairment. *Neurobiol Aging*, 28(12), 1889-1903. <https://doi.org/10.1016/j.neurobiolaging.2006.08.008>
- Han, S., Jeong, Y. Y., Sheshadri, P., & Cai, Q. (2020, Oct). Mitophagy coordination with retrograde transport ensures the integrity of synaptic mitochondria. *Autophagy*, 16(10), 1925-1927. <https://doi.org/10.1080/15548627.2020.1810919>
- Hansen, D. V., Hanson, J. E., & Sheng, M. (2018, Feb 5). Microglia in Alzheimer's disease. *J Cell Biol*, 217(2), 459-472. <https://doi.org/10.1083/jcb.201709069>
- Harrington, C. R., Mukaetova-Ladinska, E. B., Hills, R., Edwards, P. C., Montejo de Garcini, E., Novak, M., & Wischik, C. M. (1991, Jul 1). Measurement of distinct immunochemical presentations of tau protein in Alzheimer disease. *Proc Natl Acad Sci U S A*, 88(13), 5842-5846. <https://doi.org/10.1073/pnas.88.13.5842>
- Hayashi, T., Shimonaka, S., Elahi, M., Matsumoto, S. E., Ishiguro, K., Takanashi, M., Hattori, N., & Motoi, Y. (2021). Learning Deficits Accompanied by Microglial Proliferation After the Long-Term Post-Injection of Alzheimer's Disease Brain Extract in Mouse Brains. *J Alzheimers Dis*, 79(4), 1701-1711. <https://doi.org/10.3233/JAD-201002>
- He, Z., McBride, J. D., Xu, H., Changolkar, L., Kim, S.-j., Zhang, B., Narasimhan, S., Gibbons, G. S., Guo, J. L., & Kozak, M. (2020). Transmission of tauopathy strains is independent of their isoform composition. *Nature communications*, 11(1), 7.
- Holmes, B. B., DeVos, S. L., Kfoury, N., Li, M., Jacks, R., Yanamandra, K., Ouidja, M. O., Brodsky, F. M., Marasa, J., Bagchi, D. P., Kotzbauer, P. T., Miller, T. M., Papy-Garcia, D., & Diamond, M. I. (2013, Aug 13). Heparan sulfate proteoglycans mediate internalization and propagation of specific proteopathic seeds. *Proc Natl Acad Sci U S A*, 110(33), E3138-3147. <https://doi.org/10.1073/pnas.1301440110>
- Ittner, L. M., Ke, Y. D., Delerue, F., Bi, M., Gladbach, A., van Eersel, J., Wolfing, H., Chieng, B. C., Christie, M. J., Napier, I. A., Eckert, A., Staufenbiel, M., Hardeman, E., & Gotz, J. (2010, Aug 6). Dendritic function of tau mediates amyloid-beta toxicity in Alzheimer's disease mouse models. *Cell*, 142(3), 387-397. <https://doi.org/10.1016/j.cell.2010.06.036>
- Kamal, A., Stokin, G. B., Yang, Z., Xia, C. H., & Goldstein, L. S. (2000, Nov). Axonal transport of amyloid precursor protein is mediated by direct binding to the kinesin light chain subunit of kinesin-I. *Neuron*, 28(2), 449-459. [https://doi.org/10.1016/s0896-6273\(00\)00124-0](https://doi.org/10.1016/s0896-6273(00)00124-0)
- Kanaan, N. M., Cox, K., Alvarez, V. E., Stein, T. D., Poncil, S., & McKee, A. C. (2016). Characterization of early pathological tau conformations and phosphorylation in chronic traumatic encephalopathy. *Journal of Neuropathology & Experimental Neurology*, 75(1), 19-34.

- Kanaan, N. M., Morfini, G. A., LaPointe, N. E., Pigino, G. F., Patterson, K. R., Song, Y., Andreadis, A., Fu, Y., Brady, S. T., & Binder, L. I. (2011, Jul 6). Pathogenic forms of tau inhibit kinesin-dependent axonal transport through a mechanism involving activation of axonal phosphotransferases. *J Neurosci*, *31*(27), 9858-9868. <https://doi.org/10.1523/JNEUROSCI.0560-11.2011>
- Kanaan, N. M., Pigino, G. F., Brady, S. T., Lazarov, O., Binder, L. I., & Morfini, G. A. (2013, Aug). Axonal degeneration in Alzheimer's disease: when signaling abnormalities meet the axonal transport system. *Exp Neurol*, *246*, 44-53. <https://doi.org/10.1016/j.expneurol.2012.06.003>
- Kneysberg, A., Combs, B., Christensen, K., Morfini, G., & Kanaan, N. M. (2017). Axonal Degeneration in Tauopathies: Disease Relevance and Underlying Mechanisms. *Front Neurosci*, *11*, 572. <https://doi.org/10.3389/fnins.2017.00572>
- Koo, E. H., Sisodia, S. S., Archer, D. R., Martin, L. J., Weidemann, A., Beyreuther, K., Fischer, P., Masters, C. L., & Price, D. L. (1990, Feb). Precursor of amyloid protein in Alzheimer disease undergoes fast anterograde axonal transport. *Proc Natl Acad Sci U S A*, *87*(4), 1561-1565. <https://doi.org/10.1073/pnas.87.4.1561>
- Lasagna-Reeves, C. A., Castillo-Carranza, D. L., Sengupta, U., Guerrero-Munoz, M. J., Kiritoshi, T., Neugebauer, V., Jackson, G. R., & Kaye, R. (2012). Alzheimer brain-derived tau oligomers propagate pathology from endogenous tau. *Sci Rep*, *2*, 700. <https://doi.org/10.1038/srep00700>
- Lerdkrai, C., Asavapanumas, N., Brawek, B., Kovalchuk, Y., Mojtahedi, N., Olmedillas Del Moral, M., & Garaschuk, O. (2018, Feb 6). Intracellular Ca(2+) stores control in vivo neuronal hyperactivity in a mouse model of Alzheimer's disease. *Proc Natl Acad Sci U S A*, *115*(6), E1279-E1288. <https://doi.org/10.1073/pnas.1714409115>
- Levenga, J., Krishnamurthy, P., Rajamohamedsait, H., Wong, H., Franke, T. F., Cain, P., Sigurdsson, E. M., & Hoeffler, C. A. (2013, Jul 11). Tau pathology induces loss of GABAergic interneurons leading to altered synaptic plasticity and behavioral impairments. *Acta Neuropathol Commun*, *1*, 34. <https://doi.org/10.1186/2051-5960-1-34>
- Li, S., Jin, M., Koeglsperger, T., Shepardson, N. E., Shankar, G. M., & Selkoe, D. J. (2011, May 4). Soluble Abeta oligomers inhibit long-term potentiation through a mechanism involving excessive activation of extrasynaptic NR2B-containing NMDA receptors. *J Neurosci*, *31*(18), 6627-6638. <https://doi.org/10.1523/JNEUROSCI.0203-11.2011>
- Lopez-Otin, C., Blasco, M. A., Partridge, L., Serrano, M., & Kroemer, G. (2023, Jan 19). Hallmarks of aging: An expanding universe. *Cell*, *186*(2), 243-278. <https://doi.org/10.1016/j.cell.2022.11.001>
- Luna-Munoz, J., Peralta-Ramirez, J., Chavez-Macias, L., Harrington, C. R., Wischik, C. M., & Mena, R. (2008, Nov). Thiazin red as a neuropathological tool for the rapid diagnosis of

- Alzheimer's disease in tissue imprints. *Acta Neuropathol*, 116(5), 507-515. <https://doi.org/10.1007/s00401-008-0431-x>
- Luna-Viramontes, N. I., Campa-Cordoba, B. B., Ontiveros-Torres, M. A., Harrington, C. R., Villanueva-Fierro, I., Guadarrama-Ortiz, P., Garces-Ramirez, L., de la Cruz, F., Hernandez-Alejandro, M., Martinez-Robles, S., Gonzalez-Ballesteros, E., Pacheco-Herrero, M., & Luna-Munoz, J. (2020). PHF-Core Tau as the Potential Initiating Event for Tau Pathology in Alzheimer's Disease. *Front Cell Neurosci*, 14, 247. <https://doi.org/10.3389/fncel.2020.00247>
- Mate De Gerando, A., Welikovitch, L. A., Khasnavis, A., Commins, C., Glynn, C., Chun, J. E., Perbet, R., & Hyman, B. T. (2023, Aug). Tau seeding and spreading in vivo is supported by both AD-derived fibrillar and oligomeric tau. *Acta Neuropathol*, 146(2), 191-210. <https://doi.org/10.1007/s00401-023-02600-1>
- Mena, R., Edwards, P., Perez-Olvera, O., & Wischik, C. M. (1995). Monitoring pathological assembly of tau and beta-amyloid proteins in Alzheimer's disease. *Acta Neuropathol*, 89(1), 50-56. <https://doi.org/10.1007/BF00294259>
- Miao, J., Shi, R., Li, L., Chen, F., Zhou, Y., Tung, Y. C., Hu, W., Gong, C. X., Iqbal, K., & Liu, F. (2019). Pathological Tau From Alzheimer's Brain Induces Site-Specific Hyperphosphorylation and SDS- and Reducing Agent-Resistant Aggregation of Tau in vivo. *Front Aging Neurosci*, 11, 34. <https://doi.org/10.3389/fnagi.2019.00034>
- Moreno, H., Morfini, G., Buitrago, L., Ujlaki, G., Choi, S., Yu, E., Moreira, J. E., Avila, J., Brady, S. T., Pant, H., Sugimori, M., & Llinas, R. R. (2016, Jun 14). Tau pathology-mediated presynaptic dysfunction. *Neuroscience*, 325, 30-38. <https://doi.org/10.1016/j.neuroscience.2016.03.044>
- Mothes, T., Portal, B., Konstantinidis, E., Eltom, K., Libard, S., Streubel-Gallasch, L., Ingelsson, M., Rostami, J., Lindskog, M., & Erlandsson, A. (2023, Jun 17). Astrocytic uptake of neuronal corpses promotes cell-to-cell spreading of tau pathology. *Acta Neuropathol Commun*, 11(1), 97. <https://doi.org/10.1186/s40478-023-01589-8>
- Mueller, R. L., Combs, B., Alhadidy, M. M., Brady, S. T., Morfini, G. A., & Kanaan, N. M. (2021). Tau: A Signaling Hub Protein. *Front Mol Neurosci*, 14, 647054. <https://doi.org/10.3389/fnmol.2021.647054>
- Narasimhan, S., Guo, J. L., Changolkar, L., Stieber, A., McBride, J. D., Silva, L. V., He, Z., Zhang, B., Gathagan, R. J., & Trojanowski, J. Q. (2017). Pathological tau strains from human brains recapitulate the diversity of tauopathies in nontransgenic mouse brain. *Journal of neuroscience*, 37(47), 11406-11423.
- Novak, M., Wischik, C. M., Edwards, P., Pannell, R., & Milstein, C. (1989). Characterisation of the first monoclonal antibody against the pronase resistant core of the Alzheimer PHF. *Prog Clin Biol Res*, 317, 755-761. <https://www.ncbi.nlm.nih.gov/pubmed/2602435>

- Padmanabhan, P., Martinez-Marmol, R., Xia, D., Gotz, J., & Meunier, F. A. (2019, Jun 25). Frontotemporal dementia mutant Tau promotes aberrant Fyn nanoclustering in hippocampal dendritic spines. *Elife*, 8. <https://doi.org/10.7554/eLife.45040>
- Palop, J. J., & Mucke, L. (2010, Mar). Synaptic depression and aberrant excitatory network activity in Alzheimer's disease: two faces of the same coin? *Neuromolecular Med*, 12(1), 48-55. <https://doi.org/10.1007/s12017-009-8097-7>
- Perea, G., Navarrete, M., & Araque, A. (2009, Aug). Tripartite synapses: astrocytes process and control synaptic information. *Trends Neurosci*, 32(8), 421-431. <https://doi.org/10.1016/j.tins.2009.05.001>
- Pigino, G., Morfini, G., Atagi, Y., Deshpande, A., Yu, C., Jungbauer, L., LaDu, M., Busciglio, J., & Brady, S. (2009, Apr 7). Disruption of fast axonal transport is a pathogenic mechanism for intraneuronal amyloid beta. *Proc Natl Acad Sci U S A*, 106(14), 5907-5912. <https://doi.org/10.1073/pnas.0901229106>
- Poon, W. W., Carlos, A. J., Aguilar, B. L., Berchtold, N. C., Kawano, C. K., Zograbyan, V., Yaoprake, T., Shelanski, M., & Cotman, C. W. (2013, Jun 7). beta-Amyloid (A β) oligomers impair brain-derived neurotrophic factor retrograde trafficking by down-regulating ubiquitin C-terminal hydrolase, UCH-L1. *J Biol Chem*, 288(23), 16937-16948. <https://doi.org/10.1074/jbc.M113.463711>
- Roberson, E. D., Halabisky, B., Yoo, J. W., Yao, J., Chin, J., Yan, F., Wu, T., Hamto, P., Devidze, N., Yu, G. Q., Palop, J. J., Noebels, J. L., & Mucke, L. (2011, Jan 12). Amyloid-beta/Fyn-induced synaptic, network, and cognitive impairments depend on tau levels in multiple mouse models of Alzheimer's disease. *J Neurosci*, 31(2), 700-711. <https://doi.org/10.1523/JNEUROSCI.4152-10.2011>
- Saito, T., Mihira, N., Matsuba, Y., Sasaguri, H., Hashimoto, S., Narasimhan, S., Zhang, B., Murayama, S., Higuchi, M., Lee, V. M. Y., Trojanowski, J. Q., & Saido, T. C. (2019, Aug 23). Humanization of the entire murine Mapt gene provides a murine model of pathological human tau propagation. *J Biol Chem*, 294(34), 12754-12765. <https://doi.org/10.1074/jbc.RA119.009487>
- Saroja, S. R., Sharma, A., Hof, P. R., & Pereira, A. C. (2022, Sep). Differential expression of tau species and the association with cognitive decline and synaptic loss in Alzheimer's disease. *Alzheimers Dement*, 18(9), 1602-1615. <https://doi.org/10.1002/alz.12518>
- Shankar, G. M., Bloodgood, B. L., Townsend, M., Walsh, D. M., Selkoe, D. J., & Sabatini, B. L. (2007, Mar 14). Natural oligomers of the Alzheimer amyloid-beta protein induce reversible synapse loss by modulating an NMDA-type glutamate receptor-dependent signaling pathway. *J Neurosci*, 27(11), 2866-2875. <https://doi.org/10.1523/JNEUROSCI.4970-06.2007>

- Shankar, G. M., Li, S., Mehta, T. H., Garcia-Munoz, A., Shepardson, N. E., Smith, I., Brett, F. M., Farrell, M. A., Rowan, M. J., Lemere, C. A., Regan, C. M., Walsh, D. M., Sabatini, B. L., & Selkoe, D. J. (2008, Aug). Amyloid-beta protein dimers isolated directly from Alzheimer's brains impair synaptic plasticity and memory. *Nat Med*, *14*(8), 837-842. <https://doi.org/10.1038/nm1782>
- Siskova, Z., Justus, D., Kaneko, H., Friedrichs, D., Henneberg, N., Beutel, T., Pitsch, J., Schoch, S., Becker, A., von der Kammer, H., & Remy, S. (2014, Dec 3). Dendritic structural degeneration is functionally linked to cellular hyperexcitability in a mouse model of Alzheimer's disease. *Neuron*, *84*(5), 1023-1033. <https://doi.org/10.1016/j.neuron.2014.10.024>
- Stancu, I. C., Vasconcelos, B., Ris, L., Wang, P., Villers, A., Peeraer, E., Buist, A., Terwel, D., Baatsen, P., Oyelami, T., Pierrot, N., Casteels, C., Bormans, G., Kienlen-Campard, P., Octave, J. N., Moechars, D., & Dewachter, I. (2015, Jun). Templated misfolding of Tau by prion-like seeding along neuronal connections impairs neuronal network function and associated behavioral outcomes in Tau transgenic mice. *Acta Neuropathol*, *129*(6), 875-894. <https://doi.org/10.1007/s00401-015-1413-4>
- Su, J. H., Deng, G., & Cotman, C. W. (1997). Transneuronal degeneration in the spread of Alzheimer's disease pathology: immunohistochemical evidence for the transmission of tau hyperphosphorylation. *Neurobiol Dis*, *4*(5), 365-375. <https://doi.org/10.1006/nbdi.1997.0164>
- Targa Dias Anastacio, H., Matosin, N., & Ooi, L. (2022, Jun 22). Neuronal hyperexcitability in Alzheimer's disease: what are the drivers behind this aberrant phenotype? *Transl Psychiatry*, *12*(1), 257. <https://doi.org/10.1038/s41398-022-02024-7>
- Tiernan, C. T., Combs, B., Cox, K., Morfini, G., Brady, S. T., Counts, S. E., & Kanaan, N. M. (2016, Sep). Pseudophosphorylation of tau at S422 enhances SDS-stable dimer formation and impairs both anterograde and retrograde fast axonal transport. *Exp Neurol*, *283*(Pt A), 318-329. <https://doi.org/10.1016/j.expneurol.2016.06.030>
- Usenovic, M., Niroomand, S., Drolet, R. E., Yao, L., Gaspar, R. C., Hatcher, N. G., Schachter, J., Renger, J. J., & Parmentier-Batteur, S. (2015, Oct 21). Internalized Tau Oligomers Cause Neurodegeneration by Inducing Accumulation of Pathogenic Tau in Human Neurons Derived from Induced Pluripotent Stem Cells. *J Neurosci*, *35*(42), 14234-14250. <https://doi.org/10.1523/JNEUROSCI.1523-15.2015>
- Vana, L., Kanaan, N. M., Ugwu, I. C., Wu, J., Mufson, E. J., & Binder, L. I. (2011, Nov). Progression of tau pathology in cholinergic Basal forebrain neurons in mild cognitive impairment and Alzheimer's disease. *Am J Pathol*, *179*(5), 2533-2550. <https://doi.org/10.1016/j.ajpath.2011.07.044>
- Vossel, K. A., Beagle, A. J., Rabinovici, G. D., Shu, H., Lee, S. E., Naasan, G., Hegde, M., Cornes, S. B., Henry, M. L., Nelson, A. B., Seeley, W. W., Geschwind, M. D., Gorno-Tempini, M.

- L., Shih, T., Kirsch, H. E., Garcia, P. A., Miller, B. L., & Mucke, L. (2013, Sep 1). Seizures and epileptiform activity in the early stages of Alzheimer disease. *JAMA Neurol*, *70*(9), 1158-1166. <https://doi.org/10.1001/jamaneurol.2013.136>
- Vossel, K. A., Ranasinghe, K. G., Beagle, A. J., Mizuiri, D., Honma, S. M., Dowling, A. F., Darwish, S. M., Van Berlo, V., Barnes, D. E., Mantle, M., Karydas, A. M., Coppola, G., Roberson, E. D., Miller, B. L., Garcia, P. A., Kirsch, H. E., Mucke, L., & Nagarajan, S. S. (2016, Dec). Incidence and impact of subclinical epileptiform activity in Alzheimer's disease. *Ann Neurol*, *80*(6), 858-870. <https://doi.org/10.1002/ana.24794>
- Vossel, K. A., Tartaglia, M. C., Nygaard, H. B., Zeman, A. Z., & Miller, B. L. (2017, Apr). Epileptic activity in Alzheimer's disease: causes and clinical relevance. *Lancet Neurol*, *16*(4), 311-322. [https://doi.org/10.1016/S1474-4422\(17\)30044-3](https://doi.org/10.1016/S1474-4422(17)30044-3)
- Wang, Y., & Mandelkow, E. (2016). Tau in physiology and pathology. *Nature reviews neuroscience*, *17*(1), 22-35.
- Ward, S. M., Himmelstein, D. S., Lancia, J. K., & Binder, L. I. (2012, Aug). Tau oligomers and tau toxicity in neurodegenerative disease. *Biochem Soc Trans*, *40*(4), 667-671. <https://doi.org/10.1042/BST20120134>
- Witton, J., Staniaszek, L. E., Bartsch, U., Randall, A. D., Jones, M. W., & Brown, J. T. (2016, Aug 15). Disrupted hippocampal sharp-wave ripple-associated spike dynamics in a transgenic mouse model of dementia. *J Physiol*, *594*(16), 4615-4630. <https://doi.org/10.1113/jphysiol.2014.282889>
- Wu, H. Y., Hudry, E., Hashimoto, T., Kuchibhotla, K., Rozkalne, A., Fan, Z., Spires-Jones, T., Xie, H., Arbel-Ornath, M., Grosskreutz, C. L., Bacskai, B. J., & Hyman, B. T. (2010, Feb 17). Amyloid beta induces the morphological neurodegenerative triad of spine loss, dendritic simplification, and neuritic dystrophies through calcineurin activation. *J Neurosci*, *30*(7), 2636-2649. <https://doi.org/10.1523/JNEUROSCI.4456-09.2010>